Role of Intestinal Microbiota on Exogenously Induced Colitis and Associated Physiological Changes: A Comparative Analysis of DSS and Antibiotic Treatment

By

Sohini Mukhopadhyay

LIFE11201704005

National Institute of Science Education and Research (NISER), Bhubaneswar

A thesis submitted to the Board of Studies in Life Sciences

In partial fulfillment of requirementsfor the Degree

of

DOCTOR OF PHILOSOPHY

of

HOMI BHABHA NATIONAL INSTITUTE

April, 2023

Homi Bhabha National Institute[1]
Recommendations of the Viva Voce Committee

As members of the Viva Voce Committee, we certify that we have read the dissertation prepared by **Sohini Mukhopadhyay** entitled **Role of Intestinal Microbiota on Exogenously Induced Colitis and Associated Physiological Changes: A Comparative Analysis of DSS and Antibiotic Treatment** and recommend that it may be accepted as fulfilling the thesis requirement for the award of Degree of Doctor of Philosophy.

Chairman – Dr. Asima Bhattacharyya	4.8.2023
Guide / Convener – Prof. Palok Aich	Palok Aich 06 Aug 04 2023
Co-guide - Name & Signature with date (if any)	—
Examiner – Prof. Jai Kumar Kaushik	4/8/2023
Member 1- Dr. Tirumala Kumar Chowdary	04/08/23
Member 2- Dr. Ramanujam Srinivasan	04/08/23
Member 3- Dr. Sunil K Raghav	04.08.2023
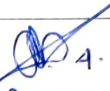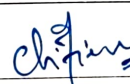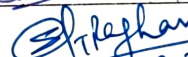
Final approval and acceptance of this thesis is contingent upon the candidate's submission of the final copies of the thesis to HBNI.

I/We hereby certify that I/we have read this thesis prepared under my/our direction and recommend that it may be accepted as fulfilling the thesis requirement.

Date: 04.08.2023

Place: NISER, Jatni

Palok Aich

Signature
Guide

[1] This page is to be included only for final submission after successful completion of viva voce.

STATEMENT BY AUTHOR

This dissertation has been submitted in partial fulfillment of requirements for an advanced degree at Homi Bhabha National Institute (HBNI) and is deposited in the library to be made available to borrowers under rules of the HBNI.

Brief quotations from this dissertation are allowable without special permission, provided that accurate acknowledgement of source is made. Requests for permission for extended quotation from or reproduction of this manuscript in whole or in part may be granted by the Competent Authority of HBNI when in his or her judgment the proposed use of the material is in the interests of scholarship. In all other instances, however, permission must be obtained from the author.

Sohini Mukhopadhyay

DECLARATION

I, hereby declare that the investigation presented in the thesis has been carried out by me. The work is original and has not been submitted earlier as a whole or in part for a degree / diploma at this or any other Institution / University.

Sohini Mukhopadhyay

Sohini Mukhopadhyay

List of Publications arising from the thesis

Journal

a. Published:

For the thesis

Differential colitis susceptibility of Th1- and Th2-biased mice: A multi-omics approach. Mukhopadhyay S, Saha S, Chakraborty S, Prasad P, Ghosh A, Aich P (2022). PLoS ONE 17(3): e0264400. https://doi.org/10.1371/journal.pone.0264400.

A comparative analysis of gut microbial dysbiosis by select antibiotics and DSS to understand the effects of perturbation on the host immunity and metabolism. Mukhopadhyay S, Ray P, Aich P (2022). Life Sciences. https://doi.org/10.1016/j.lfs.2022.121212.

Cost Effective Method for gDNA Isolation from the Cecal Content and High Yield Procedure for RNA Isolation from the Colonic Tissue of Mice. Mukhopadhyay S and Aich P (2022). Bio-protocol 12(15): e4484. DOI: 10.21769/BioProtoc.4484.

A deeper understanding of the gut microbiota of different human races in search of disease specific microbial and metabolic biomarkers. Mukhopadhyay S, Pattnaik T, Aich P. Microenviron Microecol Res. 2022;4(4):18. doi: 10.53388/MMR2022018.

Beyond the thesis

Lactobacillus rhamnosus GG reverses mortality of neonatal mice against Salmonella challenge. Naik A, Pandey U, Mukherjee R, Mukhopadhyay S, Chakraborty S, Ghosh A, Aich P (2019). Toxicology Research. https://doi.org/10.1039/c9tx00006b

b. Communicated:

For the thesis

Differential metabolite and gut microbial compositions might cause C57BL6 mice to exhibit higher stress than BALB/c mice. Mukhopadhyay S, Aich P. (Communicated)

A quantitative assessment of the gut microbial dysbiosis and regulation of host metabolism and immunity in C57BL/6 and BALb/c mice. Mukhopadhyay S, Saha D, Kar A, Aich P. (In preparation)

To distinguish the roles of direct and indirect perturbing agents on gut microbiota in differentially immune biased mice models. Mukhopadhyay S, Saha D, Kar A, Aich P. (In preparation)

Chapters in books and lectures notes

For the thesis

1. Importance of microbial diversity on health: perhaps the best tool to intervene in emerging and continuing diseases. Mukhopadhyay S, Sunaina S, Mohanty T, De A, Das A, Dwivedi I, Aich P. (Accepted)

Conferences

1. Effects of Colitis in Two Genetically Different Mouse Model in Terms of Physiology, Immunity, Metabolism and Gut Microbiota. [a]Sohini Mukhopadhyay and [b]Palok Aich. India, EMBO Symposium on "Human microbiome: Resistanceanddisease."09th–12th

November2019, NIBMG, Kalyani, India. (Presented Poster)

2. #Akkermansia muciniphila- A Potent Upcoming Probiotic to Reduce Colitis Related Disease Severity. [a]Sohini Mukhopadhyay and [b]Palok Aich. A virtual conference on "5th Biennial Conference of PAI and International Symposium". 19th-20th November 2020. NDRI, Karnal, India. (Presented Poster)

3. #Colitis Leads to Neurophysiological Changes and Impede Normal Behaviour Due to Impairment of Gut-Brain Axis. [a]Sohini Mukhopadhyay and [b]Palok Aich. "BIOSPECTRUM 2020 International Conference on Biotechnology & Biological Sciences". 19th- 21st November 2020, UEM, Kolkata, India. (Presented Poster)

4. Close Friendship: Main Culprit Behind the Spreading of Many Infectious Diseases. [a]Sohini Mukhopadhyay and [b]Palok Aich. "A Virtual Conference on: Infectious Disease, Microbiome and Public Health in the Current Scenario." 10th - 11th August 2020. NISER, Odisha, India. (Short talk)

5. Gut microbial perturbation-A pain or pleasure? [a]Sohini Mukhopadhyay and [b]Palok Aich. "HBNI-TM-LS2 Meeting". 16th – 17th February, 2023, SINP, Kolkata, India. (Presented Poster)

#Best Poster Award

[a]Presenting Author

[b]Corresponding Author   *Sohini Mukhopadhyay*

DEDICATIONS

I dedicate my thesis to the person with whom I can never seem to win an argument.

ACKNOWLEDGEMENTS

Summary

The balanced gut microbial composition of the host helps to maintain physiological homeostasis and health. A novel paradigm to understand the role of a microbe on host health is to perturb the gut microbial composition (abundance and diversity). The perturbation can be done in a direct or indirect way. We used antibiotics for direct or Dextran sulfate sodium (DSS) for indirect perturbation of the gut microbiota. All kinds of manipulations in this study was done on rodents model, in C57BL/6 (Th1 biased) and BALB/c (Th2 biased) mice.

Results from the current study revealed that antibiotic treatment had a more immediate effect on the alteration of gut microbial composition and diversity. However, the dysbiotic condition was comparatively long-lasting for the DSS-treated group. The impact of immune dysregulation was also more profound on the DSS-treated group than the antibiotic-treated groups. Moreover, the DSS-treated group of both mice strains showed typical diseased symptoms, which resembles the pathophysiology of human colitis. The current study with DSS treatment also helped us establish a new model system for studying colitis. We utilized a multi-omics approach in the current study to understand the onset and etiology of colitis.

The results revealed that a) DSS could trigger transient inflammatory responses in both C57BL/6 and BALB/c mice at higher dosage of DSS (5%), b) the Th2- bias of BALB/c mice could alleviate inflammation to restore normalcy at reduced (2.5%) DSS dosage. However, C57BL/6 mice maintained severe inflammation even at the reduced (2.5%) DSS dosage. The differential immune bias of the mice used in this study could be the primary reason for different inflammatory responses. The cause of different responses

could be due to differential a) gut barrier function, b) SCFA production, c) psychological stress responses, e.g., anxiety and depressive behavior, and d) an altered gut microbial composition in C57BL/6 and BALB/c mice. Moreover, the multi-omics approach helped us discover a) unique metabolic and microbial markers and b) key metabolic pathways associated with colitis severity. These biomarkers could be used in diagnostics and pathways to intervene and understand disease etiology.

The severity of the disease could be controlled by modifying the gut microbial composition of the host. Antibiotic is one of the most widely used approaches to treat the altered gut microbial profile of colitis patients. We tried to understand how an intervention strategy can be suggested by understanding gut microbial dysbiosis for colitis.

However, reports also suggested that repeated antibiotic exposure is probably the key reason to enhance colitis disease susceptibility.

Observation from the current study concluded that in Th1- biased C57BL/6 mice, antibiotics treatment rescued the DSS treated group from the diseased condition by activating the carbohydrate and nucleotide metabolism pathway, which converted the pro-inflammatory status of the host in an anti-inflammatory condition. On the other hand, early exposure to antibiotics increases disease susceptibility by activating pro-inflammatory lipid and amino acid metabolism pathways.

The scenario was quite different in Th2-biased BALB/c mice. Antibiotic treatment always activated the carbohydrate metabolism pathway, which ultimately provides a therapeutic effect against colitis, whether administered before or after the DSS treatment.

Table of Contents

List of figures with page numbers

Chapter: 1

Chapter: 2

Chapter: 3

Chapter: 4

Chapter: 5

Chapter: 6

List of tables with page numbers

Chapter: 6

Keywords

Gut/ intestinal microbiota; Gut dysbiosis; Physiology; Histopathology; Antibiotics; DSS; Leaky gut; Immune responses; Immune biased mice; Colitis; Cytokine action; Metagenomics; Metabonomics; SCFAs; Transcriptomics; Biomarkers; Glutamate; Stress; Anxiety; Depression; Hormones; Behavior; Therapeutic strategy; Serum metabolites; Cecal metabolite

Abbreviations

AVNM, Ampicillin-Vancomycin-Neomycin-Metronidazole; DSS, Dextran Sulfate Sodium; H & E, Hematoxylin & Eosin; FITC, Fluorescein isothiocyanate; GAPDH, glyceraldehyde-3-phosphate dehydrogenase; Cldn, Claudin; Ocln, Occludin; ZO-1 Zona Occludin-1; TNFα, Tumor Necrosis Factor α; IFNγ, Interferon γ, MPO, Myeloperoxidase; IL, Interleukin; TLR, Toll like receptor; SCFAs, Short chain fatty acids; OGTT, Oral glucose tolerance test; Th1, Type 1 helper; Th2, Type 2 helper; LDA, Linear discriminant analysis, PCA, Principal component analysis, ANOVA, Analysis of variance, IBD, Inflammatory bowel disease; qRT, Quantitative real time; PCR, Polymerase chain reaction; NMR, Nuclear magnetic resonance, gDNA, Genomic DNA, IgA, Immunoglobin A, OUT, Operational Taxonomic Unit; OD, Optical Density; CRP, C-Reactive protein; V-region, Variable region, Mt, Metabolites; M-Mt, Meta-metabolites; KEGG, Kyoto Encyclopedia of Genes and Genomes; OFT, Open field test; EPMT, Elevated plus maze test, FST, Forced swim test, TST, Tail suspension test, CRH, Corticotropin releasing hormone; ACTH, Adrenocorticotropic hormone; F/B ratio, Firmicutes to Bacteroidetes ratio, LPS, Lipopolysaccharide; PBS, Phosphate buffer saline; HPA axis, Hypothalamus–Pituitary–Adrenal gland axis.
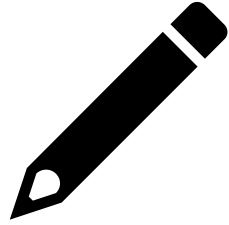
Chapter: 1

General Introduction

&

Review of Literature

1. Introduction

1.1 Health, health care strategies, and the global economy

According to linguists, from the concept of wholeness, the word Health arises. The Old Oxford dictionary suggests the word 'hælth' means 'a state or a thing that is complete in itself.' However, the newer medical health definitions emphasize the capacity to adapt to changing external and internal circumstances. So, the healthy state is an internal feedback system that stabilizes and balances our body's chemistry and creates a niche for the organs to work smoothly and efficiently with each other [1, 2]. Maintaining this homeostasis to maintain good health or to be healthy is imperative.

Health is a product of social determinants, including where one life and works, and health and healthcare inequity continues to be a pressing issue. Mental health issues were prevalent throughout the pandemic due to isolation, redundancies, job losses, and uncertainty across the population. Pressures on healthcare systems affected the mental health of healthcare workers across the globe, leading to significant burnout [3–5].

The current healthcare strategies mainly deal with interventions rather than prevention or elimination of diseases. Prevention is the best intervention strategy for any disease, which leads to a better global health scenario.

With the notion of early detection and to create a proper preventive strategy against various diseases scientists decided to sequence the whole human genome. Understanding the structural and functional information of the genetic material and the downstream biological pathways can accurately solve the mystery behind many such human diseases.

1.2 Human Genome Project: The health economic revolution

Knowing the cause or root of the disease is essential to determine the appropriate preventive measure. To solve the mystery behind many such disorders and choose the copping-up strategy better, the National Institute of Health (NIH) took the initiative in the early 1990s to sequence the entire human genome from multiple cohorts. It was a 15 years program with an investment of 3 billion dollars. Not only the genetic basis of the disorders but the economic output of the Human Genome Project (HGP) was also really noticeable. The economic and functional impacts of 2013, generated by the human genome sequencing, are $965 billion, personal income exceeding $293 billion, and 4.3 million job-years of employment [6–8].

With time researchers started to understand the mystery behind maintaining proper immunity and healthy life balance, not only the underlying fact of the genetic material of the human, but trillions of microbial symbionts of the human also play a significant role in maintaining mainly the immune balance for a healthy life.
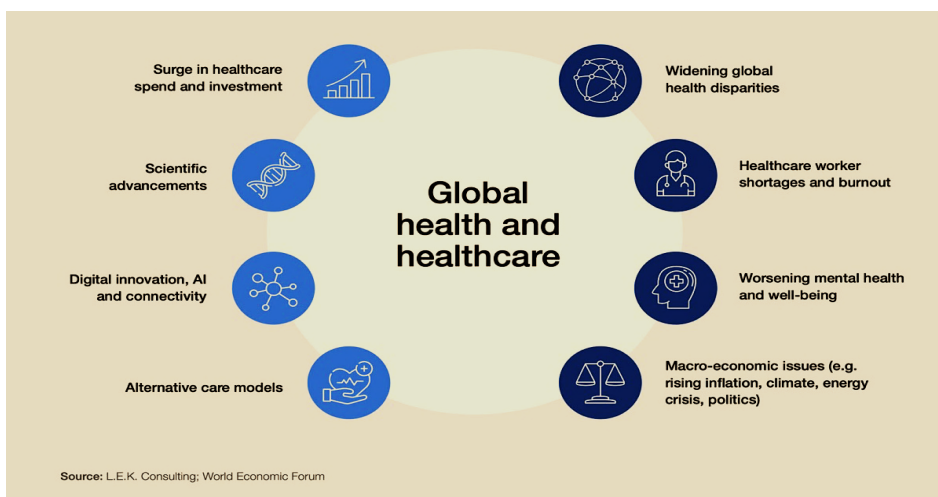
Fig. 1.1: Recent trends in global health and healthcare about health, economic, political, and environmental challenges.

The unique strategy of maintaining immune homeostasis starts following birth and is termed the 'neonatal window of opportunity.' The first significant microbial encounter happens at the time of delivery. The vaginal or the skin microbes of the mother represent the first inoculum to colonize the newborns based on the mode of delivery[9]. These complex communities of microbes, including bacteria, fungi, and viruses, colonize various surfaces of the host body, including skin, intestine, and mucosa, and control most aspects of host physiology, especially immunity. The assemblage of these microorganisms present in a particular anatomic niche with a mutual synergy is known as the 'microbiota' of that particular environment or niche. So, the mode of delivery influences immunological maturation through microbiota development [10].

From an ecological perspective, the commensal microorganisms and their host co-evolved toward mutualistic homeostasis. Such intimate relationships between microbes and the host require the proper functioning of host immunity to prevent commensals from overexploiting the host resources while maintaining immune tolerance to innocuous stimuli [11, 12]. The microbiota plays a fundamental role in the host's immune induction, maturation, and functioning. In consideration, the host evolved its immune system to maintain the symbiotic relationship with the highly diverse and evolving microbiota of various organs. So, in an immune-homeostatic condition, the immune system–microbial union build a protective response against pathogens and activate the regulatory pathways involved in maintaining tolerance to foreign bodies or antigens [13, 14].

Source: L.E.K. Consulting; World Economic Forum

Fig. 1.2: The vision for health and healthcare industries in future

1.3 Human Microbiome Project: The new era of medical science

It is obvious to maintain a healthy life balance; human needs their microbial counterpart. To better understand the concept of "Good Health," NIH extended the Human Genome Project to Human Microbiome Project (HMP) to uncover the astounding diversity of microbial populations encountered in different sites on and within the human body with a budget of $150 million [15].

HMP1

In the first phase of HMP (2012), 242 healthy individuals age 18–40 years were studied, where the microbiome was sampled from five body sites (skin, mouth, nose, colon, and vagina) and characterized for structure and diversity using 16S sequencing and a subset were shotgun sequenced to assess function.

The HMP 1 started with the notion of creating reference datasets of the microbial composition of several body sites in the "normal" condition. Purposefully they avoid using the term "healthy" in case of generating reference data sets because a healthy

microbial composition for particular human races or cohorts is not so healthy for the other races [16].

Research in the current era shows that the microbiome, especially the gut microbial composition of ethnic races, is quite different from the so-called urbanized population due to differential food habits and also for different socio-economic environments. The more primitive lifestyle and food habit of ethnic races, e.g., Hadza Hunter-gatherers of Tanzania, Yanomami Hunter-gatherers of Amazon, Bassa Population of Nigeria, Malawi Tribes of East Africa, Tribes of Botswana, Himalayan Tribes of India, is responsible for colonizing those microbes, which are pathogenic for the urbanized population. For example, the gut microbiota of ethnic populations populated with *Prevotella, Succinovibrio, Dialister, Ruminococcus, and Sutterella* is related to gut inflammation, autoimmune disorders, malnutrition, and various neurological disorders in the urbanized population [17].

The HMP1 described clearly that the concept of healthy individual is not universal.

HMP2

The second phase of HMP (2019) investigated the changes that occur in the microbiome in three conditions: the vaginal microbiome collected during 600 pregnancies, the gut microbiome in 100 individuals with inflammatory bowel disease, and host and microbial responses to dietary changes and infections in 106 individuals with pre-diabetes, whether changes in the microbiome can be related to human health and disease. Because of the short time frame of the HMP, the primary goal of these projects was to establish a correlation between microbiome changes and health/disease rather than demonstrate causation [15, 18].

HMP2 started with the notion it can successfully demonstrate correlation early in the timeline of the following diseases to establish causation in the long run.

Skin:

"Evaluation of the Cutaneous Microbiome in Psoriasis"

Psoriasis, a chronic disease involving the immune system, affecting more than 7.5 million people in the United States, appears on the skin, usually in the form of thick, red, scaly patches. Its cause is unknown. This study examines how changes in the normal cutaneous microbiome may contribute to the disease. The skin microbiome of 75 donors with and without psoriasis was examined at several taxonomic levels. Additionally, the research examined whether the immunosuppressive agents used to treat psoriasis alter the microbiome [15, 18].

Virome:

"The Human Virome in Children and Its Relationship to Febrile Illness"

An estimated 20 million visits annually to hospital emergency departments are because of fever in children with an unknown cause. This project described the human virome of blood, respiratory, and gastrointestinal samples from healthy, febrile, and immunosuppressed children [15, 18].

GI Tract:

"IBDMDB (Inflammatory Bowel Disease Multi'omics Database) Project"

IBD, including Crohn's disease and ulcerative colitis, affects millions of individuals

worldwide, with increasing incidence over the past 50 years or more coinciding with multiple factors such as westernization, urbanization, shifts in dietary patterns, antimicrobial exposure, and many more that could influence host–microbiome homeostasis. The microbiome has long been implicated in IBD, potentially as a causative or risk factor as an explanation for heterogeneity in treatment response or as a novel point of therapeutic intervention.

Therefore, to better characterize mechanisms of host–microbiome dysregulation during disease, the IBDMDB project followed 132 individuals from five clinical centres over the course of one year each as part of HMP2.

The project identified mechanistic associations of several key components that are central to the alterations seen in IBD, highlighting octanoyl carnitine, several lipids and short-chain fatty acids, the taxa *Faecalibacterium*, *Subdoligranulum*, *Roseburia*, *Alistipes*, and *Escherichia*, some at both the metagenomic and metatranscriptomic levels, and host regulators of interleukins [19].

" IPOP (The Integrated Personal 'Omics Project)"

To better understand T2D at its earliest stages, as part of HMP2, the IPOP followed 106 healthy and prediabetic individuals during quarterly periods of health, respiratory viral infection (RVI) and other perturbations over about four years. The important goal of the study was to assess host–microbiome multi-omics study for early detection of potential disease states. These included early detection of T2D, which developed differently among participants and was better detectable with varied assays; for example, haemoglobin A1c, oral glucose tolerance tests, or even continuous glucose monitoring. These results,

together with detailed characterization of glucose dysregulation over time, illustrate the heterogeneity of T2D development. Overall, the data led to microbially linked, clinically actionable health discoveries in a number of diseases in addition to T2D, including metabolic disease, cardiovascular disease, haematological or oncological conditions, and other areas; these signs were often present before symptom onset, demonstrating the power of using big data, including the microbiome, to better manage human health [18, 19].

"The Thrifty Microbiome: The Role of the Gut Microbiome in Obesity in the Amish"

Obesity is a major health problem in the United States. This project directly addresses the causes of obesity by testing the "Thrifty Microbiome Hypothesis," which poses that the gut microbiome plays a key role in human energy homeostasis. The Old Order Amish population was chosen for this study because it is genetically homogeneous and has already been characterized for many traits [18].

Vagina:

"The Microbial Ecology of Bacterial Vaginosis: A High-Resolution Longitudinal Metagenomic Analysis"

Bacterial vaginosis (BV) arises in women when the vaginal microbiome is disrupted. This project tested the hypothesis that vaginal microbiome dynamics and activities are indicators of the risk of BV. Researchers studied the metagenome and metatranscriptome in combination with metabolomics to assess the diversity of microbial species, genes, and

functions of the microbiome associated with BV [18, 19].

"The MOMS PI (Pregnancy Initiative) Project"

As part of HMP2, MOMS PI project characterized the microbiomes of pregnant women to gauge their effects on risk of Preterm birth (PTB). PTB have devastating consequences for newborn babies, including death and long-term disability. In the United States, approximately 10% of births are premature, and the incidence is even greater in lower-resource countries.

The MOMS-PI project analysed 12,039 samples from 597 pregnancies to investigate the dynamics of the microbiome and its interactions with the host during pregnancy leading to PTB [19].

Cancer of the GI Tract:

"Foregut Microbiome in Development of Esophageal Adenocarcinoma"

Esophageal adenocarcinoma (EA), the type of cancer linked to heartburn due to gastroesophageal reflux diseases (GERD), is the fastest-rising malignancy in the United States. This study focused on finding a significant association between the changes in the microbiome during the development of EA, which can be used early diagnosis and treatment of the disease, also described the possible strategies that convert the disease related microbiome to a healthy microbiome [18].

1.4 Gut microbiota, the neglected organ: perhaps the most important for maintaining the host's immune balance

HMP2 concluded that among the various microbial niche of the body, the most important and acclaimed microbial community is the intestinal or gut microbiota. Gut microflora is a positive health asset that crucially influences the structural and functional development of mucosal immunity and metabolism but is the most "neglected or forgotten organ [20, 21]."

The gastrointestinal tract or gut, with its epithelial barrier containing a total area of 400 m^2, is a complex, open, and integrated ecosystem with the highest exposure to the external environment. The gut contains at least 10^{14} microorganisms belonging to 12 different phyla and >2,000 species. The gut-associated microbiota contains 150- to 500-fold more genes than the human DNA. It is generally accepted that 1000 days after birth is the most critical timeframe for microbial colonization and associated immune developments. Any modulation in this phase can damage child growth, development, and immune maturation [22, 23]. The mode of delivery and the components of breast milk influence immunological maturation through microbial development. There are two testable immune maturation hypotheses: 'the neonatal window of opportunity and 'layered immunity.' The concept of the 'neonatal window of opportunity' postulates a non-redundant priming period of the innate and adaptive immune system after birth that sets the stage for immune homeostasis and subsequent host-microbial interaction. On the other hand, 'layered immunity' suggests that the maturation of the innate and adaptive immune system occurs in subsequent phases that depend on each other to establish a mature, homeostatic but vigilant immune system [24–26].

1.5 The "Superorganism": The most crucial player in maintaining the host's physiology and metabolism

The large diversity, stability, resilience, and symbiotic interactions of the gut microbiota with the host can act as a "superorganism" that performs the host's most vital immune and metabolic functions. It is paradoxical to note that gut microbiota functions are highly preserved among individuals. In contrast, each individual's gut microbiota is characterized by a specific combination of bacterial species due to inter-individual and intra-individual variations throughout human life [23].

The conventionally healthy gut microbiota, specifically gut bacteria of a healthy human adult, comprises six significant phyla, Firmicutes, Bacteroidetes, Actinobacteria, Proteobacteria, Fusobacteria, and Verrucomicrobia, with the two phyla Firmicutes and Bacteroidetes representing 90% of gut microbiota. The Firmicutes phylum comprises more than 200 genera, such as *Lactobacillus*, *Bacillus*, *Clostridium*, *Enterococcus,* and *Ruminicoccus,* while the *Clostridium* genus represents 95% of the Firmicutes phyla. Bacteroidetes consist of predominant genera such as *Bacteroides* and *Prevotella*. The Actinobacteria phylum is proportionally less abundant and mainly represented by the *Bifidobacterium* genus [24, 25].

The human gut not only contains a vast majority of the microbes but also harbors the body's largest pool of immune cells. The host immune system also profoundly affects the composition of the gut microbiota. Therefore, gut cells are continually exposed to a vast number of microbial antigens and metabolites but maintain perfect harmony and symbiosis with gut commensals [27].

In addition to immune development, the metabolites produced by the gut microbiota also

play a pivotal role in maintaining health homeostasis. Gut microbes produce numerous essential metabolites, such as folate, indoles, secondary bile acids, trimethylamine-N-oxide (TMAO), neurotransmitters (e.g., serotonin, gamma amino butyric acid), and also short-chain fatty acids (SCFAs). Most of the metabolites show anti-inflammatory activity, act as the primary energy source for gut epithelial cells, and some of them control the stress responses of the host [28–30].

So not only the gut microbes but the composition of gut microbiota-derived metabolites also play a crucial role in maintaining the healthy life balance of the human.

The regulatory effect of gut microflora is not limited to immunity or the metabolism of the host. Gut microbiota influences a wide range of other host processes and characteristics that were thought to depend solely on the genetic program of the host, including organ development and morphogenesis, cell proliferation, bone mass, adiposity, behavior, and stress responses.

The development of the mammalian gut is itself dependent on the composition of its microflora. Researchers have found that germ-free mice have comparatively larger cecum than normal mice. The overall intestinal surface area in germ-free mice is also reduced and impaired in brush border differentiation, so have reduced villus thickness, reduced cell regeneration, and a longer cell cycle time. The number of serotonin-producing enterochromaffin cells is also higher in the gut of germ-free mice [29, 31].

Gut microorganisms also modulate epithelial permeability in the gastrointestinal tract. For example, Gram-negative bacterium *Bacteroides thetaiotaomicron* increases the resistance of the gut to injury by inducing the expression of SPRR2A, several *Lactobacillus* strains rigidify tight junctions between epithelial cells, improve tight junction function and

reduce apoptosis rates, thus enhancing barrier integrity and facilitating wound repair after injury.

Microorganisms also modify tissue homeostasis by balancing cell renewal and death. For example, germ-free mice have reduced epithelial cell turnover in the small intestine, thus reducing IEC proliferation, crypt-to-tip cellular migration, and apoptosis [30, 32, 33].

Imbalanced cellular homeostasis can ultimately result in the development of cancer. Microorganisms could influence carcinogenesis by modulating inflammation. An increased bacterial load was detected in colonic biopsies from patients with colorectal cancer or colonic adenomas. Decreased microbial diversity is associated with obesity and inflammatory bowel disease [32, 33].

Microbes also control the bone remodeling and bone mineral density of the host. Researchers have shown that germ-free mice have a higher bone mineral density than conventional mice. T cell function, serotonin levels, and cytokine profiles could contribute to microbial modulation of bone homeostasis and a potent cause of osteoporosis [34, 35].

Gut microflora modulates several brain-derived neurotrophic factors and noradrenaline levels in different brain areas. Germ-free mice display an altered stress response, dysregulation of the hypothalamus–pituitary–adrenal gland axis, and decreased inflammatory pain perception. The neurological defects in germ-free mice can be resolved only by colonizing neonates with microbes, indicating a critical time window in which microbially induced maturation of the nervous system occurs [36–38].

The versatile role of gut microbiota is the major cause of grabbing more attention from researchers.

1.6 Dysbiosis, which deals with diseases

Dysbiosis mainly deals with the imbalance of the composition and metabolic capacity of the gut microflora. In the preceding paragraph, we mentioned a plethora of factors, e.g., genetic, epigenetic, environmental factors, lifestyle control, age, and uses of drugs, that disrupt the dynamicity of the gut microbial compositions and derange the host's homeostasis. The dysbiosis process can be categorized into three types: 1) Loss of beneficial organisms, 2) Excessive growth of potentially harmful organisms, and 3) Loss of overall microbial diversity. The types of dysbiosis are not mutually exclusive and can coincide often. Dysbiosis mainly deals with a wide range of diseases, including inflammatory bowel disease (IBD), obesity, allergic disorders, Type 1 diabetes mellitus, Type 2 diabetes, autism, obesity, colorectal cancer, liver and kidney diseases, and many more [39].

The dysbiotic or diseased gut microbiome concept is not concrete and depends upon various physiological and environmental factors. A very gross overview of dysbiosis has been described as the reduction in the proportion of anaerobes that are typically abundant in health and an increased proportion of facultative anaerobes, including Proteobacteria and Bacilli. On the other hand, such low-diversity, disease-associated microbiomes compositionally resemble the gut microbiome of infants (younger than ~2 years of age). It may be surprising that the gut microbiome of a very sick adult would resemble that of a perfectly healthy infant; this observation may be explained by the concept of 'secondary succession' where a dramatic disturbance that wipes out a complex community result in the observation of similar early succession, or 'pioneer' species [39, 40]. The low diversity, facultative anaerobe-dominated community observed in the adult gut thus may

be considered a bioindicator of disturbance with age-dependent implications for health. So, this particular type of dysbiosis may be common in many disease settings, an essential factor in understanding the compositional details of gut microflora in various diseased conditions for a better life. A detailed study about the factors and associated diseases is summarized in Fig. 1.3.

Table 1.1. *Bacterial families that dominate the adult human gut in health and during dysbiosis*

Healthy	Dysbiosis
Firmicutes	Firmicutes
Clostridia	Bacilli
Clostridiales	Lactobacillales
Lachnospiraceae (Clostridia XIVa)	Lactobacillaceae
Ruminococcaceae (Clostridia IV)	Streptococcaceae
	Enterococcaceae
Bacteroidetes	Proteobacteria
Bacteroidia	Gammaproteobacteria
Bacteroidales	Enterobacteriales
Bacteroidaceae	Enterobacteraceae
Prevotellaceae	

1.7 Composition of gut microflora and their importance in relation to various diseases

Intestinal dysbiosis typically aids in the analysis of the loss of microbial diversity (LOMD). LOMD, which is frequently present in diseased states, could be the outcome of an imbalance between prey and predators.

Intestinal dysbiosis starts with a dramatic increase in the phylum Proteobacteria, which acts as a biomarker for an unstable microbial ecology because a healthy human gut flora contains few members of this phylum [41]. While analyzing current clinical studies, a significant increase in Proteobacteria phylum is noticed in neurodegenerative disease (NDD), cardiovascular disease (CVD), Metabolic Disease (MD), Gastrointestinal Disease, Uremic and Oncological disease. Epilepsy has experienced the greatest growth among NDDs (a 23.9% increase), followed by Alzheimer's disease (14.82% increase) [42, 43]. Patients with MDs such as obesity and diabetes, show a two-fold increase in abundance, while chronic renal disease patients showed a more significant than a two-fold increase in CKD [44–46].
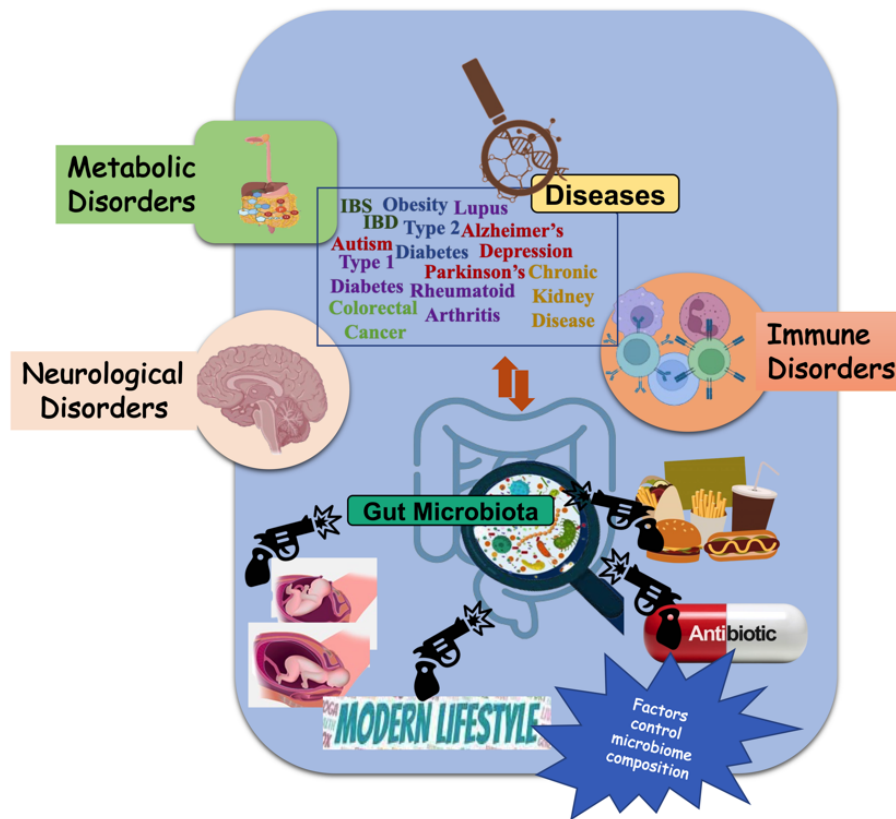
Fig. 1.3: Factors affecting gut microbial composition lead to several health disorders.

Crohn's disease (CD) and ulcerative colitis (UC), two types of IBD, however, showed distinct results. Proteobacteria abundance increased by 30.97% in CD whereas it decreased by 8.19% in UC [47]. Furthermore, Phylum is less prevalent in lung cancer patients compared to controls, who have 34.75% and 24.83% of it, respectively [48]. Acute myocardial infarction (AMI) saw a very slight increase, whereas other CVDs such as heart failure, coronary artery disease, and hypertension, showed a significant increase [49–53]. This phylum contains the well-known bacterium *Heliobacter pylori*, which has a strong link to NDDs, atherosclerosis, and colorectal cancer [54].

The ability of the Bacteroidetes phylum to adapt to the stressful gut environment has made it a successful competitor among all microorganisms. However, because it produces some by-products that are both harmful and useful, like propionate, this phylum can have an impact on the host that is both positive and detrimental. The diverse individuals in this phylum have pro- and anti-inflammatory effects [55]. Phylum quantity and composition vary greatly between different disease kinds. An intriguing finding was made regarding the prevalence of metabolic diseases: Type 2 diabetes did not significantly affect the prevalence of the phylum, which grew significantly in obese persons [44, 56]. However, the phylum significantly dropped (almost 12.6%) in patients with both Type 2 diabetes and obesity [57].

The phylum Firmicutes and the Bacteroidetes both control the gut ecology. Obesity increased the firmicutes/Bacteroidetes ratio, whereas inflammatory bowel disease, pancreatic cancer, and Alzheimer's disease decreased it [58–60]. In comparison to CD, firmicutes are more enhanced in UC [47]. Obesity was shown to have doubled, but it had slightly decreased in T2D individuals [44, 56]. The prevalence of both phyla declines in several disorders, such as epilepsy, end-stage renal disease (ESRD), and chronic heart failure [42, 50, 59]. Researchers marked reduction in Firmicutes was observed in Epilepsy, followed by chronic kidney disease [42, 46]. Oncogenic evidence indicates that this phylum has increased in colorectal cancer (CRC) and kidney cancer (KC) but that there has been no discernible change in endometrial cancer (EC) [61–63]. But more genus and species levels research will help us understand better.

Actinobacteria, one of the four major phyla, are the least numerous but significantly

impact gut homeostasis. This phylum has been the subject of numerous microbiological investigations and has been linked to a several developing illnesses. Members of this phylum are even recommended as probiotics and in treatment methods [64]. Two-fold increases in abundance were found in lung cancer and two-fold decreases in CRC while analyzing its composition in both healthy and pathological conditions [61, 65]. Among CVDs, CAD experienced a tremendous increase in abundance, followed by HF and MI [49–51]. Among All of the NDDs, a significant rise in Phylum was evident in Attention-Deficit/Hyperactivity Disorder (ADHD), while Epilepsy showed a sharp drop [42, 66]. Patients with chronic kidney disease did not show substantial variance [46]. We have tried to summarize the Phylum level abundance in different classes of disease in Fig. 1.4 in the form of Heat Map for a better understanding. The heat map shows differential distribution of the phyla for various diseases. Studies are being done to understand further at various levels of taxa using next generation sequencing methodologies.
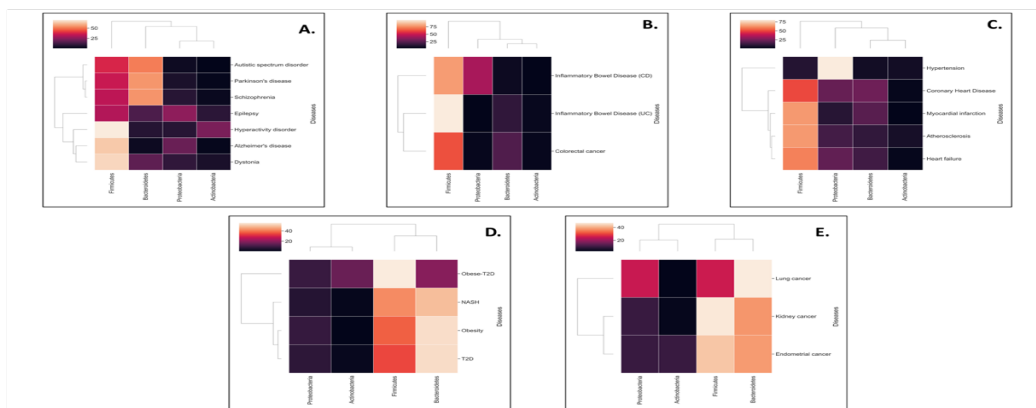
Fig. 1.4: Heat Plot of phylum abundance of different Disease Classes.

A. Neurodegenerative Disease, B. Gastro-intestinal Disease, C. Cardiovascular Disease, D. Metabolic Disease, E. Oncogenic Disease.

1.8 The molecular basis of diseases in connection with altered metagenome and metabolome

High-throughput microbial genomic sequencing advancements have considerably shed light on the alterations in the gut microbial composition and pathophysiological progression of diseases [67, 68].

The abundance of a particular microbial species might be conserved for various diseases. In contrast, some diseases are associated with the abundance of unique species and their microbial by-products or meta-metabolites. Intercommunication between the host and microbiota is made possible via metabolites and meta-metabolites. At the level of metabolome, there are two types of metabolites

Host-derived metabolites (metabolites): They are produced by the host but can be functionally controlled through co-metabolism by mutualistic machinery of both host and microbes.

Microbiota- derived metabolites (Meta-metabolites): Microbiota-derived metabolites are functionally derived and controlled by the microbial species. Talking about gut-microbial based metabolites are generally collected from fecal metabolites.

To understand the conservation and uniqueness of gut microbiome and microbiota derived metabolites across various diseases, it is necessary to study them in detail by categorizing it into different sub categories. We categorized them into 5-6 sub categories to understand the mechanism of various diseases in detail.

1.8.1 Gastrointestinal diseases

Besides colorectal cancer, gut microbiota and microbial metabolites are the key regulators of many gastrointestinal disorders. To date, it is the most explored area where the multi-

omics approaches have been used in case of disease detection, progression, and remedy [69].

Inflammatory bowel disease (IBD), which includes Crohn's disease (CD) and ulcerative colitis (UC), and celiac irritable bowel syndrome (IBS) is the most commonly occurring and most studied area of gastrointestinal disorders [70].

Case-control studies revealed that inflammatory conditions of CD suppress the growth of short-chain fatty acids (SCFAs) producing genera, *Faecalibacterium, Clostridium clustersIV and XIVb, Roseburia*, and *Ruminococcus* [70]. IBD severity is also related to differential bile acid production. Primary and secondary bile acids like taurocholic acid, cholic acid, taurochenodeoxycholic acid, glycol-deoxycholic acid, glycol-lithocholic acid, and tauro-lithocholic acid are increased, while lithocholic acid, deoxycholic acid, glycol-deoxycholic acid, glycol-lithocholic acid, and glycol-lithocholic acid are decreased in patients with IBD. Genera *Bifidobacterium* and *Clostridium clusters IV* and *XIVb* are related to altered bile acid productions.

Chronic inflammation associated with IBD also upregulates the L-arginine/nitric oxide pathway production, leading to the neoplastic transformation of the colon architecture [71].

1.8.2 Metabolic diseases

The altered and perturbed metabolic homeostasis is the major factor for another group of diseases, termed metabolic disorder. Altered gut microbiota is the major factor for this altered metabolic homeostasis. Obesity, type-2 diabetes, and Nonalcoholic fatty liver disease (NAFLD) are included under the metabolic disease umbrella.

Researchers have found that the metabolite tryptophan is the most crucial metabolite related to any kind of metabolic disorder. Tryptophan is one of the evident amino acids for bacterial catabolic action, and undergoes direct conversion into the routes that lead to kynurenine and serotonin. The kynurenine pathway yields the compound nicotinamide adenine dinucleotide (NAD+) and a number of metabolic intermediates generally referred to as "kynurenines". Kynurenine pathway intermediates dramatically reduce insulin production, excretion, and signaling [72].

Increased levels of branched-chain amino acids (BCAAs) were also observed in the blood of insulin-resistant people. The primary gut microbial species responsible for the connection between the production of BCAAs and insulin resistance were found to be *Prevotella copri* and *Bacteroides vulgatus* [73, 74].

In the case of obesity researchers have found significantly lower levels of *Bacteroides thetaiotaomicron*, a commensal that ferments glutamate.

Further analysis of global public data sets also suggests that genera *Lactobacillus* and *Provotella* are differentially abundant in all highly occurring metabolic diseases. *Streptococcus, Faecalibacterium, and Coprococcus* are also quite common in the gut microbiota of most metabolic diseases.

1.8.3 Neurological diseases

The control of several homeostatic systems inside the body is influenced by the brain and gut microbiota, the second brain of the human body. So, it is obvious that any disbalance in gut microbial homeostasis will lead to various neuronal dysfunction. The dysbiotic microbiota in the diseased condition portray an imbalance in the composition of the

genera of *Bifidobacterium* (in Autism, Schizophrenia, Epilepsy, and Parkinson's), *Dialister* (in Alzheimer's, Parkinson's, Schizophrenia), *Blautia* (in Epilepsy, Alzheimer's, Parkinson's), *Oscillospira* (in Parkinson's, Autism, Alzheimer's), *Bacteroides* (in Parkinson's, Epilepsy, Autism), *Lactobacillus* (in Parkinson's, Schizophrenia, Autism) and *Veillonella* (in Parkinson's, Schizophrenia, Autism). Most importantly, after reanalyzing the public dataset, we found the alteration in the genus Akkermensia is conserved in almost all neurological diseases, albeit in different abundances. (*0% in Autism, 5.2% in Alzheimer's, 4.85% in Parkinson's, 0.6% in Schizophrenia*, *8.7% in Epilepsy*). This data suggests that imbalance in the abundance of the *Akkermensia* genus is the most critical factor for the commonly occurring neuro disorders [75].

Not only the perturbed gut microbiota, recent clinico-biological multi-omics studies showed that host and microbiota derived metabolites also play a critical role in determining the disease severity. Previous reports revealed long-chain saturated fatty acids (17-octadecanoic-acid and cis-9,10- epoxystearic acid), sphingolipids (ceramide and dehydrophytosphingosine) were significantly high in the feces of Parkinson's patients.

Similarly, in the case of Alzheimer's disease, patients had significantly lower serum concentrations of primary bile acids (cholic acid) and higher concentrations of the secondary bile acids, deoxycholic acid, as well as its glycine and taurine conjugated forms [76].

1.9 Prolonged diseases exposure, altered behavior, and stress responses

In the previous section, we discussed the involvement of the gut microbiota and microbes-derived metabolites in neurological dysfunction. Altered neurological functions

are also highly correlated with the altered behavioral responses of an individual. The altered microbial and metabolic profile of the host due to some other diseases could be a potent factor for the activation of the stress center of the brain. Individual with prolonged illness also undergoes a variety of physiological problems, including pain and functional limitations, which are thought to be potent stressors for activating stress responses. So, the pathophysiology of the diseases acts as a potent stressor for patients [77].

The "cytokine theory of depression" deals with how proinflammatory cytokines, acting as neuromodulators, mediate the behavioral and neurochemical features of depression in case of chronic illness. The cytokine-induced hyperactivity of the HPA axis causes interference in the negative feedback of circulating corticosteroids. This dysregulation may also lower the availability of tryptophan by reducing levels of its precursor, 5-hydoxy-tryptamine (5-HT), an essential component of neuro-cellular function [78].

In addition, increased depressive affect is also associated with the production of various inflammatory cytokines, including IL-6 and C-reactive protein, in some studies. Inflammation is known to play a key role in the generation and progression of problems like atherosclerosis. Depression is also associated with enhanced platelet aggregation via alterations in serotonin and catecholamine pathways.

Levels of another pro-inflammatory cytokine, TNF-α, are associated with cachexia, and cortisol, a stress hormone associated with depression and dysregulated carbohydrate metabolism of diseased individuals [79–81].

The prolonged, painful treatment interventions are also potent enough to cause behavioral changes and activate the stress centre of the patients.

1.10 Predictive microbial and metabolic biomarkers of diseases

In the current era of microbiome research, it is quite established that gut microbiome and microbes derived metabolites are the two crucial factors that control various diseased conditions. Every disease has unique microbial and metabolic conditions that uniquely control the host's physiology, creating differences from other diseases. So, the enrichment of the disease-specific signature microbiota or metabolites in the host system can be used as a unique marker for the diagnosis and prognosis of the particular disease. This could be no invasive cost-effective options for current diagnosis method. We tried to predict some microbial and metabolic biomarkers from the already available public dataset for inflammatory, metabolic and neurological disorders.

1.10.1 Predicted microbes-metabolites biomarkers for IBD

Inflammatory Bowel Disease, most commonly known as IBD, is a disease of the human gastrointestinal tract. Dysbiosis of gut microbiota ultimately activates flares of inflammatory reactions in the human gut. Based on the localization of the inflammation in the gut, IBD can be categorized into Crohn's Disease or CD, where the inflammation use to occur in the upper GI tract, and Ulcerative Colitis, or UC is the inflammation of mainly the colon and some other portion of the lower GI tract [82–84]. In this context, it is very important to understand the interactions between the microbiome and metabolites of the host that ultimately causes differential inflammatory outcomes at different parts of the GI tract. We used the publicly available datasets to understand the relationship between microbiome and metabolome in IBD disease progression.

The Spearman correlation analysis of microbiome and metabolome data revealed a strong

correlation between 15 different bacterial species with 14 discriminant metabolites in CD patients. 7 different species, *Faecalibacterium prausnitzii, Oscillospira eae, Oscillospira guillermondii, Anaerobranca zavarzinii, Veillonella montpellierensis, Ruminococcus albus* and *Alkaliphilus crotonatoxidans* belonging to the Firmicutes phylum, 4 species, *Desulphonauticus Autotrophicus, Serratia entomophila, Escherichia albertii, and Candidatus Endobugula sertula* to the Proteobacteria phylum, another 3 species, *Dysgonomonas wimpennyi, Rikenella microfusu*s, and *Parabacteroides johnsonii* to the Bacteroidetes phylum and finally only one, *Bifidobacterium adolescentis* to the Actinobacteria phylum showed a strong association with different metabolites level of CD patients. More specifically, a strong correlation was seen between species *Oscillospira eae* with the metabolites 5β-coprostanol, 3-methyladipic acid, citric acid, methylamine, 2-hydroxy-3-methylvaleric acid, PC (16:0/3:1) and urobilin; species *Oscillospira guillermondii* showed correlation with 5β-coprostanol, methylamine, and PC (16:0/3:1); species *Desulphonauticus autotrophicus* was associated with 5β-coprostanol, 3-methyladipic acid, citric acid, methylamine, and PC (16:0/3:1) putrescine and cadaverine production and finally, the abundance of *Faecalibacterium prausnitzii* was correlated with the metabolite phenylethylamine (Fig. 1.5A, B) [85–87].

Evaluating the bacterial species and metabolites relationship in UC patients revealed strong correlations between *Pedobacter kwangyangensisvs* and *Dysgonomonas wimpennyi* with 3-methyladipic acid, 5ß-Coprostanol, 2-hydroxy-3-methylvaleric acid, citric acid, and methylamine and TMAO. 3-methyladipic acid and production also correlated with the species *Akkermansia muciniphila* and species *Alkaliphilus crotonatoxidans,* respectively (Fig. 1.5A, C) [85–87].
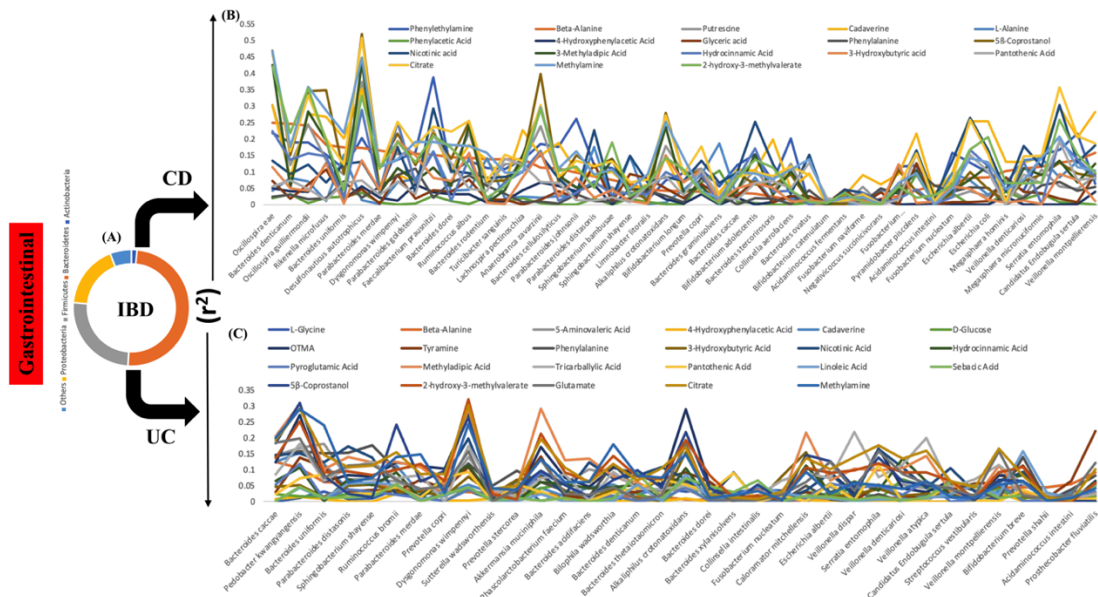
Fig. 1.5: Global correlation of the altered microbiome and metabolomic profile of IBD.

Here we depicted the altered gut microbial and metabolic changes due to IBD. We tried to establish a correlation between disease related microbial and metabolic composition to get an idea which particular genus is responsible for what kind of metabolic changes. Panel(A) demonstrates the IBD-related gut microbial changes of the host at the phylum level, and the also the correlation (Spearman) between altered gut microbiota and altered metabolism of the host due to Crohn's disease (CD) (B) and Ulcerative colitis (UC) (C).

1.10.2 Predicted microbes-metabolite biomarkers for the metabolic disorders

Obesity

Obesity or overweight is a global problem of the current century. The situation is like

that; 1 in every 5 persons is considered obese in the present scenario.

Reanalysis of various public data set showed that genera *Coprococcus, Desulfovibrio, and Ruminoclostridium* was strongly correlated with butyrate and trimethylamine productions, *Erysipelotrichaceae* and *Butyricimonas* were associated with arabinose production, and *Ruminococcaceae* and *Erysipelotrichaceae* were related with galactose production (Fig. 1.6A, C) [88, 89]. The strong association between the mentioned genera and metabolites with obesity provides us enough confidence to use them as promising biomarkers for the disease.

Type 2 Diabetes (T2D)

Type 2 Diabetes is another global burden for the healthcare system. This is also a metabolic disorder and is highly associated with the occurrence of obesity.

Available evidence showed that the gut microbiota and metabolic content were significantly altered in T2D patients. The short chain fatty acids (SCFAs) and some SCFA-producing bacteria were also remarkably changed, such as diacylglycerol.

Genera *Prevotella* and *Prevotellaceae* UCG-003 in Bacteroidetes and genera *Streptococcus*, *Weissella*, *Veillonella*, *Pseudobutyrivibrio* in Firmicutes were correlated with metabolites linolenic acid and LPC (18:2). Families Lachnospiraceae and Ruminococcaceae were associated with the production of acetate and LPC (18:2). On the other hand, the concentrations of bile acids (cholic acid, glycoursodeoxycholic acid, chenodeoxyglycocholate, and glycocholic acid) and SCFAs (acetate, propionate, and butyrate) were correlated with families of Lachnospiraceae, Ruminococcaceae, Planococcaceae, and Prevotellaceae, etc. Genera of Lachnospiraceae and Ruminococcaceae families were also correlated with the production of lipids and bile

acids (Fig. 1.6B, D) [90–92]. So the mentioned microbes and metabolites are suitable resources and promising biomarkers in the future for the detection of T2D.
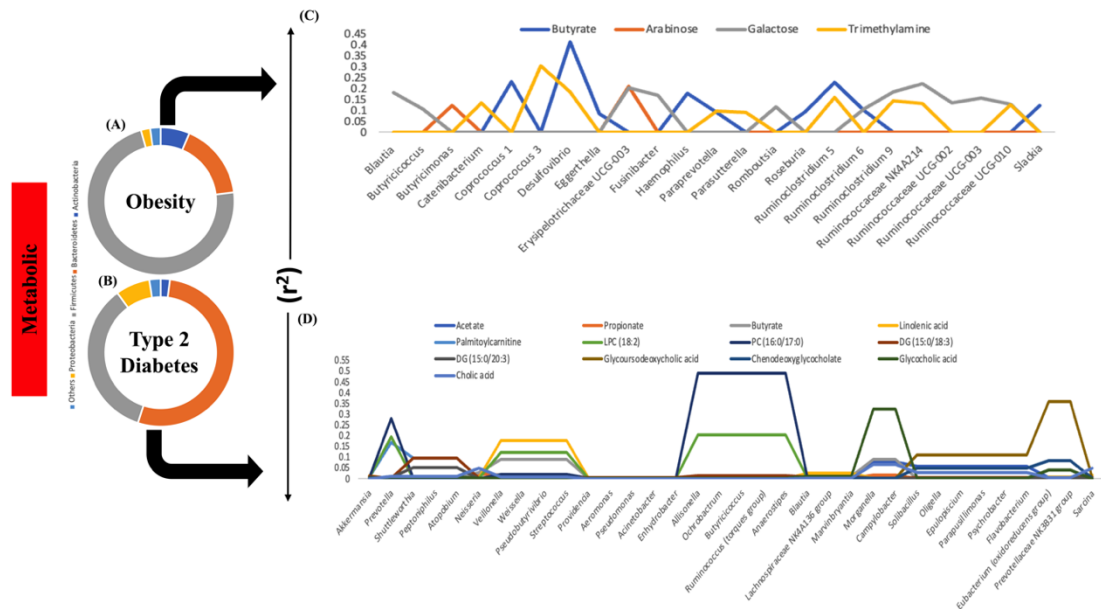
Fig. 1.6: Global correlation of the altered microbiome and metabolomic profile of Obesity and Type 2 Diabetes.

Obesity and Type 2 Diabetes related microbial and metabolic changes are demonstrated here. Correlation study explained the specific genus responsible for specific disease related metabolic changes. Changes in the gut microbial composition of obese (A) and diabetic (B) hosts in phylum level and the correlation (Spearman) between altered gut microbiota and altered metabolism of the host due to Obesity (C) and Type 2 Diabetes (D).

1.10.3 Predicted microbes-metabolites biomarkers for neuropsychiatric disorder-Autism

Available reports suggested that 6 microbial genera of the gut and 16 different

metabolites are strongly associated with the autism disease progression. The abundance of the microbial genera and metabolites were also very nicely correlated with each other. Data suggested that the genus *Lactobacilli* was correlated with the production of the metabolites fumarate, acetate, leucine, ethanol, isoleucine, phenylalanine, alanine, *Akkermansia* was associated with leucine, methionine, alanine, ethanol production, *Bifidobacteria* showed correlation with metabolites acetate, leucine, isoleucine, phenylalanine, orotate, alanine, tyrosine, uridine, methionine, 1,3-dihydroxyacetone, *Bacteroides* was responsible for the production of leucine, isoleucine, alanine, fucose, uridine, the abundance of *Prevotella* was correlated with propionate, fumarate, N-methylhydantoin and finally genera *Suttrella* had a strong association with metabolites acetate, leucine, alanine, fucose, isoleucine, phenylalanine, tyrosine, aspartate, fucose, ethanol (Fig. 1.6A, C) [93]. So, these 6 genera and their associated 16 metabolites could act as promising biomarkers for the diagnosis of autism at an early stage.

1.10.4 Predicted microbes-metabolites biomarkers for inflammatory disorder-Lupus

Systemic lupus erythematosus (SLE) or Lupus is a multifactorial autoimmune disease that can cause damage to many organs and has a global prevalence.

Previous correlation data of gut microbiome at genus level and altered lipids concentrations showed a strong association with the lupus pathogenicity. The majority of the bacteria that were correlated with altered lipid levels belong to the Firmicutes phylum. In this phylum, *Lactobacillales,* and *Erysipelotrichales, Clostridiales* are the taxa accounting for the effective correlations with disease progressions. Other phyla, including

Bacteroidetes, Actinobacteria, Fusobacteria, Proteobacteria, and Tenericutes, were also correlated to the lipids. *Proteobacteria,* which contains various pathogens, including *Escherichia- Shigella,* and *Sutterella,* were also related to altered lipid levels. The lipids, significantly correlated with the disease were mainly bile acids (deoxycholic acid, glycocholic acid, isohyodeoxycholic acid) and arachidonic acid (Fig. 1.6B, D) [94]. Altered lipid metabolism and a high abundance of the mentioned genera could be used as suitable diagnostics tools in the coming days.
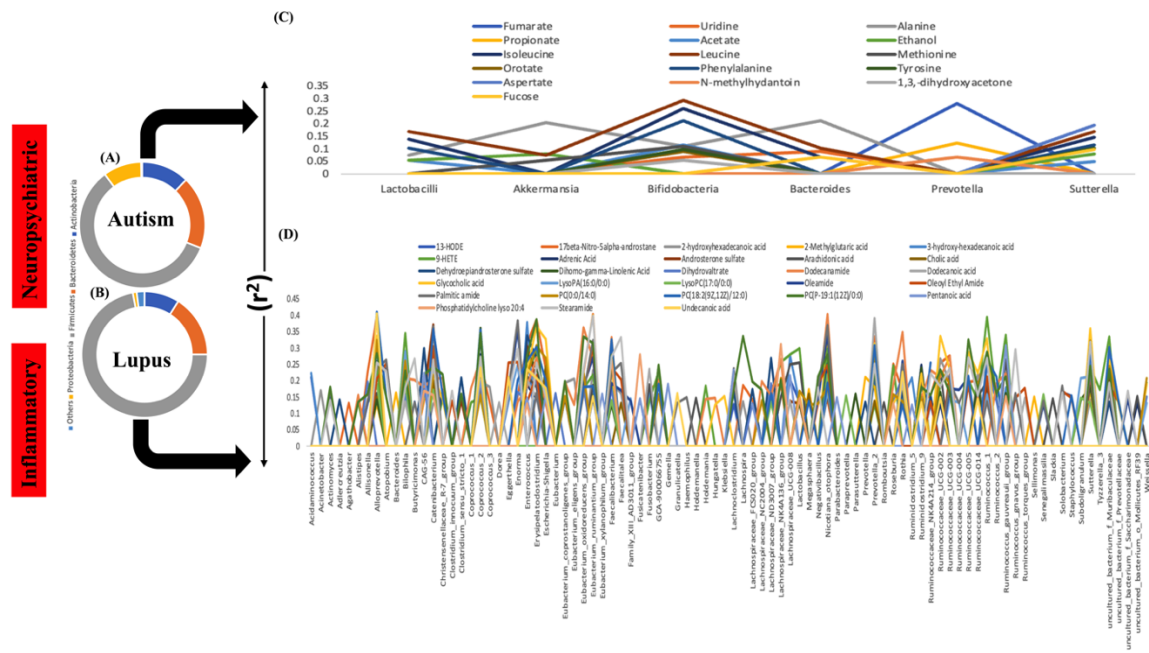
Fig. 1.7: Global correlation of the altered microbiome and metabolomic profile of Autism and Lupus.

Autism and Lupus related microbial and metabolic changes are demonstrated here. The correlation study explained the specific genus responsible for specific disease-related metabolic changes. Phylum level composition of altered gut microbiota of Autism (A) and Lupus (B) affected host and the correlation (Spearman) between altered gut microbiota

and altered metabolism of the host due to Autism (C) and Lupus (D).

1.11 Predictive μ- ∞ diagnosis method of diseases: probably the ultimate future of non-invasive & robust diagnosis strategy

Current advancements in research, availability of high throughput instruments, and robust data analysis tools push us to think to diagnose diseases using systemic approaches. The era of multi-omics approaches is currently trying to explore novel diagnostic targets and disease-specific markers using metagenomics, metabolomics, transcriptomics, and proteomics. Transcriptomics and proteomics data have the potential to detect specific genes or protein functions for a particular disease [95]. These approaches never address the host's overall physiological processes and several other downstream regulatory mechanisms. So, the best novel and non-invasive diagnostic targets and disease-specific markers could be the characterization and finding of the link between gut microbiota and host metabolism and trying to understand the functional alterations in the pathophysiology of different diseases.

Compared to other "omics," the power of metagenomic and metabolomic profiles is that these integrate the effects of gene regulation, post-transcriptional regulation, and pathway interactions. This downstream synthesis of diverse signals from microbes and metabolites ultimately reflects a meaningful physiological phenotype [96]. In addition, changes in gut microbial and metabolic abundance and diversity are induced by exogenous factors, such as environmental and dietary factors that do not affect the genome [97–100]. So, the μ- ∞ diagnosis method of diseases is "the non-biased identification and quantification of the

biological system." The accuracy and the robustness of the technology and the concept is the firm reason for researchers to consider it the future of the diagnosis process.

1.12 Various strategies of therapeutic interventions in search of a disease-free life

As the gut microbiota affects the healthy physiology of the host, it is the need of the hour to extract the therapeutic potentials of the gut microbiota, especially when drug resistance for most diseases is prevailing at its peak. Recovering the homeostasis among the gut microbial composition can help restore the body's homeostasis. This can be done in two ways: one by directly targeting the microbial population and another by inducing products that indirectly promote or effects the growth of commensal bacteria and carry out downstream functions at the cellular level, which are performed by the beneficial gut microbiota.

The oldest therapy which indirectly affects the pathogenic microbiota or tries to restore healthy gut physiology is the incorporation of antibiotics. A cocktail of antibiotics can be used to deteriorate the population of pathogenic bacteria, but with the evolutionary timeline, antibiotic resistance has developed among the bacterial population.

So, it was required to either decrease the population of pathogenic gut microbiota by some means, or increase the abundance of commensal microbiota, so they, in turn, could rule out the pathogenic bacteria. Direct incorporation of beneficial microbial species to restore the healthy microbial niche was adapted, directly targeting the gut microbial population and adding beneficiaries to it. *Lactobacilli* is the most vastly used probiotic

available in the market these days to treat diseases caused by chronic inflammation by disturbed gut microbiota [101, 102].

Gut microbiota feeds on dietary supplements and produces signaling metabolites as bi-products. Prebiotics are the nutrients required for commensal bacteria to survive and thrive. In layman's terms, prebiotics is a food source for good gut flora to flourish. In this therapeutic method, nutritional supplements like breast milk, protein diets, fibers, etc., serve as the source of prebiotics and help the species-specific strains to flourish and improve diseased conditions.

However, when the gut microbial homeostasis changes and the pro-inflammation spreads systematically, changes in chemicals and other factors send disrupted signals to the whole body, which marks the onset of a disease. The gut microbiota communicates among themselves and with the host through different chemicals released by them as a by-product of digestion called metabolites [103, 104].

These metabolites initiate receptor-mediated signaling inside the host cells, activating the transcriptional gene activation at local and systemic levels. These microbial by-product molecules interact with the immune system and modulate it depending on the type of metabolite. Gut microbes found in the colon act as bioreactors and ferment the digested dietary components to release microbial metabolites, which on one side, work as a whole endocrine system; on the other hand, train the immune system to prevent autoimmune disorders. Specific metabolites like SCFA, propionates, etc., have been found to trigger anti-inflammation pathways, which can help combat the infections and disorders caused by the dysbiosis of the gut microbial community and immune homeostasis [101–104].

Recently, several attempts have been used to replicate the gut microbial composition of a diseased person like that of a healthy individual; a direct transfer of the microbiota strategy from the healthy individual to the unhealthy one was adopted via fecal microbiota transplantation. The fecal microbiota from a healthy individual to a diseased person has been found to improve the IBD, metabolic disorder, neurological, and various conditions that are affected by dysbiosis in gut microbiota. Although this therapy is the most feasible, many associated risks of transferring other pathogens come with it [105–107].

A gut microbiota is a community of microbes consisting of viruses, fungi, and bacteria. Among the microbes, bacterial abundance is the highest. A niche of both commensal and harmful bacteria is required in the gut to keep the gut ecosystem healthy, where an excess of anything is wrong. Phages target all the bacteria and work as checkpoint gatekeepers to keep the population of any bacteria from exploding. This observation has led to the extensive use of phage particles to target pathogenic bacteria and is used as a therapy to treat various disorders caused by pathogenic microbiota [108, 109].

1.13 Regulate the bugs with bugs and maintain a healthy life

The promising potential therapeutic interventions are either the microbes/ gut bugs or their by-products. So, the main strategy of maintaining healthy homeostasis could be the kill the pathogenic bugs with the beneficial bugs.

The concept of therapy for a healthy life started thousand years ago with the concept "Let food be thy medicine, and let medicine be thy food" by Hippocrates, father of medicine. Since science is gradually trying to understand the dual role gut bugs as disease causing

agent and also as therapeutic interventions. From 2002, WHO started considering the good bugs as probiotics. Probiotics are defined as "a live organism, which provides a benefit to the host when provided in adequate quantities" [110, 111].

Since the last few decades, the science of probiotics has evolved rapidly and gained widespread acceptance as a source of effective therapies for the treatment of different metabolic disorders, including urinary, respiratory, hepatic, and neurological conditions. Ingested probiotics within the gut interact with immune cells to maintain an immunologic balance within the gastrointestinal tract because the majority of probiotics are helpful bacteria present naturally within the stomach. Therefore, the regulation of immune responses at the epithelial cells that make up the mucosal interface between host and bacteria is how the gut microbiome, probiotics, and human health interact among themselves.

A single strain or a combination of two or more strains may be present in probiotic products. Effects of probiotics cannot be generalized because they are very strain specific. Depending upon how it is used, a single strain may have unique benefits both alone and in combination [101, 103, 111, 112].

So, various combinations of probiotics can be tailor made to target several diseases as well it can be dove tailed to personalize for more precise efficacy with lesser unwanted effects for a better health.

1.14 Aims of the thesis

In this thesis, I have included the errands I ran during my Ph.D. tenure, focusing on understanding the role of direct and indirect perturbation of gut microbiota. This approach was taken to understand and characterize the role of gut bacteriome in inducing and

regulating colitis. The results revealed many novel and interesting outcomes and roles of the gut microbiome, microbial and host metabolome. Such intricate high-throughput data were tried to be put into perspective of health and microbial dysbiosis in the following chapters in the thesis.

Differential effect of gut microbial dysbiosis by select antibiotics and DSS on the host immunity and metabolism

The pattern of dysbiosis varied significantly among different dysbiotic agents. Dysbiosis patterns depend on the chemical nature of the agents or the mode of action of dysbiosis [113, 114]. The kinetics of gut dysbiosis and the capacity to restore to the normal condition also depend on the host's immune-genetic background [115, 116]. In this current study, we started our experiment with two differently immune-biased mice to observe the effect direct and indirect effect of gut microbial perturbation on host immunity and metabolism in two different immune-biased mice strains, i.e., Th1- biased C57BL/6 and Th2- biased BALB/c mice.

Differential disease susceptibility of Th1- and Th2-biased mice followed by DSS treatment

DSS treatment led to colitis like symptoms in both We mice strains. comprehensively examined the severity responses of DSS induced colitis in two immunologically bias mice strains. With a special mention, we are perhaps the first group that used a composite DSS dosage (5% for the 1st week+ 2.5% for the 2nd week) to understand all the stages of colitis in terms of severity in two different immune-biased mice models within a brief period, i.e., 2 weeks.

Differential metabolite and gut microbial compositions cause C57BL6 mice to exhibit higher stress than BALB/c mice

Altered gut microbial composition, immunity and metabolism due to development of colitis ultimately affect the stress responses of the host. The current study revealed that prolonged pro-inflammatory conditions of DSS treated C57BL/6 activate prolonged chronic stress responses and more depressive behavior than BALB/c. Like the inflammatory status, the stress response of treated BALB/c was short-lasting, and as a result, BALB/c was prone to short-lasting anxiety-related behavior or lesser depressive behavior. The depressive behavior came to the basal level at the end of the treatment. More severe inflammatory status altered the pathogenic proteobacteria level in the gut of C57BL/6 in such a way that it was never restored to the normal level till the end of the treatment.

Combinatorial effects of DSS and Antibiotics on the gut microbiota of Th1- and Th2-biased mice

Observation from the current study concluded that in Th1- biased C57BL/6 mice, antibiotics treatment rescued the DSS treated group from the diseased condition by activating the carbohydrate and nucleotide metabolism pathway, which converted the pro-inflammatory status of the host in an anti-inflammatory condition. On the other hand, early exposure to antibiotics increases disease susceptibility by activating pro-inflammatory lipid and amino acid metabolism pathways.

The scenario was quite different in Th2-biased BALB/c mice. Antibiotic treatment always activated the carbohydrate metabolism pathway, which ultimately provides a therapeutic effect against colitis, whether administered before or after the DSS treatment.

Chapter: 2

Materials and Methods

Materials & Methods

The current chapter mainly deals with the detailed materials and methods used for the present study. A detailed description of all materials and instruments used for the experiments is mentioned in this section. The methods are described succinctly and are independent enough to reproduce the experiments further.

2.1 Details of animal models and their maintenance procedures

To avoid all sorts of ethical controversies regarding using and manipulating human samples, we used mice as a model organism for conducting all the experiments related to the current study.

We used 6-8 weeks-old male C57BL/6 and BALB/c mice for the study. C57BL/6 mouse is genetically Th-1 biased, and BALB/c is Th-2 biased. All the mice were raised and inbred in a specific pathogen-free environment of the animal house facility of the school of biological sciences of NISER. We co-housed specific pathogen-free 6-8 weeks old, male C57BL/6-or BALB/c-mice with body weight in the range of 18-22g in a poly-sulfone cage using corncob as bedding material. We housed the mice of the same strains together in a pathogen-free environment with a 12h light and 12h dark cycle at a temperature of $24 \pm 3°$ in $55 \pm 3\%$ humidity. We provided traditional pelleted food (chow diet, 61.02% carbohydrate, 32.46% protein, 6.52% fat w/w) (cat# AF6000B, Krishna Valley Agrotech LLP, India) and autoclaved water ad libitum. After one week of acclimatization to the experimental area's environment, we randomly grouped the animals into different groups based on our experimental plans. Each group consisted minimum of 6 to a maximum of 10 animals according to the experimental procedures. The ethical approval for the study was taken from Committee for Control and Supervision of

Experiments on Animals, Govt. of India (CPCSEA) (IAEC, Reg. No-1634/GO/ReBi/S/12/CPCSEA, protocol number NISER/SBS/IAEC/AH-21 and 186). All the experiments were performed as per the approved guidelines.

2.2 Manipulation of the healthy state of the host using different perturbing agents

Four different perturbing agents were used to alter the normal healthy homeostasis of the hosts. All the perturbing agents alters the immune and gut microbial homeostasis directly or indirectly at any point of the treatment conditions. A single dose (Neomycin and Vancomycin) or cocktail of antibiotics (AVNM- Ampicillin, Vancomycin, Neomycin, Metronidazole) directly perturbed the gut microbial composition, which further alters the immune homeostasis of the host. On the other hand, DSS (Dextran Sulfate Sodium), a polysaccharide of microbial origin, perturbed the immune homeostasis directly, further altering the host's gut microbial composition.

- **Antibiotic dosage**

The antibiotic dosages were determined as per previous reports and FDA guidelines.

  - **Neomycin and Vancomycin treatment-** We orally gavaged two separate groups of mice with neomycin sulfate (MP Biomedicals, Illkrich, France) and vancomycin hydrochloride (MP Biomedicals, Illkrich, France) at a dose of 50mg/Kg body weight, twice a day at a gap of 12 hrs. for 7 days [117–119].

  - **AVNM treatment-** AVNM cocktail was gavaged twice a day orally with a gap of 12 hrs. for 7 days. The individual dose of each antibiotic in the cocktail was as follows; ampicillin (100mg/Kg), vancomycin

hydrochloride (50mg/Kg), neomycin sulfate (100mg/Kg), metronidazole (100mg/Kg). All the antibiotics were procured from MP Biomedicals (Illkrich, France) [120].

- **DSS dosage**

DSS treatment was through drinking water. We added DSS (M.W.-50kDa, Fisher Scientific) to autoclaved drinking water (*ad libitum*) at a concentration of 5% for the 1st week, followed by 2.5% of DSS for the 2nd week, and renewed with freshly prepared solution three times a week [121]. The dose was sufficient to alter the host's gut microbial composition.

No perturbing agent was administered in the untreated control group.

A detailed study plan is depicted in Fig. 2.1.
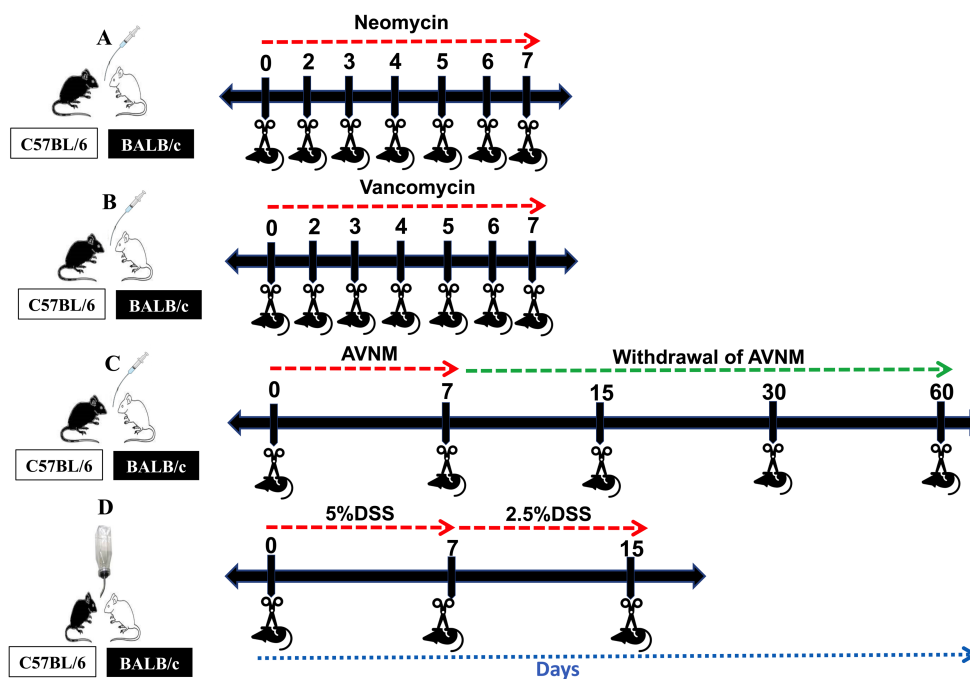
Fig. 2.1: Picture depicting the detailed experimental plans of different treatment regimes.

We continued the dose of AVNM till day 60, because in a separate experiment from our group observed that it took almost 60 days to restore the microbiota in both C57BL/6 and BALB/c mice. Whereas in all other treatment conditions we have seen the restoration of bad gut flora with a good one within 1-2 weeks in either of the mice strain. As our main notion was to quantify the strength of various perturbation process, we continued the experiments in different time scale for different perturbing agents until the gut microbial restoration.

2.3 Study the combinatorial effect of DSS and 9 antibiotics cocktail

To study both the therapeutic and detrimental effects of antibiotics we treated the mice both with DSS and a cocktail of 9 different antibiotics. The time-span of the study was for 15 days. A detailed study plan is depicted in Fig. 2.2.

- **DSS dosage**

DSS treatment was through drinking water. We added DSS (M.W.-50kDa, Fisher Scientific) to autoclaved drinking water (*ad libitum*) at a concentration of 2.5% and renewed with freshly prepared solution three times a week [121].

- **9 antibiotics cocktail dosage**

The antibiotic dosages were determined as per previous reports and FDA guidelines.

The nine antibiotics cocktail contains 100 μg/ml **Neomycin**, 50 μg/ml **Streptomycin**, 100 μg/ml **Penicillin**, 50 μg/ml **Vancomycin**, 100 μg/ml **Metronidazole**, 1 mg/ml **Bacitracin**, 125 μg/ml **Ciprofloxacin**, 100 μg/ml **Ceftazidime** and 170 μg/ml **Gentamycin** in the autoclaved drinking water.

No external chemical was administered in the untreated control group.
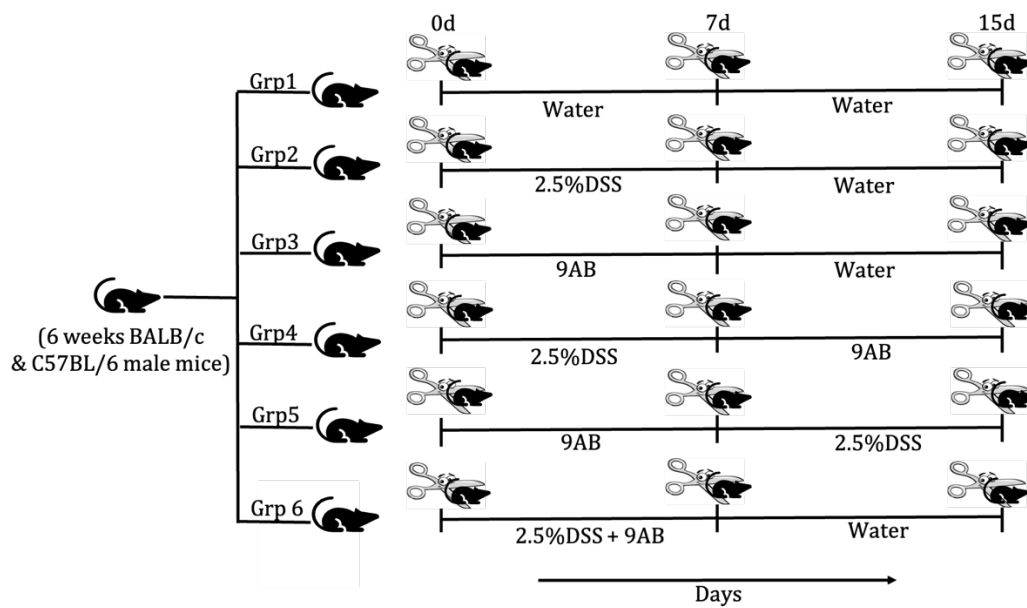
Fig. 2.2: Picture depicting the detailed experimental plans of different treatment regimes of DSS and 9 antibiotics cocktail treatments.

2.4 Zootomy, sample collections, and preservations at the different time points of the treatment

We sacrificed the mice at different time points for different treatment conditions until the restoration happened in either group of mice strains. Six mice were sacrificed for each group at each time point. Euthanasia was performed by introducing 100% carbon dioxide into a bedding-free cage initially containing room air with the lid closed at a rate sufficient to induce rapid anaesthesia, with death occurring within 2.5 minutes. Mice were sacrificed if they reached the humane endpoints of rectal prolapse, loss of >15% body weight, or signs of pain and distress including poor grooming, decreased activity, and hunched posture to alleviate the suffering of the animals.

For neomycin and vancomycin treated C57BL/6 and BALB/c mice, we sacrificed the mice every day till day 7. Whereas in AVNM treated group, we sacrificed the mice on

days 0, 7, 15, 30, and 60. For the control and DSS treated group and also for the DSS and 9 antibiotics cocktail combination groups, we collected the samples on days 0, 7, and 15.

We collected the cecal content of all the groups of mice to note the kinetics of gut microbial changes in the presence of different perturbing agents. Cecal samples were immediately snap-frozen and stored at -80°C for further use. The colon tissue samples were collected in RNALater for RNA analysis and stored at -20°C for further use. We stored the colon tissues in 4% PFA (paraformaldehyde) for histopathological examination and stored them at room temperature. To know the protein level changes in colon tissue, we snap froze the tissues and stored them at -80°C for further analysis.

Serum samples were isolated from total blood by centrifuging at 1600 rcf at 4°C for 10 minutes and stored at -20°C until further analysis.

2.5 Assessments of the physiological parameters and disease severity

We monitored the body weight changes and water intake on a day-to-day basis. We measured body weight using a weighing balance (QUINTIX 224, Sartorius, Germany, Göttingen) and water intake using a standard glass measuring cylinder (Borosil). After zootomy, we observed in some of the treatment groups, the colon length was significantly shorter than the control or other groups. We measured the colon length using a standard ruler on 0-, 7-, and 15 days post-treatment. The spleen and peritoneal fat weight were also measured using a weighing balance (QUINTIX 224, Sartorius, Germany, Göttingen) on 0-, 7-, and 15 days post-treatment.

We also scored the post dysbiosis severity level separately and independently on a scale of 0-5 based on the a) stool consistency, b) the extent of occult blood in the stool, and c) rectal bleeding of control and treated group [121].

Table. 2.1: *Disease severity score based on stool texture and rectal bleeding.*

Condition	Score
Normal + no hemoccult	0
Soft + no hemoccult	1
Soft + hemoccult	2
Soft+ very little amount of rectal bleeding	3
Very soft+ blood	4
Watery+ rectal bleeding	5

2.6 Intestinal Permeability Assay Using FITC-Dextran

We food and water starved both control and treated mice of both strains overnight and kept them in a cage without bedding to limit the coprophagic behavior [122]. We measured the mice's body weights the following morning and administered PBS dissolved FITC-dextran (100mg/ml, Cat#F7250, Sigma-Aldrich, Missouri, US) in each mouse (44mg/100g body weight) by oral gavaging following 4h of incubation. We anesthetized mice by isoflurane inhalation and collected blood using a 1ml syringe with a 25G needle by cardiac puncture. We isolated serum from the blood by centrifuging at 1600 rcf at 4°C for 10 minutes and diluted it with an equal volume of PBS. We added

100µl diluted serum in each well of a 96 well microplate in duplicate and measured fluorescence at 528 nm (emission wavelength) by exciting at 485 nm (20 nm bandwidth at both excitation and emission) [123].

2.7 Oral glucose tolerance test

The oral glucose tolerance test (OGTT) was performed at a specific time interval for some control and treatment groups. For the assay, we, food and water, starved the control and treated mice overnight, specifically for 12 hours. We measured the fasting blood glucose levels of control and treated groups just after 12 hours and orally gavaged (20-gauge gavage needle, Sigma, USA) the mice with glucose in PBS (Himedia, India) at 2g/kg body weight. Control groups were gavaged with normal PBS. We assessed the blood glucose level by using a commercial glucometer (Accu-CHEK0 Instant S Glucometer, Roche, Switzerland, Basel) at 15, 30, 60, 90 minutes after glucose administration.

2.8 Histopathological analysis of the colon tissue

We stained the mouse colon tissue sections (5µm thick) with hematoxylin-eosin (H&E) and alcian blue/PAS to address the degree of inflammation and analyzed them independently in a blinded fashion with a standard, inverted microscope (Olympus CKX53, Japan). Briefly, colon tissue samples were collected and preserved in 4% paraformaldehyde solution at room temperature for 72 hours. Tissues were processed for paraffin embedding, and multiple 5-micron sections were prepared. Slides were deparaffinized and hydrated with deionized water, followed by hematoxylin-eosin

staining and alcian blue/PAS staining separately. Slides were thoroughly washed in H2O and dehydrated through sequential alcohol grading, cleared in xylene, mounted with permanent mounting media (Vector Lab), and covered with a coverslip to watch under a microscope.

We characterized the tissue pathophysiology by using all of the following parameters such as a) presence of ulcerations, b) inflammatory cells, c) signs of edema, d) loss of crypt epithelium, e) reduction in the number of goblet cells, and f) villous blunting (g) loss of mucus layer, etc. We scored the parameters on a scale of 1-5 and listed them in a separate table [121, 124].

Table. 2.2: *The scoring method used for histopathological analysis.*

Category	Criterion	Condition	Score
Inflammatory cell infiltrate	**Leukocyte density increase** (Leukocyte density of lamina propria are infiltrated)	Minimal:<10%	1
		Mild:10-25%, scattered neutrophils	2
		Moderate:26-50%	3
		Marked:>51%, dense infiltration	4
	Extent (Expansion of leukocyte	Mucosal	1
		Mucosal and submucosal	2

		infiltration)		
		Mucosal, submucosal and transmural	3
Epithelial Changes	**Epithelial cell number increase** (Increase in epithelial cell numbers in longitudinal crypts relative to baseline epithelial cell numbers per crypt; visible as crypt elongation)	Minimal: <25%	1
		Mild: 25-35%	2 or 3
		Moderate: 36-50%	3 or 4
		Marked: >51%	4 or 5
	Goblet cell reduction (Reduction of goblet cell numbers relative to baseline goblet cell numbers per crypt)	Minimal: <20%	1 or 2
		Mild: 21-35%	2 or 3
		Moderate: 36-50%	3 or 4
		Marked: >50%	4
	Cryptitis	Based on severity	2 or 3

	(Neutrophils between crypt epithelial cells)		
	Erosion (Loss of surface epithelium)	Based on severity	1 to 4
Mucosal Architecture	**Ulceration** (Epithelial defect reaching beyond muscularis mucosae)	Based on severity	3 to 5
	Irregular crypts (Non-parallel crypts, variable crypt diameters, bifurcation, and branched crypts)	Based on severity	4 or 5
	Crypt Loss (Mucosa devoid of crypts)	Based on severity	4 or 5

		The ratio of 2:1 to 3:1	1 to 3
	Villous blunting (Villous-to-crypt-length ratio)	The ratio of 1:1 to 2:1	2 to 4
		Villous atrophy	3 to 5

2.9 RNA Extraction and Lithium Chloride Purification

We extracted the total RNA from colon tissues using a Qiagen RNeasy mini kit (Cat# 74104, Qiagen, India). In brief, we homogenized 20-25 mg of frozen colon tissue in liquid nitrogen by pestle-mortar and extracted it in RLT buffer. We (a) centrifuged the total homogenate in RLT buffer and transferred it to RNeasy mini-column followed by washing in RW1 and RPE buffer, (b) purified the samples further with LiCl to get rid of all polysaccharides, including DSS, (c) incubated RNA with 0.1 volume of 8 M LiCl diluted in nuclease-free water on ice for 2 h followed by centrifuging at 14,000 g for 30 min at 4°C, and (d) discarded the supernatant and dissolved RNA pellets in 200 µl of nuclease-free water. We repeated steps (c-d) once more before precipitating RNA at −20°C for 30 min, in 0.1 volume of 3 M sodium acetate (pH 5.2) and 2 volumes of 100% absolute ethanol. We centrifuged the RNA at 14,000 g for 30 min at 4°C. After discarding the supernatant, we washed the pellets with 100 µl of 70% ethanol and centrifuged at 14,000 g for 10 min at 4°C. We dissolved the final RNA in 30µl nuclease-free water and checked the quality and quantity of extracted RNA by measuring ODs at 230, 260, and 280nm using NanoDrop 2000 machine (Thermo Fisher Scientific, Columbus, OH, USA).

We determined the RNA concentration by nanodrop and validated it using a Qubit4 fluorometer (Invitrogen, California, USA). We assessed the RNA integrity by 2% agarose gel electrophoresis and confirmed by 4200 TapeStation instruments (Agilent, Santa Clara, CA, USA) [125].

2.10 Gene Expression by mRNA Sequencing

We submitted the samples to Agrigenome with RIN value above 8 for library preparation. Agrigenome prepared the library using TruSeq Stranded mRNA Library Prep Kit (poly-A selection) and sequenced it by the HiSeq-2500 platform (Illumina, San Diego, CA, USA). They sequenced the samples using pair-end 2×150-bp sequencing, aiming for coverage of 20 M reads. We used the Tuxedo software package for the pipeline used for data analysis. The package consists of spliced read mappers and tools that allow one to assemble transcripts, estimate their abundances, and test differential expression and regulation in RNA-Seq samples. It was a combination of open-source software and implemented peer-reviewed statistical methods. The components of the NGS data analysis pipeline for RNA-seq include Hisat2, StringTie, and Cuffdiff. We took data with a Phred score >30, alignment percentage >60. Replicate variability was significantly less and clustered according to the experimental group. Similar numbers of genes were expressed in all samples, and sort differentially expressed genes using relevant criteria, including expression level, fold change, and statistical significance [126, 127]. We used Statistixl 2.0 add-on to MS Excel for Linear Discriminant (LDA or DCA) and Principal Component Analysis (PCA) of shortlisted genes.

2.11 cDNA Preparation

We converted the mRNA from total RNA into cDNA using AffinityScript One-Step RT-PCR Kit (Cat# 600559, Agilent, Santa Clara, CA, USA) following the manufacturer's protocol. In brief, we mixed total RNA with random nonamer primer, Taq polymerase, and NT buffer. We kept the mixture at 45°C for 30 min for the synthesis of cDNA. We increased the temperature to 95°C to stop the reaction by deactivating the enzyme.

2.12 Quantitative Real-Time PCR (qRT PCR)

We set the qRT-PCR reaction in a 96 well PCR plate using a) 30 ng of cDNA as a template in the presence of 1μM/μl of each of forward (F) and reverse (R) primers (Table 2.3) for genes mentioned in Table 2.3, b) SYBR green master mix (Cat#A6002, Promega, Madison, WI, USA), and c) nuclease-free water. We performed the qRT-PCR analysis in Quantstudio 7 (Thermo Fisher Scientific, Columbus, OH, USA) using a sequence of cycles, a) a cycle for 2 minutes at 92 °C to activate DNA polymerase, b) 15 seconds at 92 °C for melting of the template, and c) 1 minute at 60 °C for primer annealing along with an extension of the chain and detection of the fluorescence for 40 cycles. A qRT-PCR analysis detects a signal by accumulating a fluorescent signal. The C_t (cycle threshold) is defined as the number of cycles required for the fluorescent signal to cross the threshold above the background level. C_t levels are inversely proportional to the template in the sample (meaning, a lower C_t value implies higher template copy numbers). We normalized the measured cycle threshold (C_t) value of a gene with the GAPDH (positive control) C_t-value, and the fold change of the desired gene was calculated to the control C_t-value

Table. 2.3: *Sequences of forward (F) and reverse (R) primers used in gene expression studies.*

Genes specific for	NCBI_ Acc. No.	The sequence of the primer used (5′-3′)
GAPDH	NM_008084	F: CATCACTGCCACCCAGAAGACTG R: ATGCCAGTGAGCTTCCCGTTCAG
TNF-α	NM_01278601	F: TGCCTATGTCTCAGCCTCTTC R: GAGGCCATTTGGGAACTTCT
IFN-γ	NM_008337.3	F: CCTTTGGACCCTCTGACTTG R: TTCCACATCTATGCCACTTGAG
MPO	NM_010824	F: CGTGTCAAGTGGCTGTGCCTAT R: AACCAGCGTACAAAGGCACGGT
CLDN-1	NM_016674	F:TGCCCCAGTGGAAGATTTACT R: CTTTGCGAAACGCAGGACAT
CLDN-2	NM_016675	F: AGGACTTCCTGCTGACATCCAG R: AATCCTGGCAGAACACGGTGCA
OCLN	NM_008756	F:GTTGAACTGTGGATTGGCAG R: AAGATAAGCGAACCTTGGCG
IL-1β	NM_008361	F: TGTAATGAAAGACGGCACACC R: TCTTCTTTGGGTATTGCTTGG
IL-6	NM_001314054	F: CTCTGCAAGAGACTTCCATCCAGT

		R: CGTGGTTGTCACCAGCATCA
IL-12p40	**NM_00130324**	F: CAATCACGCTACCTCCTCTTTT R: CAGCAGTGCAGGAATAATGTTTC
IL-17a	**NM_010552**	F: CAGACTACCTCAACCGTTCCAC R: TCCAGCTTTCCCTCCGCATTGA
IL-21	**NM_016971**	F: GCTTGAGGTGTCCAACTTCCAG R: ACTCCTCGGAACAGTTTCTCCC
IL-10	**NM_010548**	F: GCTCTTACTGACTGGCATGAG R: CGCAGCTCTAGGAGCATGTG
TLR-2	**NM_011905**	F: GAGCATCCGAATTGCATCA R: CACATGACAGAGACTCCTGAGC
TLR-4	**NM_021297**	F: TTCAGAACTTCAGTGGCTGGA R: CTGGATAGGGTTTCCTGTCAGT

2.13 Metabolite isolation and sample preparation for serum metabolomics study using ^{1}H NMR

We used the freshly isolated serum collected from the control and treated group for this study and processed the serum samples following the previously described protocol by Naik *et al.* and Ray *et al.* [128, 129]. In short, to remove the abundant serum proteins, we column (Amicon Ultra-2ml 3000 MWCO, Merck Millipore, USA) precipitate the serum by centrifugation at 4°C and at 12,000Xg. 700 μL of protein free serum was isolated from each sample and mixed with deuterium oxide (Aldrich, USA, St Louis) and pH

maintenance buffer containing the internal standard Sodium 3-(Trimethylsilyl)-1-propane sulfonate (TCI, Japan, Tokyo) and transferred into 5 mm Wilmad NMR tubes (Sigma, USA, NJ) for NMR analysis.

2.14 Metabolite isolation and sample preparation for cecal metabolomics study for ^{1}H NMR

We used freshly isolated cecal samples for metabolite isolation from the cecal samples. We used 30 mg of each cecal sample for metabolite extraction. 700 μL PBS (HiMedia, India) was added to the cecal sample to make the homogenate followed by 3-4 times of vortexing and further 3-4 rounds of sonication. Further, we centrifuged the homogenate for 10mins at 16000Xg at 4°C. 600 μL of supernatant from each sample was then transferred to a Amicon Ultra-2ml 3000 MWCO (Merck Millipore, USA) column for column precipitation by centrifugation at 4°C and at 12,000Xg. 500 μL of protein free cecal homogenate was isolated from each sample and mixed with deuterium oxide (Aldrich, USA, St Louis) and pH maintenance buffer containing the internal standard Sodium 3-(Trimethylsilyl)-1-propane sulfonate (TCI, Japan, Tokyo) and transferred into 5 mm Wilmad NMR tubes (Sigma, USA, NJ) for NMR analysis.

2.15 ^{1}H NMR Data Acquisition and Metabolite Analysis

We performed all NMR experiments at 298K on a Bruker 9.4T (400 MHz) Avance-III Nanobay solution-state NMR spectrometer equipped with a 5 mm broadband probe. We used excitation sculpting gradients with a duration of 1 ms and a strength of 14.9 G/cm for water suppression and an offset optimization using real-time 'gs' mode for each

sample. In addition, we employed a Sinc-shaped pulse of 2 ms for selective excitation of the water resonance. We recorded 64 transients for each set of experiments with an average 5s relaxation delay to ensure complete water saturation. We recorded and processed the acquired spectra by Topspin 2.1.

We used Chenomx NMR Suite7.6 (ChenomxInc., Edmonton, Canada) to identify (targeted) and quantify metabolite signals from NMR spectra. First, the Chenomx processor automatically phased, referenced the DSS peak at 0 ppm, and corrected FID files' spectra' baseline. Next, we calculated the metabolite concentrations by a profiler using Metaboanalyst 5.0 (a public software at https://www.metaboanalyst.ca). We utilize the profiler to assign and fit the metabolite peaks from the Chenomax library. We performed the pathway analysis using Metaboanalyst 5.0 software.

We identified the statistically significantly altered metabolites between two experimental conditions from the serum and cecal metabolite concentration list. Then we further shortlisted the metabolites by setting up a cut-off of 1.5 based on the relative concentration of metabolites. Next, we clustered (based on all the metabolites and significantly altered metabolites) the data based on different treatment conditions using Linear Discriminant Analysis using statistiXL 2.0 (add-in to the Windows version of Excel spreadsheet).

Finally, we used the list of significantly altered metabolites to predict biological pathways using the MetPA function of the MetaboAnalyst 5.0 software. We used KEGG pathways as reference data set for biological pathway prediction. Briefly, we manually entered the compound lists into the pathway analysis module along with the necessary metadata. The metabolite lists generated an overview plot of the predicted pathways. Similarly, to this,

we have done joint pathway analysis, where software can predict the affected biological pathways based on metabolite level changes and genetic level changes. We manually entered significantly altered metabolites and significantly altered genes available from the transcriptomics study and its proper metadata to know the collective impact of host metabolism and host genetics on the overall biological system of the host [128, 130, 131]. From the list of predicted pathways, we chose the ones with high impact scores to be altered due to different treatment conditions, giving rise to the differential disease responses based on the differential immune bias condition of the host.

2.16 Study of serum and cecal using Liquid Chromatography- Mass Spectrometry Sample Preparation

Serum and cecal samples were aliquoted for metabolome analysis. First, we aliquoted 50µl serum/ 50mg stool sample in a 1.5ml microcentrifuge tube, then 1 ml acetonitrile-methanol solution(1:1) and 5µl CPA were added, vortexed, and incubated for precipitation at 4°C for 2 hours. After precipitation, it was centrifuged at 15000 x *g* for 15mins. Upon centrifugation, the supernatant was collected into a new 1.5ml MCT tube and kept in the SpeedVac Vacuum Concentrator for 1 hour to dry. After drying, we resuspended the palate in 50µl acetonitrile-water solution using the vortex. Then again, centrifuged at 15000 x *g* for 15 mins. Finally, for the instrumental analysis, the supernatant was collected into an LC-MS tube and is ready to use for further analysis.

2.17 Metabolomics Analysis

We used a TripleTOFTM 6600 LC/MS/MS system (AB SCIEX, Foster City, CA, USA) for the identification of metabolites. A mobile phase consisting of 2 different solvents, solvent A (water, 0.1% formic acid) and solvent B (methanol, 0.1% formic acid) was used. 5 μL and 0.5 mL/min were the injection volume and flow rate, respectively. MS data were obtained between the mass range set at 50–1000 m/z in both positive and negative ionization modes.

2.18 Multivariate Data Processing and Statistical Analysis of MS-MS data

We obtained the peaks using MS- Dial software and the MassBank NIST database to identify the metabolites. And we used MetOrigin and MetaboAnalyst to identify various pathways related to the identified metabolites.

2.19 Detailed Analysis of Transcriptomics and Metabonomics Data from LDA Clustering

We performed Linear Discriminant Analysis (LDA) with the shortlisted genes, metabolites, and meta-metabolites to confirm the differential disease responses at various treatment conditions. We calculated the distance (r) between clusters, i.e., different treatment conditions on the 2D plane, to determine the differentiability of the changes of genes and metabolites based on treatment conditions and different mice strains. Distance between different clusters helped us quantify the dissimilarity in disease progression at different treatment conditions, and we named it Dissimilarity Coefficient. We also drew

the trajectory followed by different treatment conditions on the 2D plane to know the characteristics changes of genes and metabolites based on disease severity [132, 133]

Dissimilarity Coefficient (r) $= \sqrt{(x_2 - x_1)^2 + (y_2 - y_1)^2}$

Where,

r= distance between the point $x_1 y_1$ and $x_2 y_2$ (x,y depicts the different treatment conditions).

To know the role of genes and metabolites in determining the disease severity based on the host immunological background, we calculated the Disease Severity Index (D) considering 3 different parameters separately, i.e., altered genes, metabolites, and meta-metabolites expressions [134].

Disease   Severity   Index   (D)   = $\Sigma \rho_x \rho_y r_{xy}$

Where,

ρ_x= distance of point x from centre.

ρ_y= distance of point y from centre.

r_{xy}= distance between point x and y.

Σ= summation of $\rho_x \rho_y r_{xy}$ between two specific treatment conditions.

(x, y represents different treatment conditions).

We further checked the ratio of pro and anti-inflammation-related genes, metabolites, and meta-metabolites at a particular treatment condition to get an idea about the possible factors playing the main role in the activation of the host's inflammatory conditions. We have depicted the Venn diagram of shortlisted genes of C57BL/6 and BALB/c to find the common and unique genes between the two strains at various treatment conditions. Strain specific ratio of pro and anti-inflammatory genes gave us a clear idea about the reason behind differential disease severity in two different mice strains. Similarly, we have depicted the strain specific Venn diagram of shortlisted metabolites from serum and cecal content to find the common and unique metabolites from serum and cecal content at various severity levels. The ratio of pro and anti-inflammatory metabolites from serum and cecal content helps us to clear the doubt about the role of metabolites and meta-metabolites in host specific inflammatory conditions. We plotted the number of significantly altered metabolites at different treatment conditions to know whether the diseased condition was responsible for the altered chemical diversity of serum and cecal content. We also represented the Venn diagram of the number of significantly altered common and unique serum and cecal metabolites of different severity levels. This analysis helped us find the similarities and dissimilarities between the differential composition of serum and cecal metabolites at various diseased conditions, which further correlated with the disease severity.

2.20 Cecal DNA Extraction and Lithium Chloride Purification

We collected cecal samples from control and treated group of both the mice strains and stored them at −80 °C. For DNA isolation, 180-220 mg of cecal content for each sample

was mixed with 1 mL 1x sterile ice-cold PBS to make a homogenate followed by centrifugation. 600 μL of lysis buffer was added to the supernatant followed by a heat lysis at 70 °C for 30 min. Lysate was centrifuged and1 mL of Phenol- Chloroform-isoamyl alcohol was added to the supernatant followed by centrifugation and collection of the aqueous phase. 3 volumes of absolute ice-cold ethanol was added to the lysate for the precipitation of nucleic acid followed by RNase treatment. Finally 50 μL nuclease free water was added to the genomic DNA pellet.

We purified the DNA samples further with LiCl to get rid of all polysaccharides, including DSS. Briefly a) We incubated DNA on ice with 0.1 volume of 8 M LiCl for 2 h followed by centrifugation at 14,000 g for 30 min at 4°C, and (b) discarded the supernatant and dissolved DNA pellets in 200 μl of nuclease-free water. (c) We repeated steps (a-b) once more before precipitating DNA at −20°C for 30 min, in 0.1 volume of 3 M sodium acetate (pH 5.2) and 2 volumes of 100% absolute ethanol. (d) We centrifuged the DNA at 14,000 g for 30 min at 4°C and discarded the supernatant. (e) Washed the pellets with 100 μl of 70% ethanol and centrifuged at 14,000 g for 10 min at 4°C and dissolved the final DNA in 50μl nuclease-free water. We determined the quality and quantity of extracted DNA by measuring ODs at 230, 260, and 280nm using NanoDrop 2000 machine (Thermo Fisher Scientific, Columbus, OH, USA) and validated it using a Qubit4 fluorometer (Invitrogen, California, USA). We assessed the DNA integrity by 2% agarose gel electrophoresis and confirmed it by 4200 TapeStation instruments (Agilent, Santa Clara, CA, USA) [135, 136].

2.21 16S rRNA Sequencing (V3-V4 metagenomics)

We amplified V3-V4 regions of 16S rRNA gene of cecal DNA samples. For this amplification, we have used V3F: 5'-CCTACGGGNBGCASCAG-3' and V4R: 5'-GACTACNVGGGTATCTAATCC-3' primer pair [137]. In the Illumina Miseq platform, amplicons were sequenced using paired end (250bpX2) with a sequencing depth of 500823.1 ± 117098 reads. We monitored the base composition, quality, and GC content of the fastq sequence. More than 90% of the sequences had a Phred quality score above 30 and GC content nearly 40-60%. We removed conserved regions from the paired end reads. Using the FLASH program, we constructed a consensus V3-V4 region sequence by removing unwanted sequences [138, 139]. We pre-processed reads from all the samples pooled and clustered into Operational Taxonomic Units (OTUs) using the de novo clustering method based on their sequence similarity using the UCLUST program. We used QIIME for the OTU generation and taxonomic mapping [140, 141]. Finally, we identified a representative sequence for each OTU and aligned it against SILVA core set of sequences using the PyNAST program. Alignment of these representative sequences against reference chimeric data sets was done, and the RDP classifier against the SILVA OTUs database was used for taxonomic classification [141–144].

2.22 Microbiota Composition Profiling and Analysis

We further analyzed the biome file with the phylogenetic information of the OTUs and filtered OTUs for minimum counts of 2 and a prevalence of 20%. We scaled the data using the total sum scaling algorithm. We plotted the stacked bar and line plot of the phylum and genus level classification.

2.23 Microbial and Metabolite Evenness index

To get an idea about the altered microbial and metabolite diversity due to diseased conditions, we calculated the Evenness index value (E) of microbiota at the phylum level and the metabolites from serum and cecal content [19].

Evenness Index (E) = $-\Sigma E_i ln E_i$

Where,

E_i = proportion of the individual phylum/ metabolites in the total microbial/metabolite pool.

lnE_i = natural logarithm of E_i.

$-\Sigma$ = negative sum of $E_i lnE_i$ for an individual in a specific treatment condition.

2.24 Myeloperoxidase (MPO) Activity Assay

We collected the colon tissues from a control group and a treated group of mice and rapidly homogenized in 4 volumes of MPO assay buffer (5g HTAB in 1L of potassium phosphate buffer). We centrifuged tissue homogenates at 13,000 rcf for 10 minutes at 4°C to remove the insoluble debris. We performed the MPO assay per the manufacturer's protocol (Cat#MAK068, Sigma-Aldrich, St.Louis, USA). Briefly, 40 µL of MPO assay buffer and 10 µL of MPO substrate was mixed with each sample; after proper mixing kept the samples in room temperature in the dark for 120 minutes. After 120 minutes of incubation, 2 µL of stop solution was added, followed by 10 minutes of incubation at room temperature. At last, we added 50 µL of TNB reagent in each well and immediately measured the absorbance at 412nm.

2.25 C-Reactive Protein (CRP) Assay

We rapidly homogenized the colon tissue in extraction buffer (Cat#78510, Thermo Scientific, Rockford, USA) containing 1X protease inhibitor cocktail (Cat#78429, Thermo Fisher Scientific, Rockford, USA). We centrifuged tissue homogenates at 13,000 rcf for 10 minutes at 4°C to remove the insoluble debris. Protein concentration was determined using Bradford assay (Cat#5000006, Bio-Rad, USA). We performed the CRP assay per the manufacturer's protocol (Cat# ELM-CRP, RayBiotech, Norcross, GA). In sort, 100 µL of tissue homogenate was added to the each well of the ELISA plate and incubated for 2.5 hrs. at room temperature. Wells were washed thoroughly and 100 µL of biotin conjugate was added in each well and kept at room temperature for 1 hr. with gentle shaking followed by washing. 100 µL of prepared Streptavidin-HRP solution was added to each well and incubated for 45 minutes at room temperature with gentle shaking. After washing 100 µL of TMB Substrate was added to each well and incubate for 30 minutes at room temperature in the dark with gentle shaking. Lastly, we added 50 µL of Stop Solution to each well and measured the absorbance at 450 nm.

2.26 Lipocalin-2 (LCN2) Assay

We collected serum samples to perform LCN2 assay in control and treated mice groups. Protein concentration was determined using Bradford assay (Cat#5000006, Bio-Rad, USA). We completed the assay as per the manufacturer's protocol (Cat# ELM-Lipocalin-2, RayBiotech, Norcross, GA). Briefly, 100 µl of serum sample was added to each well of ELISA plate followed by a 2.5 hrs. room temperature incubation. Wells were washed

thoroughly and 100 µL of biotin conjugate was added in each well and kept at room temperature for 1 hr. with gentle shaking followed by washing. 100 µL of prepared Streptavidin-HRP solution was added to each well and incubated for 45 minutes at room temperature with gentle shaking. After washing 100 µL of TMB Substrate was added to each well and incubate for 30 minutes at room temperature in the dark with gentle shaking. Lastly, we added 50 µL of Stop Solution to each well and measured the absorbance at 450 nm.

2.27 Endotoxin Assay

We checked endotoxin levels in the serum sample of control and treated mice. We estimated the serum's protein concentration by Bradford assay (Cat#5000006, Bio-Rad, USA) and performed the endotoxin assay according to the manufacturer's protocol (Cat#L00350, Lonza, Piscataway, NJ, USA). Briefly, 100 µL of serum sample was mixed with 100 µL of LAL reagent in each assay plate well followed by a 10 minutes room temperature incubation. Lastly, 100 µL of Kinetic-QCL™ Reagent was added into each well and absorbance was measured immediately.

2.28 Detection of cecal IgA

We checked IgA levels in the cecal content of control and treated mice. We dissolved cecal contents in fecal immunoglobulin extraction buffer (1X PBS, 0.5% Tween, 0.05% Sodium Azide) containing 1X protease inhibitor cocktail (Cat#78429, Thermo Fisher Scientific, Rockford, USA) and centrifuged at 1500 rcf for 20 minutes at 4°C to isolate the supernatant. We estimated the protein concentration by Bradford assay and performed

the assay according to the manufacturer's protocol (Cat# ELM-IGA, RayBiotech, Norcross, GA). In sort, 100 µl of cecal homogenate sample was added to each well of ELISA plate followed by a 2.5 hrs. room temperature incubation. Wells were washed thoroughly, and 100 µL of biotin conjugate was added to each well and kept at room temperature for 1 hr. with gentle shaking followed by washing. 100 µL of prepared Streptavidin-HRP solution was added to each well and incubated for 45 minutes at room temperature with gentle shaking. After washing, 100 µL of TMB Substrate was added to each well and incubated for 30 minutes at room temperature in the dark with gentle shaking. Lastly, we added 50 µL of Stop Solution to each well and measured the absorbance at 450 nm.

2.29 Acetate, Butyrate, Glutamate Assays

We measured the acetate, butyrate, and glutamate levels from serum and cecal samples of control and treated mice using commercially available kits in the market, according to the manufacturer's protocol (Acetate Cat# EOAC 100, Butyrate Cat# EKBD 100, Glutamate Cat# EGLT 100, Biovision, CA, USA). For each sample, 10 µl of serum or cecal homogenate was utilized to measure the acetate, butyrate and glutamate level through a substrate-enzyme coupled colorimetric reaction at an absorbance of 570 nm.

2.30 CRH, ACTH, Cortisol Hormonal Assays

We measured the stress hormones levels CRH, ACTH, Cortisol from serum and cecal samples control and treated mice using commercially available ELISA kits. According to the manufacturer's protocol (CRH Cat# E-EL-M0351, ACTH Cat# E-EL-M0079,

Cortisol Cat# E03C0008, MyBioSource, CA, USA). The procedures for all three hormonal assays were identical. In brief, 50uL of sample was mixed with 50μL of biotinylated detection antibody in each well of ELISA plate and incubated for 45 min at 37°C followed by washing.100 μL of HRP Conjugate was added and incubated for 30 min at 37°C. After washing 90 μL of substrate reagent was added to each well followed by 15 min incubation at 37°C in dark. At last, 50 μL of stop solution was added to each well and absorbance was measured at 450nm.

2.31 Open-Field Test

Open field test is widely used to measure the psychological activity of small rodents. It measures the emotional outcome, especially the anxiety-related behavior and also the locomotor activity of the animal [145]. The open-field instrument was made up of polished wood, and the size of the chamber was 50cm (Length) x 50cm (width) x 38cm (height). The total area of the chamber was divided into two parts, center and periphery, and was marked accordingly. In an experimental setup, we placed each mouse at a time in the center of the instrument for 5 minutes to record the locomotory action of the animal. The locomotor activity was measured using a computerized video tracking system (Smart 3.0, Panlab SMART video tracking system, Harvard Apparatus). We measured the total time spent in the periphery and the center of the instrument for further analysis. The apparatus was appropriately cleaned with 70% ethanol before and after every usage [145, 146].
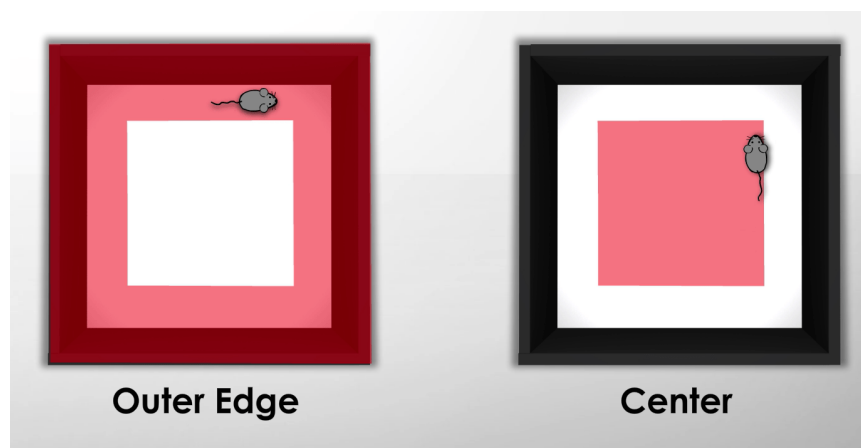
Fig. 2.3: Schema of open field apparatus

2.32 Elevated Plus-Maze Test

The elevated plus maze is a widely used behavioral assay to define anxiety-related behavior for rodents [147, 148]. The apparatus used for the elevated plus-maze test was in the configuration of a + and comprised two open arms (25 x 5 x 0.5 cm) across from each other and perpendicular to two closed arms (25 x 5 x 16 cm) with a center platform (5 x 5 x 0.5 cm). The open arms had a tiny (0.5 cm) wall to decrease the number of falls, whereas the closed arms had a high (16 cm) wall to enclose the arm. We placed the entire apparatus 50 cm above the floor and was made up of polished wood. In an experimental setup, we placed each mouse at the junction of the four arms of the maze, facing an open arm, and entries/duration in each arm were recorded by a video-tracking system (Smart 3.0, Panlab SMART video tracking system, Harvard Apparatus) and observed simultaneously for 5 min. An increase in open arm activity (duration and/or entries) reflected the anti-anxiety behavior of the mouse. The apparatus was appropriately cleaned with 70% ethanol before and after every usage [148, 149].
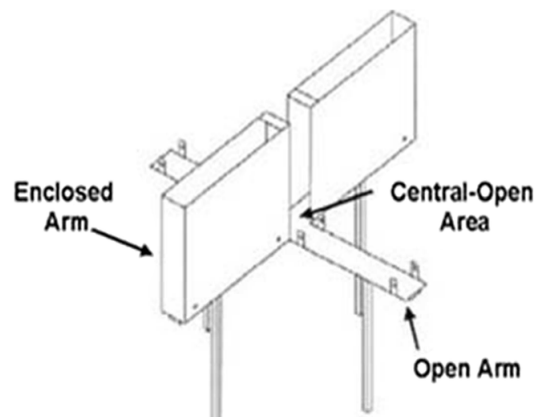
Fig. 2.4: Schema of elevated plus maze apparatus

2.33 Forced Swim Test

The forced swim test (FST) is one of the most commonly used assays for the study of depressive-like behavior in rodents [150]. Each mouse at a time was placed in an inescapable transparent tank that was filled with water, and the escape-related mobility behavior of the mouse was recorded. We used transparent Plexiglas cylindrical tanks (30 cm height x 20 cm diameters) for this study. The water level was 15 cm from the bottom, and the water temperature was 25 ± 2 °C. Each mouse was subjected to 6 min of swimming session with the last 5 min considered for the data analysis. We recorded immobility using a video-tracking system (Smart 3.0, Panlab SMART video tracking system, Harvard Apparatus) during this period. The mouse was considered to be immobile when it became static in the water without trying to escape. Those vital motions to hold its head above the water surface were not taken as immobile/static posture. We dried all the mice properly before returning to the cage. We also refilled the tank with fresh water after every experimental session [150, 151].

Fig. 2.5: Schema of forced swim apparatus

2.34 Tail Suspension Test

The Tail Suspension Test is a mouse behavioral test measuring depression-like behavior and learned helplessness [152]. The test is based on animals subjected to the short-term, inescapable stress of being suspended by their tail will develop an immobile posture. Our setup we used tail suspension boxes made of plastic with the dimensions (55 height X 60 width X 11.5 cm depth). The mouse was suspended in the middle of this compartment, and the approximate distance between the mouse's nose and the apparatus floor was 20-25 cm. An aluminium suspension bar (1 cm. height X 1 cm. width x 60 cm. length), used to suspend the tail of each mouse, was positioned on the top of the box. We adhered the mouse tail securely with the aluminium rod and recorded the mobility pattern for 6 minutes using a video-tracking system (Smart 3.0, Panlab SMART video tracking system, Harvard Apparatus). We considered last 5 minutes for the data analysis. During the analysis, we measured the immobile/static time the each mouse spent at the time of experiment. Small movements that are confined to the front legs but without the involvement of the hind legs were counted as immobility. Additionally, oscillations and pendulum-like swings that are due to the momentum gained during the earlier mobility

bouts were also excluded from the analysis. The apparatus was appropriately cleaned with 70% ethanol before and after every usage [152, 153].
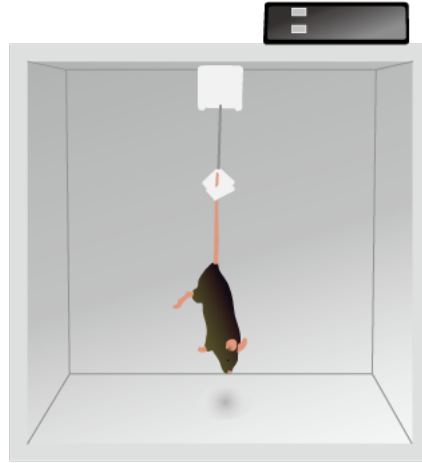
Fig. 2.6: Schema of tail suspension apparatus

2.35 Statistical Analysis

All the graphs were plotted using GraphPad Prism, version 9.0. t-test, One and Two-way ANOVA performed for statistical analysis of data as described in the figure legends. Bonferroni multiple comparison correction was performed for One and Two-way ANOVA.
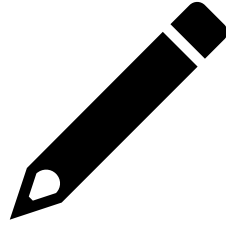
Chapter: 3

Effects of direct and indirect gut

microbial perturbations on host

physiology, immunity and metabolism

3.1 Introduction

The gut microbiota is considered one of the most "essential organ" of the human body [154–157]. Among all the physiological processes, gut microbiota plays the most crucial role in maintaining host immunity and metabolism [158]. Any alteration of gut microbial composition could affect the normal equilibrium of the host's immune responses and metabolism [159, 160]. So, to understand the role of a particular phylum or genus on host health, it is essential to modify the gut microbiota [161, 162]. Perturbation is probably the cleanest way to understand the effect of altered gut microbiota on host health [163–165].

Generally, the major gut microbial phyla include Firmicutes, Bacteroidetes, Actinobacteria, Proteobacteria, Fusobacteria, and Verrucomicrobia. Among the mentioned phyla, Firmicutes and Bacteroidetes constitute 80-90% of the gut community in a healthy condition. During the dysbiosis of gut microbiota, a drastic increase in the Proteobacteria phylum may cause an increase in the blood endotoxin level through LPS.

LPS could enhance the production of various pro-inflammatory cytokines by activating different Toll-Like Receptors (TLR4) of the gut epithelial cells [166–170].

The elevated LPS level is subsidized by the metabolic products of beneficial gut microbes. Gut microbes produce various essential metabolites, e.g., bile acids, branched amino acids, trimethylamine-N- oxide, tryptophan, indole derivatives, and, most importantly, short-chain fatty acids (SCFAs). Microbes produce SCFAs by metabolizing various dietary fibers in the host [171]. As the beneficiary effects of SCFAs, they could suppress the lipopolysaccharide (LPS) and pro-inflammatory cytokines like TNFα and IL-6 and increase the production of anti-inflammatory cytokines, IL-10 [172, 173].

To study the mechanical relationship between gut microbial dysbiosis and associated altered immune responses and metabolism, it is essential to perturb the gut microbiota externally. Antibiotics and other polysaccharides of microbial sources (e.g., DSS) act as potent perturbing agents and are used extensively for laboratory experiments. While, antibiotics are direct perturbing agents (DPA) but the DSS, which disturbs the gut epithelium structure first to affect the microbiome, is considered as indirect perturbing agent (iDPA) for gut microbes. We, therefore, hypothesized that different routes of gut microbial perturbation could control host immune responses and metabolism differentially.

In the current report, we compared the efficacy of perturbation of mouse gut microbiota by using different single antibiotics, by a cocktail of antibiotics, or by polysaccharide of the microbial source. We used individual antibiotics, e.g., neomycin, vancomycin, and a cocktail of antibiotics known as AVNM containing ampicillin, vancomycin, neomycin, and metronidazole as DPA. We used a sulfated polysaccharide, Dextran sulfate sodium (DSS) as iDPA. As stated elsewhere, all antibiotics directly target the gut microbiota and perturb it [174–176]. In contrast, DSS causes gut epithelial damage and inflammation, which ultimately causes gut microbial perturbation [177–179].

The current study revealed that the neomycin treatment caused the enrichment of the Bacteroidetes phylum, vancomycin treatment was responsible for the outgrowth of Verrucomicrobia and Proteobacteria phylum, AVNM and DSS both caused the enrichment of the phylum Proteobacteria. The outgrowth of Proteobacteria in the AVNM and DSS treated group caused permanent damage to the architecture of gut tissue, caused the leaky gut condition, and activated the severe pro-inflammatory responses. Activation

of the pro-inflammatory cascade ultimately hampered the production of SCFAs like butyrate and caused long-lasting health damage to the host.

3.2 Results

Gut microbial composition and diversity are the two critical factors in maintaining healthy gut homeostasis [180]. The degree of gut microbial dysbiosis depends on the dysbiotic agents' strength or the extent of dysbiosis and mode of action [113, 114].

In the current study, we used different perturbing agents with different strengths (in terms of the extent of dysbiosis) and modes of action to study the effect of differential gut dysbiosis on the host's physiology, immunity, and metabolism.

3.2.1 Treatment with different dysbiotic agents and their differential effects on gut dysbiosis

To perturb the healthy gut microbial composition and diversity differentially, we used different antibiotics as an individual dosage (neomycin and vancomycin) or as a cocktail (AVNM) and a sulfated polysaccharide (DSS) of microbial origin for different time scales. We continued the dosages at different time scales for different perturbing agents. We carried out the experiment until the point to determine whether there was a sign of gut microbial restoration in either of the mice strains.

For the neomycin and vancomycin treated groups, the treatment and experiment continued for 7 days in C57BL/6 and BALB/c. We continued the AVNM treatment for 7 days, followed by restoration. So the total experimental time scale was for 60 days. The treatment and the experiment were for 15 days for the DSS-treated group. We used a

comparatively higher dose for 1st 7 days, followed by a lower dosage of DSS for the last 7 days, to understand the dose-dependent gut microbial modulation of the host. A comparative analysis of differently altered gut microbiota due to different perturbing agents helped us understand its role in host immunity and metabolism.

The current study revealed that the degree of gut microbial dysbiosis depended on the dysbiotic agents' potentiality or harshness. The degree of dysbiosis and altered gut microbial composition was also highly dependent on the immune-genetic background of the host (Fig. 3.1). No significant changes was observed in the control group of both strains of mice with respect to time (Fig. 3.1A & B). So the changes we observed in gut microbial composition after treatment was the sole effect of the perturbing agents. Neomycin treatment for 7 days in C57BL/6 mice caused a significant increase in the Bacteroidetes phylum and a decrease in the Firmicutes phylum (Fig. 3.1C). The change was highest on day 3 of the antibiotic treatment in both Bacteroidetes (87%) and Firmicutes (12%) phylum (Fig. 3.1C). From day 4 onwards, the gut microbiota started recovering from the dysbiotic condition even in the presence of antibiotic treatment (Fig. 3.1C). In the case of BALB/c mice, the pattern of gut dysbiosis and restoration was remarkably different from C57BL/6 mice. There was a surge of Bacteroidetes (99%) phylum on day 2 of neomycin treatment in BALB/c and then immediately disappeared from day 3 of neomycin treatment (Fig. 3.1D). More interestingly, on day 7 of neomycin treatment, we observed the abundance of Verrucomicrobia phylum outnumbered the growth of all other phyla with an abundance of 98% (Fig. 3.1D). We considered it a sign of restoration.

Next, we treated the mice strain with a comparatively more potent antibiotic than neomycin, i.e., vancomycin. At first, vancomycin treatment caused an increase in Proteobacteria phylum in both C57BL/6 (Fig. 3.1E) and BALB/c (Fig. 3.1F) mice. In C57BL/6, we observed the highest abundance of Proteobacteria phylum on day 4 (abundance 82%) (Fig. 3.1E) of vancomycin treatment, whereas, in BALB/c, it was on day 6 (abundance 93%) (Fig. 3.1F). At the later stage of vancomycin treatment, the Proteobacteria phylum was replaced with the Verrucomicrobia phylum in both the mice strain. The abundance of Verrucomicrobia phylum was significantly higher on C57BL/6 than on the BALB/c mice. In C57BL/6, the outgrowth of the Verrucomicrobia phylum was observed from day 5 of Vancomycin treatment, with the highest abundance of 72% (Fig. 3.1E). Although Verrucomicrobia suppressed the growth of Proteobacteria on day 7 of vancomycin treatment, the abundance was significantly low in BALB/c (29%) (Fig. 3.1F) than in the C57BL/6 mice. We considered the overgrowth of the Verrucomicrobia phylum as the restoration process of the gut.

To know further the synergistic effect of multiple antibiotics on the dysbiosis pattern of the gut, we used a cocktail of four different antibiotics, i.e., AVNM (Ampicillin-Vancomycin-Neomycin-Metronidazole). Like the other two antibiotics, we continued the dose of AVNM for 7 days and found the synergistic effect of all four antibiotics was notably higher in terms of gut microbial dysbiosis. The harmful Proteobacteria phylum continued to outgrow other phyla until we withdrew the AVNM treatment after 7 days in both mice strains. Proteobacteria level was around 80% in C57BL/6 (Fig. 3.1G) and 70% in BALB/c (Fig. 3.1H) on day 7 of AVNM treatment. Phylum Bacteroidetes and Firmicutes started overgrowing after the withdrawal of AVNM treatment in both the mice

strains (Fig. 3.1G & H). But at the later stage of restoration that was on the 60th day of the experiment, we found in C57BL/6, both Bacteroidetes and Firmicutes phyla grow together with an equal abundance (Fig. 3.1G), whereas in BALB/c, Firmicutes level was considerably higher at the end of the experiment (Fig. 3.1H).

To investigate whether the degree of gut dysbiosis depends on the type of the chemical nature of the dysbiotic agent, we used a sulfated Polysaccharide, DSS. In this case, we continued the dose for 15 days in both the mice strain. Unlike the antibiotics, we haven't found the outgrowth of a particular phylum till day 7 in both the mice strains, so we continued the dose till day 15 to observe the overgrowth of a specific phylum with the prolonged treatment condition. However, the scenario was different in this case; we haven't found the outgrowth of particular phylum; instead, all 4 major phyla changed their abundance level to an extent throughout the treatment conditions in both C57BL/6 (Fig. 3.1I) and BALB/c (Fig. 3.1J) mice. There was no sign of restoration in C57BL/6 mice even on day 15 of DSS treatment; instead, the phylum Proteobacteria increased its abundance with time (Fig. 3.1I). We stopped the DSS experiment on day 15 because BALB/c started recovering from the dysbiotic condition by replacing the harmful Proteobacteria phylum with the beneficial Verrucomicrobia phylum (Fig. 3.1J), which was almost nil in C57BL/6 (Fig. 3.1I) on day 15 of DSS treatment.

A detailed statistical analysis considering time, treatment and genotype together is incorporated in the appendix section (Fig. S1) to understand how all the three factors together controlling the extent of perturbation.

3.2.2 Effect of gut microbial dysbiosis on blood glucose level

There are well-established correlational studies that increased Proteobacteria level in the gut is responsible for a high blood glucose level of the host and cause diseases like type 2 diabetes [181, 182]. The negative effect of Proteobacteria used to be nullified by the phylum Verrucomicrobia, responsible for controlling the blood glucose level of the host [129, 183, 184]. For an in-depth understanding of this fact, we chose only those two groups of mice, i.e., vancomycin treated and DSS treated mice, where the higher Proteobacteria level of the dysbiotic condition was replaced by the phylum Verrucomicrobia at the restoration phase in either group of mice strain. We quantified the blood glucose level on the 0, 3rd, and 7th days of Vancomycin treatment and 0, $7^{th,}$ and 15th days of DSS treatment in both the strains of mice. We measured the fasting glucose level and the glucose levels of 15mins, 45mins, and 90mins of post glucose administration. On day 3 of Vancomycin treatment, when the Proteobacteria level was high, the blood glucose level was higher in both C57BL/6 and BALB/c mice (Fig. 3.1K). The scenario was the opposite on day 7. A higher abundance of Verrucomicrobia was sufficient to control the blood glucose level of both C57BL/6 and BALB/c mice (Fig. 3.1K). In DSS treated mice, only in BALB/c mice, the Proteobacteria phylum was replaced with the Verrucomicrobia phylum but not in C57BL/6 mice. Our oral glucose tolerance test also corroborated with the gut microbiota data. On day 7 of DSS treatment, when the Proteobacteria level was high, both the strains had similar blood glucose levels (Fig. 3.1L). Whereas on day 15 of DSS treatment, the higher abundance of Verrucomicrobia in BALB/c compared to C57BL/6 mice was able to control the blood glucose level of the host (Fig. 3.1L). The absence of Verrucomicrobia phylum in

C57BL/6 was probably the main reason for the higher glucose level on day 15 of DSS treatment (Fig. 3.1L).

In BALB/c, irrespective of the potentiality of the dysbiotic agents at some particular point of the experimental setup, the abundance of Verrucomocrobia phylum increased. So, the pattern of restoration was similar in either of the dysbiotic agent. The scenario was different in C57BL/6. Only in the vancomycin treated group, we observed the outgrowth of the Verrucomicrobia phylum at the later stage of the antibiotic treatment. This fascinating result intended us to dig deeper into how the differential gut microbial pattern controls immunity and metabolism in C57BL/6 mice.
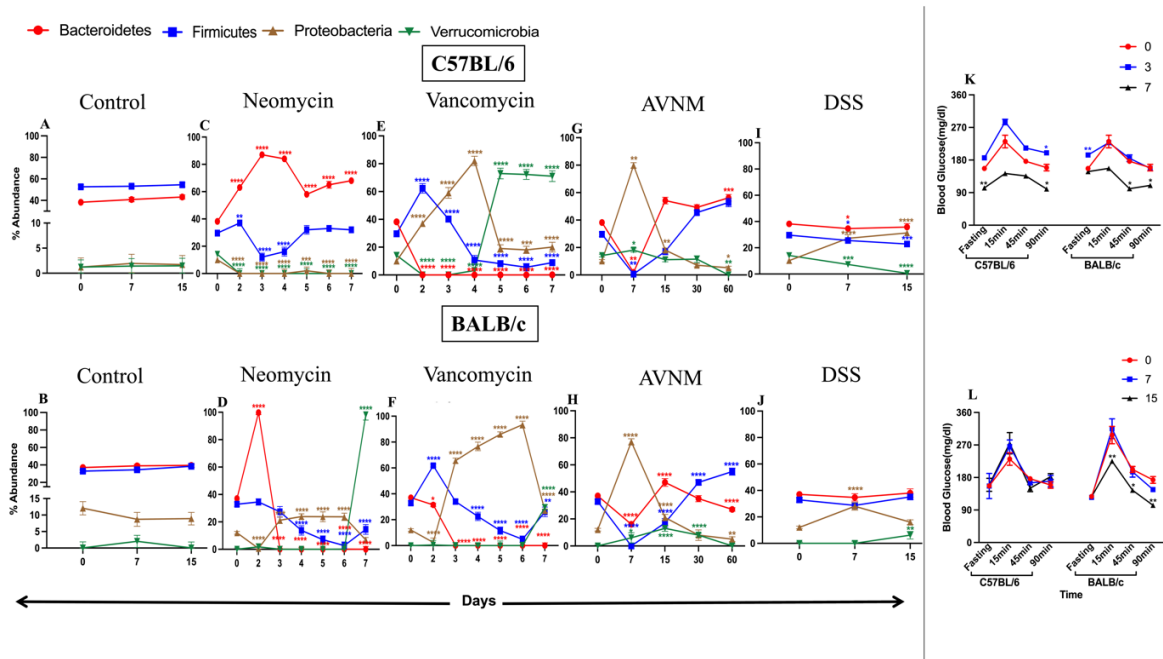
Fig. 3.1: Effect of different perturbing agents on gut microbial composition at phylum level and changes in the glucose sensitivity of the host due to altered gut microbial composition.

Kinetics of gut microbial changes of C57BL/6 and BALB/c mice followed by different antibiotics and chemical treatment at different time scales. Altered phylum level changes of C57BL/6 and BALB/c mice in the control condition (A, B) and followed by neomycin (C, D), vancomycin (E, f), AVNM (G, H), and DSS treatment (I, J). A, B represented the gut microbial composition in the control condition of C57BL/6 (A) and BALB/c (B) mice. C, D represented the alteration of the gut microbial composition followed by neomycin treatment in C57BL/6 (C) and BALB/c (D) mice. E, F represented the alteration of the gut microbial composition followed by vancomycin treatment in C57BL/6 (E) and BALB/c (F) mice. Gut microbial alteration of C57BL/6 (G) and BALB/c (H) mice, followed by antibiotic cocktail (AVNM) treatment, was examined. The effect of a potent chemical (DSS) on gut microbial composition was also observed in C57BL/6 (I) and BALB/c (J) mice.

Changes in the glucose sensitivity level were measured in C57BL/6 and BALB/c mice due to altered microbial composition. Panel (K) represented the changes in glucose sensitivity level followed by vancomycin treatment in C57BL/6 and BALB/c mice. Panel (L) represented the changes in glucose sensitivity level followed by DSS treatment in C57BL/6 and BALB/c mice.

Statistical significance was calculated by day 0 with each treatment condition using one-way ANOVA followed by the Bonferroni test. '*' corresponds to $P \leq 0.05$, ** corresponds to $P \leq 0.01$, *** corresponds to $P \leq 0.001$, **** corresponds to $P \leq 0.0001$. Error bars are shown as standard deviation from the mean value of three replicates (n = 3) for microbiome data and six replicates (n = 6) for the glucose sensitivity test.

3.2.3 Changes in gut microbial composition and diversity in C57BL/6 mice followed by the treatment of different gut microbial perturbing agents for a week

For a week, we treated the mice with four different gut perturbing agents (neomycin, vancomycin, AVNM, DSS) and studied the gut microbial composition on day 7. Observation from the current study revealed that the gut microbiota of untreated C57BL/6 mice was majorly composed of Firmicutes and Bacteroidetes phyla with a negligible percentage of Proteobacteria phylum (Fig 2A). Modulation of gut microbiota using neomycin treatment for a week caused an increase in Bacteroidetes (by 68%) and a decrease in phylum Firmicutes (by 32%) (Fig. 3.2A & Table 3.1).

On the other hand, treatment with vancomycin for the same period caused a significant increase in the phyla Verrucomicobia (by 72%) and Proteobacteria (by 20%) with a concomitant decrease in the other two major phyla Firmicutes and Bacteroidetes

In accordance, the antibiotic cocktail, AVNM, caused the outgrowth of Proteobacteria (by 80%) phylum (Fig. 3.2A & Table 3.1). Perturbation of gut microbiota with DSS for a week caused an increase of the harmful Proteobacteria phylum (by 28%) and decreased the growth of the useful Firmicutes phylum (by 25%) (Fig. 3.2A & Table 3.1).

Table. 3.1: Percent relative abundance of major phyla during control and various level of treatment conditions of the gut in C57BL/6 mice.

	% Abundance (±SD)			
	Firmicutes	Bacteroidetes	Proteobacteria	Verrucomicrobia
Control	52(±5)	38(±4)	1.8(±0.3)	1.2(±0.4)
Vancomycin	9(±2)	NIL	20(±4)	71(±6)
Significance	****	****	****	****
Neomycin	23(±4)	72(±5)	1(±0.5)	NIL
Significance	**	****	****	****
AVNM	NIL	2(±0.9)	80(±4)	18(±3)
Significance	****	***	****	**
DSS	25.55(±1.7)	34.60(±2)	27.21(±2.6)	7.31(±2)
Significance	**	*	****	***

Statistical significance was calculated between the control and each treatment condition using one-way ANOVA followed by the Bonferroni test. '*' corresponds to $P \leq 0.05$, ** corresponds to $P \leq 0.01$, *** corresponds to $P \leq 0.001$, **** corresponds to $P \leq 0.0001$, NS corresponds to non-significant.

The table represents the mean of the percent relative abundance of gut microbial phyla (n= 3) with standard deviations (±SD).

We analyzed the gut microbial composition at the genus level to further validate the phylum level observation. The major changes in genus level of gut microbiota showed that i) neomycin treatment caused an increase in the *Bacteroides* genus of Bacteroidetes phylum, ii) vancomycin treatment caused an increase in the *Akkermansia* genus of the Verrucomicrobia phylum, iii) AVNM treatment showed an elevation of *Escherichia-Shigella* genera of Proteobacteria phylum and iv) DSS treatment was responsible for overgrowth of *Helicobacter* genus of Proteobacteria phylum (Fig. 3.2B & Table 3.2).

Table. 3.2: *Percent relative abundance of major genus during control and various level of treatment conditions of the gut in C57BL/6 mice.*

% Abundance (±SD)

	A	B	C	D	E	F	G	H	I	J	K	L	M
Control	21.78 (±2.6)	37.41 (±2.0)	11.30 (±1.7)	9.10 (±1.6)	2.43 (±1.9)	NIL	3.09 (±1.5)	3.16 (±2.1)	4.56 (±3.0)	NIL	NIL	4.30 (±1.9)	NIL
Vancomycin	NIL	NIL	NIL	NIL	NIL	67.00 (±1.8)	NIL	2.00 (±1.2)	NIL	18.00 (±2.6)	12.00 (±2.5)	NIL	NIL
Significance	***	***	**	**	*	****	*	NS	*	**	**	*	NS
Neomycin	NIL	1.00	NIL	NIL	NIL	NIL	NIL	NIL	NIL	NIL	NIL	80.00 (±3.3)	NIL
Significance	***	***	**	**	*	NS	*	*	*	NS	NS	****	NS
AVNM	NIL	NIL	NIL	NIL	NIL	8.00 (±3.1)	NIL	NIL	NIL	78.00 (±2.4)	NIL	NIL	NIL
Significance	***	***	**	**	*	*	*	*	*	****	NS	*	NS
DSS	NIL	NIL	2.71 (±2)	NIL	51.97 (±2.6)	3.22 (±1.7)	NIL	NIL	NIL	NIL	NIL	5.54 (±2.6)	6.41 (±2.6)
Significance	***	***	*	**	***	*	*	*	*	NS	NS	*	**

Statistical significance was calculated between the control and each treatment condition using one-way ANOVA followed by the Bonferroni test. '*' corresponds to $P \leq 0.05$, ** corresponds to $P \leq 0.01$, *** corresponds to $P \leq 0.001$, **** corresponds to $P \leq 0.0001$, NS corresponds to non-significant.

The table represents the mean of the percent relative abundance of gut microbial Genus (n= 3) with standard deviations (±SD).

(**A-***Blautia*, **B-***Intestinimonas*, **C-***Alistipes*, **D-***Oscillibacter*, **E-***Helicobacter*, **F-***Akkermansia*, **G-***Anaerotruncus*, **H-***Desulfovibrio*, **I-***Incertae_Sedis*, **J-***Escherichia-Shigella*, **K-***Lactobacillus*, **L-***Bacteroides*, **M-***Lachnospiraceae*)

Alteration of gut microbial diversity is one of the most critical factors in understanding the extent of gut perturbation [185, 186]. Our current study observed an altered alpha diversity in phylum (Fig. 3.2C) and genus (Fig. 3.2D) levels for all the treatment conditions. We calculated the Shannon Diversity Index and observed the most affected microbial diversity in the vancomycin and AVNM treated group in phylum (Fig. 3.2C) and genus (Fig. 3.2D) levels compared to the control condition. Neomycin and DSS treated groups showed comparatively higher gut microbial diversity than vancomycin and AVNM treated groups in phylum (Fig. 3.2C) and genus (Fig. 3.2D) levels.

The altered B/F (Bacteroidetes/ Firmicutes) ratio is another prominent signature of altered gut microbial composition and diversity [187, 188]. We calculated the B/F ratio of all the treatment conditions. The highest B/F ratio was observed in the neomycin treated group due to outgrowth of Bacteroidetes phylum, and the lowest was in AVNM treated group (Fig. 3.2E).
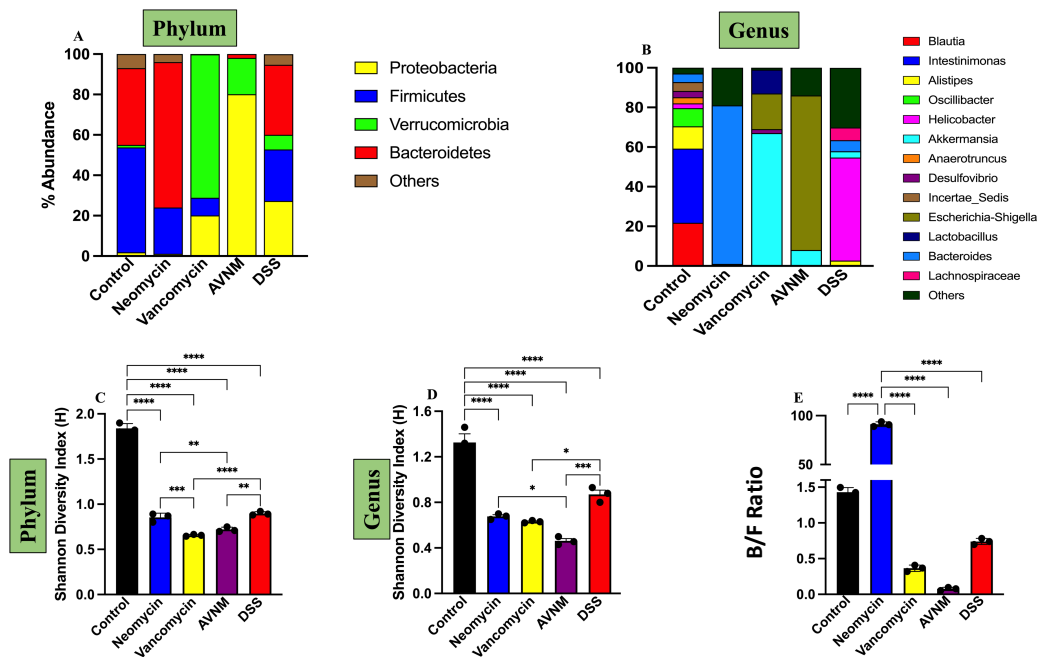
Fig. 3.2: Altered gut microbial composition and diversity at phylum and genus level for control and treated C57BL/6 mice.

Percent abundance of the gut microbial composition in untreated (control) and treated (vancomycin, neomycin, AVNM, DSS) C57BL/6 mice at phylum (A) and genus (B) level following 7 days of treatment. The percent abundance was calculated from the average values of at least 3 replicates.

Altered gut microbial diversity (Shannon diversity index) in phylum (C) and genus (D) level was calculated as the effect of altered gut microbial composition.

We also calculated the B/F (Bacteroidetes/ Firmicutes) ratio of control and treated C57BL/6 mice.

We calculated the statistical significance by comparing the values of the treated groups at various time points with their respective control groups and between the different treatment conditions through two-way ANOVA followed by the Bonferroni test. ''*

*corresponds to P ≤ 0.05, ** corresponds to P ≤ 0.01, *** corresponds to P ≤ 0.001, ****
corresponds to P ≤ 0.0001. Error bars are shown as standard deviation from the mean
value of three replicates (n = 3).*

3.2.4 Altered host physiology could be the effect of gut microbial dysbiosis

Changes in the host's physiology are another critical aspect to look for due to gut
microbial dysbiosis [121, 129]. We monitored the body weight and water intake on an
everyday basis, and other physiological changes at the end of the treatment.

We observed gradual weight loss only in DSS treated group throughout the treatment
condition compared to their time matched control (Fig. 3.3A & Table. 3.3). No weight
loss or gain was noticed in the antibiotic treated group compared to the control condition
(Fig. 3.3A & Table. 3.3).

*Table. 3.3: Day-wise change in body weight (in %) of C57BL/6 mice in various treatment
conditions.*

Days	Control	Neomycin	Vancomycin	AVNM	DSS
1	0	0	0	0	0
2	0.25 (±0.03)	0.26(±0.02)	0.27(±0.02)	0.26(±0.03)	-0.50(±0.09)
	NS	NS	NS	NS	*
3	0.38(±0.06)	0.29(±0.01)	0.31(±0.06)	0.32(±0.06)	-0.77(±0.10)
	NS	NS	NS	NS	**

4	0.41(±0.09)	0.32(±0.04)	0.33(±0.03)	0.30(±0.01)	-1.00(±0.07)
	NS	NS	NS	NS	**
5	0.48(±0.01)	0.37(±0.02)	0.41(±0.06)	0.39(±0.03)	-1.92(±0.11)
	NS	NS	NS	NS	**
6	0.52(±0.03)	0.42(±0.05)	0.56(±0.03)	0.49(±0.03)	-2.91(±0.17)
	NS	NS	NS	NS	**
7	0.57(±0.05)	0.49(±0.05)	0.57(±0.03)	0.58(±0.05)	-3.91(±0.30)
	NS	NS	NS	NS	**

We presented data as the means± SD (n=6). We calculated the statistical significance by comparing the values of the treated groups at various time points with their respective time matched control groups. We used Two-way ANOVA followed by the Bonferroni test to determine the significance level for all analyses. '*' corresponds to $P \leq 0.05$, ** corresponds to $P \leq 0.01$, *** corresponds to $P \leq 0.001$, **** corresponds to $P \leq 0.0001$, NS to corresponds non-significant.

We also measured the water intake of all the groups on an everyday basis. Although the DSS treated group's water intake was comparatively higher than the control and antibiotic treated group, there was nothing significant to mention (Fig. 3.3B & Table. 3.4).

Table. 3.4: *Day-wise water consumption (ml) of C57BL/6 mice in various treatment conditions.*

Days	Control	Neomycin	Vancomycin	AVNM	DSS
1	3.66(±1.15)	4.00(±1.00)	4.00(±1.00)	4.33(±0.57)	5.00(±1.00)
2	3.66 (±0.57)	3.66(±1.15)	4.00(±1.00)	4.00(±1.00)	6.00(±1.00)
	NS	NS	NS	NS	NS
3	3.66(±1.15)	3.66(±1.15)	4.00(±1.00)	3.66 (±0.57)	6.00(±1.00)
	NS	NS	NS	NS	NS
4	3.66 (±0.57)	3.66 (±0.57)	3.66(±1.15)	4.00(±1.00)	6.00(±1.00)
	NS	NS	NS	NS	NS
5	3.66(±1.15)	4.00(±1.00)	3.66 (±0.57)	3.66 (±0.57)	6.33(±1.15)
	NS	NS	NS	NS	NS
6	4.00(±1.00)	3.66 (±0.57)	4.00(±1.00)	4.33(±1.15)	6.00(±1.00)
	NS	NS	NS	NS	NS
7	4.00(±1.00)	3.66 (±0.57)	3.66 (±0.57)	4.33(±0.57)	6.66(±1.15)
	NS	NS	NS	NS	NS

We presented data as the means± SD (n=6). We calculated the statistical significance by comparing the values of the treated groups at various time points with their respective time matched control groups. We used Two-way ANOVA followed by the Bonferroni test to determine the significance level for all analyses. NS corresponds to non-significant.

We noticed some other physiological changes only in DSS treated group, i.e., changes in colon length, spleen size, and the amount of peritoneal fat, which were not seen in the control or antibiotic treated group. We observed the shortening of colon length in the DSS treated group compared to the other groups (Fig. 3.3C). Enlargement of the spleen was also observed after DSS treatment. We calculated the % of spleen index (spleen weight/ body weight) and found the spleen index was significantly higher in DSS treated group compared to the other groups (Fig. 3.3D). Increased peritoneal fat was another physiological anomaly observed in DSS treated group. The % of peritoneal fat index (peritoneal fat weight/ body weight) was also higher in DSS treated group compared to the other groups (Fig. 3.3E). Although none of those mentioned above changes in physiology were observed in the antibiotic treated group, noticeable changes were observed in the cecum weight of antibiotic treated groups. We calculated the cecal index (cecal weight/ body weight) and found a significant difference in the cecal index of all the antibiotic treated groups compared to the control and DSS treated groups. The changes in the cecal index were almost in AVNM and vancomycin treated groups and comparatively lower in the neomycin treated group (Fig. 3.3F).
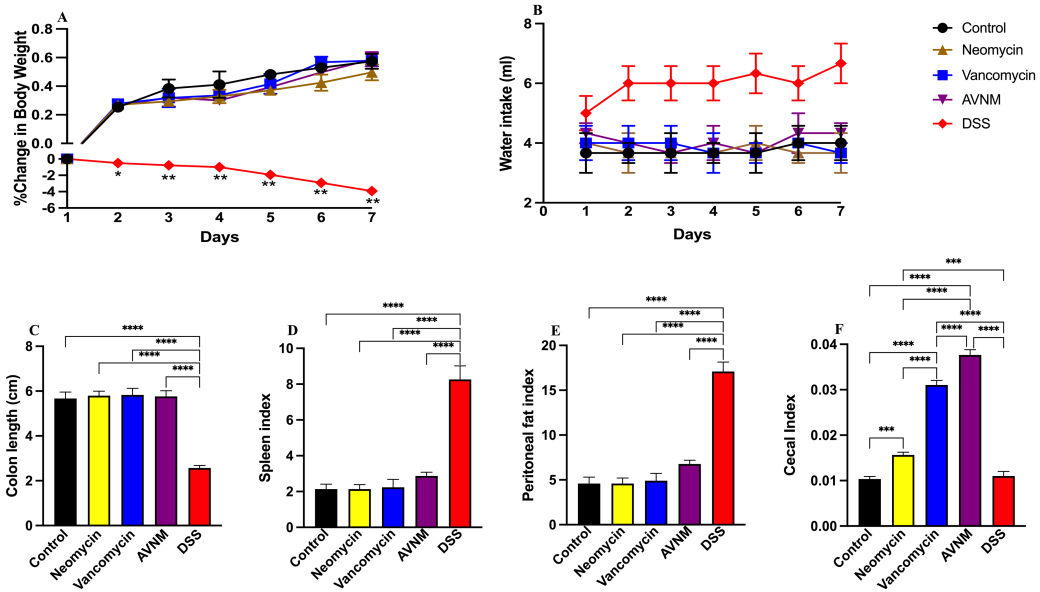
Fig. 3.3: Phenotypic changes in host following treatment with various perturbing agents.

(A) We measured the bodyweight of C57BL/6 mice every other day and plotted the % change in control and treated groups until day 7. (B) We measured water intake (in ml) of C57BL/6 mice every day for 7 days. We observed the changes in (C) Colon lengths (in cm), (D) % Spleen indices (spleen weight/body weight), (E) % Peritoneal fat indices (Peritoneal fat weight/body weight), and (F) Cecal indices (Cecal weight/body weight) between control and treated C57BL/6 mice.

We presented data as the means± SD (n=6). We used Two-way ANOVA followed by the Bonferroni test to determine the significance level for all analyses. '*' corresponds to P ≤ 0.05, ** corresponds to P ≤ 0.01, *** corresponds to P ≤ 0.001, **** corresponds to P ≤ 0.0001.

3.2.5 Histopathological assessment of gut section and alteration of gut barrier integrity

To get an idea of whether gut dysbiosis causes any changes in the morphology of gut tissue, we performed H&E staining and Alcian blue/PAS staining of the colon sections of all the control and treated groups of mice (Fig. 3.4A-J). From the histopathological analysis, we found neomycin (Fig. 3.4B & G) and vancomycin (Fig. 3.4C & H) treatment was not potent enough to change the colon tissue architecture of the host. AVNM treatment was comparatively harsh, and the changes in tissue architecture were easily differentiable compared to the control group and neomycin and vancomycin treated group (Fig. 3.4D & I). The highest changes were observed in DSS treated group. DSS treatment was potent enough to completely destroy the normal colon tissue morphology (Fig. 3.4E & J).

H&E staining of colon section of control (Fig. 3.4A), neomycin (Fig. 3.4B), and vancomycin (Fig. 3.4C) treatment revealed intact epithelium, well-defined crypt length, absence of edema, neutrophil infiltration in mucosa and submucosa, and any ulcers or lesions. Alcian blue/PAS staining showed sufficient no. of goblet cells and the intact mucus layer in control (Fig. 3.4F), neomycin (Fig. 3.4G), and vancomycin (Fig. 3.4H) treated group. In contrast, AVNM treatment destroyed epithelium, shortening crypt length, neutrophil infiltration in the mucosa (Fig. 3.4D), and loss of goblet cells and mucus layer (Fig. 3.4I). Changes in the DSS treated group was more severe, such as ulcers, lesions, shortening, loss of crypts in the whole colon, edema, neutrophil infiltration in mucosa and submucosa (Fig. 3.4E), complete loss of goblet cells and mucus

layer (Fig. 3.4J). We evaluated the severity of histopathological changes considering the parameter mentioned in Table. 3.5 and scored them accordingly. The histopathological score was highest in DSS treated group, followed by AVNM treated group (Fig. 3.4K). Higher histopathological scores revealed severe inflammatory lesions and epithelial injury, leading to epithelial cell barrier function loss in the gut [189]. We measured the gut integrity in mice treated and controlled groups to establish the compromised gut barrier function. We quantified the extent of loss of gut barrier integrity using the FITC-Dextran assay. The amount of FITC-Dextran in serum is equally proportional to the loss of gut barrier integrity. The gut-barrier integrity data supported the histopathological data. The highest loss of gut integrity was observed in DSS treated group, followed by AVNM treated group compared to the control, neomycin, and vancomycin treated group (Fig. 3.4L).

Tight junction proteins such as ZO-1, Occludin, and Claudin- 1 & 2 play a very crucial role in maintaining the gut barrier integrity of the host [190–192]. Therefore, we measured the transcription level changes of the genes responsible for maintaining gut integrity. ZO-1, Ocln, and Cldn1 are downregulated genes in leaky gut conditions, whereas Cldn2 is highly expressed in the leaky gut. We observed that ZO-1, Ocln, and Cldn1 expressions were downregulated, and Cldn2 was overexpressed only in AVNM and DSS treated groups with respect to untreated control group (Fig. 3.4M).
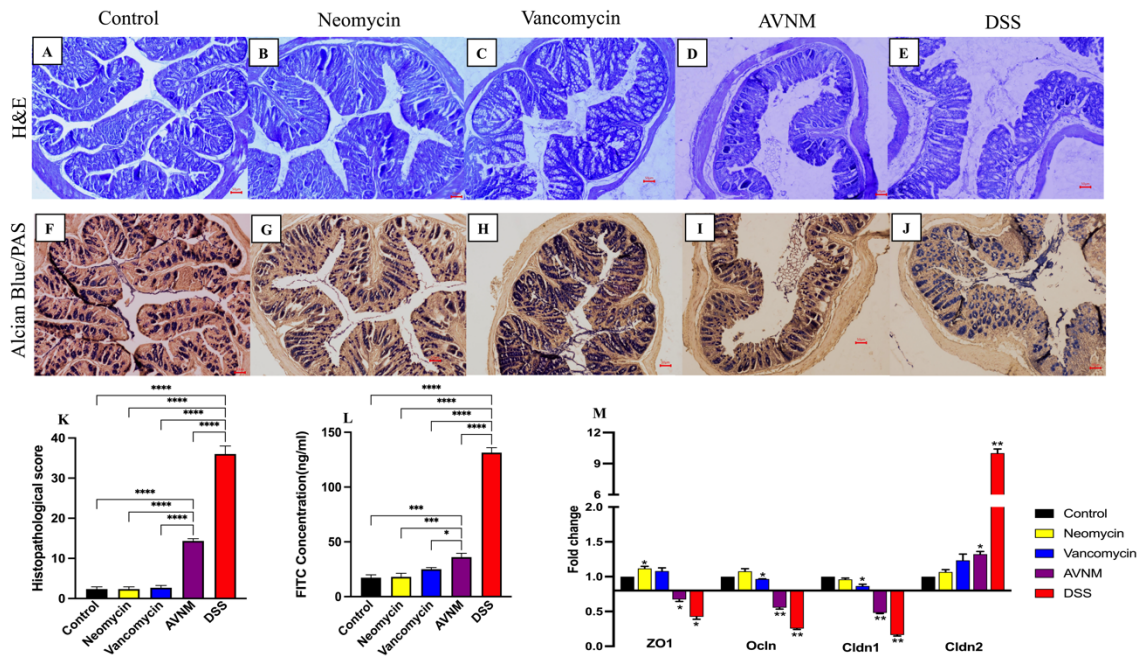
Fig. 3.4: Colon histopathology and intestinal barrier function following different treatment conditions in C57BL/6 mice.

We performed H&E staining (A-E) and Alcian Blue/PAS staining (F-J) of colon sections of control and treated C57BL/6 mice to measure the changes in epithelium and mucosal architecture and inflammatory cell infiltration. The image of the histological section of the colon via bright-field microscopy at 20X. We showed (K) histopathological scoring (H) changes in gut permeability by measuring the FITC-Dextran concentration from serum and changes in the mRNA expression of tight junction genes from colon samples in control and treated C57BL/6 mice.

We presented data as the means± SD (n=6). We performed two-way ANOVA for histopathological scoring and FITC-Dextran concentration data followed by the Bonferroni test to determine the significance level. To determine the significance level of mRNA expression data, we performed t-test. '*' corresponds to $P \leq 0.05$, ** corresponds

to $P \leq 0.01$, *** corresponds to $P \leq 0.001$, **** corresponds to $P \leq 0.0001$. (For histological analysis, pictures were taken with a magnification of 20X, scale bar 100µm).

3.2.6 Inflammatory changes in the gut due to gut microbial perturbation

Altered gut microbial composition and diversity are also responsible for altered immune gene functions in the gut. Different immune genes are either upregulated or downregulated based on the activation of the inflammatory status of the host after gut microbial dysbiosis [188, 193–195]. We measured the transcription level changes of immune genes, i.e., TNF- α, IFN-γ, IL-10 from the colon tissue. The TNF- α was upregulated in all the four treated conditions with respect to untreated control group, and expression was highest in DSS treated group (Fig. 3.5A). The IFN-γ level was upregulated only in neomycin and DSS treated group with respect to untreated control group (Fig. 3.5A). IL-10 level was also upregulated in all the groups except the AVNM, and DSS treated groups. IL-10 expression was downregulated in DSS treated mice, and no changes were observed in AVNM treated mice with respect to untreated control group (Fig. 3.5A).

To further validate the transcription level changes in the colon, we measured the protein level changes of the same cytokines in the colon and from the systemic level, i.e., in serum. Although we haven't found any significant changes in the cytokine expressions in transcription level in case of certain treatment conditions, but significant changes were observed in protein levels compared to the control condition. At the tissue level, TNF-α level was significantly upregulated in the AVNM and DSS treated group (Fig. 3.5B), whereas it was upregulated at the serum level for all the treatment conditions (Fig. 3.5C)

compared to the control condition. On the other hand, the IFN-γ level was significantly upregulated in all the treatment conditions at tissue (Fig. 3.5B) and systemic (Fig. 3.5C) levels compared to the control. IL-10 level was significantly upregulated only in the neomycin and vancomycin treated group at tissue (Fig. 3.5B) and serum (Fig. 3.5C) levels. In DSS treated group, IL-10 was significantly downregulated only at the tissue level (Fig. 3.5B) compared to the control.

3.2.7 Variation in the SCFA production after gut microbial perturbation

Gut is the main production hub for short chain fatty acids (SCFA) which are ultimately transported to the systemic level of the host. Gut microbiota is the major source of most of the SCFAs. The dysbiotic condition of the gut is one of the major rate-limiting steps for altered SCFAs productions [196–198]. Phylum Bacteroidetes is responsible for acetate and propionate production [171, 198]. We observed a high abundance of Bacteroidetes phylum in the neomycin treated condition. As a consequence, we observed the highest amount of serum acetate and propionate in the neomycin treated group compared to the other treatment conditions (Fig. 3.5D). Verrucomicrobia phylum is also responsible for propionate production [171, 199]. The high abundance of Verrucomicrobia in the vancomycin treated group was probably responsible for propionate production (Fig. 3.5D). Butyrate is produced mainly by Firmicutes [171]. The lower abundance of Firmicutes in all the treatment conditions due to dysbiosis was probably the main reason for lesser butyrate production in all the treatment conditions (Fig. 3.5D).
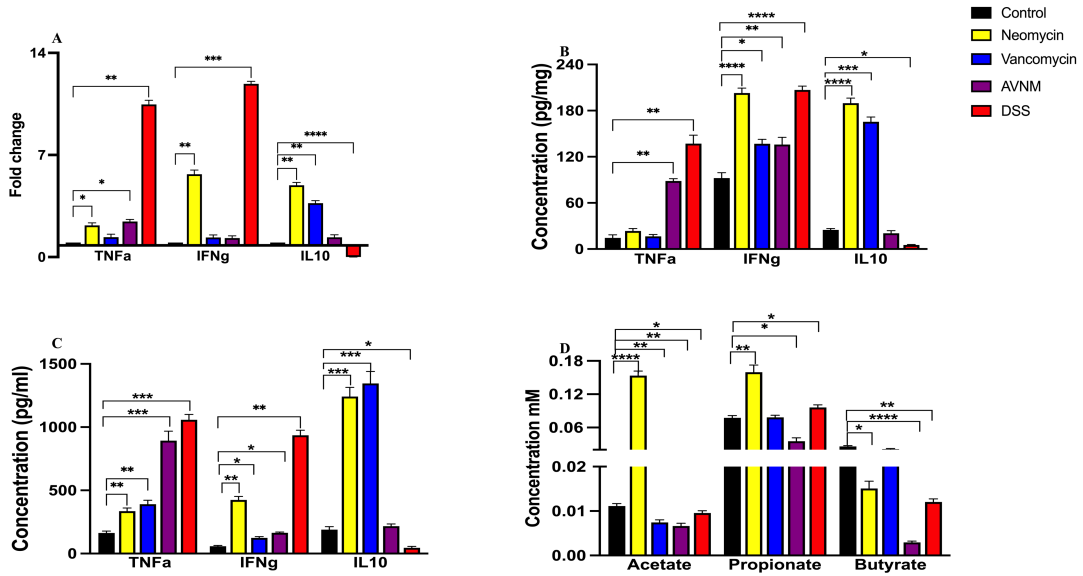
Fig. 3.5: *Expression of transcriptional and protein level inflammatory markers and abundance of short chain fatty acids in colon tissue and serum level in control and treated C57BL/6 mice.*

We quantify the changes in transcriptional expressions of inflammatory markers (A) TNFα, IFNγ & IL10 genes from the colon of control and treated C57BL/6 mice. We presented all values as means± SD for 3 biological replicates. We measured the protein level expression of the inflammatory markers (TNFα, IFNγ & IL10) from colon tissue (B) and serum samples (C) of control and treated C57BL/6 mice.

Changes in the short chain fatty acid level from serum were measured due to altered gut microbial composition and inflammatory status of the host. We measured acetate, propionate, and butyrate levels from serum samples (D) of control and treated C57BL/6 mice.

We presented data as means± SD (n=6). We performed t-test to determine the significance level. '' corresponds to P ≤ 0.05, ** corresponds to P ≤ 0.01, *** corresponds to P ≤ 0.001, **** corresponds to P ≤ 0.0001.*

3.3 Discussion

The pattern of dysbiosis varied significantly among different perturbing agents. Dysbiosis patterns depend on the chemical nature of the agents or the mode of action of perturbation [113, 114]. The kinetics of gut dysbiosis and the capacity to restore to the normal condition also depend on the host's immune-genetic background [115, 116]. In the current study, we started our experiment with two differently immune-biased mice to observe the effect of the same gut perturbing agent in two different mice strains, i.e., Th1- biased C57BL/6 and Th2- biased BALB/c mice. Data from the current study revealed that although the kinetics of dysbiosis or the composition of the perturbed gut microbiota was similar in both the mice strains, the restoration capacity was comparatively better in Th2-biased BALB/c mice. In BALB/c, gut microbiota composition was similar following restoration, irrespective of the types of dysbiotic agents. Phylum Verrucomicrobia ruled the gut at the end of all the treatment conditions. On the contrary, in C57BL/6 mice, the restoration phenomenon was very much dependent on the strength of the perturbing agents. When we treated the C57BL/6 mice with either neomycin or vancomycin, we noticed the restoration of the gut microbiota within a week, even in the presence of the perturbing agents. The AVNM treated group requires almost double the treatment time to restore normal conditions. In the DSS treated group, although BALB/c started restoring

from the dysbiotic state even in the DSS treatment, C57BL/6 could not. The more tolerogenic background of the BALB/c was probably one of the main reasons for such exciting results.

We observed an interesting pattern of gut dysbiosis irrespective of mice strains. Either individual antibiotic or the cocktail was responsible for enriching a particular phylum upon perturbation. For example, we observed a significant increase in the Verrucomicrobia phylum following treatment with vancomycin. The treatment with neomycin, on the contrary, yielded an enhanced Bacteroidetes phylum, while AVNM treatment led to the rise in Proteobacteria phylum. In contrast, DSS treatment was able to modify the abundance of all the major phyla, such as Firmicutes, Bacteroidetes, Proteobacteria, and Verrucomicrobia, of gut microbiota upon perturbation., Further studies are needed to establish the reasons of differential perturbation.

We noticed another enthralling trend in the restoration pattern in vancomycin and DSS treated C57BL/6 and BALB/c mice. The restoration trend was opposite in C57BL/6 and BALB/c in vancomycin and DSS treatment. In vancomycin treated C57BL/6, the Verrucomicrobia level (72%) was significantly higher than BALB/c (20%) at the end of the treatment. On the other hand, in DSS treated BALB/c, the Verrucomicrobial abundance (7%) was significantly higher than C57BL/6 (0%). This observation prompted us to study the role of the Verrucomicrobia in host physiology in a better way.

A previous study from our laboratory already reported that the phylum Verrucomicrobia is responsible for better glucose metabolism and insulin sensitivity [129]. To check whether the outgrowth of Verrucomicrobia in vancomycin treated C57BL/6 and DSS treated BALB/c was responsible for better glucose metabolism or not, we performed the

oral glucose tolerance test. Results supported our previous observation. We observed a higher glucose metabolism rate at the point when the Verrucomicrobia level was higher.

The differential restoration pattern of C57BL/6 intended us to study its effect on immune response and metabolism. On the other hand, the similar restoration pattern of BALB/c, irrespective of perturbing agents, forced us to discard it for further investigation.

Traditionally AVNM is taken as one of the standard gut microbial depletion agents and is responsible for the extensive loss of gut microbial diversity [200–203]. The current report observed the lowest gut microbial diversity at the genus level in AVNM treated C57BL/6 mice. More interestingly, the loss of microbial diversity was significantly higher in antibiotic treated groups compared to the DSS treated mice.

Previously it was reported that perturbation of gut microbiota related to other physiological changes of the host, such as loss or gain of body weight, changes in water intake, changes in the spleen, colon and cecum size, etc [121, 129]. The current treatment conditions also observed different physiological changes in mice, such as decreased bodyweight, shorter colon length, high spleen and peritoneal fat index in DSS treated mice, and high cecal index in antibiotics treated mice.

Altered gut microbial composition is responsible for mucosal barrier dysfunction and activation of inflammatory responses, ultimately predisposing host animals to systemic diseases [190–192, 204]. As a consequence of altered gut microbial composition, we investigated the histopathological changes in colon tissue of control and treated mice and found the loss of normal gut tissue architecture in AVNM and DSS treated mice which ultimately caused the leaky gut condition and made the gut more permeable. We also observed higher neutrophil infiltration in mucosa and submucosa of the colon tissue.

Higher neutrophil infiltration is a very prominent signature for activation of the pro-inflammatory immune responses in the host [205, 206]. We also found a strong correlation between the altered abundance of the specific gut microbes and various immune genes' expressions in the mice's colon. Increased *Akkermansia, Bacteroidetes, Escherichia-Shigella,* and *Helicobacter* like genera and decreased *Clostridia-like* genus following treatment with different perturbing agents caused significant modulation in different immune genes' expression in the colon. Altered Firmicutes and Bacteroidetes in the gut also differentially regulated the serum SCFA.

Neomycin treatment significantly enhanced the *Bacteroides* genus of Bacteroidetes phylum to increase the IFN-γ and IL-10 expressions in gut and systemic level. Previous reports have demonstrated that the increased abundance of *Bacteroides fragilis* altered various immune gene expressions in the gut [207–209]. Some selected gram-negative bacteria in the gut stimulated the production of IL-10 cytokine [208]. It is also known that members of Firmicutes phylum produce butyrate, while the *Bacteroidetes* phylum could produce acetate and propionate from dietary fibers [171]. A significant reduction of Firmicutes and elevation of Bacteroidetes, following neomycin treatment, could decrease butyrate with increased acetate and propionate concentration in mice serum. The acetate regulates different inflammatory responses of the host. It increased the IFN-γ gene expression by normalizing the IFN-γ promoter, activating histone acetylation, and chromatin accessibility by acetyl-CoA synthetase (ACSS)-dependent manner [210–212]. Acetate treatment also increased the IL-10 level of the host while it inhibited the LPS induced TNF-α secretion in the peripheral blood mononuclear cells (PBMCs) of mice [171, 213, 214]. This showed the anti-inflammatory effect of acetate supplement on the

host. In the current study, neomycin treatment caused elevated acetate release, associated with higher expression of IFN-γ and IL-10 genes.

On the other hand, in the vancomycin treated group, an increased abundance of *Akkermansia* and *Lactobacillus* genera caused the increased expression of the anti-inflammatory IL-10 gene in the colon and serum of mice. Simultaneously, no significant changes were found in the expression of pro-inflammatory genes like TNF-α and IFN-γ in either colon or serum samples. Previous studies showed that the increased abundance of *Akkermansia muciniphila* induced elevated anti-inflammatory cytokine genes in the gut [116, 129, 215]. The report also showed that *A. muciniphilla* could produce more acetate and propionate [171]. The results revealed that vancomycin-treated mice had less butyrate in serum than propionate and acetate. Hence, we concluded that vancomycin-treated mice had fewer Firmicutes (specifically *intestinimonas*) and more *A. muciniphila* [116, 129].

Following AVNM and DSS treatment, an increase in the pathogenic Proteobacteria like *E. coli*, *Shigella,* and *Helicobacter* and a decrease in the *Clostridia* group of bacteria caused a rise in TNF-α gene expression in both the group and elevation of IFN-γ in DSS treated group in the localized and systemic level. In contrast, no significant changes were found in the expression of the IL-10 gene in either colon or serum. Previous reports showed that Firmicutes, specifically the *Clostridium* group present in the gut, produced short-chain fatty acids, and these SCFAs suppressed the LPS and pro-inflammatory cytokines [172, 198]. Earlier reports also revealed that a considerable increase in

Proteobacteria phylum caused higher expression of pro-inflammatory cytokine genes in the gut [216–218]. In the current study, the lower abundance of Firmicutes phylum and a comparatively higher abundance of Proteobacteria caused a substantial decrease in all three SCFAs (acetate, propionate, and butyrate) levels in the serum of AVNM and DSS treated mice compared to the control and other antibiotic-treated groups. Following AVNM and DSS treatment, the dramatic increase in the pathogenic Proteobacteria like *E. coli, Shigella*, and *Helicobacter* and a decrease in the *Clostridia* group of bacteria caused a rise in TNF-α gene expression in the colon and serum of mice.

The current results correlated treatment of different perturbing agents with gut microbial dysbiosis and metabolism and immune responses. However, the present study did not investigate the comprehensive mechanism by which the abundance of specific gut microbiota groups regulated the expression of different cytokines and SCFA levels of the host.

3.4 Conclusion

In conclusion, the current study showed different perturbing agent-induced alteration patterns of gut microbiota and their association with various cytokines and SCFA levels of the host. Such association can be summed up as follows: Treatment with a) neomycin increased Bacteroidetes phylum to promote an anti-inflammatory response in the host, b) vancomycin enhanced Verrucomicrobia phylum to enhance anti-inflammatory responses and better glucose metabolism, c) AVNM depleted most of the microbes with a significant increase in pathogenic Proteobacteria and depletion of beneficial Verrucomicobia phylum and d) DSS caused a significant increase in pathogenic

proteobacteria phylum and decrease in beneficial Firmicutes and Verrucomicrobia phylum in both strains of mice.

In a nutshell, the outcome helps understand microbiota's role at the phylum and genus level, which could be clinically significant. The current observations are also essential in developing animal models for various infectious and metabolic disorder studies and can translate clinically.
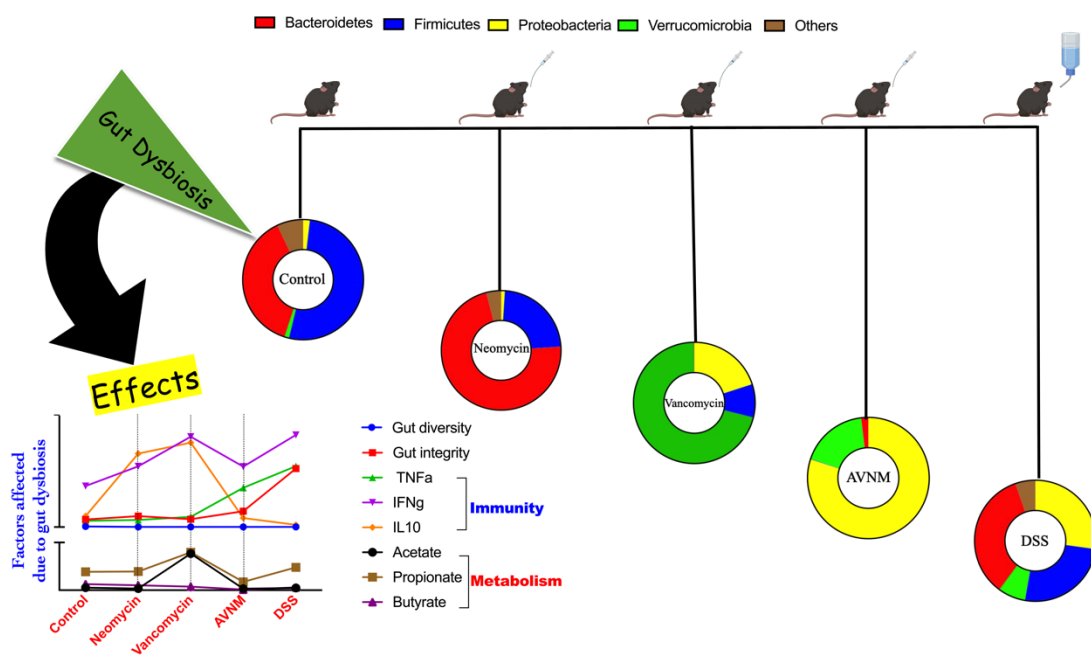
Fig. 3.6: Effects of different levels of gut microbial perturbation on host physiology, immunity and metabolism.
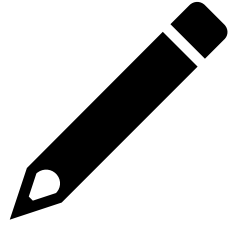
Chapter: 4

Identification of unique microbial and metabolic biomarkers at various disease severity levels of DSS induced colitis

4.1 Introduction

In the preceding chapter, we discussed how different gut perturbing agents might alter gut microbial compositions and host physiology, metabolism, and immunity. Results revealed that some perturbations were beneficial from the host perspective, while some were detrimental enough to create an elevated pro-inflammatory responses to induce colitis like syndrome.

Inflammatory Bowel Disease (IBD), consisting of Crohn's disease and ulcerative colitis, is an increasing global threat. During the 20th century, IBD was mainly a disease in westernized countries. At the turn of the 21st century, IBD became a global disease with accelerating incidence in the newly industrialized countries of Asia, South America, and Africa. The incidence of IBD in Asia is 1.4 cases per 100,000, just after the USA, with a prevalence of 1.6 cases per 100,000. In Asia, ulcerative colitis is 2-fold more likely to be diagnosed than Crohn's disease in other parts of the world. The highest incidence of colitis among Asia–the Pacific is in India at 9.3 per 100,000 persons/years [84, 219–222]. Although the condition is alarming, no unique cause has been determined for colitis. Still, its etiopathogenesis is thought to arise from genetic susceptibility to dysregulated interaction between immune factors and the enteric commensal flora. Environmental triggers, such as drug use, stress, diet, and smoking, also influence disease onset and development [223]. Research progress to date in this area indicates that colitis is a multifactorial disease. To understand the heterogeneous outcome of the disease, a systems biology approach aiming to integrate biological omics and non-omics datasets can be a

solution to resolve the complexity of the disease. The multi-omics approach is the best way to provide vast information about the therapeutic strategy and discover some clinical biomarkers that characterize disease pathogenesis.

We vigorously followed the multi-omics approach to understand colitis's disease onset and etiology in the current study. To avoid ethical issues related to human samples, we have used the mouse as a model system to study disease pathogenesis. Typically, in a colitis study, the disease is induced using chemical compounds, e.g., DSS, or by knocking out or targeting specific genes, such as regulatory cytokines. Among all these, the DSS-induced colitis mouse model is prevailing because of the similarities with human colitis and due to the rapidity, simplicity, reproducibility, and controllability [224, 225]. Different DSS dosages led to the development of robust colitis models in mice [226]. Studies reported that the optimum DSS dose varied with varying strains of mice. The optimal concentration recommended for inducing colitis was 1.5%- 3.0% in C57BL/6 (Th1 bias) and 2.5-5.0% in BALB/c (Th2 bias) mice [225, 227–229]. There is no standard optimized DSS dose available with zero mortality rates that can cause remarkable disease outcomes for the same duration independent of mice strains or immunological background. We established a common composite dose of DSS in the current study, i.e., 5% DSS for 7 days followed by 2.5% DSS for another 7 days, for both C57BL/6 and BALB/c mice.

The current report revealed that the Th1 background of C57BL/6 mice might be responsible for flares of inflammation throughout the treatment period irrespective of DSS concentration. Altered inflammatory responses disrupt the homeostasis of the host in such a way that they transformed the metabolism and gut microbial composition of the

host to create a more intense form of colitis. On the contrary, the Th2 background of BALB/c was unable to activate severe inflammatory reactions throughout the treatment condition. The severity response for the initial treatment condition was probably the outcome of the altered gut microbial composition of the host rather than the host genetic response. Lowering of DSS concentration caused recovery of the host from the diseased state. The current multi-omics study along with the vector analysis revealed that a) higher DSS concentration could not make much changes in genes and host metabolic composition but b) the gut microbial composition and microbial metabolites created a niche for that support inflammation at initial days of the disease. As the gut microbial composition and metabolic diversity were restored at lower DSS concentration, the host regained normal homeostasis and activated more anti-inflammatory responses.

We further established a few probable metabolomic and gut microbial markers independent of host immunological conditions. We observed that inflammation leads to the high amino acid and lipid metabolism in the host system, leading to the high abundance of Helicobacter genus under Proteobacteria phylum in the gut. These parameters all together create a niche for the severe form of colitis in the host. These biomarkers would help us understand the disease etiology better and could help us diagnose the disease at its early onset.

4.2 Results

We performed this study in view of the fact that colitis causes severe inflammatory changes in the host. Activation of the pro-inflammatory condition further leads to systemic level changes in the host, e.g., i) changes in gut microbial composition, ii)

alteration of serum and cecal metabolite concentration, iii) changes in gut barrier functions, and acute phase responses of the host, etc. However, the role of host genetics, mainly the immunological background of the host, in colitis related complications remains very poorly understood to date. In this study, we attempted to address the role of host genetics, more specific, the role of host immunological background in case of i) extent of inflammatory changes of the host, ii) differential changes of gut microbial composition based on host genetic background, and severity of the disease, iii) alteration of metabolite profile of host based on host genetics, disease severity, altered gut microbial composition too.

4.2.1 Colitis induction and associated inflammatory changes in the host

We administered various DSS dosages orally in C57BL/6- and BALB/c- male mice. We used untreated mice as a control in the study. We tried several doses to determine an optimum DSS amount that would not cause mortality in either of the mice strains and found 5% and 2.5% for 2 weeks as optimum for both the strains. Oral administration of DSS (5% for the 1st week +2.5% for the 2nd week) for 2 weeks induced colitis related typical and notable physiological changes e.g., loss of body weight (Fig. 4.1A), increased water intake (Fig. 4.1B), presence of fecal occult blood (Fig. 4.1C, E), diarrhea (Fig. 4.1D), rectal bleeding, and - we have used these parameters to determine the disease severity/ clinical score) in both mice strains (Fig. 4.1F, G).
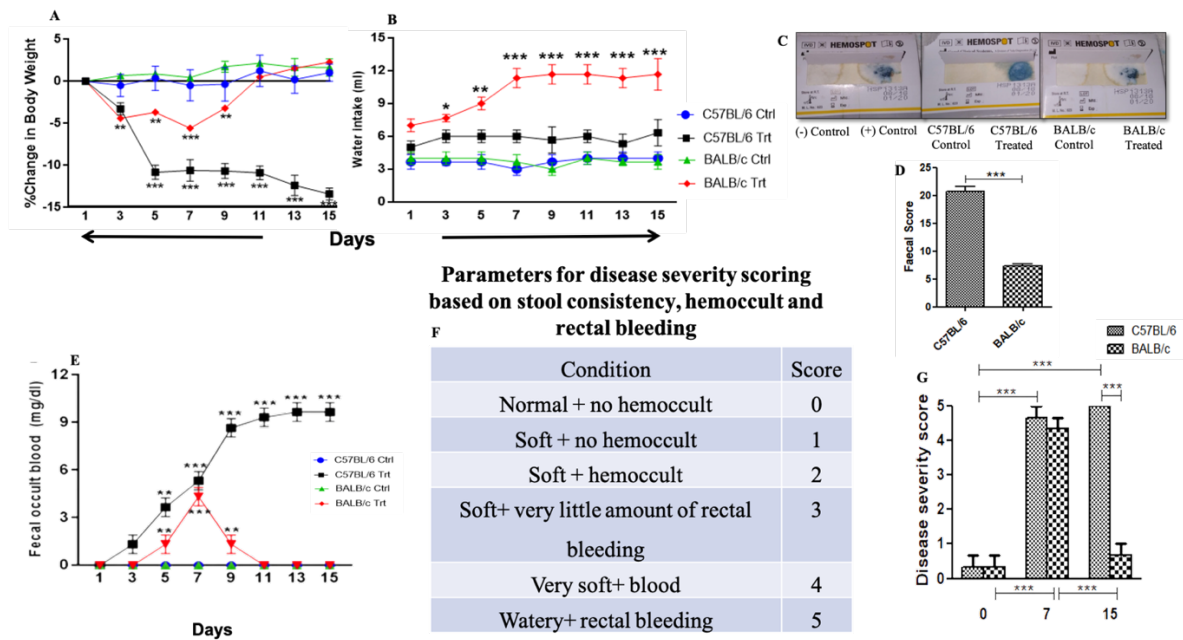
Fig. 4.1: Physiological changes and disease manifestation following treatment with DSS.

We observed the following changes in the physiology followed by DSS treatment: (A) % change in body weight & (B) water intake (in ml) of control and treated groups were measured on every alternative day till day 15 in C57BL/6 and BALB/c mice. We also observed the presence of (C) fecal occult blood, (D) stool consistency and (E) quantified the amount of the blood in the fecal samples of control and treated C57BL/6 and BALB/c mice. We scored the disease severity based on the criteria listed in panel (F) and plotted the disease severity score.

We presented data as the means ± SD (n=6). We used Two-way ANOVA followed by the Bonferroni test to determine the significance level for all analyses. * corresponds to $P<0.05$, ** corresponds to $P<0.01$, *** corresponds to $P<0.001$.

Along with the physiological alterations of the host, we measured inflammatory responses from the colon. Altered bowel/colon length (Fig. 4.2A), % spleen (Fig. 4.2B) & peritoneal fat (Fig. 4.2C) index and histopathological analysis (Fig. 4.3) was good enough to provide a distinct idea about the kinetics of disease progression in both the mice strains.
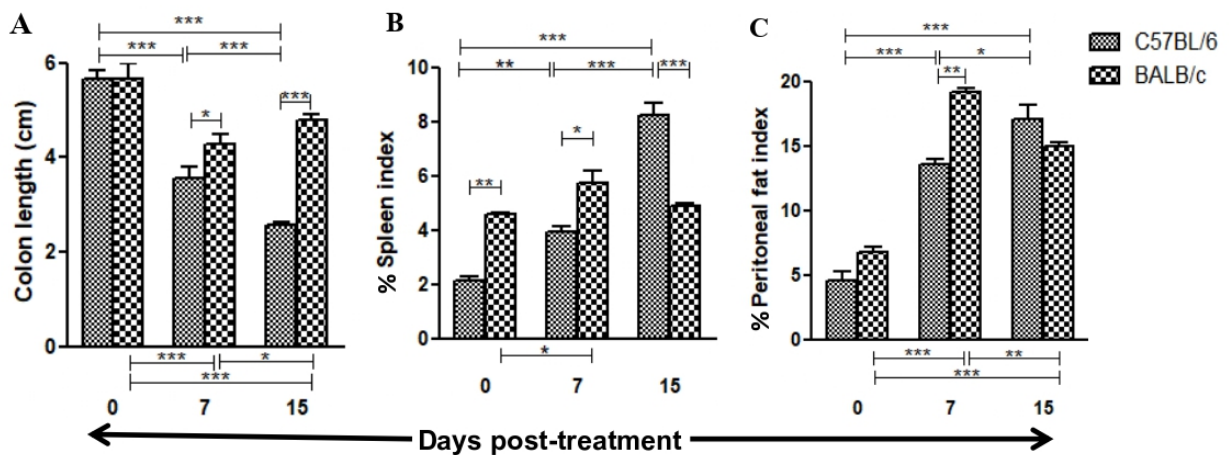
Fig. 4.2: *Altered colon length, spleen and peritoneal fat index of both mice strain followed by DSS treatment.*

*Altered (A) colon length (B) spleen & (C) peritoneal fat index showed the disease progression in both mice strains. We presented all values as means ± SD for 3 biological replicates. We performed Two-way ANOVA followed by the Bonferroni test to determine the significance level. * corresponds to P<0.05, ** corresponds to P<0.01, *** corresponds to P<0.001.*

Histopathological analysis provided us the clear idea about the changes of the gut tissue morphology due to the disease progression. We performed H&E staining (Fig. 4.3A-F) and Alcian blue/PAS staining (Fig. 4.3G-L) of the colon sections of all the control and treated groups of mice. From the histopathological analysis, we found the changes of the colon tissue architecture of is continued till end of the treatment in C57BL/6 mice (Fig. 4.3A-C, G-I). In BALB/c, highest changes in tissue architecture were observed on day 7 of the DSS treatment and by day 15 changes in tissue architecture were indifferentiable in comparison to day 0 (Fig. 4.3D-F, J-L). DSS treatment was potent enough to completely destroy the normal colon tissue morphology at the highest diseases severity level in both the mice strains.

H&E staining of colon section of control C57BL/6 (Fig. 4.3A) and BALB/c (Fig. 4.3D) revealed intact epithelium, well-defined crypt length, absence of edema, neutrophil infiltration in mucosa and submucosa, and any ulcers or lesions. Alcian blue/PAS staining also showed sufficient no. of goblet cells and the intact mucus layer in control C57BL/6 (Fig. 4.3G) and BALB/c (Fig. 4.3J) mice. In contrast, DSS treatment in both strains destroyed the epithelium, ulcers, lesions, shortening, loss of crypts in the whole colon, edema, neutrophil infiltration in mucosa and submucosa (Fig. 4.3B-C, E-F), and complete loss of goblet cells and mucus layer (Fig. 4.3H-I, K-L). The changes were highest at the highest disease severity level in both the strains, for C57BL/6, it was on day 15 & for BALB/c on day 7. Recovery of colon morphology happened on day 7 in BALB/c mice (Fig. 4.3F & L). We evaluated the severity of histopathological changes considering the parameter mentioned in materials and methods section and scored them accordingly to quantify the histopathological changes at different treatment conditions (Fig. 4.3M).
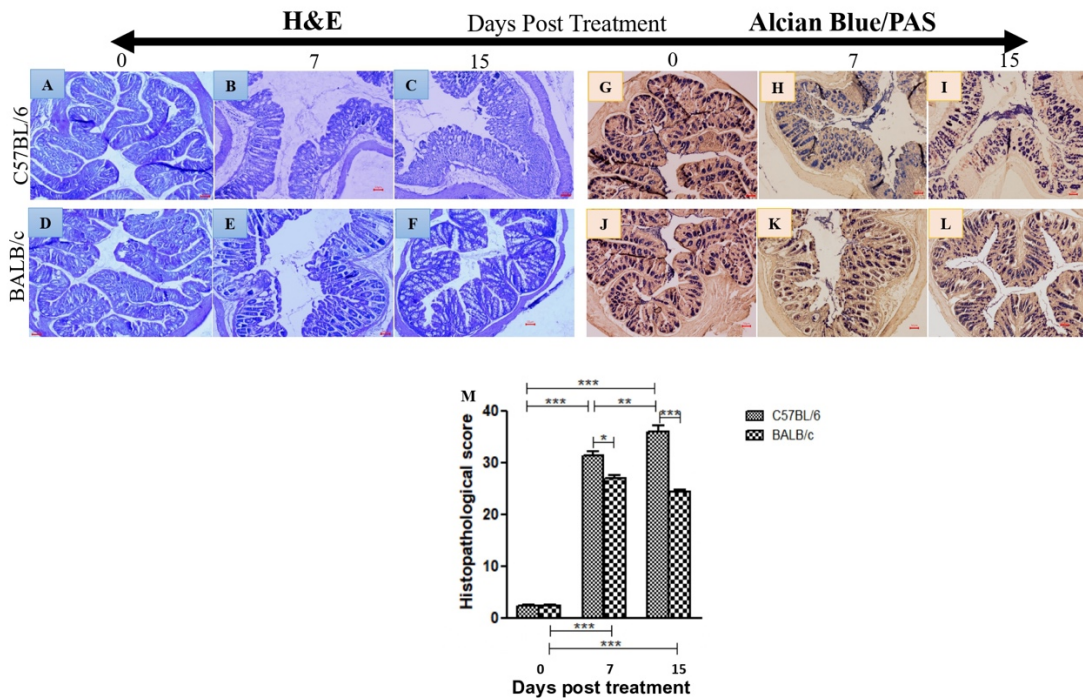
Fig. 4.3: Colon histopathology and intestinal barrier function at different disease severity of C57BL/6 and BALB/c mice.

We performed H&E staining (A-F) and Alcian Blue/PAS staining (G-L) of colon sections of control and treated C57BL/6 (A-C, G-I) and BALB/c (D-F, J-L) mice to measure the changes in epithelium and mucosal architecture and inflammatory cell infiltration. The image of the histological section of the colon via bright-field microscopy at 20X. We also (M) scored the changes and quantified the changes in gut morphology followed by DSS treatment.

We presented data as the means ± SD (n=6). We performed two-way ANOVA followed by the Bonferroni test to determine the significance level. '*' corresponds to P ≤ 0.05, ** corresponds to P ≤ 0.01, *** corresponds to P ≤ 0.001, **** corresponds to P ≤ 0.0001.

(For histological analysis, pictures were taken with a magnification of 20X, scale bar 100µm).

Data showed in the Fig. 4.2 & 4.3 clearly indicated the disease progression continued till the end of the treatment period in C57BL/6. BALB/c entered in to the recovery phase after day 7 of the DSS treatment.

As the first-line defence of host inflammatory responses, we measured the transcription level expression of Toll-Like Receptors (TLR) from the colonic tissue of mice. TLRs can recognize damage-associated molecular patterns released from damaged tissues and play a vital role in activating the other pro-inflammatory responses of the host [36,37]. We measured *Tlr2* and *Tlr4* expression of mouse colonic tissue and found that both the gene expressions were significantly higher in C57BL/6 mice than the BALB/c mice throughout the treatment condition. More surprisingly, we also found that *Tlr2* and *Tlr4* expressions continuously increased till the end of the treatment period. On the contrary, in BALB/c, both gene expressions were significantly increased until day 7 of the treatment, reaching their basal level on day 15 of the treatment (Fig. 4.4A).

Excessive TLR activation disrupts the immune homeostasis by sustained pro-inflammatory cytokines and chemokine production [38,39]. To investigate the effect of high TLR responses in the diseased condition, we analyzed transcriptional profiling of selected cytokines, i.e., *TNFα, IFNγ, IL1β, IL6, IL12, IL17, IL21, IL10*. The chosen cytokines played a crucial role in the disease progression. At the higher DSS dose (5%), gene expressions of all inflammatory markers, i.e., *TNFα, IFNγ, IL1β, IL6, IL12, IL21, and IL17*, were significantly higher in the treated group of mice compared to the control

in both the strains (Fig. 4.4B, C). In the presence of 2.5% DSS during the 2nd-week, pro-inflammatory cytokine expressions gradually increased in treated C57BL/6 mice till day 15 (Fig. 4.4B, C). We did not observe any significant upregulation in the pro-inflammatory cytokine levels in DSS-treated BALB/c mice on 2nd week of DSS treatment (Fig. 4.4B, C). We also measured the transcriptional change in *IL10* cytokine level as an activator of anti-inflammatory response. We observed significant downregulation of *IL10* (anti-inflammatory) and upregulation of pro-inflammatory genes in both treated mice strains till day 7 of the treatment condition. During the entire treatment period in C57BL/6, upregulated pro-inflammatory cytokines might be the reason for no significant upregulation of anti-inflammatory cytokine. On the contrary, anti-inflammatory cytokine level was significantly higher in the DSS-treated BALB/c group on day 15 than on day 7 of DSS treatment (Fig 4C). Expressions of all pro-inflammatory markers were substantially higher in C57BL/6 than BALB/c throughout the treatment condition, and anti-inflammatory gene expression was higher in BALB/c (Fig. 4.4B, C). We also observed the pro-inflammation related enzyme like myeloperoxidase (MPO) level also increased according to the disease severity both in C57BL/6 and BALB/c mice (Fig. 4.4D).

Activation of inflammatory cytokines, mainly *TNFα* and *IL6,* leads to the activation of the acute-phase response protein of the host [43,44]. C- reactive protein (CRP) is one of such acute-phase response proteins. We measured the CRP level from colonic tissue and found that CRP level was significantly high only on day 15 of DSS treatment in C57BL/6 mice (Fig. 4.4E).

Comparison	C57BL/6										BALB/c									
	TLR2	TLR4	TNFa	IFNg	IL1b	IL6	IL12	IL17	IL21	IL10	TLR2	TLR4	TNFa	IFNg	IL1b	IL6	IL12	IL17	IL21	IL10
0 vs 7	***	***	***	***	***	***	***	***	***	***	***	***	***	***	***	***	***	***	***	***
0 vs 15	***	***	***	***	***	***	***	***	***	***	***	***	***	***	*	*	***	***	ns	***
7 vs 15	***	***	***	***	***	***	***	***	***	ns	ns	ns	ns	ns	***	***	***	*	***	ns
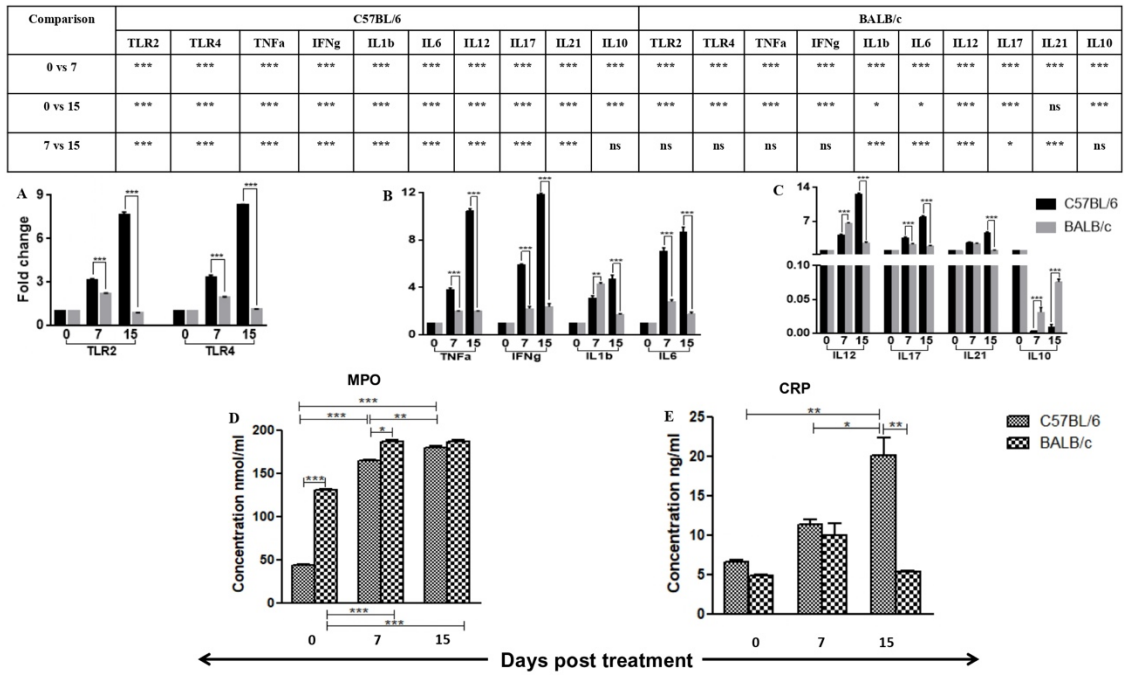
Fig. 4.4: Inflammatory responses in colon tissue following DSS treatment in C57BL/6 and BALB/c mice.

We represented the kinetics of different inflammatory responses, e.g., transcriptional expression of (A) Toll-like receptors (TLR2 and TLR4) (B) pro (TNFα, IFNγ, IL6, IL1β), (C) (IL12, IL21, IL17) & anti-(IL10) inflammatory genes and enzyme like (D) MPO following DSS treatment in both C57BL/6 and BALB/c mice. We presented all values as means± SD for 3 biological replicates. The statistical significance among various days of treatment is denoted in the tables above respective panels to avoid unnecessary clutters. We used the roman numbering system above each gene name to keep the tables and figures tidy.

(E) C- reactive protein in colon tissue of C57BL/6 and BALB/c mice was measured on days 0, 7, and 15 post-treatments to know the acute phase response of the host due to inflammation.We presented data as means± SD (n=6).

We performed Two-way ANOVA followed by the Bonferroni test to determine the significance level. [* Corresponds to P<0.05, ** corresponds to P<0.01, *** corresponds to P<0.001].

Previous reports stated that uncontrollable immune reaction in the gut microenvironment further leads to compromised gut barrier function [40]. The tight junction proteins, including occludin, claudins, and zonula occludens, play a crucial role in maintaining gut epithelial integrity [41]. As the effect of high inflammatory responses in the colon, we measured the gene expression of two tight junction proteins, i.e., *Cldn2* and *ZO1*. From the previous reports, we found that the *Cldn2* gene is highly expressed in the gut tissue of colitis patients, whereas *ZO1*is downregulated. In the current study, the expression of *Cldn2* followed the same kinetics of inflammatory responses in both the mice strains. *Cldn2* expression was highest on day 15 of DSS treatment in C57BL/6 and day 7 of DSS treatment in BALB/c. Like the other inflammatory responses, *Cldn2* expression was significantly higher in C57BL/6 than BALB/c (Fig. 4.5A). We did not find any significant changes in the gene expression of *ZO1* in either of the mice strains in any treatment condition (Fig. 4.5A).

Cldn2 gene is highly expressed in leaky gut epithelia [42]. We measured the serum FITC-Dextran level following DSS treatment to determine the gut leakiness. A high concentration of FITC-Dextran in the serum was an indication of high gut permeability.

In C57BL/6, serum FITC-Dextran level increased gradually in the treated group compared to the control and reached its highest point on day 15 of DSS treatment. BALB/c gut permeability increased until day 7 following DSS treatment and gradually decreased as the DSS dose decreased (Fig. 4.5B).

Enhanced gut permeability increased the risk of bacterial translocation from the gut lumen to the host circulatory system. It increased the chance of endotoxemia [238, 239]. We measured endotoxin (LPS) level in the serum for both mice strains. The amount of endotoxin level in serum was highest when the gut permeability was the highest. Serum endotoxin level gradually increased till day 15 in C57BL/6 treated mice, whereas, in treated BALB/c, endotoxin level increased till day 7 of DSS treatment (Fig. 4.5C). Elevated endotoxin levels in the host serum activated the host's innate defense responses by producing different antimicrobial peptides, ultimately helping the host cope with the diseased condition and maintain the system's homeostasis. Lipocalin-2 (LCN2) is one such antimicrobial peptide that plays a vital role in colitis disease pathogenesis by neutralizing the serum's excess endotoxin level [240, 241]. We measured LCN2 levels in the serum of control and treated groups of mice. In treated C57BL/6, serum LCN2 was highest on day 15 and treated BALB/c on day 7 following DSS treatment (Fig. 4.5D). So, the serum LCN2 level proportionally increased with the serum endotoxin level.

Comparison	C57BL/6		BALB/c	
	Cldn2	ZO1	Cldn2	ZO1
0 vs 7	***	ns	***	ns
0 vs 15	***	ns	ns	ns
7 vs 15	***	ns	***	ns

Comparison	C57BL/6	BALB/c
0 vs 7	***	***
0 vs 15	***	ns
7 vs 15	***	***
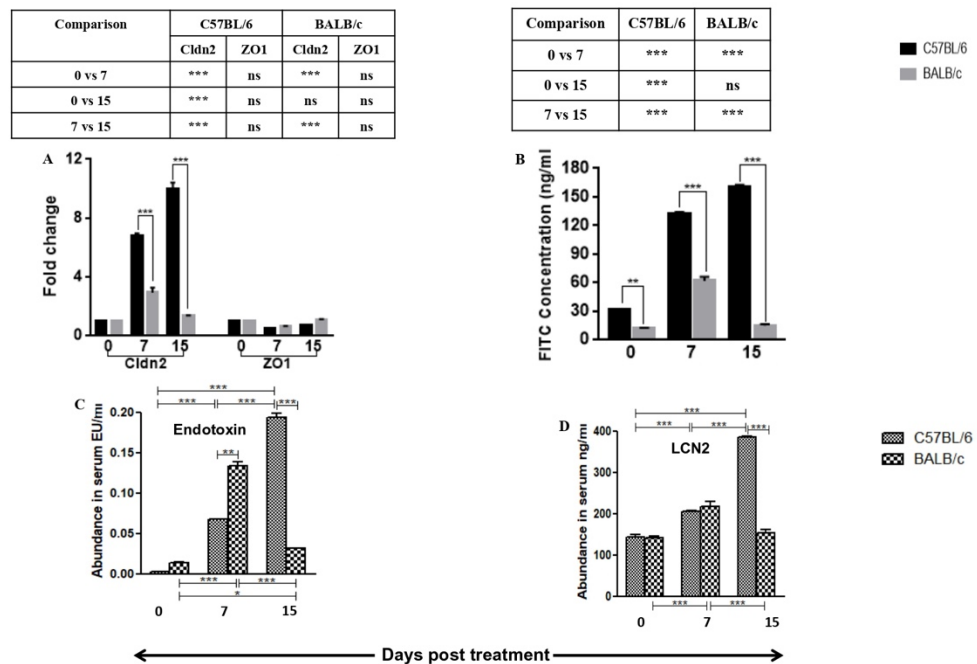
Fig. 4.5: *Evidences of compromised gut barrier functions followed by DSS treatment in C57BL/6 and BALB/c mice.*

We measured the altered expression of junction related genes (Cldn2, ZO1) due to the DSS treatment in both C57BL/6 and BALB/c mice. We presented all values as means± SD for 3 biological replicates. (B) We measured serum FITC-dextran levels in control and DSS-treated C57BL/6 and BALB/c mice to indicate intestinal permeability on days 0, 7, and 15 post-treatments as a consequence of inflammatory responses in the colon. The statistical significance among various days of treatment is denoted in the tables above respective panels to avoid unnecessary clutters. We used the roman numbering system above each gene name to keep the tables and figures tidy.

Leaky gut was probably the main cause of endotoxemia in host. We measured the (C) serum endotoxin levels of both mice strains to quantify the extent of the endotoxemia in

the circulation. Increased endotoxin production activated the production of anti-microbial peptide (D) LCN2 as a host defense mechanism to nullify the effect of endotoxemia.

We presented data as means± SD (n=6). We performed Two-way ANOVA followed by the Bonferroni test to determine the significance level. * corresponds to P<0.05, ** corresponds to P<0.01, *** corresponds to P<0.001.

4.2.2 Colitis induced transcription and metabolic level changes of two differential immune bias host

To understand the molecular basis of the differential responses of two immune bias hosts in the presence of a common DSS dose, we performed transcriptomics analysis of colon tissue and metabolomics analysis of serum and cecal content of mice. This approach allowed us to get a clear idea about the role of host genetics and metabolic profile in differential disease responses in two different strains. We compared the transcriptomics and metabolite data from different disease severity levels for both strains of mice. Our results revealed differential responses of genetics (Fig. 4.6A-F) and metabolite profile (Fig. 4.6G-N), based on which we clustered them. First, we clustered the transcriptomics data, using LDA, based on the total no. of genes expressed in the colon at different treatment conditions in both strains (Fig. 4.6A, B). Further, we shortlisted the genes based on the criteria mentioned in the methodology sections and again clustered them similarly for both strains of mice (Fig. 4.6D, E). Mice from similar treatment conditions clustered together and also clustered differentially based on different treatment conditions for both strains (Fig. 4.6A-B, 4.6D-E). The shortlisted genes from the transcriptomics data are

mainly related to the inflammatory responses of the host. In C57BL/6, genes were primarily associated with pro-inflammation, whereas in BALB/c, genes were related to anti-inflammation. We measured the distance between the clusters and the trajectory of the groups on the 2D plane to measure the extent of differential disease outcomes based on the immune background of the hosts [23,24]. From the distance and trajectory of the groups on the 2D plane, we found in C57BL/6, the distance between control and treated groups increased gradually in both analyses, i.e., LDA of total genes (Fig 6C) and LDA of shortlisted genes (Fig 6F). This analysis revealed that the gene expressions of day 15 over day 0 were more different from day 7 over day 0 (Table. 4.1). On the contrary, in BALB/c, the distance between control and treated groups was almost similar in both analyses, i.e., LDA of total genes (Fig 6C) and LDA of shortlisted genes (Fig 6F). This analysis revealed that the gene expressions of day 15 over day 0 and day 7 over day 0 were almost similar without much change (Table. 4.1). This LDA analysis showed a similar kind of trend with the previously mentioned inflammatory responses of both strains.

Similarly, we performed LDA of metabolites (serum metabolites) and meta-metabolites (cecal metabolites) data. Like transcriptomics data, we performed LDA of all the altered metabolites and meta-metabolites as well as shortlisted metabolites and meta-metabolites. In both cases (LDA of all and shortlisted metabolites and meta-metabolites), mice from different treatment conditions clustered differentially on the 2D plane in C57BL/6 mice (Fig. 4.6G, K). On the other hand, in BALB/c, mice from day 0 and day 15 clustered together and day 7 clustered differently on the 2D plane (Fig. 4.6I, M). Similar to the transcriptomics data, we calculated the distance between different treatment conditions

and trajectories on the 2D plane for metabolomics data to get an idea about the differential disease responses based on mice strains (Fig. 4.6H, L and 4.6J, N). In C57BL/6, the distance between control and treated groups increased gradually in both analyses, i.e., LDA of total metabolites (Fig. 4.6H) and meta-metabolites (Fig. 4.6L) and LDA of shortlisted metabolites (Fig. 4.6J) and meta-metabolites (Fig. 4.6N). This analysis revealed that the metabolites and meta-metabolites concentration of day 15 over day 0 were more different from day 7 over day 0 (Table. 4.1). On the contrary, in BALB/c, the distance between control and treated groups was almost similar in both analyses, i.e., LDA of total metabolites (Fig. 4.6H) and meta-metabolites (Fig. 4.6L) and LDA of shortlisted metabolites (Fig. 4.6J) and meta-metabolites (Fig. 4.6N). This analysis revealed that the metabolites and meta-metabolites concentration of day 15 over day 0 and day 7 over day 0 were almost similar without much change (Table. 4.1). Metabolomics analyses also followed the same trend of transcriptomics analyses and inflammatory responses of the hosts.
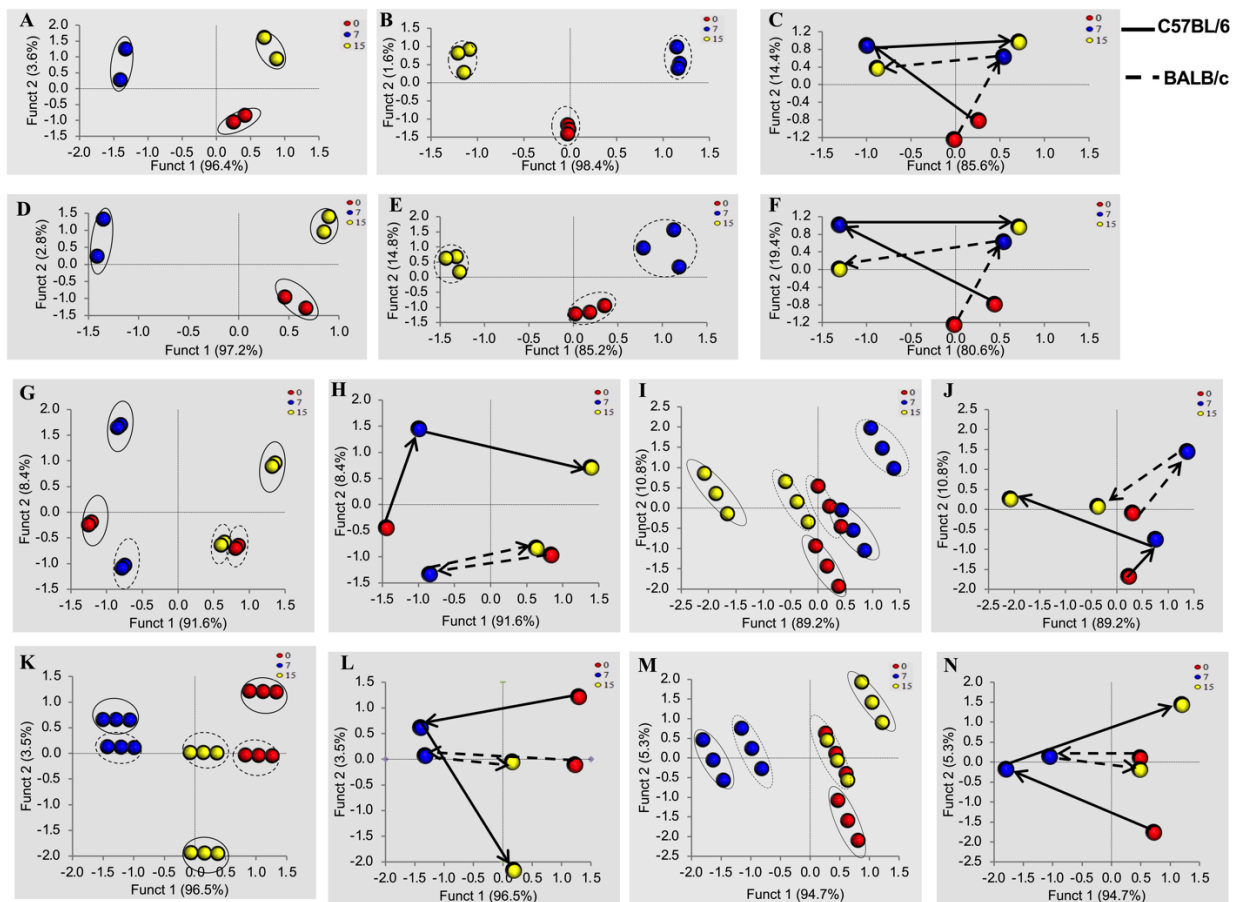
Fig. 4.6: Linear discriminant analysis of multi-omics data and the trajectory followed by different treatment conditions on the 2D plane.

We grouped the mice strain using Linear Discriminant Analysis (LDA) based on transcriptomics, metabolomics, and meta-metabolomics data according to the different treatment conditions. We showed LDA of the total gene expressed in the colon (A, B) and significantly altered genes in the colon (D, E) following DSS treatment on days 0, 7, and 15 in both C57BL/6(A, D) and BALB/c (B, E) mice. We plotted the trajectory of LDA data of total gene expression (C) and significantly altered gene expression (F) in the colon to determine the differential responses based on different treatment conditions and different

mice strains. Similarly, we showed LDA of total metabolites (G) and significantly altered metabolites (K) present in serum and total meta-metabolites (I) and significantly altered metabolites (M) present in cecal content followed by DSS treatment in both C57BL/6 and BALB/c mice. To know the differential responses based on the treatment conditions and different mice strains, we also plotted the trajectory of LDA data of total metabolites (H) and significantly altered metabolites (L) present in serum and total meta-metabolites (J) and significantly altered metabolites (N) present in cecal content. Distance between the clusters and the trajectory on the 2D plan for all the analyses is mentioned in detail in Table 4.1. This analysis gives us a better understanding of differential responses of C57BL/6 and BALB/c in the presence of an equivalent dose of DSS treatment.

Table. 4.1: *Quantitative estimation of differential responses of DSS treated C57BL/6 and BALB/c mice in terms of transcriptomics, metabolomics and meta-metabolomics using Linear Discriminant Analysis (LDA).*

Strain	Treatment Conditions	Distance (r) between groups on a 2-D plane						The trajectory followed on the 2-D plane based on different treatment conditions (DOP- ascending order)					
		T		Mt		M-Mt		T		Mt		M-Mt	
		i	ii	iii	iv	v	vi	i	ii	iii	iv	v	vi
C57BL/6	7 vs 0	1.85	1.95	2.71	1.68	1.35	2.74	CW	CW	CW	ACW	ACW	CW
	15 vs 0	2.39	2.38	2.87	3.07	2.56	3.03						
	15 vs 7	2.14	2.22	2.29	3.24	1.54	3.06						
BALB/c	7 vs 0	2.26	2.23	1.90	1.73	2.97	1.42	ACW	ACW	CW	ACW	ACW	ACW
	15 vs 0	2.26	2.21	0.96	0.61	2.10	0.18						
	15 vs 7	2.31	2.42	1.46	1.24	2.43	1.48						

Abbreviations: DOP- Days Post Treatment, T- Transcriptomics, Mt- Metabolomics, M-Mt-Meta-metabolomics, 0- Control, 7- 7 days post treatment of DSS, 15- 15 days post treatment of DSS, i- LDA was performed using all expressed genes on the particular condition, ii- LDA was performed using significantly altered genes on the particular condition, iii- LDA was performed using all metabolites present on the particular condition, iv- LDA was performed using significantly altered metabolites present on the particular condition, v- LDA was performed using all meta-metabolites present on the particular condition, vi- LDA was performed using significantly altered meta-metabolites present on the particular condition, CW- Clockwise (0-7-15 DOP), ACW- Anti-clockwise (0-15-7 DOP).

Varied distances between different clusters of transcriptomics and metabonomics data helped us understand the dissimilarity of genes, metabolites and meta-metabolites expression at different treatment conditions. We coined a new parameter, i.e., Dissimilarity Coefficient, to quantify the dissimilarities in disease responses [23,24]. We plotted the ratio of dissimilarity coefficient for different treatment conditions considering the mentioned parameters i) expressions of all altered genes and metabolites (Fig. 4.7A) ii) significantly altered genes and metabolites (Fig. 4.7B). We observed a distinct difference in the ratio of dissimilarity coefficient when we considered all altered genes and metabolites compare to the significantly altered genes and metabolites at different treatment conditions. Significantly altered parameters were thought to be the main driving force for differential disease outcomes in both strains of mice. To nullify the effect of

non-significantly altered genes and metabolites (which may not have much role in disease outcome) in the further analysis process, we considered only significantly altered genes and metabolites in successive analysis process. In C57BL/6 mice the highest amount of difference or dissimilarities was found in significantly altered metabolite expressions at 15-0 over 0-7 (Fig. 4.7B). This was a clear indication that host metabolites playing a critical role in highest disease severity on day 15 of the DSS treatment. In BALB/c, meta-metabolites or microbiota derived metabolites playing a crucial role in determining the highest disease severity on day 7 of DSS treatment. Highest dissimilarity coefficient on 7-15 over 15-0 indicated that a huge transition in meta-metabolite composition happened in between day 7 and day 15 of the treatment condition (Fig. 4.7B). To investigate the role of significantly altered genes and metabolites in disease severity, we calculated disease severity index considering the factor altered genes and metabolites in different treatment conditions [25]. Unlike the dissimilarity coefficient, role of host metabolites was highest in disease severity index in C57BL/6 on day 15-0 over 0-7 (Fig. 4.7C). On the other hand, in BALB/c role of microbial metabolites (meta-metabolites) was highest in disease severity index on day 7-15 over 15-0 (Fig. 4.7C). From further analysis, it was found that the altered genes and metabolites were either related to activation of pro or anti-inflammatory processes of host immune system. We calculated the ratio of pro- and anti-inflammatory genes, metabolites and meta-metabolites at different treatment conditions for both strains of mice. Ratio of Pro/Anti-inflammatory genes (Fig. 4.7D) metabolites and meta-metabolites (Fig. 4.7E) was highest on day 15-0 over 0-7 in C57BL/6. On the contrary, in BALB/c the ratio was highest on day 7-15 over day 15-0 for genes (Fig. 4.7D), as well as for metabolites and meta-metabolites (Fig. 4.7E). We also detected the

similarities of immunological responses between C57BL/6 and BALB/c in terms of genes. We found that, the genes involved in inflammatory processes in C57BL/6 were totally different from BALB/c and over all the total number of genes involved in pro-inflammatory processes was much higher in C57BL/6 compare to BALB/c (Fig. 4.7F). To investigate the specific role of host and microbial metabolites (metabolites & meta-metabolites) in the inflammatory process, we determined the number of unique metabolites and meta-metabolites in C57BL/6 and BALB/c. It was found that both unique host and microbial metabolites contributed equally in the disease inflammatory process in C57BL/6 (Fig. 4.7G). Whereas in BALB/c the scenario was opposite. Unique microbial metabolites took main part in activation of the inflammatory process of the host (Fig. 4.7H).

Higher disease severity was thought to be the main influencer of altered diversity (total no. of metabolites and meta-metabolites) of metabolites and meta-metabolites. We identified how the number of metabolites and meta-metabolites were changing with the varied disease severity. Increased disease severity increases the diversity of metabolites and decreases meta-metabolites' diversity in both C57BL/6 and BALB/c (Fig. 4.7I). With different treatment conditions and severity levels, we also determined how the diversity of common and unique serum and cecal metabolites were changing in C57BL/6 and BALB/c. In C57BL/6, with the increased disease severity, the diversity of unique serum metabolites increased, and the diversity of unique cecal metabolites decreased (Fig. 4.7J-L). In BALB/c, with the increased disease severity diversity of unique serum metabolites decreased, and the diversity of unique cecal metabolites increased (Fig. 4.7M-O).

The shortlisted genes responsible for differential disease progression in C57BL/6 and BALB/c mice were depicted as heatmap (Fig. 4.7P, Q) and also as tables for better understanding (Table. 4.2 & 4.3).
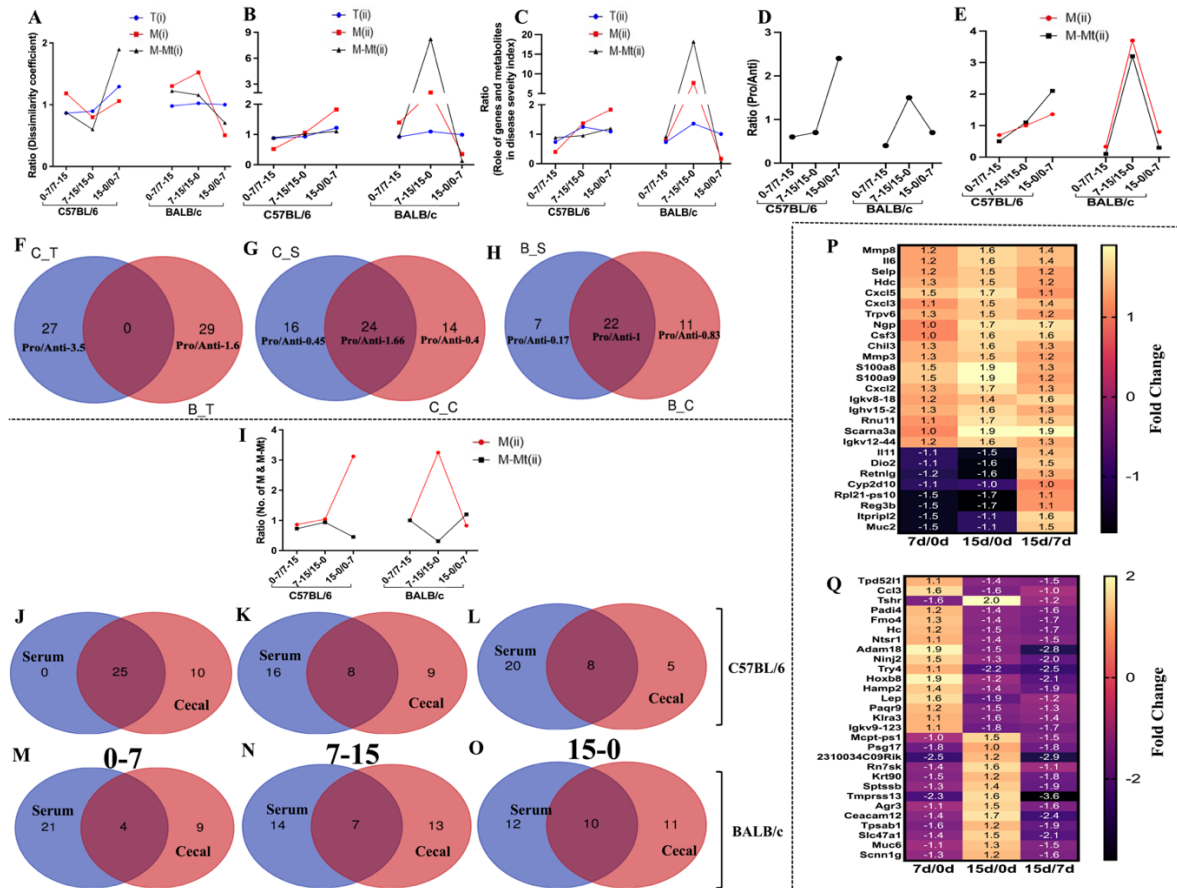
Fig. 4.7: Detailed analysis of altered transcriptomics and metabolomics status of the host at different stages of the disease.

From LDA, we have found that both mice strain formed 3 distinct clusters based on different treatment conditions. We have clustered the mice based on altered genes (T), metabolites (M), and meta-metabolites (M-Mt) expressions and measured the distances between different clusters on the 2D plane to quantify the difference between the treatment conditions. Every different cluster signifies a different treatment condition. We

have measured the distance (dissimilarity coefficient) ratio of varying treatment conditions (clusters) to observe the kinetics of altered genes, metabolites, and meta-metabolites expressions at various treatment conditions for both the strains of mice. Panel (A) depicted the ratio of distances of different clusters when we considered all (i) the altered genes, metabolites, and meta-metabolites expressions for LDA analysis. Panel (B) depicted the ratio of distances of different clusters when we considered only the significantly (ii) altered genes, metabolites, and meta-metabolites expressions for LDA analysis. Further, we assess the influence of genetic and metabolic factors in determining the disease severity index (Panel C). We have quantified the ratio of pro and anti-inflammatory genes (Panel D) metabolites and meta-metabolites (Panel E) in different treatment conditions for C57BL/6 and BALB/c to know the role of inflammation in the determination of differential disease outcomes. We have also found that significantly altered genes were very much strain specific (Panel F), and in C57BL/6 (C_T), the altered genes mainly were pro-inflammatory. In BALB/c (B_T), the altered genes were mostly related to anti-inflammation. To quantify the contributions of host metabolism and gut microbial metabolism in the inflammatory process, we calculated the ratio of significantly altered pro and anti-inflammatory metabolites from serum (S) and cecal content (C) of C57BL/6 (C) and BALB/c (B) mice. We found that in C57BL/6, host and microbial metabolites both triggered the inflammatory condition of the host (Panel G). On the contrary, in BALB/c gut microbial metabolites contribute more to trigger the inflammatory condition of the host (Panel H). To investigate how the diversity of serum and cecal metabolites altered with altered inflammatory conditions, we calculated the ratio of no. of metabolites and meta-metabolites in different disease severity for both

strains (Panel I). We also assessed how the no. of significantly altered common and unique metabolites from serum and cecal content changed along with the different treatment and disease severity levels in C57BL/6 (Panel J, K, L) BALB/c (Panel M, N, O) mice.

Table. 4.2: Significantly affected genes from transcriptomics study with their function and fold change values at different treatment conditions for C57BL/6 mice.

Sr. No.	Symbol	Full Name	Function	7d/0d	15d/0d	15d/7d
1	Mmp8	Matrix Metallopeptidase 8	Pro-inflammatory, stored in neutrophiles, help in the release of IL6,IL17 cytokines	1.2	1.6	1.4
2	Il6	Interleukin-6	Pro-inflammatory cytokine	1.2	1.6	1.4
3	Selp	Selectin P	Recruit leukocyte at the site of inflammation	1.2	1.5	1.2
4	Hdc	Histidine decarboxylase	Induced at an inflammatory site, especially in chronic inflammation	1.3	1.5	1.2

5	Cxcl5	C-X-C motif chemokine 5	Pro-inflammatory cytokine, activated by IL1 and TNFα	1.5	1.7	1.1
6	Cxcl3	C-X-C motif chemokine 3	Pro-inflammatory cytokine, involved in macrophage infiltration	1.1	1.5	1.4
7	Trpv6	Transient Receptor Potential Cation Channel Subfamily V Member 6	Shows pro-inflammatory response	1.3	1.5	1.2
8	Ngp	Neutrophilic granule protein	Increased in inflammation, works against bacterial LPS	1	1.7	1.7
9	Csf3	Colony Stimulating Factor 3	Induce expression of pro-inflammatory cytokines	1	1.6	1.6
10	Chil3	Chitinase-like protein 3	Highly expressed in inflamed tissue,	1.3	1.6	1.3

			especially colon lung			
11	Mmp3	Matrix Metallopeptidase 3	Highly expressed in inflammatory area	1.3	1.5	1.2
12	S100a8	S100 Calcium Binding Protein A8	Highly expressed in inflammatory area, recruit leukocyte and pro-inflammatory cytokine at the site of inflammation	1.5	1.9	1.3
13	S100a9	S100 Calcium Binding Protein A9	Highly expressed in inflammatory area, recruit leukocyte and pro-inflammatory cytokine at the site of inflammation	1.5	1.9	1.2
14	Cxcl2	C-X-C motif chemokine 2	Pro-inflammatory cytokine, recruit neutrophils at the pro-inflammatory site	1.3	1.7	1.3
15	Igkv8-18	Immunoglobulin kappa	Responsible for prolonged	1.2	1.4	1.6

		variable8-18	inflammation			
16	Ighv15-2	Immunoglobulin kappa variable 15-2	Responsible for prolonged inflammation	1.3	1.6	1.3
17	Rnu11	RNA, U11 Small Nuclear	Pro-inflammatory, activate TLR7 response	1.1	1.7	1.5
18	Scarna3a	Small Cajal Body-Specific RNA 3	Pro-inflammatory shows oncogenic activity	1	1.9	1.9
19	Igkv12-44	Immunoglobulin kappa variable 12-44	Responsible for prolonged inflammation	1.2	1.6	1.3
20	Il11	Interleukin-11	Anti-inflammatory cytokine	-1.1	-1.5	1.4
21	Dio2	Type II iodothyronine deiodinase	The anti-inflammatory role, suppress IL1β, COX2 expression	-1.1	-1.6	1.5
22	Retnlg	Resistin-like gamma	Involved in Th2 inflammation	-1.2	-1.6	1.3

23	Cyp2d10	Cytochrome P450 2D10	Anti-inflammatory	-1.1	-1.0	1.0
24	Rpl21-ps10	Ribosomal protein L21, pseudogene 10	Anti-inflammatory, resolve physiological inflammation	-1.5	-1.7	1.1
25	Reg3b	Regenerating islet-derived protein	Anti-inflammatory, downregulation shows more neutrophile infiltration	-1.5	-1.7	1.1
26	Itpripl2	Inositol 1,4,5-Trisphosphate Receptor Interacting Protein Like 2	Maintain endothelial permeability and Ca ion absorption	-1.5	-1.1	1.6
27	Muc2	Mucin 2	Involved in maintaining gut barrier function, Decreased at the time of gut inflammation	-1.5	-1.1	1.5

Table. 4.3: Significantly affected genes from transcriptomics study with their function and fold change values at different treatment conditions for BALB/c mice.

Sr. No.	Symbol	Full Name	Function	7d/0d	15d/0d	15d/7d
1	Tpd52l1	Tumor Protein D52 Like 1	Pro-inflammatory in nature, related to uncontrolled cell growth	1.1	-1.4	-1.5
2	Ccl3	C-C Motif Chemokine Ligand 3	Pro-inflammatory cytokine, recruit leukocytes at the pro-inflammatory site	1.6	-1.6	-1.0
3	Tshr	TSH receptor	Involved in Th2inflammation	-1.6	2.0	-1.2
4	Padi4	Peptidyl Arginine Deiminase 4	Pro-inflammatory, involved in granulocyte and macrophage development	1.2	-1.4	-1.6
5	Fmo4	Flavin Containing	Involved in TLR4 dependent	1.3	-1.4	-1.7

		Dimethylaniline Monoxygenase 4	inflammatory response, high TLR4 downregulate the expression of this gene			
6	Hc	Hemolytic complement	Pro-inflammatory activates IL1β response, recruit neutrophils at the inflammatory site	1.2	-1.5	-1.7
7	Ntsr1	Neurotensin receptor type 1	Pro-inflammatory, highly expressed in inflamed colon	1.1	-1.4	-1.5
8	Adam18	Disintegrin and metalloproteinase domain-containing protein 18	Pro-inflammatory, help in the release of TNFα	1.9	-1.5	-2.8
9	Ninj2	Ninjurin 2	Pro-inflammatory, regulate expression of IL6, IL1β, TNFα	1.5	-1.3	-2.0
10	Try4	Trypsin 4	Pro-inflammatory,	1.1	-2.2	-2.5

			induce the inflammation process			
11	Hoxb8	Homeobox protein Hox-B8	Pro-inflammatory, highly expressed in inflammatory colon	1.9	-1.2	-2.1
12	Hamp2	Hepcidin antimicrobial peptide 2	Increased in inflammation, works against bacterial LPS	1.4	-1.4	-1.9
13	Lep	Leptin	Pro-inflammatory, Induce IL2,IL12,IFNγ cytokine production	1.6	-1.9	-1.2
14	Paqr9	Progestin And AdipoQ Receptor Family Member 9	Pro-inflammatory	1.2	-1.5	-1.3
15	Klra3	killer cell lectin-like receptor	Pro-inflammatory, involve in NK cell activation	1.1	-1.6	-1.4
16	Igkv9-	Immunoglobulin	Responsible for	1.1	-1.8	-1.7

	123	kappa variable 9-123	prolonged inflammation			
17	Mcpt-ps1	Mast cell protease, pseudogene 1	Anti-inflammatory	-1.0	1.5	-1.5
18	Psg17	Pregnancy specific glycoprotein 17	Anti-inflammatory, control infections and inflammatory conditions	-1.8	1.0	-1.8
19	2310034C09Rik	-	Anti-inflammatory, downregulation cause inflammation	-2.5	1.2	-2.9
20	Rn7sk	RNA Component Of 7SK Nuclear Ribonucleoprotein	Anti-inflammatory	-1.4	1.6	-1.1
21	Krt90	Keratin 90	Anti-inflammatory, downregulation cause inflammation	-1.5	1.2	-1.8
22	Sptssb	Serine Palmitoyl transferase Small Subunit B	Anti-inflammatory, suppression of it associated with	-1.3	1.4	-1.9

			leaky gut and suppression of MUC2			
23	Tmprss13	Transmembrane Serine Protease 13	Anti-inflammatory, promote cell survival, restrict apoptosis	-2.3	1.6	-3.6
24	Agr3	Anterior Gradient 3, Protein Disulphide Isomerase Family Member	Anti-inflammatory	-1.1	1.5	-1.6
25	Ceacam 12	Carcinoembryonic antigen-related cell adhesion molecule 12	Anti-inflammatory	-1.4	1.7	-2.4
26	Tpsab1	Tryptase Alpha/Beta 1	Anti-inflammatory, control infections and sepsis	-1.6	1.2	-1.9
27	Slc47a1	Solute Carrier Family 47	Related to anti-inflammation	-1.4	1.5	-2.1

		Member 1				
28	Muc6	Mucin 6, oligomeric mucus/gel-forming	Involved in maintaining gut barrier function, Decreased at the time of gut inflammation	-1.1	1.3	-1.5
29	Scnn1g	Sodium Channel Epithelial 1 Subunit Gamma	Associated to leaky gut. Maintain electrolyte (Na, K) balance in the gut	-1.3	1.2	-1.6

The shortlisted genes from transcriptomics analysis responsible for differential disease progression in C57BL/6 (Fig. 4.7P) and BALB/c (Fig. 4.7Q) mice were depicted as the heat map in panels P and Q. Fold changes of the gene expressions were presented as a heatmap.

4.2.3 Predicted altered metabolic and immune-related pathways due to the diseased condition of the host

We calculated the fold change of significantly altered metabolites (Table. 4.4A & 4.4B) and meta-metabolites (Table. 4.5A & 4.5B) and grouped them into two parts, i) upregulated and ii) downregulated.

Table. 4.4A: Significantly affected serum metabolites from metabonomics study with their function and fold change values at different treatment conditions for C57BL/6 mice.

Sr. No.	Metabolites	Function	7d/0d	15d/0d	15d/7d
1	Fumarate	Anti-inflammatory, alleviates colitis by activating anti-oxidant and anti-inflammatory pathways	3.3	-	2.0
2	Creatine phosphate	Anti-inflammatory, alleviates the severity of colitis	3.3	-	3.8
3	Indole-3-lactate	Anti-inflammatory, controls autophagy	1.9	1.7	4.4
4	Lysine	Anti-inflammatory, controls gut mucosal inflammation	-2.7	-	-
5	Glutamine	Anti-inflammatory, help in mucosal healing in colitis	1.8	-	-
6	2,6-Dihydroxybenzoate	Anti-inflammatory, provide protection against colitis	3.0	1.7	1.8
7	2,3,4-Trihydroxybenzoate	Anti-inflammatory, provide protection against colitis	2.4	-1.7	4.0

8	Pyrocatechol	Anti-inflammatory, activate ROS to control intestinal inflammation	1.6	-1.9	3.1
9	Adenine	anti-inflammatory, alleviates inflammation	3.3	-	-1.9
10	Inosine	Anti-inflammatory, ameliorate inflammation	2.2	1.8	
11	Protocatechuate	Anti-inflammatory, controls CRP, IL6,TNFa level	2.4	-	1.7
12	Imidazole	Anti-inflammatory, prevents inflammasome formation in colitis	-2.2	-	-1.9
13	Hypoxanthine	Improves gut-barrier function	2.3	-	2.1
14	2'-Deoxyuridine	Cause neuro-gastro-intestinal encephalopathy in colitis patients	-2.8	-1.5	-
15	Niacinamide	Increase colitis related inflammation and angiogenesis	5.4	-	6.0
16	Tyrosine	Increased in colitis patient, good marker for diagnosis	1.7	-1.6	1.7

17	3-Indoxylsulfate	Indication of gut dysbiosis and increased amount of pathogenic bacteria in gut	2.2	-3.4	7.5
18	Uracil	Induce inflammation in colon	2.5	-	1.7
19	Cytosine	Induce inflammation in colon and peritoneum	3.4	3.3	-
20	NADP+	Pro-inflammatory, activate localized inflammation process	1.8	-	-
21	Quinolinate	Pro-inflammatory, elevated at the time of infection and inflammation	4.6	-1.7	7.6
22	Nicotinate	Related to colitis disease severity, inflammation	6.5	3.8	1.7
23	6-Hydroxynicotinate	Related to colitis disease severity, inflammation	3.4	1.8	1.9
24	Nicotinamide N-oxide	Related to colitis disease severity, positively correlated with hypoxia, leukocyte infiltration and inflammation	5.5	2.4	2.3
25	1-Methylnicotinamide	Related to colitis disease severity, positively correlated	2.7	-	1.8

		with hypoxia, leukocyte infiltration and inflammation			
26	Serine	anti-inflammatory, alleviates oxidative stress and inflammatory response	-	-1.5	-
27	Agmatine	Anti-inflammatory, reduce intestinal inflammation	-	-3.8	4.7
28	Catechol	Anti-inflammatory, activate ROS to control intestinal inflammation	-	-1.6	2.0
29	Maleate	Anti-inflammatory, ameliorate inflammation	-	2.6	-1.9
30	Epicatechin	Anti-inflammatory, ameliorate inflammation by blocking NF-kB pathway	-	2.2	-1.8
31	Arabinose	Exert anti-inflammatory effect in colitis	-	-1.8	-
32	Tryptophan	Reduce inflammation in colitis and help in maintaining gut barrier function	-	-3.3	2.6
33	Phenylalanine	Cause inflammation in	-	-3.2	2.8

		intestinal mucosa			
34	Ascorbate	Colitis patient content more ascorbate in the intestine	-	-1.5	
35	Glucose	High glucose exacerbate inflammation by activating TGF-B pathway	-	-2.0	-
36	5-Hydroxytryptophan	Increase the severity of colitis	-	-1.8	2.4
37	Xylose	Increased xylose indicates malabsorption of intestine due to inflammation.	-	-1.6	1.7
38	3-Hydroxykynurenine	Pro-inflammatory, elevated in colitis	-	-1.7	-
39	Pyroglutamate	Pro-inflammatory, indicator of cellular inflammatory responses	-	-6.2	4.0
40	Homocysteine	Pro-inflammatory, participate in mucosal inflammation in colitis	-	-1.6	1.8

Table. 4.4B: *Significantly affected serum metabolites from metabonomics study with their function and fold change values at different treatment conditions for BALB/c mice.*

Sr. No.	Metabolites	Function	7d/0d	15d/0d	15d/7d
1	Fumarate	Anti-inflammatory, alleviates colitis by activating anti-oxidant and anti-inflammatory pathways	3.3	5.1	1.6
2	Trigonelline	Anti-inflammatory, attenuates the inflammatory effect of Tnf-α, Il/1β and, Tlr4	2.0	-5.0	-10.1
3	Indole-3-lactate	Anti-inflammatory, controls autophagy	1.6	-	-
4	Aspartate	Anti-inflammatory, down-regulated TLR 4, NOD1, and MyD88 expression	2.0	-	-2.4
5	2,3,4-Trihydroxybenzoate	Anti-inflammatory, provide protection against colitis	2.0	11.3	5.5
6	Catechol	Anti-inflammatory, activate ROS to control intestinal inflammation	1.7	13.1	7.7
7	Adenine	anti-inflammatory, alleviates	2.0	4.2	2.2

		inflammation			
8	Maleate	Anti-inflammatory, ameliorate inflammation	3.3	6.7	2.0
9	Protocatechuate	Anti-inflammatory, controls CRP, IL6,TNFa level	3.4	9.2	2.7
10	Glutamate	Anti-inflammatory, reduce colitis disease score by activating anti-oxidants and cell proliferation	2.8	-	-1.9
11	N-Acetylglucosamine	Anti-inflammatory, used as a treatment for IBD	5.1	-	-7.2
12	Hypoxanthine	Improves gut-barrier function	2.4	4.3	1.8
13	Ascorbate	Colitis patient content more ascorbate in the intestine	3.6	-	-4.5
14	Niacinamide	Increase colitis related inflammation and angiogenesis	2.4	10.3	4.2
15	5-Hydroxytryptophan	Increase the severity of colitis	1.5	1.7	-
16	Tyrosine	Increased in colitis patient, good marker for diagnosis	1.9	-	-
17	Uracil	Induce inflammation in colon	2.7	4.3	1.6
18	Cytosine	Induce inflammation in colon	5.1	6.6	-

		and peritoneum			
19	Quinolinate	Pro-inflammatory, elevated at the time of infection and inflammation	2.5	2.1	-
20	N-Acetylaspartate	Pro-inflammatory, related to tumor growth and adipogenesis	5.8	-	-8.5
21	Homocysteine	Pro-inflammatory, participate in mucosal inflammation in colitis	1.8	-1.7	-3.1
22	6-Hydroxynicotinate	Related to colitis disease severity, inflammation	11.4	-	-2.9
23	Nicotinate	Related to colitis disease severity, inflammation	5.0	5.9	-
24	Nicotinamide N-oxide	Related to colitis disease severity, positively correlated with hypoxia, leukocyte infiltration and inflammation	4.1	2.1	-1.9
25	2,6-Dihydroxybenzoate	Anti-inflammatory, provide protection against colitis	-	10.7	6.5
26	Gallate	Anti-inflammatory, reduced the expression of COX2, IL-6, TNFα	-	7.9	6.0

27	Pyrocatechol	Anti-inflammatory, activate ROS to control intestinal inflammation	-	12.0	9.6
28	Adenine	anti-inflammatory, alleviates inflammation	-	4.2	2.2
29	3-Indoxylsulfate	Indication of gut dysbiosis and increased amount of pathogenic bacteria in gut	-	7.7	5.1
30	Epicatechin	Anti-inflammatory, protective effect mediated by increasing antioxidation and by the inhibition of NF-κB pathway	-	-	2.8
31	Arabinose	Exert anti-inflammatory effect in colitis	-	-	-1.8

Table. 4.5A: *Significantly affected cecal metabolites from metabonomics study with their function and fold change values at different treatment conditions for C57BL/6 mice.*

Sr. No.	Metabolites	Function	7d/0d	15d/0d	15d/7d
1	Guanosine	Anti-inflammatory and anti-oxidative, block the activation of NF-KB	28.3	-	-

		pathway			
2	Serine	anti-inflammatory, alleviates oxidative stress and inflammatory response	-3.8	-2.5	-
3	Indole-3-acetate	Anti-inflammatory, reduce macrophage inflammation	-3.4	-	-34.2
4	Vanillate	Anti-inflammatory, stops neutrophile migration	-2.1	21.4	-45.5
5	Lactulose	Anti-inflammatory, used as prebiotic for colitis treatment	-3.4	-7.0	-2.0
6	Adenine	anti-inflammatory, alleviates inflammation	75.9	-	-
7	Inosine	Anti-inflammatory, ameliorate inflammation	21.0	-	-
8	Imidazole	Anti-inflammatory, prevents inflammasome formation in colitis	2.9	-	14.2
9	Arabinose	Exert anti-inflammatory effect in colitis	-3.0	-12.1	4.1
10	Hypoxanthine	Improves gut-barrier function	78.5		

11	Niacinamide	Increase colitis related inflammation and angiogenesis	26.4	15.4	4.2
12	3-Indoxylsulfate	Indication of gut dysbiosis and increased amount of pathogenic bacteria in gut	2.3	54.7	23.6
13	Uracil	Induce inflammation in colon	2.0	44.0	90.0
14	Cytidine	Induce inflammation in colon and peritoneum	11.8	8.4	-
15	Cytosine	Induce inflammation in colon and peritoneum	1.9	70.8	38.1
16	Quinolinate	Pro-inflammatory, elevated at the time of infection and inflammation	55.8	25.5	-
17	3-Hydroxykynurenine	Pro-inflammatory, elevated in colitis	-3.5	29.0	101.4
18	Mannitol	Pro-inflammatory, elevated in colitis	-3.5	-3.2	-
19	Nicotinate	Related to colitis disease severity, inflammation	60.3	41.3	4.3
20	6-	Related to colitis disease	47.7	11.8	11.8

	Hydroxynicotinate	severity, inflammation			
21	Nicotinamide N-oxide	Related to colitis disease severity, positively correlated with hypoxia, leukocyte infiltration and inflammation	32.6	11.9	13.6
22	Ascorbate	Colitis patient content more ascorbate in the intestine	-3.5	-3.6	-
23	Taurine	Anti-inflammatory, attenuates carcinogenicity in colitis	-	-32.7	-22.0
24	Glycine	Anti-inflammatory, attenuates the activation of pro-inflammatory cytokine and chemokine in colitis	-	-8.6	-2.5
25	Cellobiose	Anti-inflammatory, attenuates the activation of pro-inflammatory cytokines in colitis	-	-41.1	-28.6
26	Trehalose	Anti-inflammatory, maintain autophagic flux	-	-24.5	-13.6

		and reduce the severity of colitis			
27	myo-Inositol	Anti-inflammatory, reduces β-catenin activation in colitis	-	-27.3	
28	Gallate	Anti-inflammatory, reduced the expression of COX2, IL-6, TNFα	-	21.4	-18.0
29	Pyrocatechol	Anti-inflammatory, activate ROS to control intestinal inflammation	-	228.9	-212.2
30	Catechol	Anti-inflammatory, activate ROS to control intestinal inflammation	-	227.3	-211.5
31	Histamine	Cause allergic enteropathy in colitis	-	-28.7	-13.2
32	Glucose	High glucose exacerbate inflammation by activating TGF-B pathway	-	-37.2	-40.6
33	Xylose	Increased xylose indicates malabsorption of intestine due to inflammation.	-	-42.5	-48.3

34	Quinolinate	Pro-inflammatory, elevated at the time of infection and inflammation	-	25.5	-
35	Homocysteine	Pro-inflammatory, participate in mucosal inflammation in colitis	-	3.1	13.1
36	N-Acetylaspartate	Pro-inflammatory, related to tumor growth and adipogenesis	-	9.5	8.5
37	Pyroglutamate	Pro-inflammatory, indicator of cellular inflammatory responses	-	4.0	6.0
38	Tyrosine	Increased in colitis patient, good marker for diagnosis	-	1.9	3.9
39	myo-Inositol	Anti-inflammatory, reduces β-catenin activation in colitis	-	-	-24.8
40	Maleate	Anti-inflammatory, ameliorate inflammation	-	-	-5.4
41	Protocatechuate	Anti-inflammatory, controls CRP, IL6,TNFa level	-	-	63.0

Table. 4.5B: *Significantly affected cecal metabolites from metabonomics study with their function and fold change values at different treatment conditions for BALB/c mice.*

Sr. No.	Metabolites	Function	7d/0d	15d/0d	15d/7d
1	Guanosine	Anti-inflammatory and anti-oxidative, block the activation of NF-KB pathway	-4.0	-6.0	-
2	Fumarate	Anti-inflammatory, alleviates colitis by activating anti-oxidant and anti-inflammatory pathways	-5.3	-	6.2
3	Serine	anti-inflammatory, alleviates oxidative stress and inflammatory response	4.0	-5.6	-22.5
4	Lactulose	Anti-inflammatory, used as prebiotic for colitis treatment	13.0	-	-35.7
5	Pyrocatechol	Anti-inflammatory,	-5.6	-	6.2

		activate ROS to control intestinal inflammation			
6	Catechol	Anti-inflammatory, activate ROS to control intestinal inflammation	-5.6	-	6.2
7	Adenine	anti-inflammatory, alleviates inflammation	-6.4	-	5.3
8	Protocatechuate	Anti-inflammatory, controls CRP, IL6,TNFa level	-6.2	-	6.4
9	Imidazole	Anti-inflammatory, prevents inflammosome formation in colitis	-6.0	-	6.4
10	Ascorbate	Colitis patient content more ascorbate in the intestine	5.7	-12.5	-74.0
11	Arabinose	Exert anti-inflammatory effect in	20.0	-	-57.9

		colitis			
12	Hypoxanthine	Improves gut-barrier function	-6.3	-	-
13	3-Indoxylsulfate	Indication of gut dysbiosis and increased amount of pathogenic bacteria in gut	-6.2	-	6.5
14	Uracil	Induce inflammation in colon	-6.4	-	6.4
15	Cytosine	Induce inflammation in colon and peritoneum	-6.2	-	6.3
16	Mannitol	Mannitol excretion is high in colitis	6.2	-	-54.2
17	Quinolinate	Pro-inflammatory, elevated at the time of infection and inflammation	-6.5	-	5.1
18	3-Hydroxykynurenine	Pro-inflammatory, elevated in colitis	6.8	-	-50.2
19	6-	Related to colitis	-4.3	-	3.9

	Hydroxynicotinate	disease severity, inflammation			
20	Nicotinamide N-oxide	Related to colitis disease severity, positively correlated with hypoxia, leukocyte infiltration and inflammation	-7.3	-1.5	4.3
21	Homocysteine	Pro-inflammatory, participate in mucosal inflammation in colitis	3.1	-	-
22	N-Acetylaspartate	Pro-inflammatory, related to tumor growth and adipogenesis	45.5	-	-
23	Niacinamide	Increase colitis related inflammation and angiogenesis	84.2	-4.1	-
24	Tyrosine	Increased in colitis patient, good marker for diagnosis	3.9	-	-
25	Pyroglutamate	Pro-inflammatory,	10.0	-	-

		indicator of cellular inflammatory responses			
26	Inosine	Anti-inflammatory, ameliorate inflammation	-	-5.0	-
27	Cytidine	Induce inflammation in colon and peritoneum	-	-7.7	-7.9
28	Nicotinate	Related to colitis disease severity, inflammation	-	-4.2	-3.6
29	2,6-Dihydroxybenzoate	Anti-inflammatory, provide protection against colitis	-	-	6.4
30	2,3,4-Trihydroxybenzoate	Anti-inflammatory, provide protection against colitis	-	-	6.4
31	Gallate	Anti-inflammatory, reduced the expression of COX2, IL-6, TNFα	-	-	6.2
32	Vanillate	Anti-inflammatory,	-	-	-14.4

		stops neutrophile migration			
33	Maleate	Anti-inflammatory, ameliorate inflammation	-	-	4.5

Using the KEGG pathway as a reference dataset, we predicted the altered metabolic pathways using these upregulated and downregulated metabolites and meta-metabolites. We named these pathways as upregulated and downregulated pathways of different treatment conditions. We represented the pathway names with a unique number. Pathway names with their corresponding unique pathway numbers were enlisted in Table. 4.6. We plotted the bar graph with the topmost impacted pathways in various diseased conditions. The pathway analysis found that the pathways related to carbohydrate and nucleotide metabolisms were upregulated in the less severe condition of the disease and downregulated in the severe form of the disease in both strains. In C57BL/6, pathways predicted from shortlisted metabolites (Fig. 4.8A, E) and meta-metabolites (Fig. 4.8C, G) related to carbohydrate and nucleotide metabolism were upregulated on day 7 over day 0 (Fig. 4.8A, C) and downregulated on day 15 over day 0 and day 15 over day 7 (Fig. 4.8E, G). On the other hand, in BALB/c, pathways predicted from metabolites were upregulated day 15 over day 0 and day 15 over day 7 (Fig. 4.8B). For meta-metabolites, it was on day 15 over day 7 (Fig. 4.8D). However, in BALB/c, we had not found any downregulated carbohydrate and nucleotide metabolism pathways from the pathways predicted from metabolites, but for meta-metabolites, it was on day 7 over day 0 (Fig.

4.8H). Pathways related to amino acid and lipid metabolism were upregulated when the disease severity was highest in both mice strains and successively downregulated at the less severe colitis. In C57BL/6, the predicted pathways from metabolites (Fig. 4.8A, E) and meta-metabolites (Fig. 4.8C, G), related to amino acid and lipid metabolisms were upregulated on day 15 over day 0 and day 15 over day 7 (Fig. 4.8A, C) and downregulated on day 7 over day 0 (Fig. 4.8E, G). In BALB/c, the predicted pathways from metabolites (Fig. 4.8B, F) and meta-metabolites (Fig. 4.8D, H) related to the amino acid and lipid metabolisms were upregulated on day 7 over day 0 (Fig. 4.8B, D) and downregulated on day 15 over day 0 as well as day 15 over day 7 (Fig. 4.8F, H).
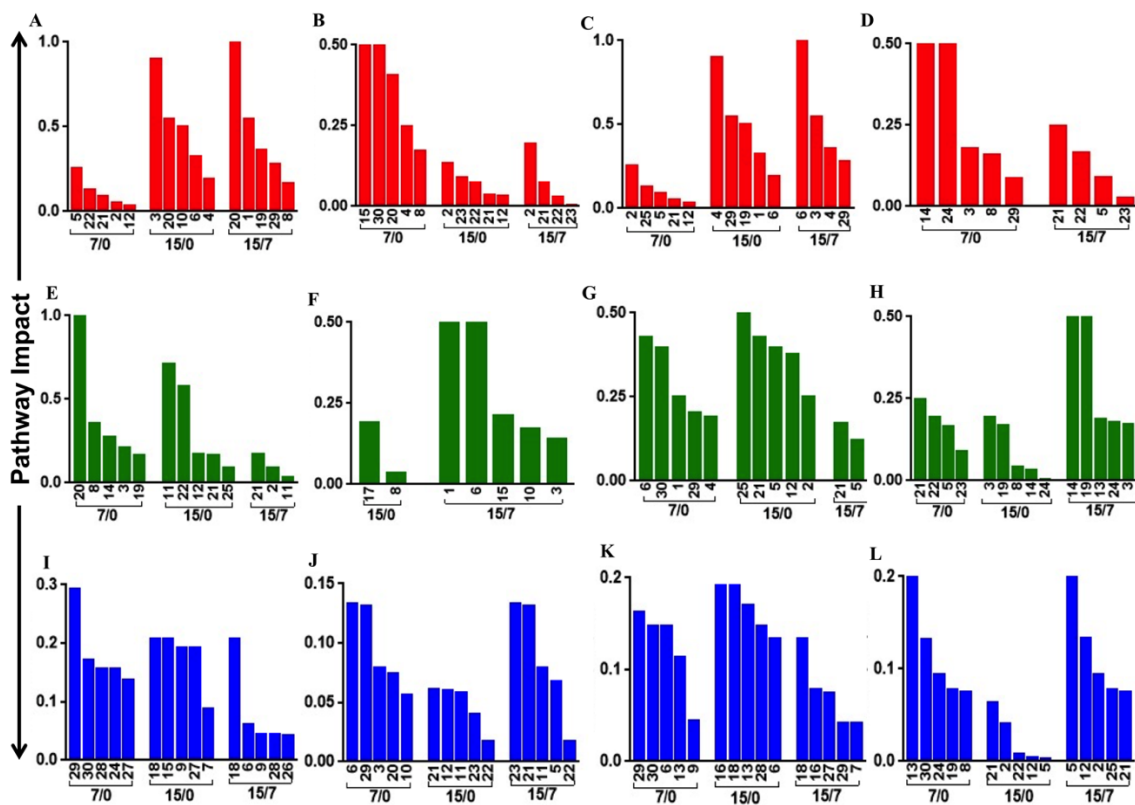
Fig. 4.8: *Majorly impacted pathways due to the altered metabolic and inflammatory responses in the presence of DSS treatment.*

(A, B) Majorly impacted pathways due to altered metabolites' upregulation at various treatment conditions in serum in C57BL/6 (A) and BALB/c (B) mice. (C, D) Majorly impacted pathways due to altered metabolites' upregulation at various treatment conditions in cecal content in C57BL/6 (C) and BALB/c (D) mice. (E, F) Majorly impacted pathways due to altered metabolites' downregulation at various treatment conditions in serum in C57BL/6 (E) and BALB/c (F) mice. (G, H) Majorly impacted pathways due to altered metabolites' downregulation at various treatment conditions in cecal content in C57BL/6 (G) and BALB/c (H) mice. (I, J) Primarily impacted pathways due to the alteration of serum metabolites and changes in the host's inflammatory responses in both C57BL/6 (I) and BALB/c (J) mice. (K, L) Primarily impacted pathways due to the alteration of cecal metabolites (meta-metabolites) and changes in the host's inflammatory responses in both C57BL/6 (K) and BALB/c (L) mice. We represented the pathway names with numbers to avoid unnecessary clutters. We have enlisted the pathway names with their corresponding pathway numbers in Table. 4.6.

We performed a correlation analysis for C57BL/6 (Table. 4.7A) and BALB/c (Table. 4.7B) and found that carbohydrate and nucleotide metabolisms were positively correlated with anti-inflammation. In contrast, amino acid and lipid metabolism were positively correlated with pro-inflammation (Table. 4.7A & B). This correlation analysis is well corroborated with our experimental observations.

We perform a joint pathway analysis to know the collective effect of gene-level and metabolite-level changes on the host system. This analysis considered both shortlisted

genes and shortlisted metabolites and meta-metabolites to predict the biological pathways. Pathway names with their corresponding unique pathway numbers were enlisted in Table. 4.6. Interestingly, we found that in C57BL/6, the highly impacted pathways from these two joint analyses, i.e., transcriptomics and metabolites (Fig. 4.8I) and transcriptomics and meta-metabolites (Fig. 4.8K), were mainly related to pro-inflammation related pathways along with the metabolic pathways. Pathways related to Toll-Like receptor, NOD- Like receptor, IL17, TNFα signaling, cytokine-cytokine receptor interactions were affected along with different metabolic pathways. Either one or more of these immune-related pathways were activated in all the treatment conditions, i.e., day 7 over day 0, day 15 over day 0, and day 15 over day 7. In BALB/c, the highly impacted pathways from these two joint analyses, i.e., transcriptomics and metabolites (Fig. 4.8J) and transcriptomics and meta-metabolites (Fig. 4.8L), no inflammation-related pathways were affected. Only metabolic pathways were involved in all the treatment conditions, i.e., day 7 over day 0, day 15 over day 0, and day 15 over day 7. This observation supports the point more strongly; the immune background of the host plays a crucial role in determining the disease severity of colitis.

Table. 4.6: *Pathway name and its corresponding pathway no. used in the main figure panel.*

Pathway No.	Pathway Name
1	Alanine, aspartate and glutamate metabolism
2	Amino sugar and nucleotide sugar metabolism
3	Arginine and proline metabolism
4	Arginine metabolism
5	Ascorbate and aldarate metabolism
6	beta-Alanine metabolism
7	Chemokine signalling pathway
8	Cysteine and methionine metabolism
9	Cytokine-cytokine receptor interaction
10	D-Glutamine and D-glutamate metabolism
11	Fructose and mannose metabolism
12	Galactose metabolism
13	Glycerolipid metabolism
14	Glycine, serine and threonine metabolism
15	Histidine metabolism
16	IL-17 signalling pathway
17	Inositol phosphate metabolism
18	NOD-like receptor signalling pathway
19	Phenylalanine metabolism

20	Phenylalanine, tyrosine and tryptophan metabolism
21	Purine metabolism
22	Pyrimidine metabolism
23	Pyruvate metabolism
24	Sphingolipid metabolism
25	Starch and sucrose metabolism
26	Th17 cell differentiation
27	TNF signalling pathway
28	Toll-like receptor signalling pathway
29	Tryptophan metabolism
30	Tyrosine metabolism

4.2.4 Altered gut microbial composition of diseased C57BL/6 and BALB/c

Transcriptional activation TLRs, other inflammatory cytokines, and compromised gut barrier function were the clear indication for the altered gut microbial composition of diseased hosts. Activation of the host's inflammatory responses was the effect of more no. of gram-negative pathogenic bacteria in the gut. LPS (Lipopolysaccharide) secreted by these bacteria bind with the TLRs and activate the downstream pro-inflammatory pathways [45]. We investigated the gut microbial composition of treated groups and their time match controls at different diseased conditions for both strains. Data from our study revealed that the gut microbial composition of control C57BL/6 (Fig. 4.9A) and BALB/c (Fig. 4.9B) overtly belongs to the phyla Bacteroidetes and Firmicutes (Fig. 4.9A, B). The abundance of the phyla Bacteroidetes (Fig. 4.9C) and Firmicutes (Fig. 4.9D) were

reduced, while the abundance of Proteobacteria (gram-negative pathogens) phylum (Fig. 4.9E) was increased significantly on day 7 and day 15 of DSS treated animals compared to their time-matched control. The proteobacteria level reached maximum by day 15 (32% of total abundance) in treated C57BL/6 and by day 7 (29% of total abundance) in treated BALB/c (Fig 4.9E). After day 7 of DSS-treated BALB/c showed a significantly different gut microbiota profile with the appearance of phylum, Verrucomicrobia, absent in treated C57BL/6 on day 15 (Fig. 4.9F). A sudden increase in Bacteroidetes, Firmicutes, and Verrucomicrobia phyla, on day 15 of DSS-treated BALB/c replaced the predominance of Proteobacteria phylum (Fig. 4.9F). This result again supports our previous observation about the differential responses of two different immune-bias mice in the presence of a common DSS dose.

Since each phylum contains various genera, it is crucial to know the significant changes in the abundance and diversity at the genus level following DSS treatment in C57BL/6 (Fig. 4.9G) and BALB/c (Fig. 4.9H). At the genus level, the gut microbiota of untreated time-matched control of either type of mice majorly composed of genus Bacteroides and Alistipes of Bacteroidetes phylum and genus Lachnospiraceae from Firmicutes phylum. In the DSS treated condition, the abundance of Bacteroides (Fig. 4.9I), Alistipes (Fig. 4.9J), and Lachnospiraceae (Fig. 4.9K) significantly decreased and predominated by the genus Helicobacter (Fig. 4.9L) from Proteobacteria phylum in both the strains. The abundance of Helicobacter genus was highest on day 15 of DSS treatment in C57BL/6 and day 7 in BALB/c (Fig. 4.9L). In BALB/c, similar to the phylum level, the genus belongs to the Bacteroidetes (genus-Alistipes), Firmicutes (genus- Lachnospiraceae), and Verrucomicrobia (genus- Akkermensia) phyla replace the predominancy of genus

Helicobacter of Proteobacteria phylum (Figs 4.9J-M). In C57BL/6, no such changes were observed on day 15 of DSS treatment.

The above results revealed that along with the disease severity, a load of pathogenic Proteobacteria in the gut significantly increased till the end of the DSS treatment in C57BL/6. In DSS-treated BALB/c, as the disease severity decreased after day 7 of DSS treatment, the abundance of Proteobacteria also significantly reduced in the gut.

In addition, we further determined the changes in the diversity (the diversity and evenness in the distribution of microbial and metabolite composition) of gut microbial composition and metabolites and meta-metabolites diversity along with the altered disease severity [19]. The diversity Evenness index at the microbial phylum level showed a significant gradual decrease in diversity throughout the treatment condition in C57BL/6 compared to their time-matched control. On the contrary, in BALB/c, on day 7, we observed a substantial reduction in the diversity in the treatment condition compared to their time-matched control (Fig. 4.9N). Diversity Evenness index of serum and cecal metabolites behaved oppositely. Serum metabolite diversity increased with the disease severity (Fig. 4.9R) in both strains compared to their time matched control (Fig. 4.9O). On the contrary, cecal metabolite diversity decreased with the disease severity (Fig. 4.9R) in both strains compared to their time matched control (Fig. 9P). The ratio of Evenness index of treatment/control condition also supports the mentioned observation in both strains (Fig. 4.9Q). The disease severity score was calculated using the criteria mentioned in Fig. 4.1F.
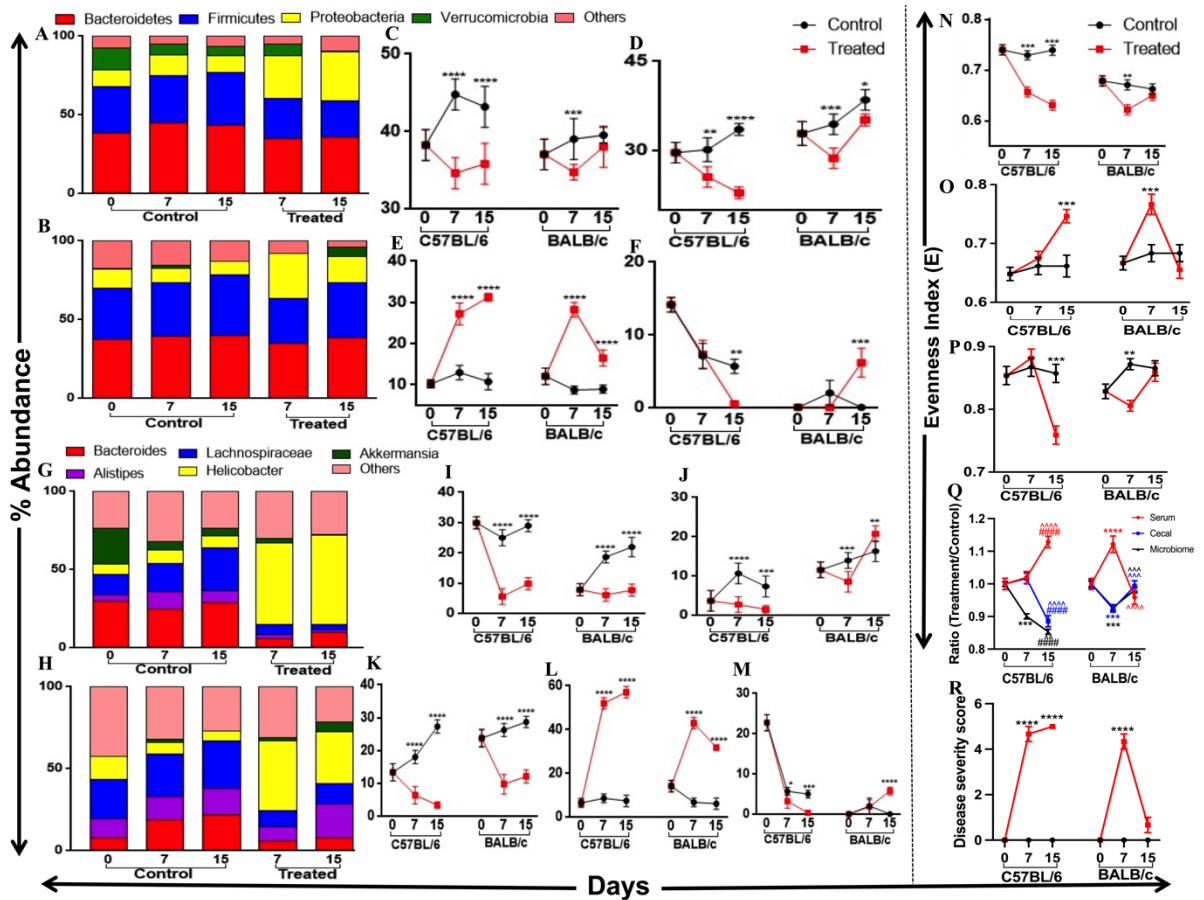
Fig. 4.9: Phylum and genus level changes in gut microbial composition and altered metabolic and microbial diversity due to altered disease severity.

Stack bar showing the relative changes in major phyla of gut microbiota in control and DSS treated C57BL/6 (A) and BALB/c (B) mice. We have plotted the abundance of major phyla of control and its respective treated group for both the mice strains for better understanding. (C, D, E, F) depicts the following phylum respectively- Bacteroidetes, Firmicutes, Proteobacteria, Verrucomicrobia. Panel (H, I) represents the relative changes in the genus level of gut microbiota in control and DSS treated C57BL/6 (H) and BALB/c (I) mice. Similarly, like phylum, we have plotted the abundance of the different genus of control and its respective treated group for both the mice strains for better

understanding. (I, J, K, L, M) depicts the following genus respectively- Bacteroides, Alistipes, Lachnospiraceae, Helicobacter, Akkermensia. (N) Further, we calculated the changes in gut microbial diversity and represented the kinetics of phylum-level diversity by calculating the Equitability (Evenness) index (E) of gut microbiota for both control and treated groups of mice for both the strains. Altered gut microbial composition and diversity could be the main reason for the altered metabolic profile and diversity of the host. (O, P) We represented the kinetics of metabolite (O) and meta-metabolite diversity (P) by calculating the equitability index of metabolite and mete-metabolite composition for both control and treated groups C57BL/6 and BALB/c mice. (Q) We also calculated the (treatment/control) ratio of microbial and metabolic Evenness index (E) of C57BL/6 and BALB/c mice to get a comprehensive idea of microbial and metabolic changes based on disease severity. (R) Disease severity score was calculated to get an idea how altered microbial and metabolic profiles affect disease severity followed by DSS treatment.

We presented all values as means± SEM for 3 biological replicates. We performed Two-way ANOVA followed by the Bonferroni test to determine the significance level. */#/^ corresponds to $P<0.05$, ** /##/^^corresponds to $P<0.01$, ***/###/^^^ corresponds to $P<0.001$, ****/####/^^^^ corresponds to $P<0.0001$. (In panel Q, * symbolizes the comparison between day 0 and day 7, # symbolizes the comparison between day 0 and day 15, ^ symbolizes the comparison between day 7 and day 15).

4.2.5 Microbiota regulated metabolic pathways of diseased C57BL/6 and BALB/c

Reports from previous studies suggested that the specific phylum is responsible for the metabolism of particular nutrients. Not all phyla can metabolize all kinds of nutrients,

e.g., Phyla i) Bacteroidetes and Verrucomicrobia are responsible for carbohydrate metabolism ii) Firmicutes is responsible for nucleotide metabolism iii) Proteobacteria is responsible for amino acid and lipid metabolism [46–48].

In this current study, we observed a positive correlation between the i) abundance of Bacteroidetes and Verrucomicrobia and carbohydrate metabolism ii) abundance of Firmicutes with nucleotide metabolism iii) abundance of Proteobacteria with amino acid and lipid metabolism in both the strains (Table. 4.7A & B). We also found a positive correlation between anti-inflammation, the abundance of Bacteroidetes, Firmicutes, and carbohydrate and nucleotide metabolism. On the other hand, pro-inflammation, the abundance of Proteobacteria and amino acid, and lipid metabolism were positively correlated (Table. 4.7A & B). We already mentioned in previous sections that as the colitis disease severity increased, carbohydrate and nucleotide metabolism became downregulated and amino acid and lipid metabolism upregulated. This section plotted the already predicted metabolic pathways acquired from the metabolites and meta-metabolites data, with the responsible phyla for the upregulation or downregulation of these pathways.

Table. 4.7A: Correlation analysis between inflammatory parameters, microbial abundance (phylum level) and metabolic pathways in C57BL/6 mice.

	1	2	3	4	5	6	7	8	9	10	11	12	13	14	15	16	17	18	19	20	21
1	1.00																				
2	0.30	1.00																			
3	0.99	0.32	1.00																		
4	0.98	0.15	0.98	1.00																	
5	0.96	0.03	0.96	0.99	1.00																
6	0.86	0.22	0.85	0.93	0.97	1.00															
7	0.99	0.35	0.99	0.98	0.95	0.84	1.00														
8	0.99	0.24	0.99	0.99	0.98	0.89	0.99	1.00													
9	0.99	0.17	0.99	0.99	0.99	0.92	0.98	0.99	1.00												
10	-0.74	-0.42	-0.73	-0.84	-0.90	-0.98	-0.71	-0.78	-0.83	1.00											
11	0.93	0.07	0.92	0.98	0.99	0.99	0.91	0.95	0.97	-0.93	1.00										
12	-0.39	-0.76	-0.37	-0.52	-0.62	-0.80	-0.34	-0.44	-0.51	0.91	-0.70	1.00									
13	0.87	0.21	0.86	0.94	0.97	0.99	0.84	0.90	0.93	-0.98	0.99	-0.79	1.00								
14	0.99	0.27	0.99	0.99	0.97	0.88	0.99	0.99	0.99	-0.76	0.94	-0.42	0.89	1.00							
15	-0.92	-0.10	-0.91	-0.97	-0.99	-0.99	-0.90	-0.94	-0.96	0.94	-0.99	0.72	-0.99	-0.93	1.00						
16	-0.98	-0.10	-0.97	-0.99	-0.99	-0.95	-0.97	-0.99	-0.99	0.86	-0.99	0.57	-0.95	-0.98	0.98	1.00					
17	-0.95	-0.02	-0.94	-0.98	-0.99	-0.98	-0.93	-0.96	-0.98	0.92	-0.99	0.66	-0.98	-0.96	0.99	0.99	1.00				
18	0.85	0.24	0.84	0.92	0.96	0.99	0.83	0.88	0.92	-0.98	0.98	-0.81	0.99	0.87	-0.99	-0.94	-0.98	1.00			
19	-0.08	-0.97	-0.10	-0.07	-0.19	-0.43	-0.13	-0.02	-0.06	0.61	-0.29	0.89	-0.42	-0.05	0.32	0.13	0.25	-0.45	1.00		
20	-0.46	-0.98	-0.48	-0.32	-0.20	-0.05	-0.51	-0.41	-0.34	0.25	-0.11	0.64	-0.03	-0.43	0.08	0.27	0.15	-0.07	0.92	1.00	
21	0.97	0.53	0.97	0.92	0.86	0.71	0.98	0.95	0.93	-0.55	0.81	-0.15	0.72	0.96	-0.79	-0.90	-0.84	0.70	-0.33	-0.67	1.00

Table. 4.7B: *Correlation analysis between inflammatory parameters, microbial abundance (phylum level) and metabolic pathways in BALB/c mice.*

	1	2	3	4	5	6	7	8	9	10	11	12	13	14	15	16	17	18	19	20	21
1	1.00																				
2	0.10	1.00																			
3	0.74	0.60	1.00																		
4	0.80	0.52	0.99	1.00																	
5	0.01	1.00	0.67	0.59	1.00																
6	0.22	0.95	0.82	0.76	0.97	1.00															
7	0.05	0.99	0.71	0.64	0.99	0.98	1.00														
8	0.49	0.82	0.95	0.91	0.87	0.96	0.90	1.00													
9	0.18	1.00	0.53	0.45	0.99	0.92	0.97	0.77	1.00												
10	-0.72	-0.62	-0.99	-0.99	-0.69	-0.84	-0.73	-0.96	-0.56	1.00											
11	0.05	1.00	0.64	0.56	0.99	0.96	0.99	0.85	0.99	-0.66	1.00										
12	-0.34	-0.97	-0.39	-0.29	-0.94	-0.84	-0.92	-0.66	-0.99	0.42	-0.96	1.00									
13	0.15	0.99	0.55	0.47	0.99	0.93	0.98	0.79	0.99	-0.58	0.99	-0.98	1.00								
14	0.12	0.99	0.58	0.50	0.99	0.94	0.99	0.81	0.99	-0.61	0.99	-0.97	0.99	1.00							
15	-0.48	-0.92	-0.23	-0.14	-0.88	-0.74	-0.85	-0.53	-0.95	0.26	-0.90	0.99	-0.94	-0.93	1.00						
16	-0.95	-0.41	-0.49	-0.57	-0.32	-0.10	-0.27	-0.19	-0.48	0.46	-0.36	0.62	-0.46	-0.42	0.74	1.00					
17	0.53	-0.89	-0.17	-0.08	-0.85	-0.70	-0.82	-0.48	-0.93	0.21	-0.87	0.98	-0.92	-0.90	0.99	0.77	1.00				
18	0.06	0.99	0.72	0.65	0.99	0.99	0.99	0.90	0.97	-0.74	0.99	-0.92	0.98	0.98	-0.84	-0.26	-0.81	1.00			
19	-0.79	-0.53	-0.99	-0.99	-0.61	-0.78	-0.66	-0.92	-0.47	0.99	-0.58	0.32	-0.49	-0.52	0.16	0.55	0.10	-0.66	1.00		
20	-0.24	-0.94	-0.83	-0.78	-0.97	-0.99	-0.98	-0.97	-0.91	0.85	-0.96	0.83	-0.92	-0.93	0.73	0.07	0.69	-0.98	0.79	1.00	
21	0.27	0.98	0.45	0.36	0.96	0.88	0.95	0.71	0.99	-0.48	0.97	-0.99	0.99	0.99	-0.97	-0.56	-0.96	0.94	-0.38	-0.87	1.00

Abbreviations: 1, *TLR2*; 2, *TLR4*; 3, *TNFα*; 4, *IFNγ*; 5, *IL1b*; 6, *IL6*; 7, *IL12*; 8, *IL17*; 9, *IL21*; 10, *IL10*; 11, *Cldn2*; 12, *ZO1*; 13, Gut Permeability; 14, C-Reactive Protein; 15, Bacteroidetes; 16, Verrucomicrobia; 17, Firmicutes; 18, Proteobacteria; 19, Carbohydrate Metabolism; 20, Nucleotide Metabolism; 21, Amino acid and Lipid Metabolism

As the abundance of Bacteroidetes (Fig. 4.10C, G) and Verrucomicrobia (Fig. 4.10D, H) decreased with the disease severity, carbohydrate metabolism also downregulated in C57BL/6 (Fig. 4.10A, B; 4.10A- pathways predicted from serum metabolites, 4.10B- pathways predicted from cecal metabolites) and BALB/c (Fig. 4.10E, F; 4.10E- pathways predicted from serum metabolites, 4.10F- pathways predicted from cecal metabolites) mice. The same trend was followed by nucleotide metabolism. Nucleotide metabolism (Fig. 4.10I, J, L, M) and abundance of Firmicutes (Fig. 4.10K, N) phylum became downregulated with disease severity in C57BL/6 (Fig. 4.10I, J; 4.10I- pathways predicted from serum metabolites, 4.10J- pathways predicted from cecal metabolites) and BALB/c (Fig. 4.10L, M; 4.10L- pathways predicted from serum metabolites, 4.10M- pathways predicted from cecal metabolites) mice. On the contrary, as the disease severity increased, the abundance of Proteobacteria increased (Fig. 4.10Q, T). This further leads to the upregulation of amino acid and lipid metabolism pathways in C57BL/6 (Fig. 4.10O, P; 4.10O- pathways predicted from serum metabolites, 4.10P- pathways predicted from cecal metabolites) and BALB/c (Fig. 4.10R, S; 4.10R- pathways predicted from serum metabolites, 4.10S- pathways predicted from cecal metabolites) mice.
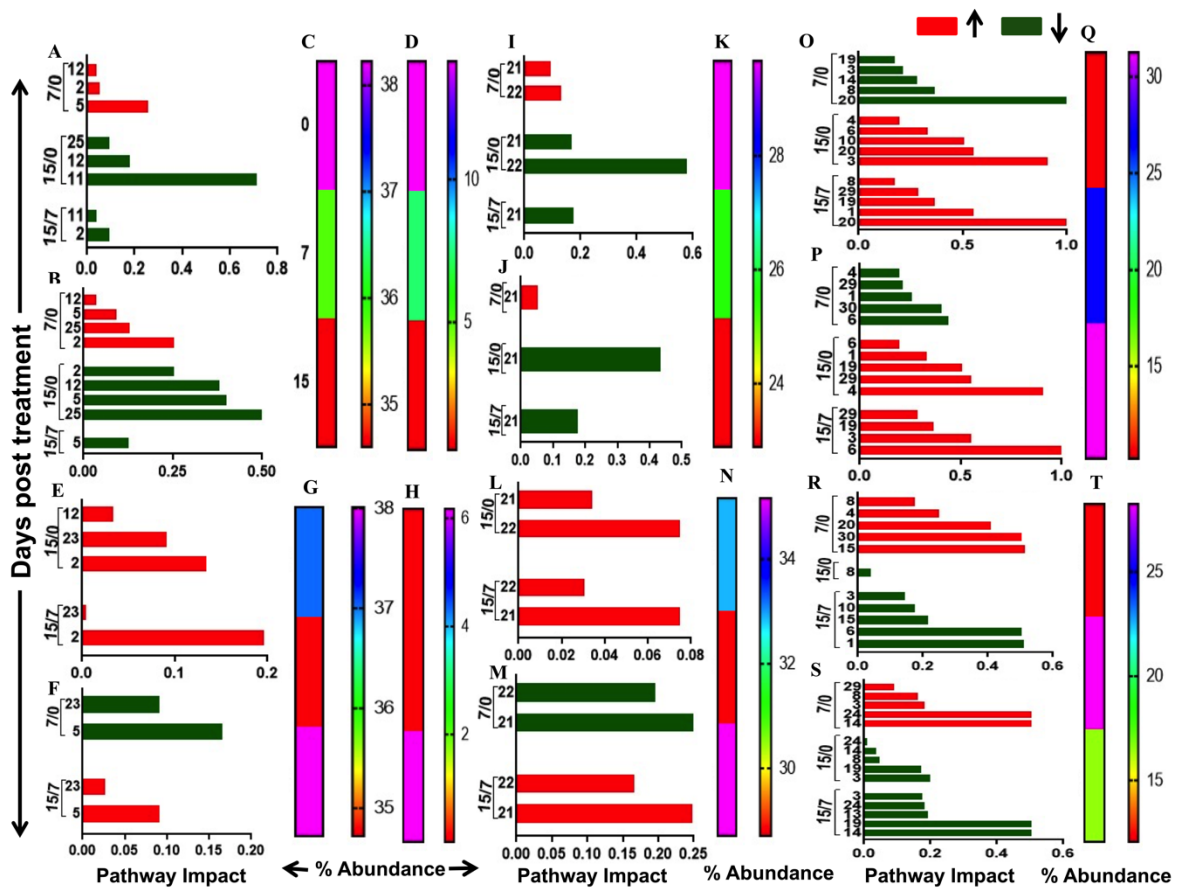
Fig. 4.10: Majorly impacted metabolic pathways in different treatment conditions and the corresponding bacterial phyla responsible for the metabolic changes.

We have categorized the metabolic pathways into four different groups- i) Carbohydrate metabolism, ii) Nucleotide metabolism, iii) Amino acid metabolism, and iv) Lipid metabolism. Bacteroidetes and Verrucomicrobia are responsible for affected Carbohydrate metabolism. Firmicutes are responsible for affected Nucleotide metabolism. Proteobacteria are responsible for affected Amino acid and Lipid metabolism. In C57BL/6 mice, (A, B) represents the affected carbohydrate metabolism in serum (A) and cecal (B) level, (I, J) represents the affected nucleotide metabolism in serum (I) and cecal (J) level and (O, P) represents the affected amino acid and lipid

metabolism in serum (O) and cecal (P) level. (C, D, K, Q) represents the phylum level abundance of Bacteroidetes, Verrucomicrobia, Firmicutes, and Proteobacteria, respectively, in gut microbiota along with its corresponding metabolic process. In BALB/c mice, (E, F) represents the affected carbohydrate metabolism in serum (E) and cecal (F) level, (L, M) represents the affected nucleotide metabolism in serum (L) and cecal (M) level and (R, S) represents the affected amino acid and lipid metabolism in serum (R) and cecal (S) level. (G, H, N, T) represents the phylum level abundance of Bacteroidetes, Verrucomicrobia, Firmicutes, and Proteobacteria, respectively, in gut microbiota along with its corresponding metabolic process. We represented the pathway names with numbers to avoid unnecessary clutters. We have enlisted the pathway names with their corresponding pathway numbers in Table. 4.6.

4.2.6 The probable mechanism of different metabolic conversion and the associated gut microbial genus at the different inflammatory states of the host

So the overall observations of all the experiments gave us a crystal clear idea that host-immune background is the major regulatory factor in determining colitis disease severity. Host immune bias is crucial in activating inflammatory responses, altering the host's metabolic and gut microbial composition in the diseased condition. Increased amino acid metabolism in inflammatory conditions leads to a high amount of lactate and glutamate production. We observed a high amount of butyrate production from its precursor molecules in the control or recovery condition. The gut microbial genus responsible for butyrate production was predominant at the disease's control and recovery phase. The

probable mechanism of the metabolic interconversions at particular inflammatory conditions is depicted in Fig. 4.11.
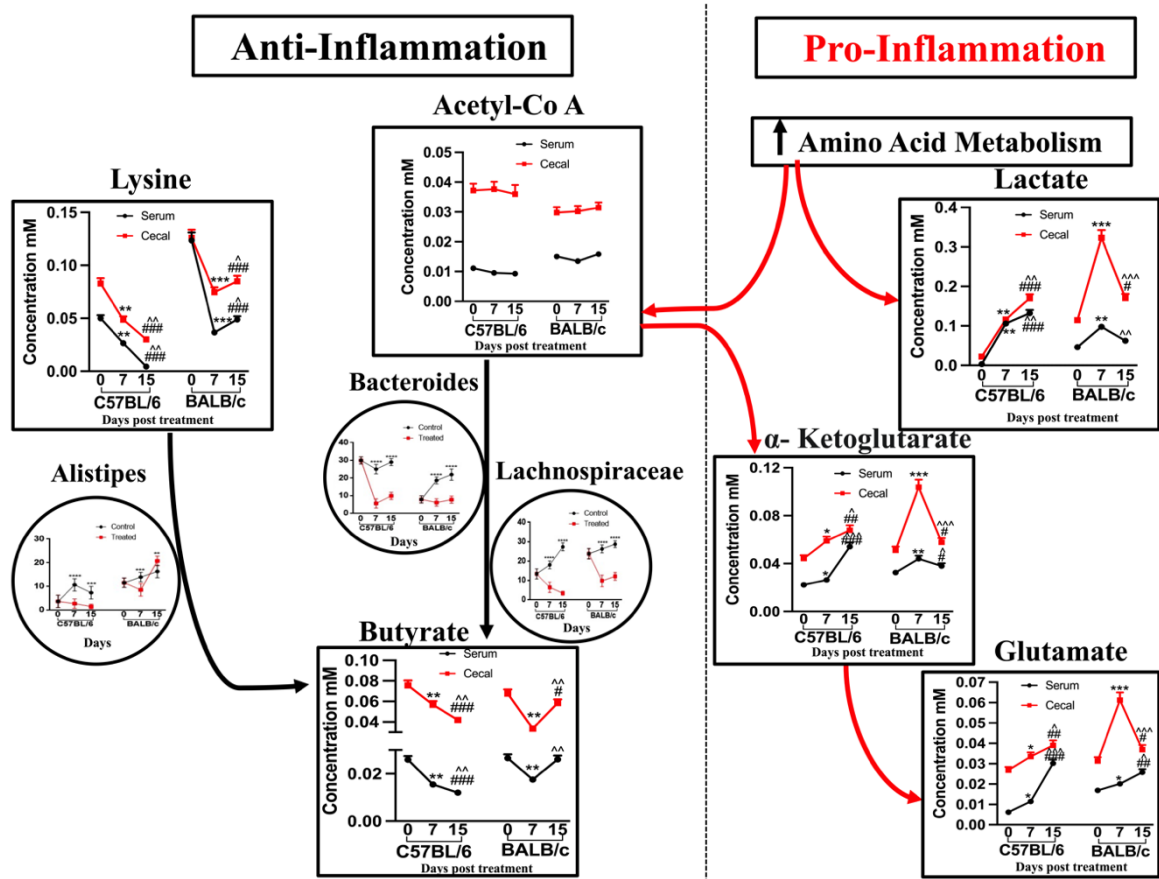
Fig. 4.11: A predictive schema of different regulatory metabolic pathways and associated microbial genus contributing to the varied inflammatory condition at different severity levels of the disease in C57BL/6 and BALB/c mice.

We performed Two-way ANOVA followed by the Bonferroni test to determine the significance level. */#/^ corresponds to P<0.05, ** /##/^^corresponds to P<0.01, ***/###/^^^ corresponds to P<0.001, ****/####/^^^^ corresponds to P<0.0001. *

symbolizes the comparison between day 0 and day 7, # symbolizes the comparison between day 0 and day 15, ^ symbolizes the comparison between day 7 and day 15.

4.3 Discussion

We comprehensively examined the severity responses of DSS induced colitis in two immunologically bias mice strains. With a special mention, we are perhaps the first group that used a composite DSS dosage (5% for the 1st week+ 2.5% for the 2nd week) to understand all the stages of colitis in terms of severity in two different immune-biased mice models within a brief period, i.e., 2 weeks. Data from the gene-based inflammatory study and multi-omics approach revealed that in the presence of a higher dosage (5% for the 1st week), the extent of colonic inflammation and other metabolic and gut microbial changes were almost similar for both strains of mice. At the lower continuing dosage (2.5% for the 2nd week) of DSS, the inflammatory condition was more pronounced and severe in C57BL/6, whereas BALB/c started recovering from the inflammatory state and reaching the normal healthy condition.

Like human colitis, DSS caused damages to intestinal epithelial cells and activated the host's inflammatory responses [49]. After colitis induction in both mice strains, damage-associated molecular markers were released by the damaged colon tissue bound with the Toll-Like Receptors (mainly Tlr2 and Tlr4) and activated flares of inflammatory responses first-line defense mechanism of hosts. Activation of TLRs further activates monocytes and macrophages by using the nucleotide-binding oligomerization domain 2 protein (NOD2) pathway [36,37]. Activation of monocytes and macrophages produced an array of soluble pro-inflammatory cytokines, e.g., TNF-α, IFN-γ [38,50,51]. IL-12 and

IL-21 also mediate IFN-γ secretion due to Th1 mediated pro-inflammatory response [52,53]. TNF-α exerts its pro-inflammatory effects through increased production of IL-1β and IL-6 [54]. IL-1β and IL-6 produced by damaged and inflamed tissue stimulate the production of another inflammatory cytokine, i.e., IL17 [55].

The present study revealed that *TLR2* and *TLR4* genes activated significant pro-inflammatory responses in both mice strains on the 1st week of DSS treatment. We observed a significant upregulation of all the pro-inflammatory mediators (*TNF-α, IFN-γ, IL6, IL1β, IL12, IL21, IL17, MPO*). C57BL/6 followed the trend till the end of the treatment. In BALB/c, no further upregulation was observed in the gene expression of pro-inflammatory mediators on the 2nd week. In some of cases, the expression of pro-inflammatory genes tends to reach their basal level. To know the reason for the amelioration of colitis severity in BALB/c, we checked the expression of one of the most crucial anti-inflammatory mediators, IL10. CD4+ Th2 cells trigger the secretion of IL-10 as an anti-inflammatory response of the host [56]. As we expected, the *IL10* gene expression was upregulated in BALB/c as the disease severity decreased. No such upregulation of *IL10* expression was observed in C57BL/6 in any of the treatment conditions. Activation of the pro-inflammatory pathway has many other consequences in the host system, such as activating host acute phase response protein [43,44,51]. In the current study, we observed significant upregulation of CRP in C57BL/6 on day 15 of the treatment but not in any treatment conditions in BALB/c mice.

Activation of the intestinal pro-inflammatory responses is the critical factor for the breakdown of intestinal tissue homeostasis. Severe inflammatory reactions in intestinal epithelium ultimately led to leaky gut formation [40,57]. A transmembrane protein known

as the Tight Junction (TJ) proteins regulates gut permeability in healthy conditions. TJ proteins maintain gut permeability by forming heteropolymer strands at the apical pole of the basolateral membrane of gut epithelia [41,58]. Cldn2 and ZO1 are two TJ proteins involved in colitis disease pathology. The *Cldn2* gene is highly expressed in the gut tissue of colitis patients, whereas *ZO1*is downregulated [40–42,59]. The current study revealed that gut barrier function became compromised with an upregulation of *Cldn2* gene expression in colon tissue as the disease severity increased. No change was observed in *ZO1* gene expression in either of the mouse strains. The *Cldn2* gene is highly expressed in leaky gut epithelia [42]. The leaky gut condition of both strains was corroborating with the *Cldn2* expression level. studies reported enhanced intestinal permeability increased the risk of bacterial translocation to the host circulatory system and might cause endotoxemia (endotoxin in the blood) [238, 242]. Data from the current study also revealed endotoxemia in leaky gut conditions. Epithelial cells produce a diverse arsenal of antimicrobial peptides that kill or inhibit microorganisms' growth and protect from endotoxin secreted by gram-negative bacteria [254, 255]. Lipocalin-2 is one such antimicrobial peptide highly expressed in colitis patients, which binds with the ferric-siderophore complex of bacteria to inhibit bacterial growth [247, 256].

In the present study, we observed significantly high Lipocalin-2 expression at the highest severity point of the disease for both strains.

To dig deeper, how the host immune background reacts to the diseased condition differently, we evaluated systemic level changes of the host. Transcriptomics and the untargeted metabonomics approach helped us assess the systemic changes in two different mice strains in diseased conditions. LDA analysis of colon transcriptomics data

and metabonomics study from serum and cecal content deciphered the change in individual animals of both strains and further clustered them based on the differential disease outcome. Varied trajectory and Dissimilarity Coefficient (distance) between different clusters on the 2D plane revealed the extent of differential responses, in gene and metabolite level, between different severity levels in two different mice strains [23,24]. Increased Dissimilarity Coefficient between different clusters indicated more intense differential respond between different treatment conditions. With increased dissimilarity between clusters, the disease severity index of both the strains was also increased [25]. The genes, metabolites, and meta-metabolites involved in the higher disease severity index were mainly related to the activation of the pro-inflammatory responses in the host. The genes that were involved in pro-inflammation were intensely host specific. The Th1 immune background C57BL/6 was probably the main reason for activating more pro-inflammatory genes compared to BALB/c throughout the diseased condition. The role of the host and microbial metabolites in the disease process was also quite different in C57BL/6 and BALB/c. In C57BL/6, the unique host and microbial metabolites both contributed equally to the activation of the host's inflammatory responses. In contrast the unique microbial metabolites were the major influencer in activating host inflammatory responses in BALB/c mice. Varied disease severity was hypothesized to be the main reason for altered host and microbial metabolic diversity. Increased disease severity might be the main reason for increased diversity of serum/host metabolites and decreased diversity of cecal/microbial metabolites in both strains of mice. However, the number of unique serum metabolites were increased with the disease severity in C57BL/6 and decreased in BALB/c. In the case of cecal metabolites, the total

opposite trend was found. The number of unique serum metabolites was reduced with the disease severity in C57BL/6 and increased in BALB/c. From the mentioned observation, this can be concluded that in C57BL/6 altered number of unique host or serum metabolites had a greater influence in disease severity. In contrast, an altered number of unique microbial or cecal metabolites had a more significant impact on the disease severity of BALB/c. So, in a nutshell, data from LDA analysis revealed that disease severity responses were extremely different from each other on days 0, 7, and 15 of DSS treatment in C57BL/6. In BALB/c day 0 and 15 resembles the same level of severity compared to day 7 of DSS treatment.

The shortlisted genes, metabolites, and meta-metabolites used in LDA analysis were further used to predict multiple biological pathways responsible for exerting differential disease outcomes in the host. Due to the altered metabolic condition of the host, altered biological pathways were categorized into two parts. Amino acid and lipid metabolism pathways were upregulated as the severity of the disease increased in both strains. Upregulation of carbohydrate and nucleotide metabolism was thought to be one of the main reasons for easing the diseased condition in BALB/c. Observation from the earlier study prompted increased CD4+ cell population, and IL22 cytokine expression in colitis patients was tightly correlated with upregulation of carbohydrate and nucleotide metabolism and downregulation of amino acid and lipid metabolism. High CD4+ and IL22 expressions collectively create potent anti-inflammatory reactions to ameliorate the inflammatory state of the disease [257–263]. As the inflammatory condition was more concentrated in C57BL/6, it showed a continuous upregulation in amino acid and lipid metabolism throughout the treatment period. Lesser disease load was strong enough to

activate the carbohydrate and nucleotide metabolism at the less severe form of the disease in BALB/c. Extremely severe inflammatory reactions in C57BL/6 were potent enough to activate other inflammation-related biological pathways. The genetic and metabolic joint pathway prediction revealed that along with the metabolic pathways, pathways related to inflammatory reactions, e.g., Toll-Like receptor, NOD- Like receptor, IL17, TNFα signaling, cytokine-cytokine receptor interactions were upregulated throughout the treatment conditions. No such changes were observed in BLAB/c. From the observation, this can be concluded that non-significant differences in the gene level at the diseased condition compared to control might be the reason for protecting the diseased state. Altered metabolic functions were thought to be a factor for the modified gut microbial composition of the host, followed by DSS treatment. Previous reports suggested that the host's upregulated amino acid and lipid metabolism is the consequence of the high Proteobacterial load in the gut. LPS secreted by this phylum activates the downstream inflammatory responses [66–68]. A kinetics study of the gut microbial composition revealed that as the inflammation and amino acid and lipid metabolism increase with time, Proteobacterial abundance, mainly the abundance of genus Helicobacter, increased in the gut content C57BL/6. In BALB/c, we observed a surge in the Proteobacterial level in the gut on day 7 of DSS treatment. On day 15 of DSS treatment, Proteobacterial abundance was suppressed by 3 other phyla, i.e., Bacteriodetes, Verrucomicrobia, and Firmicutes. It is already well established that Bacteroidetes and Verrucomicrobia are responsible for increased carbohydrate metabolism, and Firmicutes are responsible for nucleotide metabolism [244, 245, 266]. A high abundance of Bacteriodetes,

Verrucomicrobia, and Firmicutes, activated carbohydrate and nucleotide metabolism, which further triggered the anti-inflammatory responses in BALB/c.

Varying disease severity, the altered gut microbial composition was the probable reason for the increased abundance of one particular microbial phylum or a group of host or microbial metabolites, which would repress the abundance of other phyla or metabolites. As a sequela, the overall evenness index of the gut microbiota and metabolites would change [129, 134]. In the current study, we observed an increase in Proteobacteria phylum with the disease severity associated with a decrease in gut microbiota diversity. Gut microbial evenness index was significantly decreased in C57BL/6. On the contrary, in BALB/c, the gut microbial evenness index was significantly reduced on day 7 and restored on day 15 of the DSS treatment. This might be another possible reason for less severe disease outcomes in BALB/c.

In the case of metabolic evenness index, microbial metabolite evenness index followed the same trend of microbial evenness index, whereas the opposite trend was observed in the case of host metabolite evenness index. From here, this can be concluded that the host and its gut microbial counterpart contributed separately in differential disease severity of both strains of mice.

Increased amino acid metabolism at the highest inflammatory condition of the disease in both strains of mice prompted us to investigate the downstream mechanism of change in the host and microbial metabolic profile and their role in disease severity. A probable mechanism of varied disease severity is clearly explained in the study. The severe inflammatory condition leads to acidosis by producing a high amount of lactate and glutamate from acetyl-CoA [70–74]. In the control and recovery state of the disease,

production of the high amount of short chain fatty acid, butyrate, from lysine and acetyl-CoA was the key metabolic product to maintain the anti-inflammatory condition of the host [75–77]. The notable genus responsible for the interconversion of butyrate from lysine and acetyl-CoA were Alistipes, Bacteroides, and Lachnospiraceae [78,79]. Increased abundance of Alistipes, Bacteroides, and Lachnospiraceae on day 15 of the treatment condition led to the production of a high amount of butyrate and activated the anti-inflammatory responses in BALB/c. No such notable change in beneficial microbial genus and metabolites ultimately caused a prolonged disease severity in C57BL/6.

4.4 Conclusion

The present study could conclude that the oral administration of a specific (5% for one week followed by 2.5% for the 2nd week) DSS dose could produce reproducible colitis in C57BL/6 BALB/c mice. DSS-induced colitis activated the Th1 immune responses in the host system. Thus, the immunological background of C57BL/6 mice might have directed to exhibit immense severity response. We noticed a time-dependent increase in inflammation and disease severity after lowering the DSS dosage. Th2 immunological background of BALB/c, on the contrary, perhaps helped the mice to maintain a low disease severity compared to C57BL/6.

Observation from a multi-omics study prompted that the Th1-skewed immune background of C57BL/6 altered the host's overall homeostasis by altering the host's genetic, metabolic, and microbial composition. Altered genes, metabolites, and gut microbiota collectively created a niche for flares of extremely severe inflammatory reactions. The tolerogenic nature of BALB/c could control the inflammation to regain its

normal homeostasis very easily. Activation of anti-inflammatory responses protected BALB/c from the activation of long-term inflammatory reactions, which further control its genetic, metabolic, and gut-microbial composition.

More interestingly, in C57BL/6, the disease severity was mainly host factor-driven. Activation of more pro-inflammatory genes and host metabolites was the main reason for altered disease severity. Gut microbiota and its associated metabolites had a less critical role in disease severity due to less activation of pro-inflammatory microbial metabolites. On the contrary, altered gut microbial composition and its associated microbial changes had more stake in determining disease severity in BALB/c. Activation of more pro-inflammatory microbial metabolites than host metabolites and genes is the probable reason for this hypothesis.

Although C57BL/6 and BALB/c exerted different severity responses in a common DSS dose, the pattern of metabolic and gut microbial changes was similar in both strains at the highest severity of the disease. Inflammation leads to the high amino acid and lipid metabolism, leading to the high abundance of Helicobacter genus under Proteobacteria phylum in the gut of the host. These parameters all together create a niche for the severe form of colitis in the host. The amino acid and lipid metabolism pathways and the mentioned genus Helicobacter could be a very promising and efficient biomarker in the characterization of colitis irrespective of the immune-bias condition of the host. On the other hand high abundance of short chain fatty acid butyrate and Alistipes, Bacteroides and Lachnospiraceae genus could be used as a potent biomarker in the determination of the recovery phase of the disease. These biomarkers might also help understand the disease etiology better and diagnose the disease early.
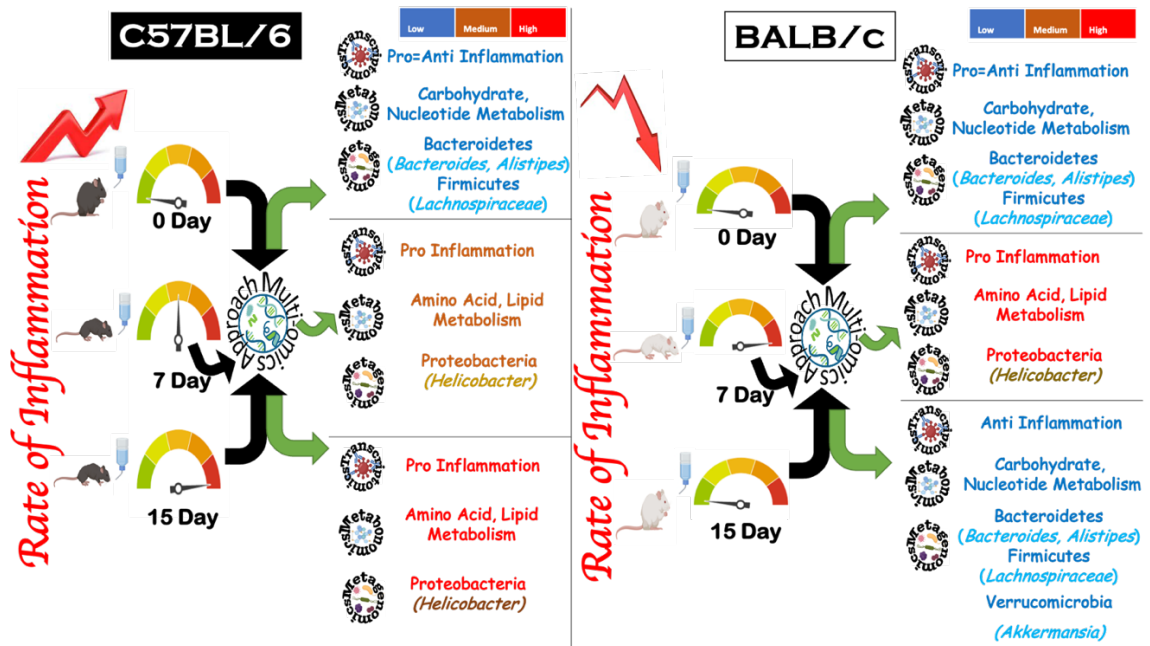
Fig. 4.12: Schema represented the probable inflammatory, metabolic, and microbial biomarkers of colitis at various disease severity conditions in Th1 & Th2 skewed immune conditions.
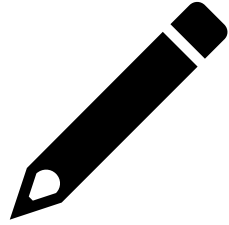
Chapter: 5

Effects of altered immune homeostasis on host metabolism, stress, and behavior

5.1 Introduction

In our preceding chapter, we have discussed how the altered immune status of the two differently immune-biased mice controls the disease severity and other important physiological processes, even the gut microbial composition of the host. In this context, it is essential to understand the importance of immune-homeostasis or immunostasis in maintaining a healthy life balance. In healthy conditions, immune homeostasis is maintained by balancing T-helper cell activity. The primary function of Th1 cells is to create a niche for pro-inflammation; Th2, on the other hand, has some regulatory effect in controlling pro-inflammation [277, 278]. Disbalance in Th1 and Th2 homeostasis is the host's fundamental cause of various inflammatory and autoimmune diseases. Even a localized pro-inflammation in any part of the body may ultimately activate the pro-inflammatory responses at the systemic level and could be potent enough to alter the gut microbial composition of the host.

For example, localized inflammation in the gut causes a leaky gut condition and forms a passage for transferring all the host and microbiota derived pro-inflammatory factors at the systemic level [204, 236].

The pro-inflammatory factors in the circulatory system ultimately cross the blood-brain barrier, affect the central nervous system, and finally activate the host's stress responses. Therefore, the host suffers anxiety and depression [279]. Perturbed gut microbiota due to gut inflammation also hampers the production of beneficiary short-chain fatty acids (SCFA) from its precursors' molecules. Gut inflammation and perturbed microbial and metabolic condition are also the leading cause of altered stress hormones productions by entero-endocrine cells in the gut, which further cause a disbalance in the crosstalk of the

gut-brain. Altered gut-brain crosstalk is ultimately responsible for the anxiety and depressive behavior of the host [280–282].

It is, therefore, imperative to study the defense biology of the Th1 and Th2-biased hosts by modulating their immunity. As discussed earlier, we have used two mice strains, C57BL/6 (Th1-biased) and BALB/c (Th2-biased), as the model system. To know the effect of a similar level of immune modulation in Th1 and Th2 biased mice, we used a composite dose of DSS for two weeks (5% DSS for 1st week followed by 2.5% DSS for 2nd week) to induce the inflammation of different severity levels, just like the previous chapter [121].

The results revealed that the Th1 responses of Th2 biased mice were short but intense. The tolerogenic nature of Th2- biased mice brought back the immune homeostasis at the end of the treatment. On the contrary, the Th1 biased mice showed immense inflammatory responses even at lower DSS doses. This observation suggested extremely imbalanced immune homeostasis of the Th1-biased host. Once the Th1 responses got activated, it was challenging to regain normalcy even in the absence of the inflammation-causing agent. Investigation of other physiological changes revealed that inflammation in the gut caused a) compromised gut barrier function, b) excess production of metabolite glutamate c) altered or lesser production of SCFA, mainly acetate and butyrate from glutamate by gut microbiota, c) activation of stress responses like associated anxiety and depressive behavior, and d) an altered gut microbial composition in both mice strains, when the Th1 immune responses were in the activated state. On a special note, prolonged and more intense pro-inflammation and more robust gut microbial alteration caused chronic depressive behavior in Th1 biased mice. Th2 biased BALB/c was more prone to

acute anxiety and able to cope with the depressive condition at the end of the treatment. Altogether, this study could be important and relevant for understanding the mechanism of inflammation and stress alleviation.

5.2 Results

The host's immune status is so important that it could determine the extent of pro-inflammation in a diseased condition, the level of psychological stress and stress hormones, the behavior of the host, and the composition of the gut microbiome.

To know the effects of differential immune responses in C57BL/6 (Th1-biased)- and BALB/c (Th2-biased)- mice, we administered DSS in drinking water. Untreated mice were used as a control in the current study. To investigate the host's inflammatory and other systemic changes, a genome-wide analysis of gene expressions of the colon sample of both mice strains was performed.

5.2.1 Genome-wide analysis of gene expressions of colon sample to know the local and systemic changes of the host

We performed a genome-wide analysis of gene expressions (RNA-seq analysis) from colonic samples before and after the induction of the inflammation and shortlisted differentially expressed genes using the criteria mentioned in the methodology section. KEGG enrichment analysis of shortlisted genes (Fig. 5.1A) suggested the enrichment of inflammatory (pro and anti) pathways, complement pathways, different nucleotide-sugar-amino acid, and short-chain fatty acid metabolism pathways, stress responses of host and stress associated hormonal changes, and pathways related to other bone-related

inflammatory diseases. According to the Z-Score analysis of enriched pathway, we found that the pathways related to either pro-inflammation, i.e., IL-17 signaling pathway, chemokine signaling pathway, complement, and coagulation cascade, had higher Z-Score values in treated C57BL/6 than untreated control mice. The Z-score was the highest on day 15 following DSS treatment. In BALB/c, the Z-Score values of pro-inflammatory pathways were the highest on day 7 of DSS treatment and tried to reach the control values on post-day 7. IL-10 signaling, mainly related to the anti-inflammation, showed an opposite expression trend between two strains of mice. The Z-Score of the IL-10 signaling pathway was continuously decreased throughout the treatment condition in C57BL/6. High Z-Score of IL-10 on day 15 of DSS treatment compared to day 7 was probably the main reason for the lower Z-Score of pro-inflammatory pathways on day 15 compared to day 7 in BALB/c. Except for the short-chain fatty acid metabolism, the Z-Score of other pathways mentioned in Fig. 5.1A, followed the same trend as the pro-inflammatory pathways. The Z-Score value of short-chain fatty acid metabolism decreased along with the increased inflammatory condition in both the mice strains.

To understand which genes in a system, contribute to synergistic mechanisms of inflammation, we analyzed Principal Component Analysis (PCA) of differentially expressed shortlisted genes derived from RNA-Seq data (Fig. 5.1a). In PCA analysis, the genes expressed differentially and not overlapped or clustered with any other genes in any treatment conditions were further shortlisted and thought to play the most critical role in the inflammatory process. Using PCA clustering, we classified the shortlisted gene expressions into three modules based on the functions of the genes. In Fig. 5.1a, b, the clusters marked with blue, red, and black lines contained pro & anti-inflammatory and gut

barrier function-related genes. In C57BL/6 i) Genes, associated with pro-inflammation (*Igkv12-44, Scarna3a, Rnu11, Itpripl2, Muc2, Ighv15-2, Trpv6, Mmp3, Cxcl5, Chil3, Cxcl2, Igkv8-18*), gut barrier function (*Itpripl2, Muc2*), are clustered together. Although genes associated with anti-inflammation (*Dio2, Rpl21-ps10, Retnlg, Reg3b)* also clubbed together at a distinctly different location from inflammatory genes (Fig. 5.1a). We observed similar gene clustering trends in BALB/c. But the genes associated with i) pro-inflammation (*Padi4, Igkv9-123, Lep, Tpd52ll, Ccl3, Try4, Hc, Hoxb8, Adam18*) ii) gut barrier function (*Scnn1g, Muc6) and* iii) anti-inflammation (*Tmprss13, Sptssb, 2310034C09Rik, Rn7sk, Ceacam12, Slc47a1)* in BALB/c were different from C57BL/6 (Fig. 5.1b). Although genes of similar functions behaved similarly in either of the mice strains, the genes and their expressions differed for each strain. We did not find any common genes among differentially expressed genes between the two mice strains.

Further, we wanted to observe the severity of other systemic changes in the host based on their immunological background.

5.2.2 Pro-Inflammation is associated with the lower short-chain fatty acid production of the host

The host's immune status could determine the extent of a) stress level and hormones, b) the behavior of the host, and c) the role of the gut microbiome.

We found that activation of the pro-inflammatory pathways of the host was responsible for the significantly lower amount of short-chain fatty acids production (e.g., acetate and butyrate). We observed that the abundance of acetate (Fig. 5.1B, C) and butyrate (Fig.

5.1D, E) in both serum and cecal samples decreased and reached the minimum on the 15th day following DSS treatment C57BL/6. While for BALB/c, serum SCFAs went minimum on day 7 and reverted to the control value on day15 of DSS treatment. In contrast, the cecal acetate and butyrate levels decreased on day 7 and recovered to a certain extent on day 15, but not entirely to normalcy. The host probably tried to bring back the systemic anomaly to the normal condition by training the acetate and butyrate to the serum or systemic level.
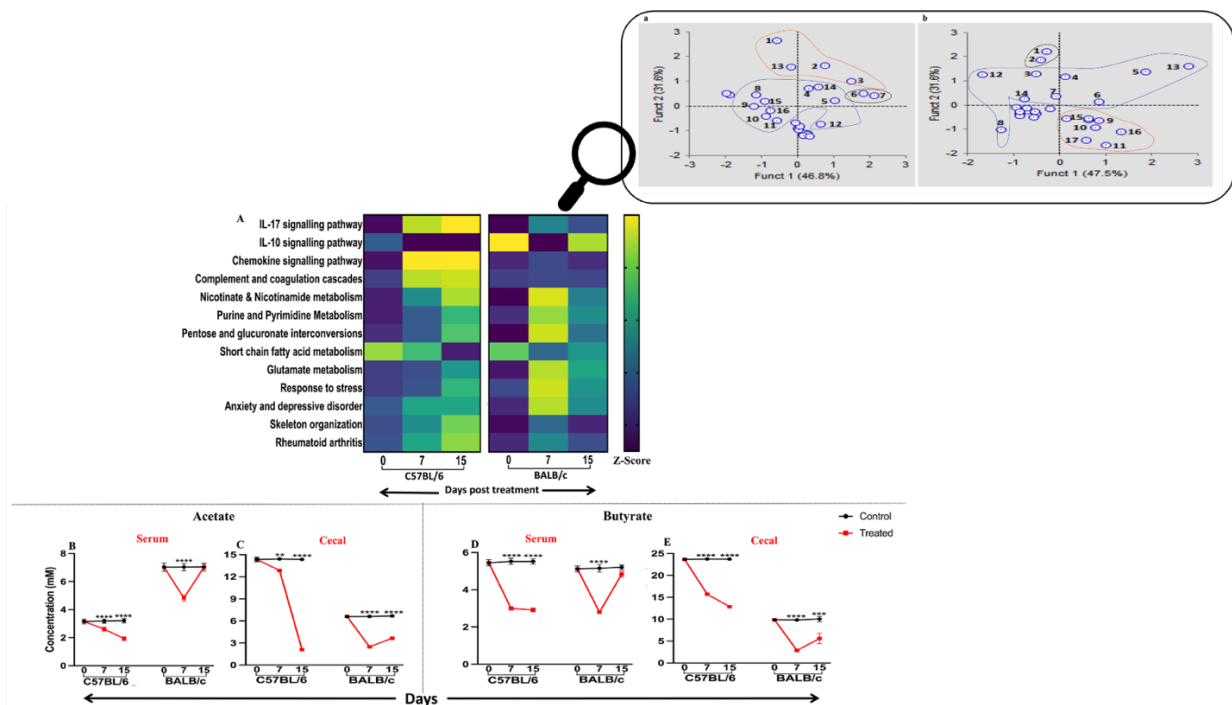
Fig. 5.1: Inflammatory pathways following DSS treatment and various inflammatory responses in the gut and systemic level of the Th1 and Th2 biased mice.

The most impacted inflammation associated pathways, in the gut of Th1 and Th2 biased mice, are shown in a heatmap (A).

Principal Component Analysis or PCA of differentially expressed inflammatory genes responsible altered pathway functions in C57BL/6 (a) and BALB/c (b) mice presented in the inset. PCA analysis revealed that genes with similar functions clustered together. The genes shown in panels B and C are represented by numbers as described below to avoid clutter.

1. Reg3b, 2. Retnlg, 3. Rpl21-ps10, 4. Trpv6, 5. Ighv15-2, 6. Muc2, 7. Itpripl2, 8. Mmp3, 9. Cxcl5, 10. Chil3, 11. Cxcl2, 12. Igkv8-18, 13. Dio2, 14. Rnu11, 15. Scarna3a, 16. Igkv12-44 for C57BL/6 (B). 1.Scnn1g, 2. Muc6, 3. Igkv9-123, 4. Lep, 5. Tpd52l1, 6. Padi4, 7. Ccl3, 8. Try4, 9. Tmprss13, 10. Sptssb, 11. 2310034C09Rik, 12. Hc, 13. Hoxb8, 14. Adam18, 15. Rn7sk, 16. Ceacam12, 17. Slc47a1 for BALB/c (C). Cluster marked with blue, red and black line contained pro & anti-inflammatory and gut barrier function-related genes, respectively.

We showed the short-chain fatty acids acetate (B, C) and butyrate (D, E) in serum (B, D) and cecal content (C, E) in C57BL/6 and BALB/c mice.

We calculated the statistical significance by comparing the values of the treated groups at various time points with their respective control groups through two-way ANOVA followed by the Bonferroni test. The number of stars indicate the significance level e.g., '*' (P ≤ 0.05), '**' (P ≤ 0.01), '***' (P ≤ 0.001), '****' (P ≤ 0.0001). Error bars shown are ±1 SD from the mean value of three replicates (n = 6).

5.2.3 Increased glutamate production further activated the stress responses of the host

The RNA-Seq analysis provided the clue that the pro-inflammatory status of the host was positively correlated with the glutamate metabolism of the host. The source of the glutamate was either the host or microbial counterpart [279, 283]. We observed increased serum and cecal glutamate and the increased pro-inflammatory status of the host in both strains of mice (Fig. 5.2). In C57BL/6, the highest serum and cecal glutamate production happened on day 15 of the DSS treatment, and in BALB/c, it was on day 7 of the post-treatment condition. Serum glutamate production of BALB/c recovered by day 15 of the post-treatment condition, whereas cecal glutamate level was not fully recovered by the end of the treatment condition (Fig. 5.2).

We observed that the circulatory (serum) and intestinal (gut) glutamate abundance was inversely proportional to circulatory and intestinal SCFA levels, i.e., acetate and butyrate. From the current study, we found that a comparatively lower abundance of the genus *Akkermansia* (6%) and *Bacteroides* (26%) in C57BL/6 restricted the conversion of glutamate to acetate (Fig. 5.2). Similarly lesser abundance of genus *Bacteroides* (26%) and *Lachnospiraceae* (10%) halted the conversion of butyrate from glutamate (Fig. 5.2). In contrast, BALB/c was able to cope up the acetate and butyrate production from glutamate at the later stage of the disease.
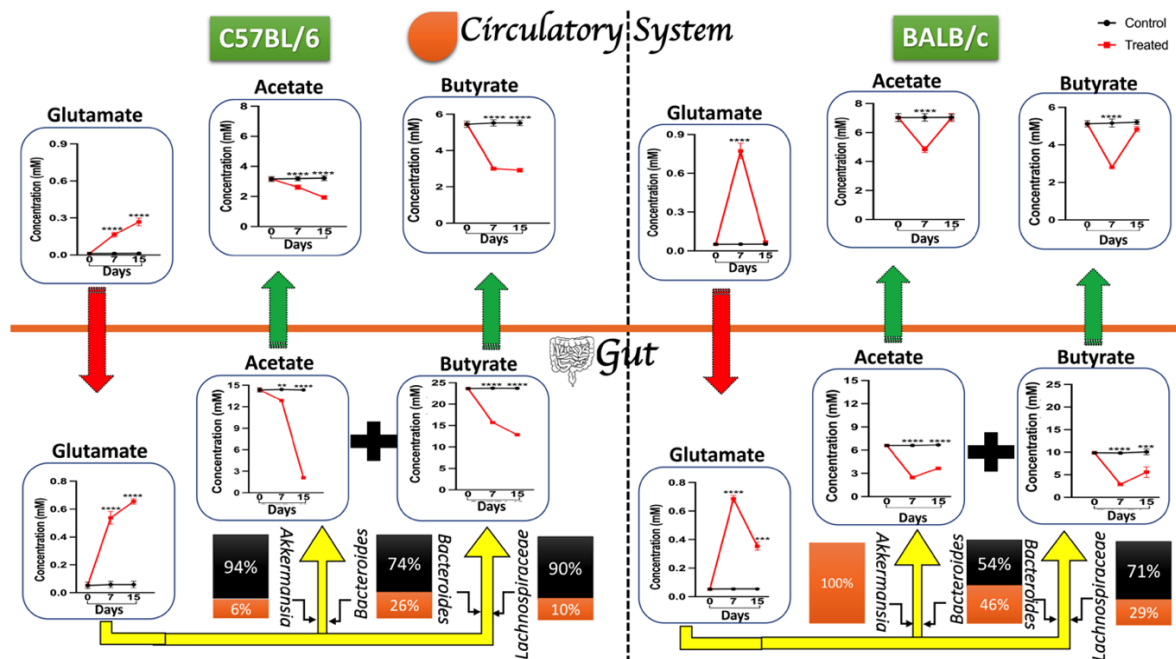
Fig. 5.2: Gut microbiota is the key determinant of the fate of glutamate in Th1 and Th2 biased mice.

We proposed a predictive mechanism of conversion of circulatory and intestinal (gut) glutamate by the gut microbial counterpart of the Th1 and Th2 biased host.

We calculated the statistical significance by comparing the values of the treated groups at various time points with their respective control groups through two-way ANOVA followed by the Bonferroni test. '*' corresponds to $P \leq 0.05$, ** corresponds to $P \leq 0.01$, *** corresponds to $P \leq 0.001$, **** corresponds to $P \leq 0.0001$. Error bars are shown as standard deviation from the mean value of six replicates (n = 6).

In normal healthy conditions, the excess systemic glutamate never crosses the blood-brain barrier of the host. A leaky gut is one of the significant factors when glutamate crosses

the blood-brain barrier of the host and enters the central nervous system (CNS) [284, 285]. A high glutamate concentration in the CNS activates the HPA (Hypothalamus-Pituitary-Adrenal) axis and further triggers the cascades of the release of stress-related hormones, e.g., CRH (Corticotrophin Releasing Hormone), ACTH (Adrenocorticotrophic Hormone), and Cortisol [286, 287]. Cortisol plays a significant role in the host's stress outcome, controlling the inflammation in the gut and maintaining the cross talk between gut and brain. Higher inflammation in the gut also activates the HPA axis and triggers the stress responses of the host [288–290].

In our study, high glutamate concentration and leaky gut condition due to inflammation cause a considerable infiltration of glutamate in the CNS, further activating the HPA axis in both mice strains (Fig. 5.3A). High gut inflammation at the treated condition created a niche for activating the HPA axis and the production of stress hormones in the gut by entero-endocrine cells. To justify the HPA axis activation, we measured the CRH, ACTH, and cortisol hormone levels in serum and cecal samples for both mice strains. In C57BL/6, the highest abundance of serum and cecal CRH (Fig. 5.3B), ACTH (Fig. 5.3C), and cortisol (Fig. 5.3D) was on day 15 and day 7 in BALB/c following DSS treatment. Serum CRH (Fig. 5.3B), ACTH (Fig. 5.3C), and cortisol (Fig. 5.3D) production of BALB/c recovered by day 15 of the post-treatment condition, whereas cecal CRH (Fig. 5.3B), ACTH (Fig. 5.3C), and cortisol (Fig. 5.3D) levels were not fully recovered by the end of the treatment condition.
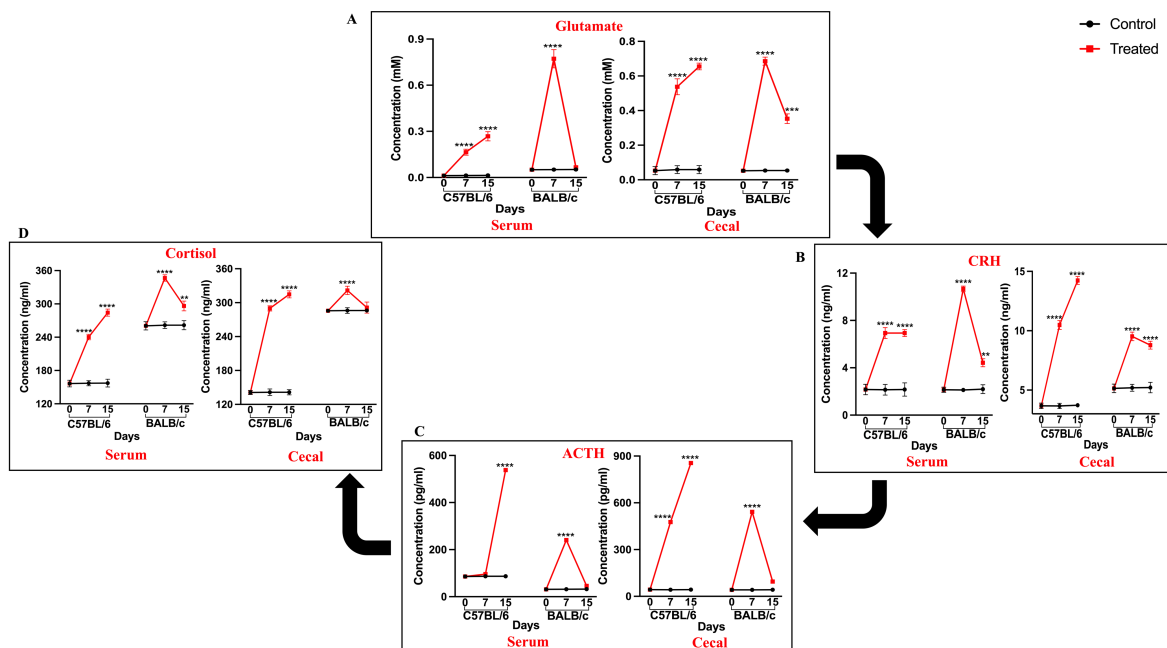
Fig. 5.3: Predictive mechanism of activation of distinctive stress responses in Th1 and Th2 biased mice due to various levels of gut inflammation.

We showed the glutamate (A), CRH (B), ACTH (C), and cortisol (D) concentrations in serum and the gut content of Th2 biased mice.

We calculated the statistical significance by comparing the values of the treated groups at various time points with their respective control groups through two-way ANOVA followed by the Bonferroni test. '*' corresponds to $P \leq 0.05$, ** corresponds to $P \leq 0.01$, *** corresponds to $P \leq 0.001$, **** corresponds to $P \leq 0.0001$. Error bars are shown as standard deviation from the mean value of three replicates (n = 6).

5.2.4 Measurement of anxiety and depression in Th1 and Th2-biased mice

High levels of stress hormones in systemic level and gut content in treated Th1 and Th2 bias mice indicated the host's behavioral anomaly. In the current study, open-field test (OFT) and elevated plus maze test (EPMT) were used to measure the anxiety levels, and forced swim test (FST), and tail suspension test (TST) were used to measure the depression level of mice [145, 148, 150, 152]. We monitored the behavior of the control and treated mice every other day till the study was over. The open-field test revealed a higher anxiety level in both mice strains until the end of the treatment period than in the respective time-matched control. The time spent in the periphery of the open field apparatus started increasing from day 5 of the treatment condition in both strains (Fig. 5.4A, B). It increased for C57BL/6 continuously till the end of the treatment condition (Fig. 5.4A). While for BALB/c, the anxiety level started decreasing from day 9 of the treatment but never came to the basal level even at the end of the treatment (Fig. 5.4B).

The elevated plus-maze test revealed the same pattern as OFT in treated C57BL/6 and BALB/c mice. At a higher level of anxiety, both the strains spent more time in the closed arm of the EPM apparatus. During EPMT, C57BL/6 started showing anxiety-like behavior from day 5 and gradually increased up to day 15 (Fig. 5.4C). On the other hand, treated BALB/c started showing anxiety-like behavior from day 3, and the anxiety level was almost similar till the end of the treatment condition (Fig. 5.4D). The lower level of stress hormones in the second week compared to the first week of treatment condition was also unable to control the anxiety-like behavior in BALB/c.

To measure the effect of prolonged stress, we quantify the depression level in both mice strains using the FST and TST. In both behavior tests, we measured the activity level of

the mice. Lesser activity or the animal's higher immobility than their time-matched control in FST and TST was considered depression-like behavior. In both FST (Fig. 5.4E) and TST (Fig. 5.4G), the static time increased in treated C57BL/6 mice until day 15. However, in BALB/c, the static time or depression level in both FST (Fig. 5.4F) and TST (Fig. 5.4H) increased until day 7 and gradually started decreasing from day 9 of the treatment and came to normalcy at the end of the treatment. In conclusion, the Th1 background of C57BL/6 induced more depressive behavior after the inflammatory modulation with DSS. Th2 background of BALB/c was somehow able to cope with the depressive behavior at the lower inflammatory stage, but the level of anxiety was uncontrollable even at the lower inflammatory status of BALB/c.
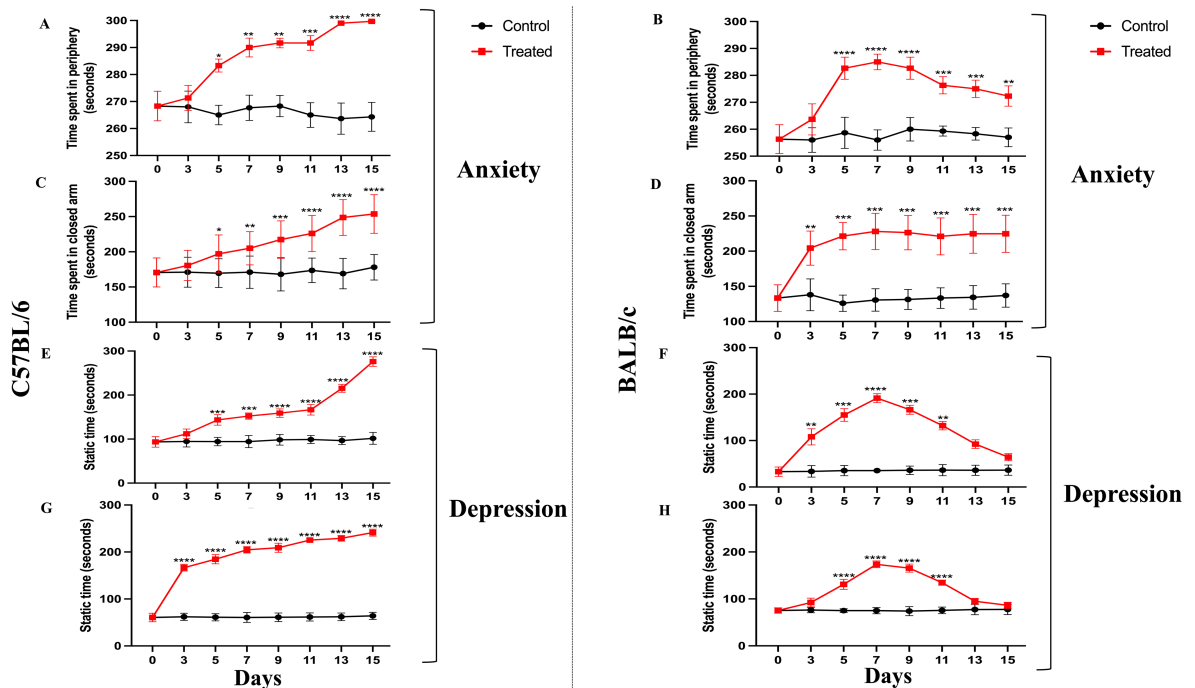
Fig. 5.4: Differential anxiety and depression-related behavioral responses of Th1 and Th2 mice at varied inflammatory conditions of the gut.

We measured the anxiety and depression levels of Th1 (C57BL/6) and Th2 (BALB/c) biased mice from different behavioral experiments. We detected the anxiety level of control and treated mice using the open-field test (OFT) (A, B) and elevated plus-maze test (EPMT) (C, D). OFT data were showing time spent in the periphery (in seconds) for DSS-treated and untreated control C57BL/6 (A) and BALB/c (B) mice, EPMT data showing time spent in the closed arms (in seconds) for DSS-treated and untreated control C57BL/6 (C) and BALB/c (D) mice during the various inflammatory status of the gut. We detected the level of depression in both strains of mice using the forced swim test (FST) (E, F) and tail suspension test (TST) (G, H). We calculated the immobility (static) time (in seconds) of treated and control C57BL/6 (E, G) and BALB/c (F, H) mice in FST and TST at the different inflammatory conditions of the gut to measure the depression level.

We calculated the statistical significance by comparing the values of the treated groups at various time points with their respective control groups through two-way ANOVA followed by the Bonferroni test. '*' corresponds to $P \leq 0.05$, ** corresponds to $P \leq 0.01$, *** corresponds to $P \leq 0.001$, **** corresponds to $P \leq 0.0001$. Error bars are shown as standard deviation from the mean value of ten replicates (n = 10).

The trajectory pathway of control and treated mice in OFT and EPMT and the activity measurement in FST and TST were depicted in Fig. 5.5.
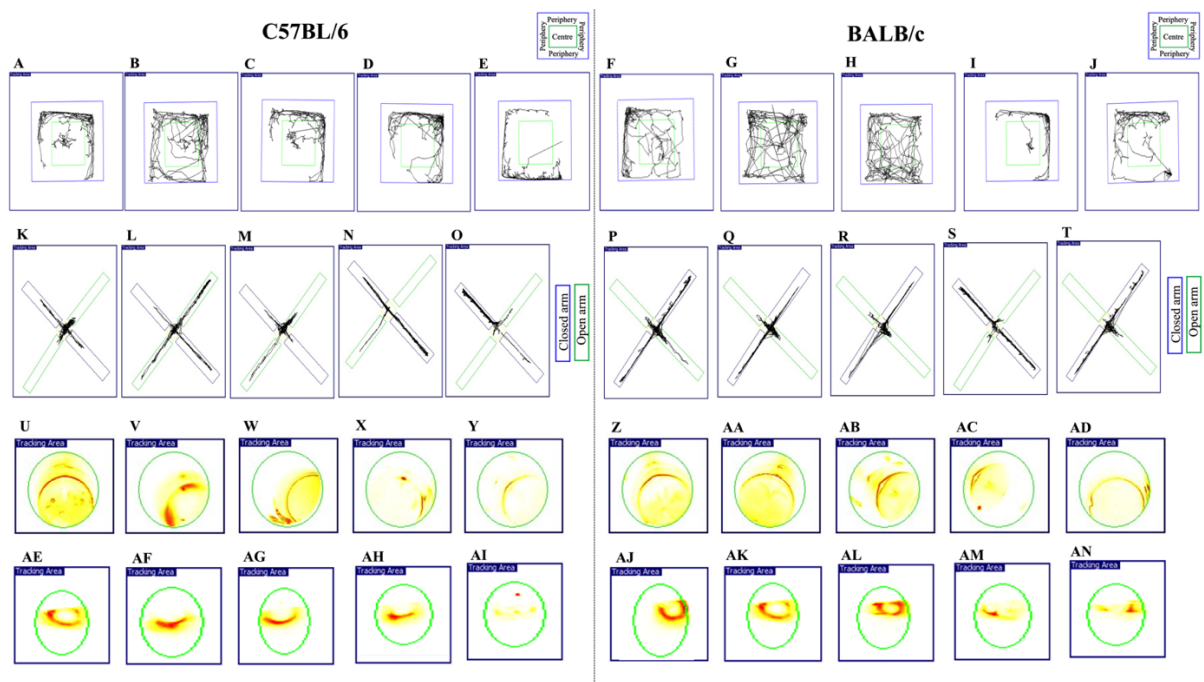
Fig. 5.5: Images showing the trajectory paths of mice in open-field and elevated plus-maze instrument and the mobile or active state in forced swim and tail suspension test.

(A-E) and (F-J) showing the locomotor activities of C57BL/6 (A-E) and BALB/c (F-J) mice at different locations of open field instruments of treated animals at varying levels of gut inflammation and their respective control group. (A, B, C) represented the trajectory of control C57BL/6 mice on days 0, 7, and 15, respectively. (D, E) represented the trajectory of treated C57BL/6 mice on days 7 and 15, respectively. In BALB/c, (F, G, H) represented the trajectory of control mice on days 0, 7, and 15, respectively. (I, J) represented the trajectory of treated BALB/c mice on days 7 and 15, respectively.

(K-O) and (P-T) showing the locomotor activities of C57BL/6 (K-O) and BALB/c (P-T) mice at different locations of the elevated plus-maze instrument of treated animals at a different level of gut inflammation and their respective control group. (K, L, M) represented the trajectory of control C57BL/6 mice on days 0, 7, and 15, respectively. (N,

O) represented the trajectory of treated C57BL/6 mice on days 7 and 15, respectively. In BALB/c, (P, Q, R) represented the trajectory of control mice on days 0, 7, and 15, respectively. (S, T) represented the trajectory of treated BALB/c mice on days 7 and 15, respectively.

(U-Y) and (Z-AD) showing the activity level or the mobile state of C57BL/6 (U-Y) and BALB/c (Z-AD) in the forced swim test. (U, V, W) showing the activity level of control C57BL/6 mice underwater on days 0, 7, and 15, respectively. (X, Y) showing the activity level of treated C57BL/6 mice underwater on days 7 and 15, respectively. (Z, AA, AB) showing the activity level of control BALB/c mice underwater on days 0, 7, and 15, respectively. (AC, AD) showing the activity level of treated BALB/c mice underwater on days 7 and 15, respectively.

Similarly, (AE-AI) and (AJ-AN) shows the activity level or the mobile state of C57BL/6 (AE-AI) and BALB/c (AJ-AN) in the tail suspension test. (AE, AF, AG) showing the activity level of control C57BL/6 mice under the tail suspended condition on days 0, 7, and 15, respectively. (AH, AI) showing the activity level of treated C57BL/6 mice under the tail suspended condition on days 7 and 15, respectively. (AJ, AK, AL) showing the activity level of control BALB/c mice under the tail suspended condition on days 0, 7, and 15, respectively. (AM, AN) showing the activity level of treated BALB/c mice under the tail suspended condition on days 7 and 15, respectively.

All the trajectory pathways and activity of the mice were measured by Smart 3.0, Panlab SMART video tracking system, Harvard Apparatus.

5.2.5 Stress levels and roles of gut microbiota in both mice strains

The current study revealed the gut microbial changes were detrimental in the case of C57BL/6 but beneficial for BALB/c. A lower abundance of genus *Akkermansia* (6%), *Bacteroides* (26%), and *Lachnospiraceae* (10%) compared to control restricted the production of anti-inflammatory short-chain fatty acids from glutamate and created a niche for more pro-inflammation. Whereas, in BALB/c increase of the beneficial *Akkermansia* (100%), *Bacteroides* (46%), and *Lachnospiraceae* (29%) genus further restored the production of short-chain fatty acids from glutamate at the end of the treatment and helped BALB/c from copping up from the diseased condition.

Previously, we also mentioned that activated inflammatory responses due to DSS treatment were responsible for the higher abundance of Proteobacteria (gram-negative pathogens) phylum at the highest severity level in both strains. In congruence with other factors reported in this study, the highest abundance of Proteobacteria was reached on day 15 for C57BL/6 and day 7 for BALB/c [121].

In a different context, we also reported that the Proteobacterial abundance could be associated with mice's altered behavior [116]. The current study reiterated the Proteobacterial association with the percent (%) anxiety and depression levels of mice. We calculated the percent anxiety level using the formula previously reported by our group [116]. In C57BL/6, the rate of increase of Proteobacterial abundance was not proportional to the rise in the rate of % anxiety (Fig. 5.6A), whereas Proteobacterial abundance was strongly proportionate with the increase in the rate of % depression (Fig. 5.6B).

Similarly, in BALB/c, although the Proteobacterial level decreased on day 15 of the

treatment condition, the % anxiety was not reduced even on day 15 of treatment (Fig. 5.6C). On the other hand, a decrease in Proteobacterial level on day 15 of the treatment condition reduced the % depression level on day 15 (Fig. 5.6D). So gut Proteobacteria level played a critical role in determining the depression level in both the mice strains.

Reports also suggested that a higher F/B (Firmicutes/ Bacteroidetes) ratio is responsible for more intense stress responses in the host [291, 292]. The current study revealed a significantly high F/B ratio only on day 15 of the treated condition in C57BL/6 compared to its time-matched control. No such increase was observed in treated BALB/c mice (Fig. 5.6E).

Perturbed gut microbial composition and leaky gut due to pro-inflammation prompted us to measure the secretory IgA (sIgA) level in the gut content of both strains of mice. sIgA is a significant modulator of gut microbial composition and distribution. We observed, the basal IgA level of control BALB/c was notably higher than control C57BL/6 mice (Fig. 5.6F). A significant decrease in the IgA level of treated mice was probably because of gut microbial dysbiosis. Cecal IgA level reduced gradually until day 15 in treated C57BL/6; however, the IgA level started to increase on day 15 of treated BALB/c compared to day 7 of treatment. Previous studies reported that the sIgA level is directly proportional to the gut microbial diversity [116, 293]. We compared the gut microbial diversity (Shannon index) and IgA level dynamics for both mice strains (Fig. 5.6F). The results revealed that the altered gut microbial profile directly affects the IgA abundance in both mice strains following treatment with DSS but with different kinetics of alteration and restoration.
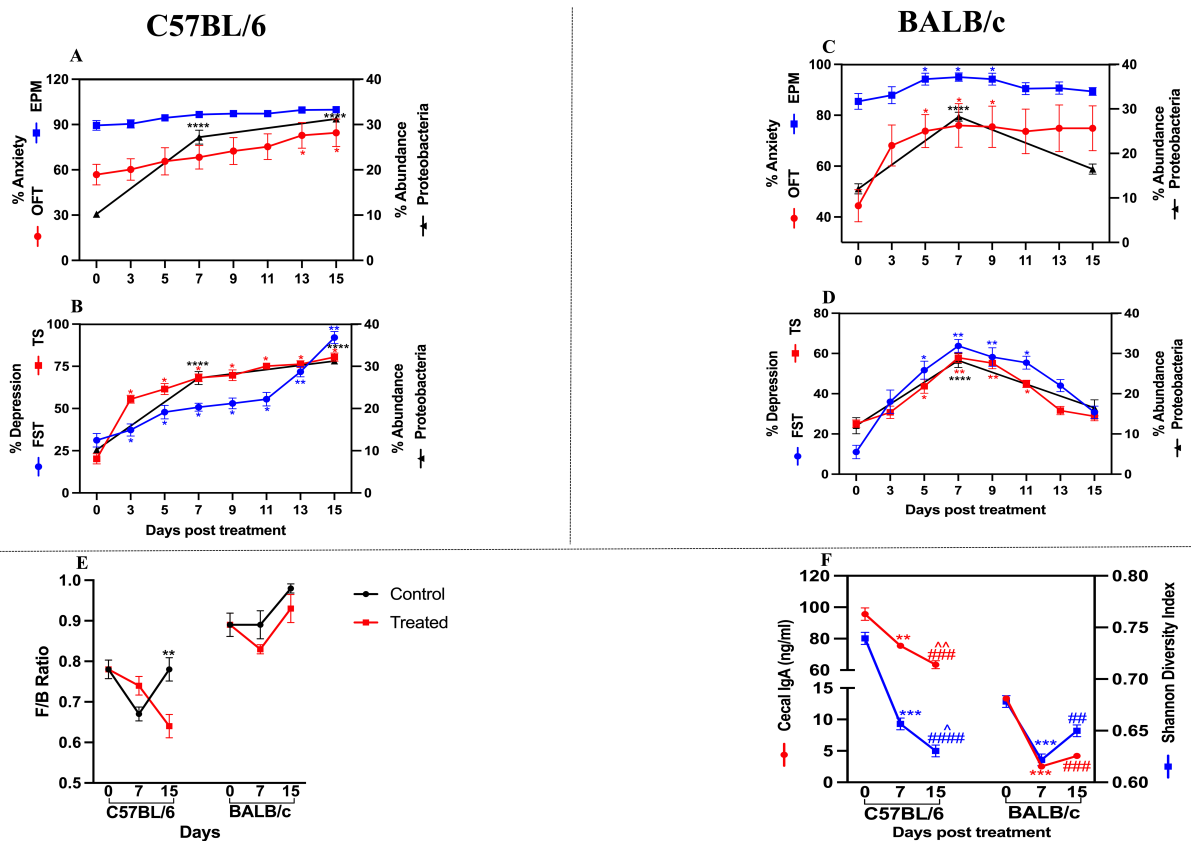
Fig. 5.6: *Altered gut microbiota associated behavioral changes in Th1 and Th2 biased mice at different inflammatory conditions of the gut.*

Altered gut microbial composition, especially the altered proteobacteria level at various treatment conditions, was probably responsible for altered % anxiety either/or % depression in C57BL/6 (A, B) and BALB/c (C, D) mice. OFT and EPMT behavioral experiment measured the % anxiety level, and FST and TST determined the % depression level. Statistical significance was calculated by day 0 with other treatment conditions using two-way ANOVA followed by the Bonferroni test. '' corresponds to P ≤ 0.05, ** corresponds to P ≤ 0.01, *** corresponds to P ≤ 0.001, **** corresponds to P ≤ 0.0001.*

Error bars are shown as standard deviation from the mean value of ten replicates (n = 10) for behavior and three replicates (n=3) for proteobacterial levels in the gut.

Altered F/B (Firmicutes/ Bacteroidetes) ratio is also thought to be a result of intense stress responses of host. We calculated the F/B ratio I at various treatment conditions in C57BL/6 and BALB/c mice I.

Compromised gut microbial diversity at various inflammatory conditions altered IgA secretion in the gut. Double Y-axis graph (D) of Shannon diversity index and secretary (cecal) IgA showing the altered gut microbial diversity and altered level of the secretory IgA due to inflammation in the gut. Statistical significance was calculated by day 0 with other treatment conditions using two-way ANOVA followed by the Bonferroni test. We presented all values as means ± SD for 3 biological replicates. */#/^ corresponds to P ≤ 0.05, ** /##/^^corresponds to P ≤ 0.01, ***/###/^^^ corresponds to P ≤ 0.001, ****/####/^^^^ corresponds to P ≤ 0.0001. (* symbolizes the comparison between day 0 and day 7, # symbolizes the comparison between day 0 and day 15, ^ symbolizes the comparison between day 7 and day 15).

5.3 Discussion

In the current study, we have used C57BL/6 (Th1) and BALB/c (Th2) mice to study the physiological responses by inducing a pro-inflammatory state using DSS. Although the significant inflammation was localized in the colon of the gut, the effect was systemic.

The RNA-Seq analysis revealed that the pro-inflammatory status of the host was positively correlated with the glutamate metabolism of the host. We observed that the

increase in serum and cecal glutamate was equally proportionate with the increased pro-inflammatory status of the host in either strain of mice. The source of the glutamate was either the host or its gut microbial counterpart. This glutamate is the precursor molecule of the two most important short-chain fatty acids, i.e., acetate and butyrate, which further control the inflammatory status of the host. Genera *Akkermansia*, *Bacteroides*, and *Lachnospiraceae* are the major producer of acetate and butyrate from glutamate in the gut [275, 276, 294–296]. Perturbation of these gut genera restricts the short-chain fatty acids production and create a niche for pro-inflammation and which ultimately causes the leaky gut condition of the host. The excess glutamate further crosses the blood-brain barrier and reaches the central nervous system (CNS) in an inflamed, leaky gut condition [279, 287]. Previous studies revealed that Glutamate played a vital role in activating the HPA (Hypothalamus-Pituitary-Adrenal) axis to trigger the host's stress responses [279, 286, 287, 297].

Glutamate could further activate the production of the cascade of CRH-ACTH-Cortisol hormones from the paraventricular nucleus and adrenal cortex of the brain, respectively. Enteroendocrine cells in the gut also produce CRH-ACTH-Cortisol simultaneously [298–305]. All the stress hormones are further transported to the bloodstream of the host.

In the current experimental condition, perturbed microbial condition restrict the production of short-chain fatty acids (acetate & butyrate) from glutamate. Further create a niche for the production of more pro-inflammatory cytokines in the gut, which could further activate the HPA axis to maintain the host's gut-brain crosstalk and trigger the host's stress responses. Lower SCFAs, higher inflammatory cytokines produced by the inflamed gut, and high glutamate levels in serum and cecal were sufficient to activate the

HPA axis of the host. Inflammatory cytokines and high glutamate levels established the niche for gut-brain crosstalk and triggered the cascade of CRH- ACTH- Cortisol production (Fig 3). High levels of CRH- ACTH- Cortisol in the diseased condition showed a significant surge in the stress responses of the host. We established a detailed mechanism of stress responses of Th1 and Th2-biased mice at different levels of the pro-inflammatory state of the host. The stress response of both the mice strains was directly proportional to the pro-inflammation level of the host. Higher pro-inflammation created a higher amount of stress responses in the host.

Higher stress responses of Th1 and Th2 biased mice at higher inflammatory conditions were the clear indication for activation of anxiety and depression-like behavior in the host. Anxiety results from comparatively shorter stress responses, and if it persists for a longer time and then it becomes converted into depression [297, 306, 307]. The current study revealed that Th1-biased C57BL/6 showed anxiety-like behavior that turned into depression throughout the treatment. Although BALB/c showed anxiety-like behavior throughout the treatment, the depression level became normal at the end of the treatment. This data suggested that Th1 immune status was responsible for chronic stress, whereas Th2 immune status triggered acute stress responses.

Earlier reports suggested that the high Proteobacterial abundance and higher Firmicutes/Bacteroidetes ratio in the gut microbiota are responsible for triggering anxiety or depressive behavior in mice [116, 291, 292, 308–310].

Moreover, the major phylum which plays the most crucial role in creating a niche for pro-inflammation is Proteobacteria [199, 280, 311–313]. We further validated that Proteobacterial abundance was increased in both mice strains as a sequela of increased

pro-inflammation. The gut Proteobacterial level was directly proportional to the % depression of both mice strains. The significantly higher F/B on day 15 of treated C57BL/6 and the higher Proteobacterial abundance than treated BALB/c probably triggered more intense depressive behavior in C57BL/6.

The differential increase of Proteobacteria phylum that could repress the abundance of other phyla may explain the varying inflammatory status of the two mice strains. Consequently, the overall diversity of the gut microbiota is changed [134, 242]. The current study revealed that an increase in Proteobacteria reduced the gut microbial diversity and enhanced pro-inflammation. Gut microbial diversity (Shannon diversity) was significantly decreased in C57BL/6. On the contrary, in BALB/c, the gut microbial diversity was significantly reduced till day 7 and restored by the 15th day of the treatment. This restoration might be another advantage of the Th2 background of a host.

Studies reported that gut microbial diversity depended on the IgA level of the host [116, 314–316]. In the current study, as the gut microbiota's alpha diversity (Shannon diversity index) decreased in treated conditions, the sIgA level also decreased in both mice strains compared to their time-matched control. The pro-inflammatory state in treated BALB/c restored the gut microbial diversity and the sIgA level. No such restoration was observed in treated C57Bl/6 throughout the treatment condition.

5.4 Conclusion

The present study could conclude that prolonged pro-inflammatory conditions of treated C57BL/6 activate prolonged chronic stress responses and more depressive behavior than BALB/c. Like the inflammatory status, the stress response of treated BALB/c was short-

lasting, and as a result, BALB/c was prone to short-lasting anxiety-related behavior or lesser depressive behavior. The depressive behavior came to the basal level at the end of the treatment. Restoration of beneficial gut microbial genera *Akkermansia*, *Bacteroides*, and *Lachnospiraceae* protected BALB/c from the diseased condition at the end of the treatment by converting the stress causing glutamate to anti-inflammatory acetate and butyrate. On the other hand, more severe inflammatory status altered the pathogenic proteobacteria level in the gut of C57BL/6 in such a way that it was never restored to the normal level till the end of the treatment. Treated BALB/c restored the healthy gut microbial composition after 1st week of DSS treatment. This current study will help us know how the host's inflammatory or immunological background controls the host's overall physiologyh, starting from maintaining gut barrier integrity, SCFA production, activation of stress responses and associated behavioral outcomes, and finally, the gut microbial composition of the host. This study will explain the importance of studying the differential immunobiology of Th1 and Th2-biased hosts.

Effects of Perturbed Immune-Homeostasis	Days					
	0		**7**		**15**	
	C57BL/6	BALB/c	C57BL/6	BALB/c	C57BL/6	BALB/c
Gut inflammation						
Gut leakiness						
*SCFA level						
Stress responses						
Gut dysbiosis						

*SCFA- Short Chain Fatty Acid
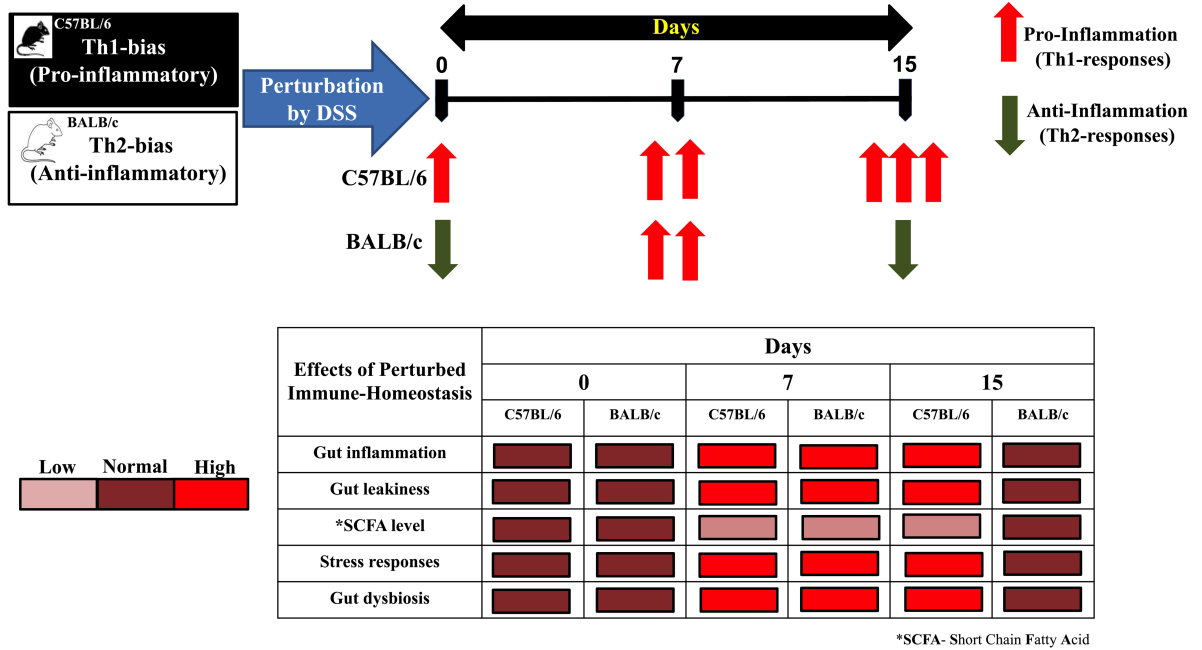
Fig. 5.7: Altered immune status of the host leads to altered gut microbial composition followed by altered behavioral and stress responses.
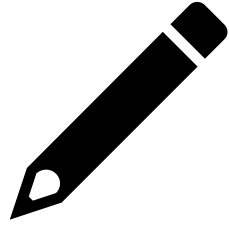
Chapter: 6

For the improvement of diagnosis and treatment plans, mapping the gut microbiota and metabolites of colitis before and after therapeutic interventions.

6.1 Introduction

From our previous investigations and experimental plans, we may conclude that the disease colitis is a multifactorial and systemic disease. Even while the disease's early inflammation is limited to the gut, as it progresses, it may impact all of our body's critical systems, including physiology, immunity, metabolism, and endocrine

signals connected to stress, anxiety, depression, behavior, and many other things. Another significant alteration could be the altered gut microbial composition of the host [317–319]. Still, the alterations in the biological mechanisms that drive gut microbial alterations remain unknown. Also, it is unclear yet, whether the microbial alterations represent a cause or consequence of the disease. The primary notion of our research was to understand the complex mechanism of colitis pathogenesis. Whether it is an effect of uncontrolled immune reactions or the composition of the gut flora and gut flora-derived metabolites or host metabolites controls the pathogenesis and progression of the disease. From our understanding, we tried to establish some microbial and metabolic biomarkers of the disease for non-invasive and cost-effective diagnosis of different stages of colitis. The microbial and metabolic biomarkers could also be an excellent target for therapeutic interventions. Alteration of the diseased microbial and metabolic profile to a healthy one will try to eradicate the cause of the disease from its root [121] .

The most well-known and potential therapeutic strategy for controlling colitis is different antibiotics [320–322]. Antibiotics could prevent the disease condition at the early onset of the disease by altering the gut microbial composition of the patients. Long-term antibiotic administration could lead to other health hazards and other diseases. More interestingly,

the so-called lifesaving antibiotic can become a threat for colitis later in life if consumed extensively in early life [323–325].

The dual nature of antibiotic perturbation provoked us to study the perturbation pattern and kinetics of antibiotics before and after the colitis disease onset. In this study, we aimed to understand the detrimental or therapeutic effect of antibiotics on disease pathogenesis using the perspective of gut microbial and metabolic intervention of the host physiology. From our previous chapters, we got a precise idea that the altered microbial and metabolic profile could be a plausible cause of any kind of systemic intervention of the host. So, in this context, the best way to understand the effect of pre and post-administration of antibiotics on the modulation of colitis disease susceptibility is through gut microbial and metabolic interventions.

In our previous chapters, we have already proved that the Th1- C57BL/6 had more intense responses against any physiological manipulations than Th2- BALB/c. To get a more profound idea about how the pre and post-antibiotic treatment could modulate the gut microbiota and metabolic profile of the disease colitis in these two differently immune-biased mice models.

The current antibiotic treatment strategy used to treat colitis is a cocktail of different antibiotics which can target other gut microbial populations in the gut ecosystem. So, with this notion, we used a cocktail of 9 different antibiotics with a diverse target population in the gut instead of any single antibiotic dosage.

The 9antibiotic cocktail (9AB)'s composition and modes of action are listed in Table. 6.1.

Table. 6.1: *Detail compositions, mode of actions, and target microbiota of 9 antibiotics cocktail*

Sr. No.	Antibiotic	Concentration (µg/ml)	Mode of Action	Target Microbiota
1	Penicillin	100	Inhibits cell wall formation	Gram positive bacteria
2	Vancomycin	50	Inhibits RNA synthesis	Gram positive bacteria (mainly *Firmicutes*)
3	Neomycin	100	Inhibits protein synthesis	Gram positive and Gram negative bacteria (mainly *Firmicutes and Proteobacteria*)
4	Metronidazole	100	Inhibits protein synthesis	Gram negative bacteria (mainly *Bacteroidetes*)
5	Bacitracin	1000	Inhibits peptidoglycan synthesis	Gram positive bacteria
6	Streptomycin	50	Inhibits protein synthesis	Gram positive and Gram negative bacteria
7	Ciprofloxacin	125	Inhibits DNA replication	Gram positive bacteria (mainly *Firmicutes*)
8	Ceftazidime	100	Weakens the cell wall	Gram negative bacteria
9	Gentamicin	170	Inhibits protein synthesis	Gram positive bacteria (mainly *Firmicutes and Actinobacteria*)

We have used 2.5% dextran sulfate sodium (DSS) to induce colitis-like symptoms in both mice strains. The dose was potent enough to create colitis-like pathology in both the mice strains.

Data from current observation revealed that in Th1- biased C57BL/6 mice, antibiotics treatment rescued the DSS-treated group from the diseased condition by activating the carbohydrate and nucleotide metabolism pathway, which converted the pro-inflammatory status of the host into an anti-inflammatory condition. On the other hand, early exposure to antibiotics increases disease susceptibility by activating pro-inflammatory lipid and amino acid metabolism pathways.

The scenario was quite different in Th2-biased BALB/c mice. The antibiotic treatment activates the carbohydrate metabolism pathway, which ultimately provides a therapeutic effect against colitis, whether administered before or after the DSS treatment.

We also tried to understand the role of microbes and microbiota-derived metabolites in such surprising outcomes. We tried to map the microbiota with its metabolites for future diagnosis and therapeutic intervention strategies for colitis.

6.2 Results

In the current study, we treated both C57BL/6 and BALB/c with 5 different treatment combinations to understand the role of antibiotics in disease progression or role in the therapeutic intervention.

We administered five different treatments through drinking water: i) 7 days 9 antibiotics cocktail treatment followed by 7 days regular autoclaved drinking water (7D 9AB + 7D H2O), ii) 7 days DSS treatment followed by 7 days regular autoclaved drinking water (7D DSS + 7D H2O), iii) 7 days 9 antibiotics cocktail treatment followed by 7 days DSS treatment (7D 9AB + 7D DSS), iv) 7 days DSS treatment followed by 7 days 9 antibiotics cocktail treatment (7D DSS + 7D 9AB) and, v) 7 days 9 antibiotics cocktail and DSS treatment together followed by 7 days regular autoclaved drinking water(7D 9AB&DSS + 7D H2O) in C57BL/6 and BALB/c male mice. We used untreated mice as the control in this study.

6.2.1 Altered host physiology at different treatment conditions in C57BL/6 and BALB/c mice

To know the effect of pre and post-administration of antibiotics on the disease physiology of the host, we checked specific parameters that clearly indicate the colitis disease

progression or regression. We checked the changes in i) body weight, ii) cecal index, iii) colon length, and iv) gut permeability level.

Results revealed that the control group of mice of both strains showed no significant changes in their physiology with time.

We observed that the effect on the body weight changes was more severe when we administered 9 antibiotics cocktails before DSS treatment in both mice strains. C57BL/6 (Fig. 6.1A) had prolonged and significantly more adverse body weight alterations than BALB/c (Fig. 6.1B). Administration of 9 antibiotics cocktail after disease induction rescued the mice from the alteration of the body weight due to the disease in both mice strains. Another interesting observation we noted when we were treating the mice with 9 antibiotics and DSS together the loss of body weight was significantly higher in BALB/c (Fig. 6.1B) than in C57BL/6 (Fig. 6.1A).

We also observed other phenotypic changes, e.g., colon length and cecal index, due to various treatments.

Results revealed that when we administered only 9 antibiotics cocktail or DSS as a single dose or 9 AB & DSS combinatorial dose for 1st 7days of the treatment, we haven't found any significant alterations of colon length in either of the mice strains (Fig. 6.1C).. In contrast, in case of a cecal index, we observed a substantial increase of cecal index in C57BL/6 mice when treated with 9 AB and 9 AB & DSS together (Fig. 6.1D). In case of BALB/c the changes in the cecal index were observed in only 9 AB & DSS treatment group (Fig. 6.1D). Moreover the increase of cecal index was significantly higher in C57BL/6 than BALB/c (Fig. 6.1D).

The scenario was quite different when we treated the mice with antibiotics before and after the colitis disease manifestation. We observed significant alterations in colon length in C57BL/6 mice when we administered the antibiotics before disease manifestation. Post-treatment antibiotics rescued the mice from such phenotypic changes (Fig. 6.1E). No significant alterations in colon length were observed in BALB/c mice (Fig. 6.1E). Contrarily, we observed a considerable rise in the cecal index in the C57BL/6 both before and after antibiotic treatment (Fig. 6.1F).

The BALB/c post-antibiotic treatment group increased the cecal index (Fig. 6.1F). The cecal index changes were negligible in BALB/c than C57BL/6 (Fig. 6.1F).

6.2.2 Quantification of the gut permeability level at various treatment conditions

Our previous experimental observation found that gut permeability alterations are one of the main pathophysiology of colitis. To know how the pre and post-treatment of antibiotics control the leakiness of the gut, we administered the FITC-dextran. We measured its concentration in serum after a specific time interval in both mice strains. When we treated the mice with only DSS, we found an increased gut permeability in both strains. The permeability was significantly higher in C57BL/6 compared to BALB/c. No changes were observed in the permeability at the time of only antibiotics treatment in both strains (Fig. 6.2A). But when we treated the mice with antibiotics before disease manifestation, the leakiness of the gut increased drastically in C57BL/6 mice. In contrast, antibiotic treatment after disease manifestation rescued the C57BL/6 mice from the leaky gut symptom (Fig. 6.2B).

In BALB/c, no such effect was noticed. Antibiotic therapy, both pre and after, could not alter the intestinal permeability in BALB/c mice in this way.

A summary of the highest physiological changes is mentioned in Table. 6.2 for a better understanding.
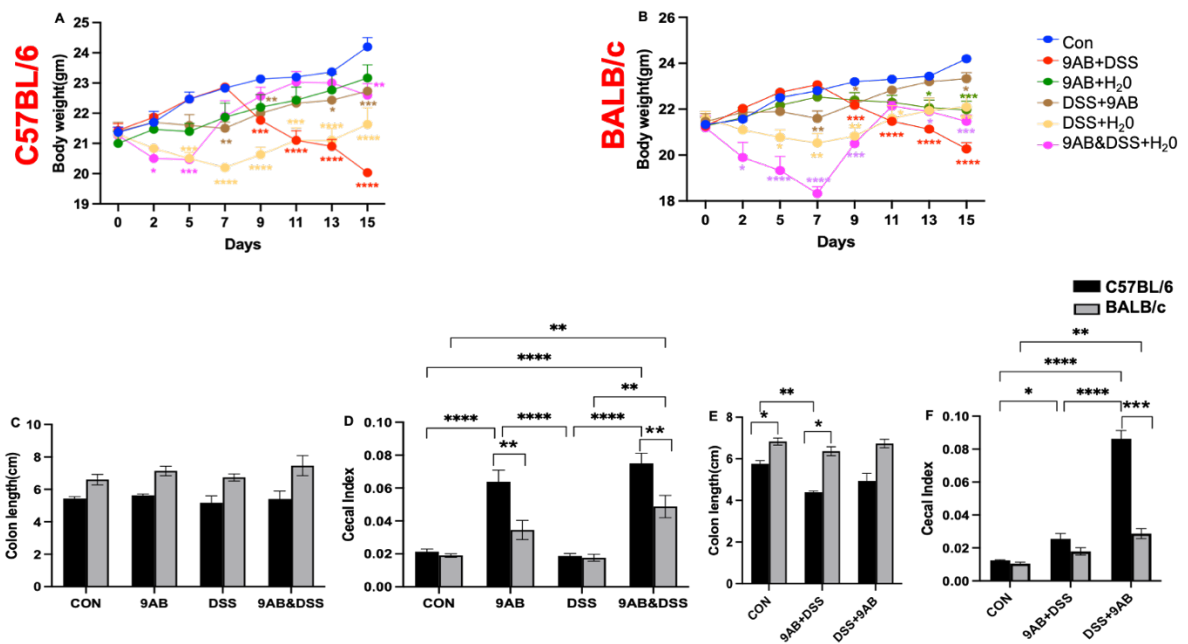
Fig. 6.1: Altered host physiology in C57BL/6 and BALB/c followed by different combinations of 9 antibiotics and DSS treatments.

We measured the body weight of the control and treated C57BL/6 (A) and BALB/c (B) mice on every alternative day until day 15. We also observed the alterations of colon length (C & E) and cecal index (D & F) in both mice strains.
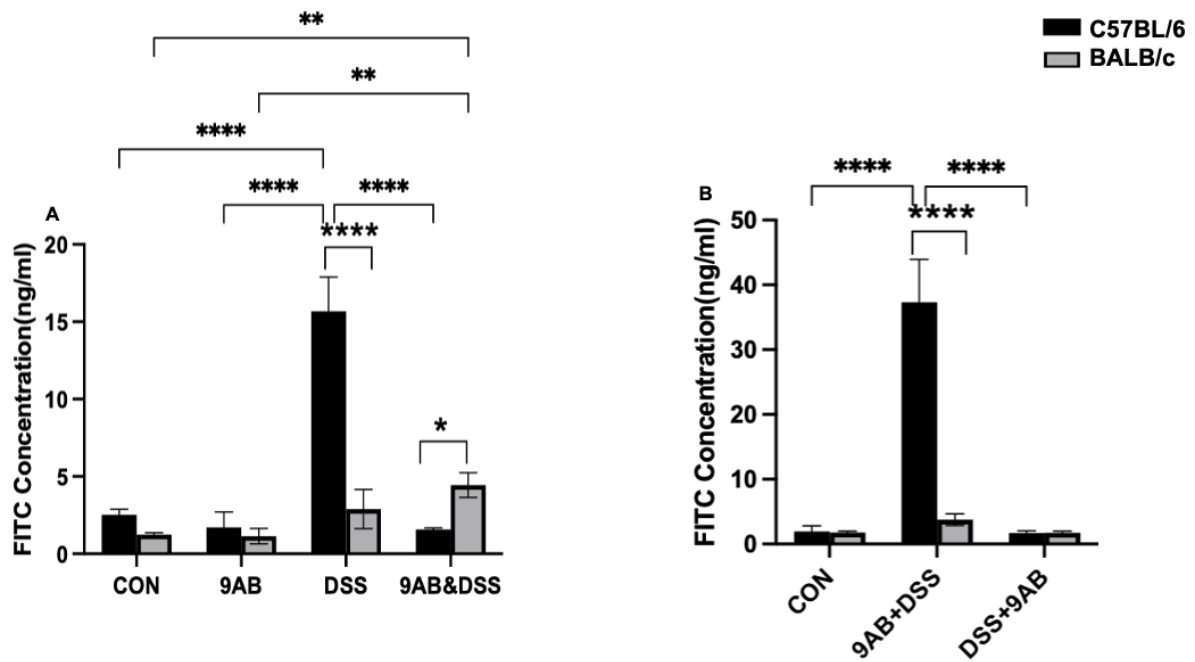
Fig. 6.2: Changes in the gut permeability level of both mice strain at different treatment conditions.

We measured the serum FITC concentration on day 7 (A) and day 15 (B) of control and treated C57BL/6 and BALB/c mice to quantify the leakiness of the gut due to various treatment conditions.

Table. 6.2: *Summary of most adverse physiological changes at different treatment conditions in C57BL/6 and BALB/c mice.*

Conditions	C57BL/6	BALB/c
Body weight	9AB+DSS	9AB&DSS
Cecal Index	• 9AB • 9AB&DSS	• 9AB • 9AB&DSS
Colon Length	9AB+DSS	----
Gut Permeability	• 9AB • 9AB+DSS	----

6.2.3 Characteristics of metabolic alterations of the diseased host due to pre and post-treatment of the antibiotics in C57BL/6 and BALB/c mice

To understand the molecular basis of the differential outcomes of the antibiotics' treatment in the disease severity level, we tried to understand the host's involvement in various metabolic processes. We performed the metabonomics study of serum and cecal content to understand the alterations of the metabolic profile of the host and its microbial counterpart.

We tried to connect the different metabolic changes in the host and gut microbiota levels and how these two separate metabolic processes control the host physiology and, thus, differential disease outcomes.

In the current observation, we found alterations of carbohydrate and lipid metabolisms when treating the C57BL/6 mice only with a single dose of either 9 antibiotics cocktail or

DSS. In the antibiotic treatment group, we found altered carbohydrate and lipid metabolism in the serum level and carbohydrate and vitamin metabolism at the cecal level (Fig. 6.3A). When we treated the mice with DSS, we observed an increased carbohydrate metabolism in the serum level and carbohydrate and lipid metabolism in cecal level (Fig. 6.3B).

On the other hand, 9 antibiotic treatments in BALB/c showed an increased carbohydrate and amino acid metabolism (Fig. 6.4A). DSS treatment caused alterations in lipid metabolism (Fig. 6.4B).

We also treated C57BL/6 (Fig. 6.5A) and BALB/c (Fig. 6.5B) mice with a combinatorial dose of 9AB & DSS. We found alterations in carbohydrate, lipid, and amino acid metabolism at the serum level and lipid and amino acid metabolism at a cecal level in both mice strains.
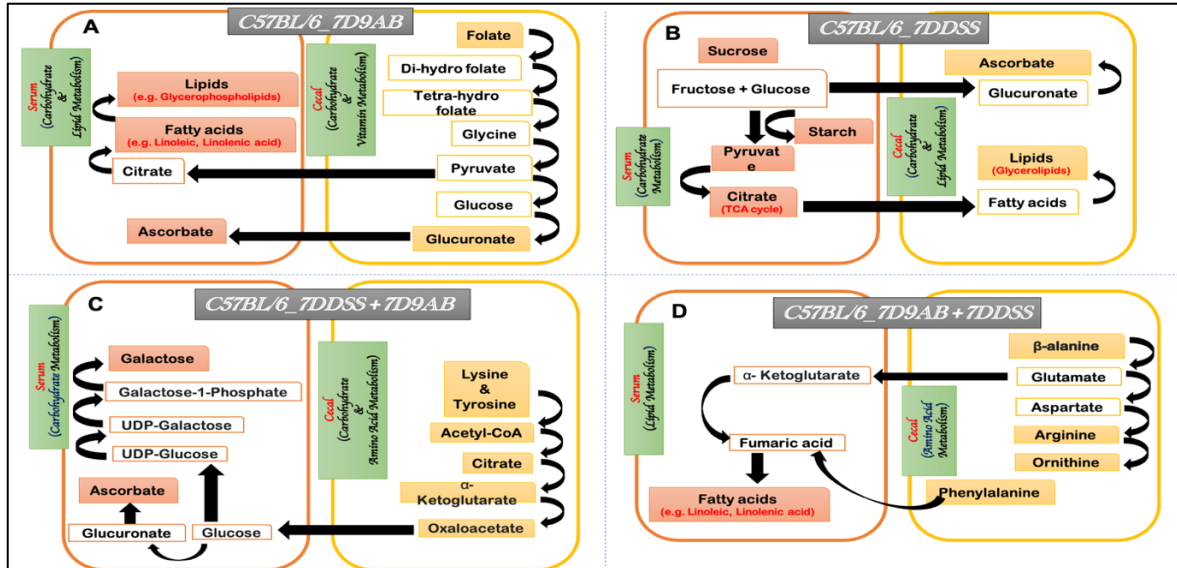
Fig. 6.3: *Predictive metabolic pathways that control the disease outcome due to pre and post-treatment of antibiotics in C57BL/6 mice.*

We connected the metabolic pathways involved in the different disease outcome and their role in controlling the disease pathology. Panel (A) and (B) depict altered metabolism due to antibiotics and DSS treatment. Panel (C) and (D) explained the metabolic alterations due to the post and pre-treatment of antibiotics in colitis disease outcomes, respectively.

From the previous literature and our previous observation, we noted that carbohydrate metabolism was related to the anti-inflammatory responses of the host. In comparison, amino acid and lipid metabolisms activated the pro-inflammatory responses [121]. When we treated the mice with a single dose of antibiotics, we observed activation of the carbohydrate metabolism in both mice strains, which has a protective role for the host.

A similar discovery was made when we administered a 9-antibiotic cocktail to C57BL/6 (Fig. 6.3C) and BALB/c (Fig. 6.4C) mice after the colitis disease manifested. Post antibiotics treatment rescued the mice from the disease by activating the anti-inflammatory carbohydrate metabolism pathway in the host systemic or serum level. The cecal level inflammatory amino acid and lipid metabolism pathway ultimately converted to the beneficial carbohydrate metabolism when reached both the host's circulatory or systemic level (Fig. 6.3C, 6.4C).
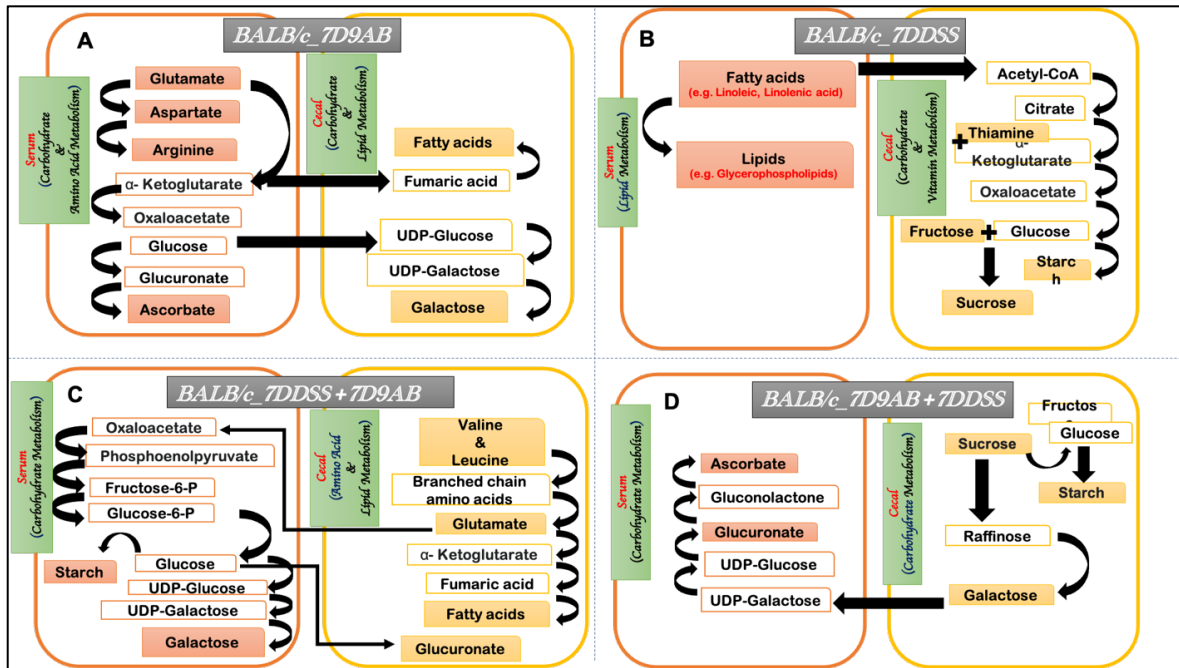
Fig. 6.4: *Predictive metabolic pathways that control the disease outcome due to pre and post-treatment of antibiotics in BALB/c mice.*

We connected the metabolic pathways involved in the different disease outcome and their role in controlling the disease pathology. Panel (A) and (B) depict the altered metabolism due to antibiotics and DSS treatment, respectively. Panel (C) and (D) explained the metabolic alterations due to the post and pre-treatment of antibiotics in colitis disease outcomes, respectively.

Pre-treatment with antibiotics before colitis disease manifestation also protected BALB/c mice by upregulating the carbohydrate metabolism process both in gut microbial and systemic levels (Fig. 6.4D). The scenario was different for C57BL/6. Although the post-treatment of antibiotics protected the mice from the disease conditions, pre-treatment activated the pro-inflammatory amino acid metabolism in the microbiota level, which

ultimately led to the activation of inflammatory lipid metabolism at the systemic level and increased the susceptibility of the colitis (Fig. 6.3D).
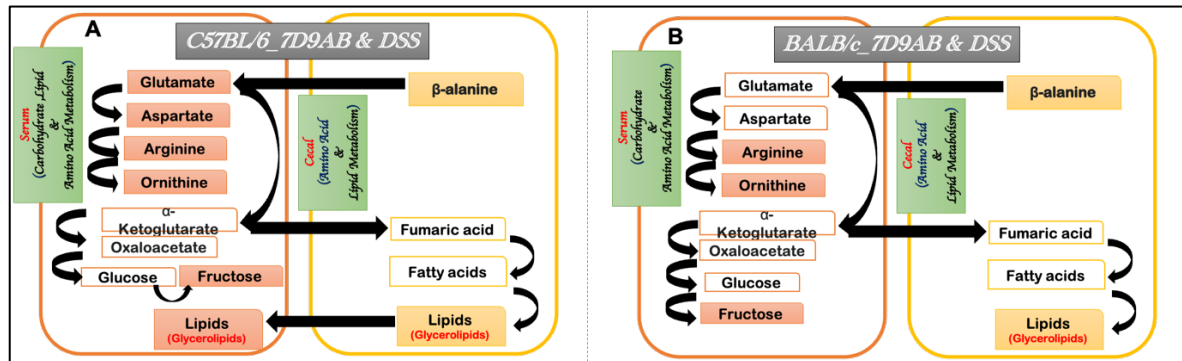
Fig. 6.5: Predictive metabolic pathways when antibiotics and DSS are administered in C57BL/6 and BALB/c mice.

Panel (A) and (B) described the altered metabolic status of C57BL/6 and BALB/c, respectively, when we administered antibiotics and DSS together.

6.2.4 Microbiota and microbiota-derived metabolites probably the major controlling factor of the diseased conditions

Altered cecal metabolism resulted from altered microbiota due to various treatment conditions. We tried to establish the relationship between altered gut microbial conditions and affected metabolism. We shortlisted the various impacted metabolism at different treatment conditions and the responsible specific microorganism for the particular metabolic processes. We emphasized those metabolic processes commonly altered in microbiota and host levels and marked them with a tick (✓) in the respective figure panel and summarized in Table. 6.3. We found the altered metabolic pathways were very time specific and unique for treatment conditions (Fig. 6.6, 6.7) in both strains of mice.

The metabolic pathways in the control condition in C57BL/6 (Fig. 6.6A) and BALB/c (Fig. 6.6B) mice were quite different, along with their microbial counterpart. When treated with antibiotics, we haven't found a common pathway that was altered in both mice strains' host and microbiota levels (Fig. 6.6C, D).

When treated with DSS and a combination of DSS & 9 AB, the metabolic and microbial alterations in serum and cecal levels were similar in C57BL/6 (Fig. 6.6C) and BALB/c (Fig. 6.6D) mice.
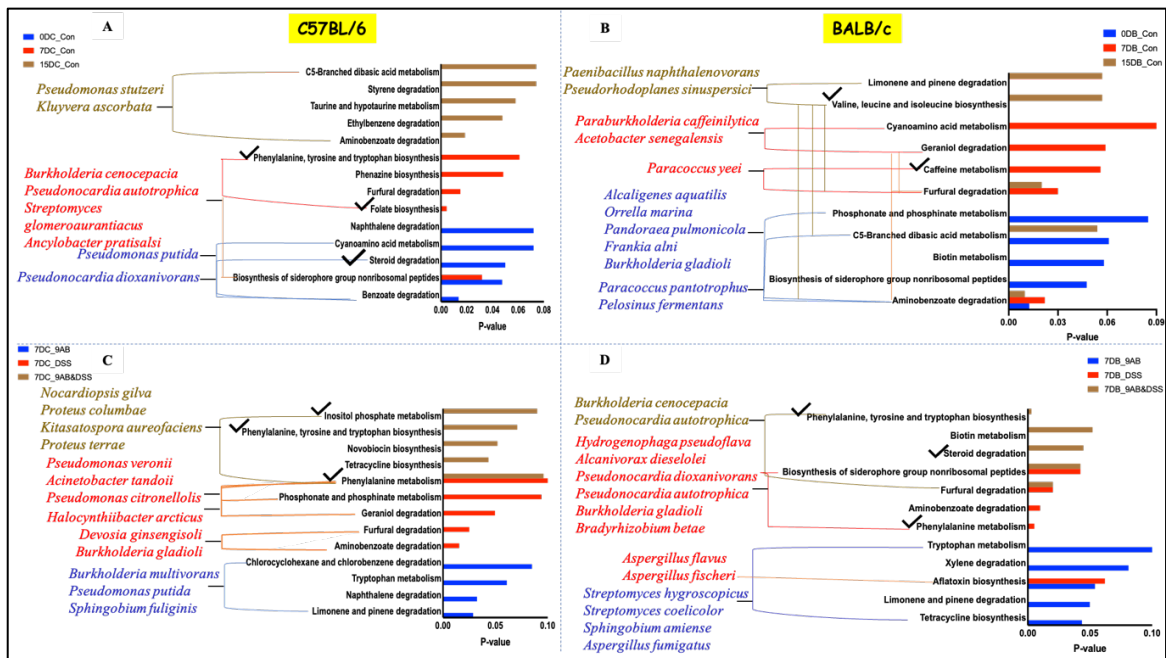
Fig. 6.6: Altered metabolic processes of the host and the responsible gut microbiota in C57BL/6 and BALB/c mice.

(A) & (B) represent the metabolic and microbial alterations in control conditions of C57BL/6 (A) and BALB/c (B) mice. Alterations of metabolic and microbial flora, when treated individually by 9 AB, DSS, and combinations of 9AB & DSS in C57BL/6 and BALB/c, were shown in panels (C) & (D), respectively.

Pre and post-treatment of antibiotics altered the metabolic and microbial status of two different hosts in very different ways (Fig. 6.7). So, the microbiota and microbiota-derived metabolites were the critical determinants of the overall systemic alterations of the host in diseased and treatment periods.
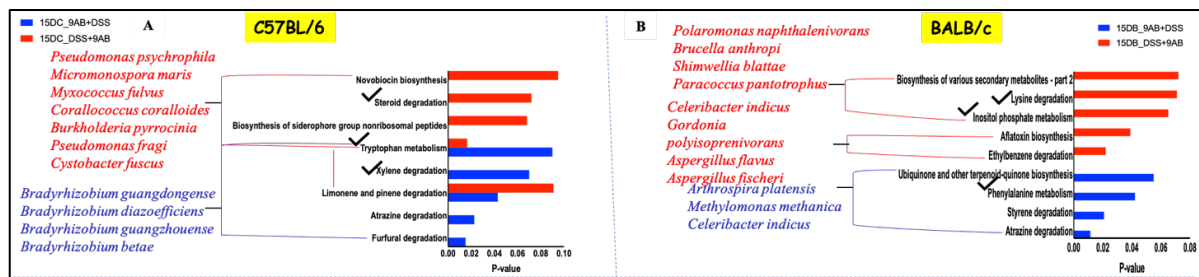
Fig. 6.7: Alterations of the host's metabolic and gut microbial status due to pre and post-treatment of 9 AB in colitis disease manifestation.

(A) depicted the metabolic and microbial changes in C57BL/6 and (B) in BALB/c.

We also tried to shortlist the most important metabolic pathways for altered physiology at different treatment conditions and the main responsible microorganisms related to the particular metabolic process (Table. 6.3).

We found the shortlisted microorganisms were mainly from the phylum of proteobacteria. The metabolic processes are mainly amino acid and lipid metabolism, which ultimately make all the differences between different treatment regimes.

Table. 6.3: *Summary of altered metabolic and microbial flora at various treatment conditions.*

Pathway Name	Producing Species	Respective Phylum
Phenylalanine, Tyrosine, Tryptophan Metabolism	• *Burkholderia cenocepacia* • *Pseudonocardia autotrophica*	• **Proteobacteria** • **Actinobacteria**
Folate Biosynthesis	• *Streptomyces glomeroaurantiacus* • *Ancylobacter pratisals*	• **Actinobacteria** • **Proteobacteria**
Valine, Leucine, Isoleucine Metabolism	• *Paenibacillus naphthalenovorans* • *Pseudorhodoplanes sinuspersici*	• **Firmicutes** • **Proteobacteria**
Inositol Phosphate Metabolism	• *Proteus columbae* • *Kitasatospora aureofaciens* • *Proteus terrae*	• **Proteobacteria** • **Actinobacteria** • **Proteobacteria**
Caffeine Metabolism	• *Paracoccus yeei*	• **Proteobacteria**

6.3 Discussion

In the present experimental setup, we tried to understand the role of antibiotics in modulating gut microflora and microflora-derived metabolites and further the host metabolism in controlling the colitis disease susceptibility in two differently immune-biased hosts.

Reports from case-control studies revealed that antibiotic treatment is the most common treatment strategy for colitis. Antibiotics provide a protective role against colitis by modulating the gut microbial profile of the host [320–322]. But the major question arises when we find pieces of literature that describe that early life exposure to too many antibiotics ultimately leads to increased colitis susceptibility and a more severe form of the disease [323–325]. But the underlying mechanism of the dual role of antibiotics in determining disease susceptibility is unknown to the group of medical practitioners or

researchers. In this study, we tried to understand the complex role of antibiotics in modulating the gut microflora and further the host's metabolism in deciding the disease severity when treated before and after the disease manifestation.

We experimented on two differently immune-biased mice to know if there is any effect on the host's immune status when considering the treatment strategies of the diseased individual.

We observed the first significant evidence shreds of differences in the physiologic processes of the two different hosts against a particular treatment regime. The physical or phenotypic changes were significantly more severe in Th1- biased host (C57BL/6) than in Th2 (BALB/c) [124, 326, 327]. The pattern of severity response against a particular treatment regime is also quite different in two immune-biased hosts. Results revealed that the pre-treatment of the antibiotics increased the kinetics of the body weight loss in C57BL/6 mice but not in BALB/c when they developed colitis. Antibiotic treatment after colitis development rescued the mice from body weight loss in C57BL/6. In BALB/c, both pre-and post-treatment of antibiotics provided a protective measure against the disease. From our previous experimental plans, we have seen antibiotic treatments were responsible for the increased cecal index of the host. We observed pre and post-treatment antibiotics hadn't any more significant adverse effects on both the hosts.

We have shown development of colitis ultimately leads to the shortening of colon length as the severity increases. Here, we found the highest shortening of colon length in C57BL/6 mice when given early exposure to the antibiotics before developing the disease. In BALB/c, no such changes were observed. A significant symptom to be mentioned in colitis patients is a leaky gut due to the uncontrolled inflammatory

responses of the gut tissue. Our data showed that pre-exposure to antibiotics ultimately led to a more perforated gut than when there was no early antibiotic exposure in C57BL/6 but not in BALB/c.

Phenotypic changes and changes in gut integrity imparted the idea that early life exposure to antibiotics has some detrimental effect on the Th1 host in developing more severe colitis than the no antibiotic-exposed group. The th2 host is independent of this hypothesis. This observation prompted us to discover the underlying mechanism of these surprising results regarding the metabolic and associated gut microbial alterations. Metabonomics studies of host and microbial metabolites revealed that the changes were highly metabolism driven. Pathway prediction analysis from the shortlisted metabolites imparted the possible reason for exerting the same antibiotics' differential effect, showing the dual role in colitis susceptibility based on the treatment time. When C57BL/6 mice were exposed to antibiotics before the onset of the disease, we notic ed an enhanced lipid and amino acid metabolism. The same antibiotic treatment provided a therapeutic effect when administered after the disease development by upregulating the carbohydrate metabolism. Data from the previous study also revealed that the more impacted amino acid and lipid metabolism has a very high impact on activating the inflammatory responses and creating a niche for the more severe form of colitis. On the other hand, observation from the earlier study prompted an increased CD4+ cell population, and IL22 cytokine expression in colitis patients was tightly correlated with the upregulation of carbohydrate and nucleotide metabolism and downregulation of amino acid and lipid metabolism. High CD4+ and IL22 expressions collectively create

potent anti-inflammatory reactions to alleviate the inflammatory state of the disease [121, 257–262, 328].

In Th2- biased BALB/c, the effects of antibiotics were always protective. Antibiotic treatment modifies the host metabolism to protect against colitis by activating the anti-inflammatory carbohydrate metabolism irrespective of antibiotics pre or post-treatment. The major contributors to the altered metabolic processes of the hosts are their gut microbial counterparts. So, we predicted probably the gut microbial population is the critical player in changing the metabolism and thus the altered disease severity based on the pre and post-exposure of antibiotics. We tried to map the metabolic pathways with their probable microbial counterpart. We found the metabolic pathways were very much organism-specific, and an increase of one particular species of microbes can ultimately control more than one metabolic process, which further influences the disease severity. The altered metabolic pathways and the responsible gut microflora were very much dependent on the immuno-genetic background of the host. We found separate metabolic pathways and microflora in C57BL/6 and BALB/c mice. We also tried to shortlist the significant metabolic pathways altered at systemic and gut levels. We thought they had the highest effect on the differential role of antibiotics and the disease outcome. We found the significant gut microbiota responsible for altered metabolism was coming under the phylum proteobacteria and actinobacteria. Earlier, we also established higher abundance of proteobacteria in the gut was correlated with more amino acid metabolism. So, early exposure to the antibiotic ultimately increased the proteobacteria levels in the gut, which activated the amino acid and lipid metabolism of the host and thus created a more severe disease outcome. The disease colitis itself causes the increase of the proteobacteria level

in the gut, or rather, a higher proteobacteria level can lead to colitis-like diseases. So a proteobacterial storm in the gut due to early exposure to antibiotics and the disease itself could lead to a more severe disease outcome.

6.4 Conclusion

In this chapter, we tried to understand the detrimental and therapeutic effects of antibiotics against the disease of colitis. It is important to note that the antibiotic could perform a dual role as a) therapy and b) perturbing agent. We tried to understand this mechanism regarding metabolic and gut microbial alterations. We also tried it to predict the gut microbial profile with their metabolic counterpart. With this notion, we shortlisted some metabolic pathways specific to a specific disease condition and their specific microbial counterpart. So, if we can examine the metabolic profiles or pathways from a particular disease condition, we could map the gut microbial profile without any so-called metagenomic sequencing procedure.
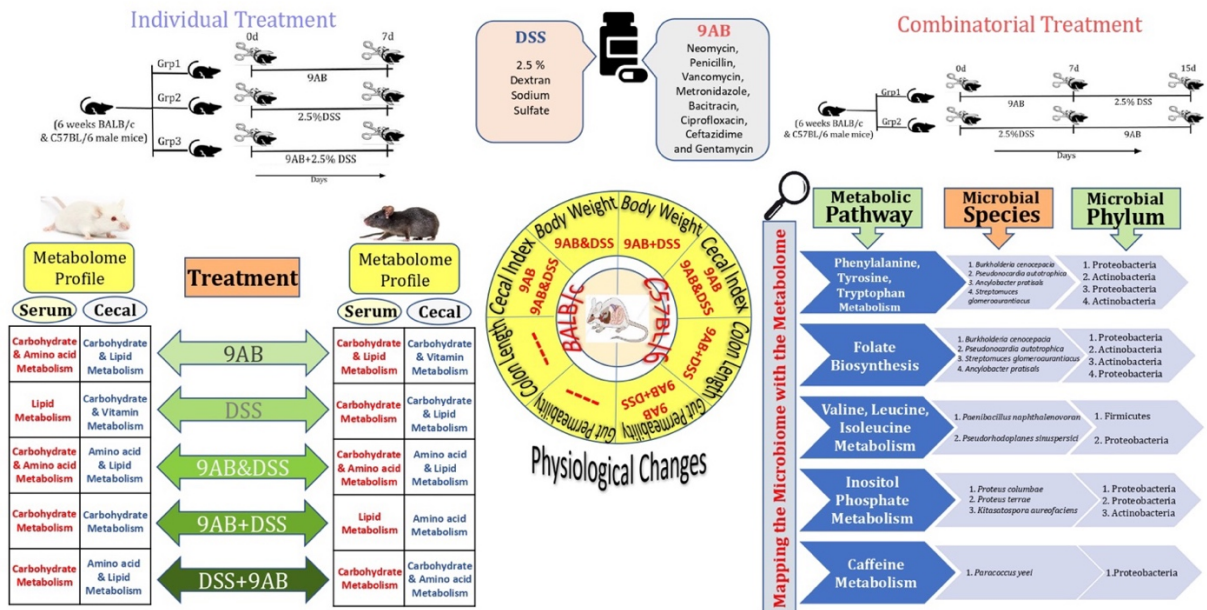
Fig. 6.8: Schema represented the effect of early life exposure to antibiotics on colitis susceptibility and the therapeutic interventions of antibiotics in terms of physiology, metabolism, and altered gut microbial compositions.
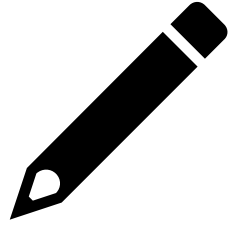
Chapter: 7

Conclusion

7. Conclusion

To give colitis patients a better quality of life, we began our thesis with the idea of an early, non-invasive diagnosis. Ethically it is challenging to work with human subjects. So, to accomplish our goal, we used the mouse model to comprehend the pathology of the disease and intervention techniques. We tried comprehending the condition from altered immunity, metabolism, and gut microbial profile viewpoints.

To create the disease in a mouse model, we employed Dextran sulphate sodium (DSS). To comprehend how the gut microbial pattern differs in colitis patients from antibiotic perturbation, we also utilized the well-known antibiotic that perturbs the gut.

According to the current study, antibiotic treatment affected the makeup and diversity of gut microbes more quickly. For the group receiving DSS, however, the dysbiotic condition persisted for a more extended period. The DSS-treated group had immunological dysregulation more severely than the antibiotic-treated groups.

For a deeper understanding of the heterogeneous outcome of colitis, we have used a systems biology approach aiming to integrate biological omics, and non-omics datasets can be a solution to resolve the complexity of the disease.

The finding showed that a) at higher DSS dosages (5 percent), both C57BL/6 and BALB/c mice might experience transitory inflammatory reactions, and b) at lower DSS dosages (2.5 percent), BALB/c mice's Th2-bias could minimize inflammation and help the animals return to normal.

Even at the lower (2.5 percent) DSS dosage, C57BL/6 mice exhibited significant inflammation

Varied inflammatory reactions may have been caused mainly by the animals in this study's investigation having different immunological biases.

Variable gut barrier function, SCFA synthesis, psychological stress reactions, such as anxiety and depressive behavior, and changed gut microbial composition in C57BL/6 and BALB/c mice may all contribute to the different responses. Additionally, the multi-omics technique enabled us to identify a) unique metabolic and microbial markers and b) key metabolic pathways associated with colitis severity. These biomarkers could be used in diagnostics and pathways to intervene and understand disease etiology.

 The severity of the disease could be controlled by modifying the gut microbial composition of the host. The antibiotic is one of the most widely used approaches to treat the altered gut microbial profile of colitis patients. We tried to understand how an intervention strategy can be suggested by understanding gut microbial dysbiosis for colitis.

However, reports also suggested that repeated antibiotic exposure is probably the key reason to enhance colitis disease susceptibility.

The experimental data revealed that in Th1- biased C57BL/6 mice, antibiotics treatment rescued the DSS-treated group from the diseased condition. On the other hand, early exposure to antibiotics increases disease susceptibility.

The scenario was quite different in Th2-biased BALB/c mice. Antibiotic treatment always provides a therapeutic effect against colitis, whether administered before or after the DSS treatment.

So, for the Th1 host, host immune status is the main controlling factor for the disease severity, which further causes microbial dysbiosis and leads to different physiological changes. Whereas, in the Th2 host, microbial dysbiosis is the primary factor for the disease

severity, restoration of gut microbial flora altered the diseased condition to a healthy one. Host immune status probably provides the extra advantage of restoring fast in the Th2 host.

Lastly, the observed metabolic pathways and microbial species could be a potential biomarker to diagnose colitis in the near future, aiming to map the microbiome with the metabolome.

The discovered metabolic pathways and microbial species may serve as a possible biomarker to detect colitis quickly.
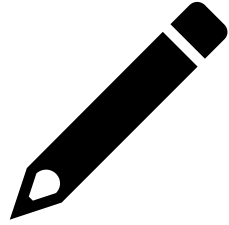
Chapter: 8

References

8. Reference:

1. Brüssow H (2013) What is health? Microb Biotechnol 6:341–348. https://doi.org/10.1111/1751-7915.12063

2. Saracci R (1997) The world health organisation needs to reconsider its definition of health. BMJ 314:1409–1409. https://doi.org/10.1136/bmj.314.7091.1409

3. Alegría M, NeMoyer A, Falgàs Bagué I, et al (2018) Social Determinants of Mental Health: Where We Are and Where We Need to Go. Curr Psychiatry Rep 20:95. https://doi.org/10.1007/s11920-018-0969-9

4. Deferio JJ, Breitinger S, Khullar D, et al (2019) Social determinants of health in mental health care and research: a case for greater inclusion. Journal of the American Medical Informatics Association 26:895–899. https://doi.org/10.1093/jamia/ocz049

5. Singu S, Acharya A, Challagundla K, Byrareddy SN (2020) Impact of Social Determinants of Health on the Emerging COVID-19 Pandemic in the United States. Front Public Health 8:. https://doi.org/10.3389/fpubh.2020.00406

6. Hood L, Rowen L (2013) The human genome project: big science transforms biology and medicine. Genome Med 5:79. https://doi.org/10.1186/gm483

7. Lander ES, Linton LM, Birren B, et al (2001) Initial sequencing and analysis of the human genome. Nature 409:860–921. https://doi.org/10.1038/35057062

8. Venter JC, Adams MD, Myers EW, et al (2001) The Sequence of the Human Genome. Science (1979) 291:1304–1351. https://doi.org/10.1126/science.1058040

9. Hornef MW, Torow N (2020) 'Layered immunity' and the 'neonatal window of opportunity' – timed succession of non-redundant phases to establish mucosal

host–microbial homeostasis after birth. Immunology 159:15–25. https://doi.org/10.1111/imm.13149

10. Torow N, Hornef MW (2017) The Neonatal Window of Opportunity: Setting the Stage for Life-Long Host-Microbial Interaction and Immune Homeostasis. The Journal of Immunology 198:557–563. https://doi.org/10.4049/jimmunol.1601253

11. Zheng D, Liwinski T, Elinav E (2020) Interaction between microbiota and immunity in health and disease. Cell Res 30:492–506. https://doi.org/10.1038/s41422-020-0332-7

12. Belkaid Y, Hand TW (2014) Role of the Microbiota in Immunity and Inflammation. Cell 157:121–141. https://doi.org/10.1016/j.cell.2014.03.011

13. Wu H-J, Wu E (2012) The role of gut microbiota in immune homeostasis and autoimmunity. Gut Microbes 3:4–14. https://doi.org/10.4161/gmic.19320

14. Lazar V, Ditu L-M, Pircalabioru GG, et al (2018) Aspects of Gut Microbiota and Immune System Interactions in Infectious Diseases, Immunopathology, and Cancer. Front Immunol 9:. https://doi.org/10.3389/fimmu.2018.01830

15. Turnbaugh PJ, Ley RE, Hamady M, et al (2007) The Human Microbiome Project. Nature 449:804–810. https://doi.org/10.1038/nature06244

16. Nash AK, Auchtung TA, Wong MC, et al (2017) The gut mycobiome of the Human Microbiome Project healthy cohort. Microbiome 5:153. https://doi.org/10.1186/s40168-017-0373-4

17. Mukhopadhyay S, Pattnaik T, Aich P (2022) A deeper understanding of the gut microbiota of different human races in search of disease specific microbial and metabolic biomarkers. Microenvironment and Microecology Research 4:18.

https://doi.org/10.53388/MMR2022018

18. Peterson J, Garges S, Giovanni M, et al (2009) The NIH Human Microbiome Project. Genome Res 19:2317–2323. https://doi.org/10.1101/gr.096651.109

19. (2019) The Integrative Human Microbiome Project. Nature 569:641–648. https://doi.org/10.1038/s41586-019-1238-8

20. O'Hara AM, Shanahan F (2006) The gut flora as a forgotten organ. EMBO Rep 7:688–693. https://doi.org/10.1038/sj.embor.7400731

21. Bocci V (1992) The Neglected Organ: Bacterial Flora Has a Crucial Immunostimulatory Role. Perspect Biol Med 35:251–260. https://doi.org/10.1353/pbm.1992.0004

22. Lazar V, Ditu L-M, Pircalabioru GG, et al (2018) Aspects of Gut Microbiota and Immune System Interactions in Infectious Diseases, Immunopathology, and Cancer. Front Immunol 9:. https://doi.org/10.3389/fimmu.2018.01830

23. Sommer F, Bäckhed F (2013) The gut microbiota — masters of host development and physiology. Nat Rev Microbiol 11:227–238. https://doi.org/10.1038/nrmicro2974

24. (2012) Structure, function and diversity of the healthy human microbiome. Nature 486:207–214. https://doi.org/10.1038/nature11234

25. Qin J, Li R, Raes J, et al (2010) A human gut microbial gene catalogue established by metagenomic sequencing. Nature 464:59–65. https://doi.org/10.1038/nature08821

26. Hornef MW, Torow N (2020) 'Layered immunity' and the 'neonatal window of opportunity' – timed succession of non-redundant phases to establish mucosal

host–microbial homeostasis after birth. Immunology 159:15–25. https://doi.org/10.1111/imm.13149

27. Hosseinkhani F, Heinken A, Thiele I, et al (2021) The contribution of gut bacterial metabolites in the human immune signaling pathway of non-communicable diseases. Gut Microbes 13:. https://doi.org/10.1080/19490976.2021.1882927

28. Skonieczna-Żydecka K, Jakubczyk K, Maciejewska-Markiewicz D, et al (2020) Gut Biofactory—Neurocompetent Metabolites within the Gastrointestinal Tract. A Scoping Review. Nutrients 12:3369. https://doi.org/10.3390/nu12113369

29. Man AWC, Zhou Y, Xia N, Li H (2020) Involvement of Gut Microbiota, Microbial Metabolites and Interaction with Polyphenol in Host Immunometabolism. Nutrients 12:3054. https://doi.org/10.3390/nu12103054

30. Park J, Kotani T, Konno T, et al (2016) Promotion of Intestinal Epithelial Cell Turnover by Commensal Bacteria: Role of Short-Chain Fatty Acids. PLoS One 11:e0156334. https://doi.org/10.1371/journal.pone.0156334

31. Thursby E, Juge N (2017) Introduction to the human gut microbiota. Biochemical Journal 474:1823–1836. https://doi.org/10.1042/BCJ20160510

32. von Frieling J, Fink C, Hamm J, et al (2018) Grow With the Challenge – Microbial Effects on Epithelial Proliferation, Carcinogenesis, and Cancer Therapy. Front Microbiol 9:. https://doi.org/10.3389/fmicb.2018.02020

33. Ramachandran A, Madesh M, Balasubramanian KA (2000) Apoptosis in the intestinal epithelium: Its relevance in normal and pathophysiological conditions. J Gastroenterol Hepatol 15:109–120. https://doi.org/10.1046/j.1440-1746.2000.02059.x

34. Seely KD, Kotelko CA, Douglas H, et al (2021) The Human Gut Microbiota: A Key Mediator of Osteoporosis and Osteogenesis. Int J Mol Sci 22:9452. https://doi.org/10.3390/ijms22179452

35. Bhardwaj A, Sapra L, Tiwari A, et al (2022) "Osteomicrobiology": The Nexus Between Bone and Bugs. Front Microbiol 12:. https://doi.org/10.3389/fmicb.2021.812466

36. Carabotti M, Scirocco A, Maselli MA, Severi C (2015) The gut-brain axis: interactions between enteric microbiota, central and enteric nervous systems. Ann Gastroenterol 28:203–209

37. Martin CR, Osadchiy V, Kalani A, Mayer EA (2018) The Brain-Gut-Microbiome Axis. Cell Mol Gastroenterol Hepatol 6:133–148. https://doi.org/10.1016/j.jcmgh.2018.04.003

38. Cryan JF, O'Riordan KJ, Cowan CSM, et al (2019) The Microbiota-Gut-Brain Axis. Physiol Rev 99:1877–2013. https://doi.org/10.1152/physrev.00018.2018

39. DeGruttola AK, Low D, Mizoguchi A, Mizoguchi E (2016) Current Understanding of Dysbiosis in Disease in Human and Animal Models. Inflamm Bowel Dis 22:1137–1150. https://doi.org/10.1097/MIB.0000000000000750

40. Kriss M, Hazleton KZ, Nusbacher NM, et al (2018) Low diversity gut microbiota dysbiosis: drivers, functional implications and recovery. Curr Opin Microbiol 44:34–40. https://doi.org/10.1016/j.mib.2018.07.003

41. Shin N-R, Whon TW, Bae J-W (2015) Proteobacteria: microbial signature of dysbiosis in gut microbiota. Trends Biotechnol 33:496–503. https://doi.org/10.1016/j.tibtech.2015.06.011

References

42. Şafak B, Altunan B, Topçu B, Eren Topkaya A (2020) The gut microbiome in epilepsy. Microb Pathog 139:103853. https://doi.org/10.1016/j.micpath.2019.103853

43. Liu P, Wu L, Peng G, et al (2019) Altered microbiomes distinguish Alzheimer's disease from amnestic mild cognitive impairment and health in a Chinese cohort. Brain Behav Immun 80:633–643. https://doi.org/10.1016/j.bbi.2019.05.008

44. Shah V, Lambeth SM, Carson T, et al (2015) Composition Diversity and Abundance of Gut Microbiome in Prediabetes and Type 2 Diabetes. J Diabetes Obes 2:108–114. https://doi.org/10.15436/2376-0949.15.031

45. Méndez-Salazar EO, Ortiz-López MG, Granados-Silvestre M de los Á, et al (2018) Altered Gut Microbiota and Compositional Changes in Firmicutes and Proteobacteria in Mexican Undernourished and Obese Children. Front Microbiol 9:. https://doi.org/10.3389/fmicb.2018.02494

46. Lun H, Yang W, Zhao S, et al (2019) Altered gut microbiota and microbial biomarkers associated with chronic kidney disease. Microbiologyopen 8:e00678. https://doi.org/10.1002/mbo3.678

47. Alam MT, Amos GCA, Murphy ARJ, et al (2020) Microbial imbalance in inflammatory bowel disease patients at different taxonomic levels. Gut Pathog 12:1. https://doi.org/10.1186/s13099-019-0341-6

48. Zhang W-Q, Zhao S-K, Luo J-W, et al (2018) Alterations of fecal bacterial communities in patients with lung cancer. Am J Transl Res 10:3171–3185

49. Han Y, Gong Z, Sun G, et al (2021) Dysbiosis of Gut Microbiota in Patients With Acute Myocardial Infarction. Front Microbiol 12:.

https://doi.org/10.3389/fmicb.2021.680101

50.   Sun W, Du D, Fu T, et al (2022) Alterations of the Gut Microbiota in Patients With Severe Chronic Heart Failure. Front Microbiol 12:. https://doi.org/10.3389/fmicb.2021.813289

51.   Zhu Q, Gao R, Zhang Y, et al (2018) Dysbiosis signatures of gut microbiota in coronary artery disease. Physiol Genomics 50:893–903. https://doi.org/10.1152/physiolgenomics.00070.2018

52.   Yan Q, Gu Y, Li X, et al (2017) Alterations of the Gut Microbiome in Hypertension. Front Cell Infect Microbiol 7:. https://doi.org/10.3389/fcimb.2017.00381

53.   Qin J, Li R, Raes J, et al (2010) A human gut microbial gene catalogue established by metagenomic sequencing. Nature 464:59–65. https://doi.org/10.1038/nature08821

54.   Gorlé N, Bauwens E, Haesebrouck F, et al (2021) Helicobacter and the Potential Role in Neurological Disorders: There Is More Than Helicobacter pylori. Front Immunol 11:. https://doi.org/10.3389/fimmu.2020.584165

55.   Flint HJ, Duncan SH (2014) Bacteroides and Prevotella. In: Encyclopedia of Food Microbiology. Elsevier, pp 203–208

56.   Duan M, Wang Y, Zhang Q, et al (2021) Characteristics of gut microbiota in people with obesity. PLoS One 16:e0255446. https://doi.org/10.1371/journal.pone.0255446

57.   Ahmad A, Yang W, Chen G, et al (2019) Analysis of gut microbiota of obese individuals with type 2 diabetes and healthy individuals. PLoS One 14:e0226372.

https://doi.org/10.1371/journal.pone.0226372

58. Magne F, Gotteland M, Gauthier L, et al (2020) The Firmicutes/Bacteroidetes Ratio: A Relevant Marker of Gut Dysbiosis in Obese Patients? Nutrients 12:1474. https://doi.org/10.3390/nu12051474

59. Stojanov S, Berlec A, Štrukelj B (2020) The Influence of Probiotics on the Firmicutes/Bacteroidetes Ratio in the Treatment of Obesity and Inflammatory Bowel disease. Microorganisms 8:1715. https://doi.org/10.3390/microorganisms8111715

60. Vogt NM, Kerby RL, Dill-McFarland KA, et al (2017) Gut microbiome alterations in Alzheimer's disease. Sci Rep 7:13537. https://doi.org/10.1038/s41598-017-13601-y

61. Wang T, Cai G, Qiu Y, et al (2012) Structural segregation of gut microbiota between colorectal cancer patients and healthy volunteers. ISME J 6:320–329. https://doi.org/10.1038/ismej.2011.109

62. Chen Y, Ma J, Dong Y, et al (2022) Characteristics of Gut Microbiota in Patients With Clear Cell Renal Cell Carcinoma. Front Microbiol 13:. https://doi.org/10.3389/fmicb.2022.913718

63. Zhao S-S, Chen L, Yang J, et al (2022) Altered Gut Microbial Profile Accompanied by Abnormal Fatty Acid Metabolism Activity Exacerbates Endometrial Cancer Progression. Microbiol Spectr. https://doi.org/10.1128/spectrum.02612-22

64. Binda C, Lopetuso LR, Rizzatti G, et al (2018) Actinobacteria: A relevant minority for the maintenance of gut homeostasis. Digestive and Liver Disease 50:421–428.

https://doi.org/10.1016/j.dld.2018.02.012

65. Zhuang H, Cheng L, Wang Y, et al (2019) Dysbiosis of the Gut Microbiome in Lung Cancer. Front Cell Infect Microbiol 9:. https://doi.org/10.3389/fcimb.2019.00112

66. Aarts E, Ederveen THA, Naaijen J, et al (2017) Gut microbiome in ADHD and its relation to neural reward anticipation. PLoS One 12:e0183509. https://doi.org/10.1371/journal.pone.0183509

67. Wei LQ, Cheong IH, Yang GH, et al (2021) The Application of High-Throughput Technologies for the Study of Microbiome and Cancer. Front Genet 12:. https://doi.org/10.3389/fgene.2021.699793

68. Fouhy F, Ross RP, Fitzgerald GF, et al (2012) Composition of the early intestinal microbiota. Gut Microbes 3:203–220. https://doi.org/10.4161/gmic.20169

69. Gorkiewicz G, Moschen A (2018) Gut microbiome: a new player in gastrointestinal disease. Virchows Archiv 472:159–172. https://doi.org/10.1007/s00428-017-2277-x

70. Wang Y, Gao X, Zhang X, et al (2021) Microbial and metabolic features associated with outcome of infliximab therapy in pediatric Crohn's disease. Gut Microbes 13:. https://doi.org/10.1080/19490976.2020.1865708

71. Li M, Yang L, Mu C, et al (2022) Gut microbial metabolome in inflammatory bowel disease: From association to therapeutic perspectives. Comput Struct Biotechnol J 20:2402–2414. https://doi.org/10.1016/j.csbj.2022.03.038

72. Ganesan R, Jeong J-J, Kim DJ, Suk KT (2022) Recent Trends of Microbiota-Based Microbial Metabolites Metabolism in Liver Disease. Front Med (Lausanne) 9:.

https://doi.org/10.3389/fmed.2022.841281

73. Pedersen HK, Gudmundsdottir V, Nielsen HB, et al (2016) Human gut microbes impact host serum metabolome and insulin sensitivity. Nature 535:376–381. https://doi.org/10.1038/nature18646

74. Gojda J, Cahova M (2021) Gut Microbiota as the Link between Elevated BCAA Serum Levels and Insulin Resistance. Biomolecules 11:1414. https://doi.org/10.3390/biom11101414

75. Ou Z, Deng L, Lu Z, et al (2020) Protective effects of Akkermansia muciniphila on cognitive deficits and amyloid pathology in a mouse model of Alzheimer's disease. Nutr Diabetes 10:12. https://doi.org/10.1038/s41387-020-0115-8

76. MahmoudianDehkordi S, Arnold M, Nho K, et al (2019) Altered bile acid profile associates with cognitive impairment in Alzheimer's disease—An emerging role for gut microbiome. Alzheimer's & Dementia 15:76–92. https://doi.org/10.1016/j.jalz.2018.07.217

77. Sirois FM, Molnar DS, Hirsch JK (2015) Self-Compassion, Stress, and Coping in the Context of Chronic Illness. Self and Identity 14:334–347. https://doi.org/10.1080/15298868.2014.996249

78. Grygiel-Górniak B, Limphaibool N, Puszczewicz M (2019) Cytokine secretion and the risk of depression development in patients with connective tissue diseases. Psychiatry Clin Neurosci 73:302–316. https://doi.org/10.1111/pcn.12826

79. Ting EY-C, Yang AC, Tsai S-J (2020) Role of Interleukin-6 in Depressive Disorder. Int J Mol Sci 21:2194. https://doi.org/10.3390/ijms21062194

80. Berk M, Williams LJ, Jacka FN, et al (2013) So depression is an inflammatory

disease, but where does the inflammation come from? BMC Med 11:200. https://doi.org/10.1186/1741-7015-11-200

81. Bermudez EA, Rifai N, Buring J, et al (2002) Interrelationships Among Circulating Interleukin-6, C-Reactive Protein, and Traditional Cardiovascular Risk Factors in Women. Arterioscler Thromb Vasc Biol 22:1668–1673. https://doi.org/10.1161/01.ATV.0000029781.31325.66

82. von Stein P, Lofberg R, Kuznetsov N V., et al (2008) Multigene Analysis Can Discriminate Between Ulcerative Colitis, Crohn's Disease, and Irritable Bowel Syndrome. Gastroenterology 134:1869–1881. https://doi.org/10.1053/j.gastro.2008.02.083

83. Joossens M, Huys G, Cnockaert M, et al (2011) Dysbiosis of the faecal microbiota in patients with Crohn's disease and their unaffected relatives. Gut 60:. https://doi.org/10.1136/gut.2010.223263

84. Ng SC, Tang W, Ching JY, et al (2013) Incidence and Phenotype of Inflammatory Bowel Disease Based on Results From the Asia-Pacific Crohn's and Colitis Epidemiology Study. Gastroenterology 145:158-165.e2. https://doi.org/10.1053/j.gastro.2013.04.007

85. Santoru ML, Piras C, Murgia A, et al (2017) Cross sectional evaluation of the gut-microbiome metabolome axis in an Italian cohort of IBD patients. Sci Rep 7:9523. https://doi.org/10.1038/s41598-017-10034-5

86. Reiman D, Layden BT, Dai Y (2021) MiMeNet: Exploring microbiome-metabolome relationships using neural networks. PLoS Comput Biol 17:e1009021. https://doi.org/10.1371/journal.pcbi.1009021

References

87. Mallick H, Franzosa EA, McIver LJ, et al (2019) Predictive metabolomic profiling of microbial communities using amplicon or metagenomic sequences. Nat Commun 10:3136. https://doi.org/10.1038/s41467-019-10927-1

88. EJTAHED H-S, ANGOORANI P, SOROUSH A-R, et al (2020) Gut microbiota-derived metabolites in obesity: a systematic review. Biosci Microbiota Food Health 39:65–76. https://doi.org/10.12938/bmfh.2019-026

89. Jaimes JD, Slavíčková A, Hurych J, et al (2021) Stool metabolome-microbiota evaluation among children and adolescents with obesity, overweight, and normal-weight using 1H NMR and 16S rRNA gene profiling. PLoS One 16:e0247378. https://doi.org/10.1371/journal.pone.0247378

90. Dong L, Han L, Duan T, et al (2020) Integrated microbiome–metabolome analysis reveals novel associations between fecal microbiota and hyperglycemia-related changes of plasma metabolome in gestational diabetes mellitus. RSC Adv 10:2027–2036. https://doi.org/10.1039/C9RA07799E

91. Menni C, Zhu J, Le Roy CI, et al (2020) Serum metabolites reflecting gut microbiome alpha diversity predict type 2 diabetes. Gut Microbes 11:1632–1642. https://doi.org/10.1080/19490976.2020.1778261

92. Zhao L, Lou H, Peng Y, et al (2019) Comprehensive relationships between gut microbiome and faecal metabolome in individuals with type 2 diabetes and its complications. Endocrine 66:526–537. https://doi.org/10.1007/s12020-019-02103-8

93. Laghi L, Mastromarino P, Prosperi M, et al (2021) Are Fecal Metabolome and Microbiota Profiles Correlated with Autism Severity? A Cross-Sectional Study on

ASD Preschoolers. Metabolites 11:654. https://doi.org/10.3390/metabo11100654

94. He J, Chan T, Hong X, et al (2020) Microbiome and Metabolome Analyses Reveal the Disruption of Lipid Metabolism in Systemic Lupus Erythematosus. Front Immunol 11:. https://doi.org/10.3389/fimmu.2020.01703

95. Preter V De, Verbeke K (2013) Metabolomics as a diagnostic tool in gastroenterology. World J Gastrointest Pharmacol Ther 4:97. https://doi.org/10.4292/wjgpt.v4.i4.97

96. Yoshida M, Hatano N, Nishiumi S, et al (2012) Diagnosis of gastroenterological diseases by metabolome analysis using gas chromatography–mass spectrometry. J Gastroenterol 47:9–20. https://doi.org/10.1007/s00535-011-0493-8

97. Ooi M, Nishiumi S, Yoshie T, et al (2011) GC/MS-based profiling of amino acids and TCA cycle-related molecules in ulcerative colitis. Inflammation Research 60:831–840. https://doi.org/10.1007/s00011-011-0340-7

98. Bjerrum JT, Nielsen OH, Hao F, et al (2010) Metabonomics in Ulcerative Colitis: Diagnostics, Biomarker Identification, And Insight into the Pathophysiology. J Proteome Res 9:954–962. https://doi.org/10.1021/pr9008223

99. Bajpai J, Sinha BN, Srivastava AN (1975) Clinical study of Volkmann's ischemic contracture of the upper limb. Int Surg 60:162–4

100. Grover M, Herfarth H, Drossman DA (2009) The Functional–Organic Dichotomy: Postinfectious Irritable Bowel Syndrome and Inflammatory Bowel Disease–Irritable Bowel Syndrome. Clinical Gastroenterology and Hepatology 7:48–53. https://doi.org/10.1016/j.cgh.2008.08.032

101. Day RL, Harper AJ, Woods RM, et al (2019) Probiotics: current landscape and

future horizons. Future Sci OA 5:. https://doi.org/10.4155/fsoa-2019-0004

102. Hassan ZH, Hugenholtz F, Zoetendal EG, Smidt H (2022) Future Perspectives of Probiotics and Prebiotics in Foods and Food Supplements. In: Good Microbes in Medicine, Food Production, Biotechnology, Bioremediation, and Agriculture. Wiley, pp 69–88

103. Floch MH, Kim A (2014) Clinical Insights: Probiotics, Prebiotics and Gut Health. Future Medicine Ltd, Unitec House, 2 Albert Place, London N3 1QB, UK

104. Cunningham M, Azcarate-Peril MA, Barnard A, et al (2021) Shaping the Future of Probiotics and Prebiotics. Trends Microbiol 29:667–685. https://doi.org/10.1016/j.tim.2021.01.003

105. Gupta S, Allen-Vercoe E, Petrof EO (2016) Fecal microbiota transplantation: in perspective. Therap Adv Gastroenterol 9:229–239. https://doi.org/10.1177/1756283X15607414

106. Giles EM, D'Adamo GL, Forster SC (2019) The future of faecal transplants. Nat Rev Microbiol 17:719–719. https://doi.org/10.1038/s41579-019-0271-9

107. Chen C-C, Chiu C-H (2022) Current and future applications of fecal microbiota transplantation for children. Biomed J 45:11–18. https://doi.org/10.1016/j.bj.2021.11.004

108. Lin DM, Koskella B, Lin HC (2017) Phage therapy: An alternative to antibiotics in the age of multi-drug resistance. World J Gastrointest Pharmacol Ther 8:162. https://doi.org/10.4292/wjgpt.v8.i3.162

109. Brives C, Pourraz J (2020) Phage therapy as a potential solution in the fight against AMR: obstacles and possible futures. Palgrave Commun 6:100.

https://doi.org/10.1057/s41599-020-0478-4

110. Wegener G (2014) 'Let food be thy medicine, and medicine be thy food': Hippocrates revisited. Acta Neuropsychiatr 26:1–3. https://doi.org/10.1017/neu.2014.3

111. Martín R, Langella P (2019) Emerging Health Concepts in the Probiotics Field: Streamlining the Definitions. Front Microbiol 10:. https://doi.org/10.3389/fmicb.2019.01047

112. Shruthi B, Deepa N, Somashekaraiah R, et al (2022) Exploring biotechnological and functional characteristics of probiotic yeasts: A review. Biotechnology Reports 34:e00716. https://doi.org/10.1016/j.btre.2022.e00716

113. Jackson MA, Verdi S, Maxan M-E, et al (2018) Gut microbiota associations with common diseases and prescription medications in a population-based cohort. Nat Commun 9:2655. https://doi.org/10.1038/s41467-018-05184-7

114. Vich Vila A, Collij V, Sanna S, et al (2020) Impact of commonly used drugs on the composition and metabolic function of the gut microbiota. Nat Commun 11:362. https://doi.org/10.1038/s41467-019-14177-z

115. Li Y, Sui L, Zhao H, et al (2022) Differences in the Establishment of Gut Microbiota and Metabolome Characteristics Between Balb/c and C57BL/6J Mice After Proton Irradiation. Front Microbiol 13:. https://doi.org/10.3389/fmicb.2022.874702

116. Ray P, Pandey U, Das D, Aich P (2021) Vancomycin-Induced Changes in Host Immunity and Behavior: Comparative Genomic and Metagenomic Analysis in C57BL/6 and BALB/c Mice. Dig Dis Sci 66:. https://doi.org/10.1007/s10620-020-

References

06729-x

117. Patel S, Preuss C V., Bernice F (2022) Vancomycin

118. Pepin J (2008) Vancomycin for the Treatment of *Clostridium difficile* Infection: For Whom Is This Expensive Bullet Really Magic? Clinical Infectious Diseases 46:1493–1498. https://doi.org/10.1086/587656

119. Miglioli PA, Allerberger F, Calabrò GB, Gaion RM (2001) Effects of daily oral administration of rifaximin and neomycin on faecal aerobic flora in rats. Pharmacol Res 44:373–375. https://doi.org/10.1006/phrs.2001.0869

120. Zarrinpar A, Chaix A, Xu ZZ, et al (2018) Antibiotic-induced microbiome depletion alters metabolic homeostasis by affecting gut signaling and colonic metabolism. Nat Commun 9:2872. https://doi.org/10.1038/s41467-018-05336-9

121. Mukhopadhyay S, Saha S, Chakraborty S, et al (2022) Differential colitis susceptibility of Th1- and Th2-biased mice: A multi-omics approach. PLoS One 17:e0264400. https://doi.org/10.1371/journal.pone.0264400

122. Jensen T, Kiersgaard M, Sørensen D, Mikkelsen L (2013) Fasting of mice: a review. Lab Anim 47:225–240. https://doi.org/10.1177/0023677213501659

123. (2014) http://www.bio-protocol.org/e1289 Vol 4, Iss 22, Nov 20, 2014. 4:20–23

124. Mukhopadhyay S, Ray P, Aich P (2023) A comparative analysis of gut microbial dysbiosis by select antibiotics and DSS to understand the effects of perturbation on the host immunity and metabolism. Life Sci 312:121212. https://doi.org/10.1016/j.lfs.2022.121212

125. Viennois E, Chen F, Laroui H, et al (2013) Dextran sodium sulfate inhibits the activities of both polymerase and reverse transcriptase: Lithium chloride

purification, a rapid and efficient technique to purify RNA. BMC Res Notes 6:360. https://doi.org/10.1186/1756-0500-6-360

126. Cardinale CJ, Wei Z, Li J, et al (2014) Transcriptome Profiling of Human Ulcerative Colitis Mucosa Reveals Altered Expression of Pathways Enriched in Genetic Susceptibility Loci. PLoS One 9:e96153. https://doi.org/10.1371/journal.pone.0096153

127. Ashton JJ, Boukas K, Davies J, et al (2020) Ileal transcriptomic analysis in paediatric Crohn's disease reveals IL17- and NOD- signalling expression signatures in treatment-naïve patients and identifies epithelial cells driving differentially expressed genes. J Crohns Colitis jjaa236:. https://doi.org/10.1093/ecco-jcc/jjaa236

128. Naik AK, Pandey U, Mukherjee R, et al (2019) Lactobacillus rhamnosus GG reverses mortality of neonatal mice against Salmonella challenge. Toxicol Res (Camb) 8:361–372. https://doi.org/10.1039/C9TX00006B

129. Ray P, Pandey U, Aich P (2021) Comparative analysis of beneficial effects of vancomycin treatment on Th1- and Th2-biased mice and the role of gut microbiota. J Appl Microbiol 130:1337–1356. https://doi.org/10.1111/jam.14853

130. Xia J, Wishart DS (2011) Metabolomic Data Processing, Analysis, and Interpretation Using MetaboAnalyst. Curr Protoc Bioinformatics 34:. https://doi.org/10.1002/0471250953.bi1410s34

131. Chong J, Wishart DS, Xia J (2019) Using MetaboAnalyst 4.0 for Comprehensive and Integrative Metabolomics Data Analysis. Curr Protoc Bioinformatics 68:. https://doi.org/10.1002/cpbi.86

References

132. (2020) Practical Machine Learning for Data Analysis Using Python. Elsevier

133. (2020) An Industrial IoT Approach for Pharmaceutical Industry Growth. Elsevier

134. Epps KY, Comerford NB, Reeves IJB, et al (2007) Chemical diversity – highlighting a species richness and ecosystem function disconnect. Oikos 116:. https://doi.org/10.1111/j.2007.0030-1299.15853.x

135. Hong Y-K, Coury DA, Polne-Fuller M, Gibor A (1992) LITHIUM CHLORIDE EXTRACTION OF DNA FROM THE SEAWEED PORPHYRA PERFORATA (RHODOPHYTA)1. J Phycol 28:717–720. https://doi.org/10.1111/j.0022-3646.1992.00717.x

136. Arif IA, Bakir MA, Khan HA, et al (2010) A Simple Method for DNA Extraction from Mature Date Palm Leaves: Impact of Sand Grinding and Composition of Lysis Buffer. Int J Mol Sci 11:3149–3157. https://doi.org/10.3390/ijms11093149

137. Takahashi S, Tomita J, Nishioka K, et al (2014) Development of a Prokaryotic Universal Primer for Simultaneous Analysis of Bacteria and Archaea Using Next-Generation Sequencing. PLoS One 9:e105592. https://doi.org/10.1371/journal.pone.0105592

138. Kim JJ, Shajib MdS, Manocha MM, Khan WI (2012) Investigating Intestinal Inflammation in DSS-induced Model of IBD. Journal of Visualized Experiments. https://doi.org/10.3791/3678

139. Mysara M, Njima M, Leys N, et al (2017) From reads to operational taxonomic units: an ensemble processing pipeline for MiSeq amplicon sequencing data. Gigascience 6:. https://doi.org/10.1093/gigascience/giw017

140. Caporaso JG, Kuczynski J, Stombaugh J, et al (2010) QIIME allows analysis of

high-throughput community sequencing data. Nat Methods 7:335–336. https://doi.org/10.1038/nmeth.f.303

141.   Purcell R V., Visnovska M, Biggs PJ, et al (2017) Distinct gut microbiome patterns associate with consensus molecular subtypes of colorectal cancer. Sci Rep 7:11590. https://doi.org/10.1038/s41598-017-11237-6

142.   DeSantis TZ, Hugenholtz P, Larsen N, et al (2006) Greengenes, a Chimera-Checked 16S rRNA Gene Database and Workbench Compatible with ARB. Appl Environ Microbiol 72:5069–5072. https://doi.org/10.1128/AEM.03006-05

143.   Frank DN, St. Amand AL, Feldman RA, et al (2007) Molecular-phylogenetic characterization of microbial community imbalances in human inflammatory bowel diseases. Proceedings of the National Academy of Sciences 104:13780–13785. https://doi.org/10.1073/pnas.0706625104

144.   Kastenberger I, Lutsch C, Herzog H, Schwarzer C (2012) Influence of Sex and Genetic Background on Anxiety-Related and Stress-Induced Behaviour of Prodynorphin-Deficient Mice. PLoS One 7:e34251. https://doi.org/10.1371/journal.pone.0034251

145.   Seibenhener ML, Wooten MC (2015) Use of the Open Field Maze to Measure Locomotor and Anxiety-like Behavior in Mice. Journal of Visualized Experiments. https://doi.org/10.3791/52434

146.   Gould TD, Dao DT, Kovacsics CE (2009) The Open Field Test

147.   Lister RG The use of a plus-maze to measure anxiety in the mouse

148.   Walf AA, Frye CA (2007) The use of the elevated plus maze as an assay of anxiety-related behavior in rodents. Nat Protoc 2:322–328.

References

https://doi.org/10.1038/nprot.2007.44

149. Komada M, Takao K, Miyakawa T (2008) Elevated plus maze for mice. Journal of Visualized Experiments. https://doi.org/10.3791/1088

150. Yankelevitch-Yahav R, Franko M, Huly A, Doron R (2015) The forced swim test as a model of depressive-like behavior. Journal of Visualized Experiments 2015:. https://doi.org/10.3791/52587

151. Can A, Dao DT, Arad M, et al (2011) The mouse forced swim test. Journal of Visualized Experiments. https://doi.org/10.3791/3638

152. Cryan JF, Mombereau C, Vassout A (2005) The tail suspension test as a model for assessing antidepressant activity: Review of pharmacological and genetic studies in mice. Neurosci Biobehav Rev 29:571–625

153. Can A, Dao DT, Terrillion CE, et al (2011) The tail suspension test. Journal of Visualized Experiments. https://doi.org/10.3791/3769

154. Chen Y, Zhou J, Wang L (2021) Role and Mechanism of Gut Microbiota in Human Disease. Front Cell Infect Microbiol 11:. https://doi.org/10.3389/fcimb.2021.625913

155. O'Hara AM, Shanahan F (2006) The gut flora as a forgotten organ. EMBO Rep 7:688–693. https://doi.org/10.1038/sj.embor.7400731

156. Wang B, Yao M, Lv L, et al (2017) The Human Microbiota in Health and Disease. Engineering 3:71–82. https://doi.org/10.1016/J.ENG.2017.01.008

157. Ding R, Goh W-R, Wu R, et al (2019) Revisit gut microbiota and its impact on human health and disease. J Food Drug Anal 27:623–631. https://doi.org/10.1016/j.jfda.2018.12.012

158. Lin L, Zhang J (2017) Role of intestinal microbiota and metabolites on gut homeostasis and human diseases. BMC Immunol 18:2. https://doi.org/10.1186/s12865-016-0187-3

159. Martin AM, Sun EW, Rogers GB, Keating DJ (2019) The Influence of the Gut Microbiome on Host Metabolism Through the Regulation of Gut Hormone Release. Front Physiol 10:. https://doi.org/10.3389/fphys.2019.00428

160. Wu H-J, Wu E (2012) The role of gut microbiota in immune homeostasis and autoimmunity. Gut Microbes 3:4–14. https://doi.org/10.4161/gmic.19320

161. Langdon A, Crook N, Dantas G (2016) The effects of antibiotics on the microbiome throughout development and alternative approaches for therapeutic modulation. Genome Med 8:39. https://doi.org/10.1186/s13073-016-0294-z

162. Kho ZY, Lal SK (2018) The Human Gut Microbiome – A Potential Controller of Wellness and Disease. Front Microbiol 9:. https://doi.org/10.3389/fmicb.2018.01835

163. Durack J, Lynch S V. (2019) The gut microbiome: Relationships with disease and opportunities for therapy. Journal of Experimental Medicine 216:20–40. https://doi.org/10.1084/jem.20180448

164. Angoa-Pérez M, Zagorac B, Francescutti DM, et al (2020) Effects of a high fat diet on gut microbiome dysbiosis in a mouse model of Gulf War Illness. Sci Rep 10:9529. https://doi.org/10.1038/s41598-020-66833-w

165. Schwartz DJ, Langdon AE, Dantas G (2021) Correction to: Understanding the impact of antibiotic perturbation on the human microbiome. Genome Med 13:26. https://doi.org/10.1186/s13073-021-00846-6

References

166. Steimle A, Autenrieth IB, Frick J-S (2016) Structure and function: Lipid A modifications in commensals and pathogens. International Journal of Medical Microbiology 306:290–301. https://doi.org/10.1016/j.ijmm.2016.03.001

167. Hawkesworth S, Moore SE, Fulford AJC, et al (2013) Evidence for metabolic endotoxemia in obese and diabetic Gambian women. Nutr Diabetes 3:e83–e83. https://doi.org/10.1038/nutd.2013.24

168. Boutagy NE, McMillan RP, Frisard MI, Hulver MW (2016) Metabolic endotoxemia with obesity: Is it real and is it relevant? Biochimie 124:11–20. https://doi.org/10.1016/j.biochi.2015.06.020

169. Akira S, Hemmi H (2003) Recognition of pathogen-associated molecular patterns by TLR family. Immunol Lett 85:85–95. https://doi.org/10.1016/S0165-2478(02)00228-6

170. Rallabhandi P, Awomoyi A, Thomas KE, et al (2008) Differential Activation of Human TLR4 by *Escherichia coli* and *Shigella flexneri* 2a Lipopolysaccharide: Combined Effects of Lipid A Acylation State and TLR4 Polymorphisms on Signaling. The Journal of Immunology 180:1139–1147. https://doi.org/10.4049/jimmunol.180.2.1139

171. Parada Venegas D, De la Fuente MK, Landskron G, et al (2019) Short Chain Fatty Acids (SCFAs)-Mediated Gut Epithelial and Immune Regulation and Its Relevance for Inflammatory Bowel Diseases. Front Immunol 10:. https://doi.org/10.3389/fimmu.2019.00277

172. Vinolo MAR, Rodrigues HG, Nachbar RT, Curi R (2011) Regulation of Inflammation by Short Chain Fatty Acids. Nutrients 3:858–876.

https://doi.org/10.3390/nu3100858

173. Morrison DJ, Preston T (2016) Formation of short chain fatty acids by the gut microbiota and their impact on human metabolism. Gut Microbes 7:189–200. https://doi.org/10.1080/19490976.2015.1134082

174. Palleja A, Mikkelsen KH, Forslund SK, et al (2018) Recovery of gut microbiota of healthy adults following antibiotic exposure. Nat Microbiol 3:1255–1265. https://doi.org/10.1038/s41564-018-0257-9

175. Yassour M, Vatanen T, Siljander H, et al (2016) Natural history of the infant gut microbiome and impact of antibiotic treatment on bacterial strain diversity and stability. Sci Transl Med 8:. https://doi.org/10.1126/scitranslmed.aad0917

176. Lange K, Buerger M, Stallmach A, Bruns T (2016) Effects of Antibiotics on Gut Microbiota. Digestive Diseases 34:260–268. https://doi.org/10.1159/000443360

177. Maeda S, Hsu L-C, Liu H, et al (2005) *Nod2* Mutation in Crohn's Disease Potentiates NF-κB Activity and IL-1ß Processing. Science (1979) 307:734–738. https://doi.org/10.1126/science.1103685

178. Natividad JMM, Petit V, Huang X, et al (2012) Commensal and Probiotic Bacteria Influence Intestinal Barrier Function and Susceptibility to Colitis in Nod1−/−;Nod2−/− Mice. Inflamm Bowel Dis 18:1434–1446. https://doi.org/10.1002/ibd.22848

179. Kiesler P, Fuss IJ, Strober W (2015) Experimental Models of Inflammatory Bowel Diseases. Cell Mol Gastroenterol Hepatol 1:154–170. https://doi.org/10.1016/j.jcmgh.2015.01.006

180. Wu H-J, Wu E (2012) The role of gut microbiota in immune homeostasis and

autoimmunity. Gut Microbes 3:4–14. https://doi.org/10.4161/gmic.19320

181. Larsen N, Vogensen FK, van den Berg FWJ, et al (2010) Gut Microbiota in Human Adults with Type 2 Diabetes Differs from Non-Diabetic Adults. PLoS One 5:e9085. https://doi.org/10.1371/journal.pone.0009085

182. Zhang Z, Tian T, Chen Z, et al (2021) Characteristics of the gut microbiome in patients with prediabetes and type 2 diabetes. PeerJ 9:e10952. https://doi.org/10.7717/peerj.10952

183. Egshatyan L, Kashtanova D, Popenko A, et al (2016) Gut microbiota and diet in patients with different glucose tolerance. Endocr Connect 5:1–9. https://doi.org/10.1530/EC-15-0094

184. Craciun C-I, Neag M-A, Catinean A, et al (2022) The Relationships between Gut Microbiota and Diabetes Mellitus, and Treatments for Diabetes Mellitus. Biomedicines 10:308. https://doi.org/10.3390/biomedicines10020308

185. Minter MR, Zhang C, Leone V, et al (2016) Antibiotic-induced perturbations in gut microbial diversity influences neuro-inflammation and amyloidosis in a murine model of Alzheimer's disease. Sci Rep 6:30028. https://doi.org/10.1038/srep30028

186. Schwartz DJ, Langdon AE, Dantas G (2020) Understanding the impact of antibiotic perturbation on the human microbiome. Genome Med 12:82. https://doi.org/10.1186/s13073-020-00782-x

187. Magne F, Gotteland M, Gauthier L, et al (2020) The Firmicutes/Bacteroidetes Ratio: A Relevant Marker of Gut Dysbiosis in Obese Patients? Nutrients 12:1474. https://doi.org/10.3390/nu12051474

188. Forbes JD, Van Domselaar G, Bernstein CN (2016) The Gut Microbiota in

Immune-Mediated Inflammatory Diseases. Front Microbiol 7:. https://doi.org/10.3389/fmicb.2016.01081

189. Clayburgh DR, Shen L, Turner JR (2004) A porous defense: the leaky epithelial barrier in intestinal disease. Laboratory Investigation 84:282–291. https://doi.org/10.1038/labinvest.3700050

190. Luettig J, Rosenthal R, Barmeyer C, Schulzke JD (2015) Claudin-2 as a mediator of leaky gut barrier during intestinal inflammation. Tissue Barriers 3:1–2. https://doi.org/10.4161/21688370.2014.977176

191. Weber CR, Nalle SC, Tretiakova M, et al (2008) Claudin-1 and claudin-2 expression is elevated in inflammatory bowel disease and may contribute to early neoplastic transformation. Laboratory Investigation 88:1110–1120. https://doi.org/10.1038/labinvest.2008.78

192. Cherradi S, Martineau P, Gongora C, Del Rio M (2019) Claudin gene expression profiles and clinical value in colorectal tumors classified according to their molecular subtype. Cancer Manag Res Volume 11:1337–1348. https://doi.org/10.2147/CMAR.S188192

193. Lazar V, Ditu L-M, Pircalabioru GG, et al (2018) Aspects of Gut Microbiota and Immune System Interactions in Infectious Diseases, Immunopathology, and Cancer. Front Immunol 9:. https://doi.org/10.3389/fimmu.2018.01830

194. Richards AL, Muehlbauer AL, Alazizi A, et al (2019) Gut Microbiota Has a Widespread and Modifiable Effect on Host Gene Regulation. mSystems 4:. https://doi.org/10.1128/mSystems.00323-18

195. Zheng D, Liwinski T, Elinav E (2020) Interaction between microbiota and

immunity in health and disease. Cell Res 30:492–506. https://doi.org/10.1038/s41422-020-0332-7

196. van der Hee B, Wells JM (2021) Microbial Regulation of Host Physiology by Short-chain Fatty Acids. Trends Microbiol 29:700–712. https://doi.org/10.1016/j.tim.2021.02.001

197. Deleu S, Machiels K, Raes J, et al (2021) Short chain fatty acids and its producing organisms: An overlooked therapy for IBD? EBioMedicine 66:103293. https://doi.org/10.1016/j.ebiom.2021.103293

198. Morrison DJ, Preston T (2016) Formation of short chain fatty acids by the gut microbiota and their impact on human metabolism. Gut Microbes 7:189–200. https://doi.org/10.1080/19490976.2015.1134082

199. Morrison DJ, Preston T (2016) Formation of short chain fatty acids by the gut microbiota and their impact on human metabolism. Gut Microbes 7:. https://doi.org/10.1080/19490976.2015.1134082

200. Cho Y, Abu-Ali G, Tashiro H, et al (2018) The Microbiome Regulates Pulmonary Responses to Ozone in Mice. Am J Respir Cell Mol Biol 59:346–354. https://doi.org/10.1165/rcmb.2017-0404OC

201. Ochoa-Repáraz J, Mielcarz DW, Ditrio LE, et al (2009) Role of Gut Commensal Microflora in the Development of Experimental Autoimmune Encephalomyelitis. The Journal of Immunology 183:6041–6050. https://doi.org/10.4049/jimmunol.0900747

202. Jena PK, Sheng L, Liu H-X, et al (2017) Western Diet–Induced Dysbiosis in Farnesoid X Receptor Knockout Mice Causes Persistent Hepatic Inflammation

after Antibiotic Treatment. Am J Pathol 187:1800–1813. https://doi.org/10.1016/j.ajpath.2017.04.019

203. Nakamura YK, Metea C, Karstens L, et al (2016) Gut Microbial Alterations Associated With Protection From Autoimmune Uveitis. Investigative Opthalmology & Visual Science 57:3747. https://doi.org/10.1167/iovs.16-19733

204. Clayburgh DR, Shen L, Turner JR (2004) A porous defense: the leaky epithelial barrier in intestinal disease. Laboratory Investigation 84:282–291. https://doi.org/10.1038/labinvest.3700050

205. Luo L, Zhang S, Wang Y, et al (2014) Proinflammatory role of neutrophil extracellular traps in abdominal sepsis. American Journal of Physiology-Lung Cellular and Molecular Physiology 307:L586–L596. https://doi.org/10.1152/ajplung.00365.2013

206. Jainu M, Shyamala Devi CS (2005) Attenuation of neutrophil infiltration and proinflammatory cytokines by Cissus quadrangularis: a possible prevention against gastric ulcerogenesis. J Herb Pharmacother 5:33–42

207. Johansson MA, Saghafian-Hedengren S, Haileselassie Y, et al (2012) Early-Life Gut Bacteria Associate with IL-4−, IL-10− and IFN-γ Production at Two Years of Age. PLoS One 7:e49315. https://doi.org/10.1371/journal.pone.0049315

208. Hessle C, Andersson B, Wold AE (2000) Gram-Positive Bacteria Are Potent Inducers of Monocytic Interleukin-12 (IL-12) while Gram-Negative Bacteria Preferentially Stimulate IL-10 Production. Infect Immun 68:3581–3586. https://doi.org/10.1128/IAI.68.6.3581-3586.2000

209. Cohen-Poradosu R, McLoughlin RM, Lee JC, Kasper DL (2011) Bacteroides

fragilis–Stimulated Interleukin-10 Contains Expanding Disease. J Infect Dis 204:363–371. https://doi.org/10.1093/infdis/jir277

210. Qiu J, Villa M, Sanin DE, et al (2019) Acetate Promotes T Cell Effector Function during Glucose Restriction. Cell Rep 27:2063-2074.e5. https://doi.org/10.1016/j.celrep.2019.04.022

211. Siska PJ, Rathmell JC (2016) Metabolic Signaling Drives IFN-γ. Cell Metab 24:651–652. https://doi.org/10.1016/j.cmet.2016.10.018

212. Brown MA, Rad PY, Halonen MJ (2003) Method of birth alters interferon-gamma and interleukin-12 production by cord blood mononuclear cells. Pediatric Allergy and Immunology 14:106–111. https://doi.org/10.1034/j.1399-3038.2003.00015.x

213. Soliman ML, Puig KL, Combs CK, Rosenberger TA (2012) Acetate reduces microglia inflammatory signaling *in vitro*. J Neurochem 123:555–567. https://doi.org/10.1111/j.1471-4159.2012.07955.x

214. Soliman ML, Combs CK, Rosenberger TA (2013) Modulation of Inflammatory Cytokines and Mitogen-activated Protein Kinases by Acetate in Primary Astrocytes. Journal of Neuroimmune Pharmacology 8:287–300. https://doi.org/10.1007/s11481-012-9426-4

215. Lindenberg F, Krych L, Fielden J, et al (2019) Expression of immune regulatory genes correlate with the abundance of specific Clostridiales and Verrucomicrobia species in the equine ileum and cecum. Sci Rep 9:12674. https://doi.org/10.1038/s41598-019-49081-5

216. Qi H, Gao Y, Li Y, et al (2019) Induction of Inflammatory Macrophages in the Gut and Extra-Gut Tissues by Colitis-Mediated Escherichia coli. iScience 21:474–489.

https://doi.org/10.1016/j.isci.2019.10.046

217. Jones-Hall YL, Nakatsu CH (2016) The Intersection of TNF, IBD and the Microbiome. Gut Microbes 7:58–62. https://doi.org/10.1080/19490976.2015.1121364

218. Holzheimer RG (2001) Antibiotic induced endotoxin release and clinical sepsis: a review. J Chemother 13 Spec No 1:159–72. https://doi.org/10.1179/joc.2001.13.Supplement-2.159

219. Kaplan GG, Ng SC (2017) Understanding and Preventing the Global Increase of Inflammatory Bowel Disease. Gastroenterology 152:313-321.e2. https://doi.org/10.1053/j.gastro.2016.10.020

220. Ng SC, Kaplan G, Banerjee R, et al (2016) 78 Incidence and Phenotype of Inflammatory Bowel Disease From 13 Countries in Asia-Pacific: Results From the Asia-Pacific Crohn's and Colitis Epidemiologic Study 2011-2013. Gastroenterology 150:S21. https://doi.org/10.1016/S0016-5085(16)30195-0

221. Alatab S, Sepanlou SG, Ikuta K, et al (2020) The global, regional, and national burden of inflammatory bowel disease in 195 countries and territories, 1990–2017: a systematic analysis for the Global Burden of Disease Study 2017. Lancet Gastroenterol Hepatol 5:17–30. https://doi.org/10.1016/S2468-1253(19)30333-4

222. Singh P, Ananthakrishnan A, Ahuja V (2017) Pivot to Asia: inflammatory bowel disease burden. Intest Res 15:138. https://doi.org/10.5217/ir.2017.15.1.138

223. Kumar M, Garand M, Al Khodor S (2019) Integrating omics for a better understanding of Inflammatory Bowel Disease: a step towards personalized medicine. J Transl Med 17:419. https://doi.org/10.1186/s12967-019-02174-1

224. Melgar S, Karlsson A, Michaëlsson E (2005) Acute colitis induced by dextran sulfate sodium progresses to chronicity in C57BL/6 but not in BALB/c mice: Correlation between symptoms and inflammation. Am J Physiol Gastrointest Liver Physiol 288:1328–1338. https://doi.org/10.1152/ajpgi.00467.2004

225. Okayasu I, Hatakeyama S, Yamada M, et al (1990) A novel method in the induction of reliable experimental acute and chronic ulcerative colitis in mice. Gastroenterology 98:694–702. https://doi.org/10.1016/0016-5085(90)90290-H

226. Chassaing B, Aitken JD, Malleshappa M, Vijay-Kumar M (2015) DSS Protocol. Curr Protoc Immunol 27:1–19. https://doi.org/10.1037/a0032811.Child

227. Wirtz S, Popp V, Kindermann M, et al (2017) Chemically induced mouse models of acute and chronic intestinal inflammation. Nat Protoc 12:1295–1309. https://doi.org/10.1038/nprot.2017.044

228. Dieleman LA, Palmen MJHJ, Akol H, et al (1998) Chronic experimental colitis induced by dextran sulphate sodium (DSS) is characterized by Th1 and Th2 cytokines. Clin Exp Immunol 114:385–391. https://doi.org/10.1046/j.1365-2249.1998.00728.x

229. Tsuchiya T, Fukuda S, Hamada H, et al (2003) Role of γδT Cells in the Inflammatory Response of Experimental Colitis Mice. The Journal of Immunology 171:5507–5513. https://doi.org/10.4049/jimmunol.171.10.5507

230. El-Zayat SR, Sibaii H, Mannaa FA (2019) Toll-like receptors activation, signaling, and targeting: an overview. Bull Natl Res Cent 43:187. https://doi.org/10.1186/s42269-019-0227-2

231. Pandey S, Singh S, Anang V, et al (2015) Pattern Recognition Receptors in Cancer

Progression and Metastasis. Cancer Growth Metastasis 8:CGM.S24314. https://doi.org/10.4137/CGM.S24314

232. Yan Y, Kolachala V, Dalmasso G, et al (2009) Temporal and spatial analysis of clinical and molecular parameters in dextran sodium sulfate induced colitis. PLoS One 4:8. https://doi.org/10.1371/journal.pone.0006073

233. Lacy P, Stow JL (2011) Cytokine release from innate immune cells: association with diverse membrane trafficking pathways. Blood 118:9–18. https://doi.org/10.1182/blood-2010-08-265892

234. Sproston NR, Ashworth JJ (2018) Role of C-reactive protein at sites of inflammation and infection. Front Immunol 9:1–11. https://doi.org/10.3389/fimmu.2018.00754

235. Clos TW Du, Clos TW Du (2018) Function of C-reactive protein Function of C-reactive protein. Ann Med 2000; 32: 274-278 3890:274–278. https://doi.org/10.3109/07853890009011772

236. Chelakkot C, Ghim J, Ryu SH (2018) Mechanisms regulating intestinal barrier integrity and its pathological implications. Exp Mol Med 50:1–9. https://doi.org/10.1038/s12276-018-0126-x

237. Weber CR, Nalle SC, Tretiakova M, et al (2008) Claudin-1 and claudin-2 expression is elevated in inflammatory bowel disease and may contribute to early neoplastic transformation. Laboratory Investigation 88:1110–1120. https://doi.org/10.1038/labinvest.2008.78

238. Guo S, Al-Sadi R, Said HM, Ma TY (2013) Lipopolysaccharide Causes an Increase in Intestinal Tight Junction Permeability in Vitro and in Vivo by Inducing

Enterocyte Membrane Expression and Localization of TLR-4 and CD14. Am J Pathol 182:375–387. https://doi.org/10.1016/j.ajpath.2012.10.014

239. Pizzorno J (2014) Toxins From the Gut. Integr Med (Encinitas) 13:8–11

240. Stallhofer J, Friedrich M, Konrad-Zerna A, et al (2015) Lipocalin-2 Is a Disease Activity Marker in Inflammatory Bowel Disease Regulated by IL-17A, IL-22, and TNF-α and Modulated by IL23R Genotype Status. Inflamm Bowel Dis 1. https://doi.org/10.1097/MIB.0000000000000515

241. Thorsvik S, Damås JK, Granlund A vB, et al (2017) Fecal neutrophil gelatinase-associated lipocalin as a biomarker for inflammatory bowel disease. J Gastroenterol Hepatol 32:128–135. https://doi.org/10.1111/jgh.13598

242. Rojo ÓP, San Román AL, Arbizu EA, et al (2007) Serum lipopolysaccharide-binding protein in endotoxemic patients with inflammatory bowel disease. Inflamm Bowel Dis 13:269–277. https://doi.org/10.1002/ibd.20019

243. Huang X, Fang S, Yang H, et al (2017) Evaluating the contribution of gut microbiome to the variance of porcine serum glucose and lipid concentration. Sci Rep 7:14928. https://doi.org/10.1038/s41598-017-15044-x

244. Mohamed FF, Hady MM, Kamel NF, Ragaa NM (2020) The impact of exogenous dietary nucleotides in ameliorating Clostridium perfringens infection and improving intestinal barriers gene expression in broiler chicken. Vet Anim Sci 10:100130. https://doi.org/10.1016/j.vas.2020.100130

245. Flint HJ, Scott KP, Duncan SH, et al (2012) Microbial degradation of complex carbohydrates in the gut. Gut Microbes 3:289–306. https://doi.org/10.4161/gmic.19897

246. Eichele DD, Kharbanda KK (2017) Dextran sodium sulfate colitis murine model: An indispensable tool for advancing our understanding of inflammatory bowel diseases pathogenesis. World J Gastroenterol 23:6016–6029. https://doi.org/10.3748/wjg.v23.i33.6016

247. Toyonaga T, Matsuura M, Mori K, et al (2016) Lipocalin 2 prevents intestinal inflammation by enhancing phagocytic bacterial clearance in macrophages. Sci Rep 6:1–13. https://doi.org/10.1038/srep35014

248. Masoodi I, Tijjani BM, Wani H, et al (2011) Biomarkers in the management of ulcerative colitis: A brief review. GMS German Medical Science 9:1–7. https://doi.org/10.3205/000126

249. Pallone F, Monteleone G (1998) Interleukin 12 and Th1 responses in inflammatory bowel disease. Gut 43:735–736. https://doi.org/10.1136/gut.43.6.735

250. Muzes G, Molnár B, Tulassay Z, Sipos F (2012) Changes of the cytokine profile in inflammatory bowel diseases. World J Gastroenterol 18:5848–5861. https://doi.org/10.3748/wjg.v18.i41.5848

251. Fuss IJ (2008) Is the Th1/Th2 paradigm of immune regulation applicable to IBD? Inflamm Bowel Dis 14:S110–S112. https://doi.org/10.1002/ibd.20683

252. Sanchez-Muñoz F, Dominguez-Lopez A, Yamamoto-Furusho JK (2008) Role of cytokines in inflammatory bowel disease. World J Gastroenterol 14:4280–4288. https://doi.org/10.3748/wjg.14.4280

253. Ito R, Kita M, Shin-Ya M, et al (2008) Involvement of IL-17A in the pathogenesis of DSS-induced colitis in mice. Biochem Biophys Res Commun 377:12–16. https://doi.org/10.1016/j.bbrc.2008.09.019

254. Kim JM (2014) Antimicrobial Proteins in Intestine and Inflammatory Bowel Diseases. Intest Res 12:20. https://doi.org/10.5217/ir.2014.12.1.20

255. Zharkova MS, Orlov DS, Golubeva OYu, et al (2019) Application of Antimicrobial Peptides of the Innate Immune System in Combination With Conventional Antibiotics—A Novel Way to Combat Antibiotic Resistance? Front Cell Infect Microbiol 9:. https://doi.org/10.3389/fcimb.2019.00128

256. Lu F, Inoue K, Kato J, et al (2019) Functions and regulation of lipocalin-2 in gut-origin sepsis: A narrative review. Crit Care 23:1–8. https://doi.org/10.1186/s13054-019-2550-2

257. Davenport M, Poles J, Leung JM, et al (2014) Metabolic Alterations to the Mucosal Microbiota in Inflammatory Bowel Disease. Inflamm Bowel Dis 20:723–731. https://doi.org/10.1097/MIB.0000000000000011

258. Sugimoto K, Ogawa A, Mizoguchi E, et al (2008) IL-22 ameliorates intestinal inflammation in a mouse model of ulcerative colitis. Journal of Clinical Investigation. https://doi.org/10.1172/JCI33194

259. Hainzl E, Stockinger S, Rauch I, et al (2015) Intestinal Epithelial Cell Tyrosine Kinase 2 Transduces IL-22 Signals To Protect from Acute Colitis. The Journal of Immunology 195:5011–5024. https://doi.org/10.4049/jimmunol.1402565

260. Yang Y, Jobin C (2014) Microbial imbalance and intestinal pathologies: connections and contributions. Dis Model Mech 7:1131–1142. https://doi.org/10.1242/dmm.016428

261. Grimble GK (1994) Dietary nucleotides and gut mucosal defence. Gut 35:S46-51. https://doi.org/10.1136/gut.35.1_suppl.s46

262. Le Floc'h N, Melchior D, Obled C (2004) Modifications of protein and amino acid metabolism during inflammation and immune system activation. Livest Prod Sci 87:37–45. https://doi.org/10.1016/j.livprodsci.2003.09.005

263. Oliphant K, Allen-Vercoe E (2019) Macronutrient metabolism by the human gut microbiome: major fermentation by-products and their impact on host health. Microbiome 7:91. https://doi.org/10.1186/s40168-019-0704-8

264. Moon CD, Young W, Maclean PH, et al (2018) Metagenomic insights into the roles of Proteobacteria in the gastrointestinal microbiomes of healthy dogs and cats. Microbiologyopen 7:e00677. https://doi.org/10.1002/mbo3.677

265. Stark RM, Suleiman MS, Hassan IJ, et al (1997) Amino acid utilisation and deamination of glutamine and asparagine by Helicobacter pylori. J Med Microbiol 46:793–800. https://doi.org/10.1099/00222615-46-9-793

266. Pan L, Han P, Ma S, et al (2020) Abnormal metabolism of gut microbiota reveals the possible molecular mechanism of nephropathy induced by hyperuricemia. Acta Pharm Sin B 10:249–261. https://doi.org/10.1016/j.apsb.2019.10.007

267. Xu L (2004) Effect of glutamate on inflammatory responses of intestine and brain after focal cerebral ischemia. World J Gastroenterol 11:. https://doi.org/10.3748/wjg.v11.i5.733

268. Rindflesch TC, Blake CL, Cairelli MJ, et al (2018) Investigating the role of interleukin-1 beta and glutamate in inflammatory bowel disease and epilepsy using discovery browsing. J Biomed Semantics 9:. https://doi.org/10.1186/s13326-018-0192-y

269. Hove H, Mortensen PB (1995) Influence of intestinal inflammation (IBD) and

small and large bowel length on fecal short-chain fatty acids and lactate. Dig Dis Sci 40:. https://doi.org/10.1007/BF02065554

270. Naseer M, Gandhi J, Chams N, Kulairi Z (2017) Stercoral colitis complicated with ischemic colitis: a double-edge sword. BMC Gastroenterol 17:. https://doi.org/10.1186/s12876-017-0686-6

271. Vernia P, Caprilli R, Latella G, et al (1988) Fecal Lactate and Ulcerative Colitis. Gastroenterology 95:. https://doi.org/10.1016/S0016-5085(88)80078-7

272. Segain J-P (2000) Butyrate inhibits inflammatory responses through NFkappa B inhibition: implications for Crohn's disease. Gut 47:. https://doi.org/10.1136/gut.47.3.397

273. Geirnaert A, Calatayud M, Grootaert C, et al (2017) Butyrate-producing bacteria supplemented in vitro to Crohn's disease patient microbiota increased butyrate production and enhanced intestinal epithelial barrier integrity. Sci Rep 7:. https://doi.org/10.1038/s41598-017-11734-8

274. Zhang M, Zhou Q, Dorfman RG, et al (2016) Butyrate inhibits interleukin-17 and generates Tregs to ameliorate colorectal colitis in rats. BMC Gastroenterol 16:. https://doi.org/10.1186/s12876-016-0500-x

275. Pryde SE, Duncan SH, Hold GL, et al (2002) The microbiology of butyrate formation in the human colon. FEMS Microbiol Lett 217:. https://doi.org/10.1111/j.1574-6968.2002.tb11467.x

276. Vital M, Howe AC, Tiedje JM (2014) Revealing the Bacterial Butyrate Synthesis Pathways by Analyzing (Meta)genomic Data. mBio 5:. https://doi.org/10.1128/mBio.00889-14

277. Kidd P (2003) Th1 / Th2 Balance Th1/Th2 Balance: The Hypothesis, its Limitations, and Implications for Health and Disease

278. Van Eden W, Van der Zee R, Van Kooten P, et al (2002) Balancing the immune system: Th1 and Th2. In: Annals of the Rheumatic Diseases

279. Baj A, Moro E, Bistoletti M, et al (2019) Glutamatergic signaling along the microbiota-gut-brain axis. Int J Mol Sci 20

280. Luo Y, Zeng B, Zeng L, et al (2018) Gut microbiota regulates mouse behaviors through glucocorticoid receptor pathway genes in the hippocampus. Transl Psychiatry 8:. https://doi.org/10.1038/s41398-018-0240-5

281. Foster JA, Rinaman L, Cryan JF (2017) Stress & the gut-brain axis: Regulation by the microbiome. Neurobiol Stress 7:. https://doi.org/10.1016/j.ynstr.2017.03.001

282. Luczynski P, McVey Neufeld K-A, Oriach CS, et al (2016) Growing up in a Bubble: Using Germ-Free Animals to Assess the Influence of the Gut Microbiota on Brain and Behavior. International Journal of Neuropsychopharmacology 19:. https://doi.org/10.1093/ijnp/pyw020

283. Mazzoli R, Pessione E (2016) The neuro-endocrinological role of microbial glutamate and GABA signaling. Front Microbiol 7

284. Houtepen LC, Schür RR, Wijnen JP, et al (2017) Acute stress effects on GABA and glutamate levels in the prefrontal cortex: A 7T 1 H magnetic resonance spectroscopy study. Neuroimage Clin 14:. https://doi.org/10.1016/j.nicl.2017.01.001

285. Musazzi L, Treccani G, Popoli M (2015) Functional and Structural Remodeling of

References

Glutamate Synapses in Prefrontal and Frontal Cortex Induced by Behavioral Stress. Front Psychiatry 6:. https://doi.org/10.3389/fpsyt.2015.00060

286. Levy BH, Tasker JG (2012) Synaptic regulation of the hypothalamic–pituitary–adrenal axis and its modulation by glucocorticoids and stress. Front Cell Neurosci 6:. https://doi.org/10.3389/fncel.2012.00024

287. Zelena D, Mergl Z, Makara GB (2005) Glutamate agonists activate the hypothalamic–pituitary–adrenal axis through hypothalamic paraventricular nucleus but not through vasopressinerg neurons. Brain Res 1031:. https://doi.org/10.1016/j.brainres.2004.10.034

288. Vanuytsel T, van Wanrooy S, Vanheel H, et al (2014) Psychological stress and corticotropin-releasing hormone increase intestinal permeability in humans by a mast cell-dependent mechanism. Gut 63:. https://doi.org/10.1136/gutjnl-2013-305690

289. Larauche M, Kiank C, Tache Y (2009) Corticotropin releasing factor signaling in colon and ileum: regulation by stress and pathophysiological implications. J Physiol Pharmacol 60 Suppl 7:

290. Sun Y, Li L, Xie R, et al (2019) Stress Triggers Flare of Inflammatory Bowel Disease in Children and Adults. Front Pediatr 7:. https://doi.org/10.3389/fped.2019.00432

291. F. Ahmed NAK (2019) Managing the F:B Ratio in DM; A Review of the Roleof Firmicutes and Bacteroidetes in Diabetes Mellitus. Adv Complement Altern Med 4:295–298

292. Ried K, Travica N, Sali A (2018) The Effect of Kyolic Aged Garlic Extract on Gut

Microbiota, Inflammation, and Cardiovascular Markers in Hypertensives: The GarGIC Trial. Front Nutr 5:. https://doi.org/10.3389/fnut.2018.00122

293. Fransen F, Zagato E, Mazzini E, et al (2015) BALB/c and C57BL/6 Mice Differ in Polyreactive IgA Abundance, which Impacts the Generation of Antigen-Specific IgA and Microbiota Diversity. Immunity 43:527–540. https://doi.org/10.1016/j.immuni.2015.08.011

294. Louis P, Flint HJ (2017) Formation of propionate and butyrate by the human colonic microbiota. Environ Microbiol 19:29–41. https://doi.org/10.1111/1462-2920.13589

295. Mirzaei R, Bouzari B, Hosseini-Fard SR, et al (2021) Role of microbiota-derived short-chain fatty acids in nervous system disorders. Biomedicine & Pharmacotherapy 139:111661. https://doi.org/10.1016/j.biopha.2021.111661

296. Van den Abbeele P, Ghyselinck J, Marzorati M, et al (2022) The Effect of Amino Acids on Production of SCFA and bCFA by Members of the Porcine Colonic Microbiota. Microorganisms 10:762. https://doi.org/10.3390/microorganisms10040762

297. Varghese FP, Brown ES (2001) The Hypothalamic-Pituitary-Adrenal Axis in Major Depressive Disorder: A Brief Primer for Primary Care Physicians. Prim Care Companion J Clin Psychiatry 3:. https://doi.org/10.4088/pcc.v03n0401

298. Fukudo S (2007) Role of corticotropin-releasing hormone in irritable bowel syndrome and intestinal inflammation. J Gastroenterol 42:. https://doi.org/10.1007/s00535-006-1942-7

299. EVANSON NK, HERMAN JP (2015) Role of Paraventricular Nucleus Glutamate

Signaling in Regulation of HPA Axis Stress Responses. Interdiscip Inf Sci 21:. https://doi.org/10.4036/iis.2015.B.10

300. Wittmann G, Lechan RM, Liposits Z, Fekete C (2005) Glutamatergic innervation of corticotropin-releasing hormone- and thyrotropin-releasing hormone-synthesizing neurons in the hypothalamic paraventricular nucleus of the rat. Brain Res 1039:. https://doi.org/10.1016/j.brainres.2005.01.090

301. Clarke G, Grenham S, Scully P, et al (2013) The microbiome-gut-brain axis during early life regulates the hippocampal serotonergic system in a sex-dependent manner. Mol Psychiatry 18:666–673. https://doi.org/10.1038/mp.2012.77

302. Uren Webster TM, Rodriguez-Barreto D, Consuegra S, Garcia de Leaniz C (2020) Cortisol-Related Signatures of Stress in the Fish Microbiome. Front Microbiol 11:. https://doi.org/10.3389/fmicb.2020.01621

303. Fukudo S, Nomura T, Hongo M (1998) Impact of corticotropin-releasing hormone on gastrointestinal motility and adrenocorticotropic hormone in normal controls and patients with irritable bowel syndrome. Gut 42:. https://doi.org/10.1136/gut.42.6.845

304. Foster JA, Rinaman L, Cryan JF (2017) Stress & the gut-brain axis: Regulation by the microbiome. Neurobiol Stress 7:. https://doi.org/10.1016/j.ynstr.2017.03.001

305. Lefebvre H, Thomas M, Duparc C, et al (2016) Role of ACTH in the Interactive/Paracrine Regulation of Adrenal Steroid Secretion in Physiological and Pathophysiological Conditions. Front Endocrinol (Lausanne) 7:. https://doi.org/10.3389/fendo.2016.00098

306. Nandam LS, Brazel M, Zhou M, Jhaveri DJ (2019) Cortisol and Major Depressive Disorder-Translating Findings From Humans to Animal Models and Back. Front Psychiatry 10:. https://doi.org/10.3389/fpsyt.2019.00974

307. Schroeder A, Notaras M, Du X, Hill R (2018) On the Developmental Timing of Stress: Delineating Sex-Specific Effects of Stress across Development on Adult Behavior. Brain Sci 8:. https://doi.org/10.3390/brainsci8070121

308. Jang H-M, Lee K-E, Lee H-J, Kim D-H (2018) Immobilization stress-induced Escherichia coli causes anxiety by inducing NF-κB activation through gut microbiota disturbance. Sci Rep 8:. https://doi.org/10.1038/s41598-018-31764-0

309. Park AJ, Collins J, Blennerhassett PA, et al (2013) Altered colonic function and microbiota profile in a mouse model of chronic depression. Neurogastroenterology & Motility 25:. https://doi.org/10.1111/nmo.12153

310. Soto M, Herzog C, Pacheco JA, et al (2018) Gut microbiota modulate neurobehavior through changes in brain insulin sensitivity and metabolism. Mol Psychiatry 23:. https://doi.org/10.1038/s41380-018-0086-5

311. Khan I, Ullah N, Zha L, et al (2019) Alteration of Gut Microbiota in Inflammatory Bowel Disease (IBD): Cause or Consequence? IBD Treatment Targeting the Gut Microbiome. Pathogens 8:. https://doi.org/10.3390/pathogens8030126

312. Forbes JD, Van Domselaar G, Bernstein CN (2016) The Gut Microbiota in Immune-Mediated Inflammatory Diseases. Front Microbiol 7:. https://doi.org/10.3389/fmicb.2016.01081

313. Zeng MY, Inohara N, Nuñez G (2017) Mechanisms of inflammation-driven bacterial dysbiosis in the gut. Mucosal Immunol 10:.

https://doi.org/10.1038/mi.2016.75

314. Gutzeit C, Magri G, Cerutti A (2014) Intestinal IgA production and its role in host-microbe interaction. Immunol Rev 260:. https://doi.org/10.1111/imr.12189

315. Cao AT, Yao S, Gong B, et al (2012) Th17 Cells Upregulate Polymeric Ig Receptor and Intestinal IgA and Contribute to Intestinal Homeostasis. The Journal of Immunology 189:4666–4673. https://doi.org/10.4049/jimmunol.1200955

316. Fransen F, Zagato E, Mazzini E, et al (2015) BALB/c and C57BL/6 Mice Differ in Polyreactive IgA Abundance, which Impacts the Generation of Antigen-Specific IgA and Microbiota Diversity. Immunity 43:. https://doi.org/10.1016/j.immuni.2015.08.011

317. Segerstrom SC, Miller GE (2004) Psychological Stress and the Human Immune System: A Meta-Analytic Study of 30 Years of Inquiry. Psychol Bull 130:601–630. https://doi.org/10.1037/0033-2909.130.4.601

318. Slavich GM, Irwin MR (2014) From stress to inflammation and major depressive disorder: A social signal transduction theory of depression. Psychol Bull 140:774–815. https://doi.org/10.1037/a0035302

319. Furman D, Campisi J, Verdin E, et al (2019) Chronic inflammation in the etiology of disease across the life span. Nat Med 25:1822–1832. https://doi.org/10.1038/s41591-019-0675-0

320. Nitzan O (2016) Role of antibiotics for treatment of inflammatory bowel disease. World J Gastroenterol 22:1078. https://doi.org/10.3748/wjg.v22.i3.1078

321. Ledder O (2019) Antibiotics in inflammatory bowel diseases: do we know what we're doing? Transl Pediatr 8:42–55. https://doi.org/10.21037/tp.2018.11.02

322. Carter MJ (2004) Guidelines for the management of inflammatory bowel disease in adults. Gut 53:v1–v16. https://doi.org/10.1136/gut.2004.043372

323. Mark-Christensen A, Lange A, Erichsen R, et al (2022) Early-Life Exposure to Antibiotics and Risk for Crohn's Disease: A Nationwide Danish Birth Cohort Study. Inflamm Bowel Dis 28:415–422. https://doi.org/10.1093/ibd/izab085

324. Agrawal M, Sabino J, Frias-Gomes C, et al (2021) Early life exposures and the risk of inflammatory bowel disease: Systematic review and meta-analyses. EClinicalMedicine 36:100884. https://doi.org/10.1016/j.eclinm.2021.100884

325. Faye AS, Allin KH, Iversen AT, et al (2023) Antibiotic use as a risk factor for inflammatory bowel disease across the ages: a population-based cohort study. Gut 72:663–670. https://doi.org/10.1136/gutjnl-2022-327845

326. Watanabe H, Numata K, Ito T, et al (2004) INNATE IMMUNE RESPONSE IN TH1- AND TH2-DOMINANT MOUSE STRAINS. Shock 22:460–466. https://doi.org/10.1097/01.shk.0000142249.08135.e9

327. Mills CD, Kincaid K, Alt JM, et al (2000) M-1/M-2 macrophages and the Th1/Th2 paradigm. J Immunol 164:6166–73. https://doi.org/10.4049/jimmunol.164.12.6166

328. Oliphant K, Allen-Vercoe E (2019) Macronutrient metabolism by the human gut microbiome: major fermentation by-products and their impact on host health. Microbiome 7:. https://doi.org/10.1186/s40168-019-0704-8

Appendix

9. Appendix
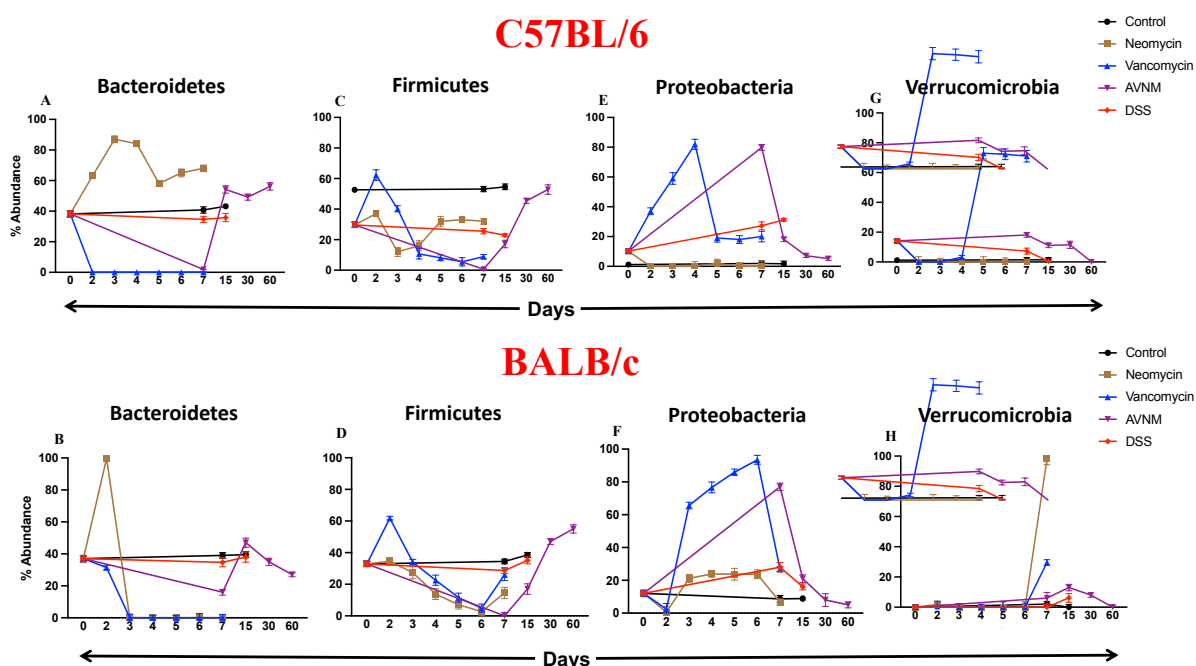
Fig. S1: Effect of different perturbing agents on gut microbial composition at phylum level.

Kinetics of gut microbial changes of C57BL/6 and BALB/c mice followed by different antibiotics and chemical treatment at different time scales. Alteration in the phylum level composition of C57BL/6 and BALB/c mice in control condition and followed by various treatment is depicted here. (A, B) represents the changes in Bacteroidetes phylum, (C, D), in Firmicutes phylum, (E, f), in Proteobacteria and (G, H), in Verrucomicrobia phylum followed by different treatment conditions in both strains. To avoid the clutter in the figure a detailed statistical analysis considering time x treatment x genotype is mentioned in the separate table and is available in the following link https://github.com/sohinitista/Thesis_data/tree/383ab4c76009e568c8a2ba5314799e1a276942d1

Spearman (r²)	Phenylethyl amine	Beta-Alanine	Putrescine	Cadaverine	L-Alanine	Phenylacetic Acid	4-Hydroxyphenylacetic Acid	Glyceric acid	Phenylalanine	5ß-Coprostanol	Nicotinic acid	3-Methyladipic Acid	Hydrocinnamic Acid	3-Hydroxybutyric acid	Pantothenic Acid	Citrate	Methylamine	2-hydroxy-3-methylvalerate
Oscillospira eae	0.21762225	0.24990001	0.30305025	0.30239001	0.04247721	0.02042041	0.04963984	0.07284601	0.02480625	0.46936201	0.13344009	0.42562576	0.22344529	0.11471769	0.05546025	0.46090521	0.46771921	0.42003361
Bacteroides denticanum	0.18905104	0.24681024	0.12103441	0.08311689	0.08208225	0.03268864	0.04084441	0.01855044	0.03045025	0.15015625	0.09308601	0.0529	0.13734436	0.05022081	0.07458361	0.16232841	0.175561	0.21855625
Oscillospira guilliermondii	0.18974736	0.241081	0.24512401	0.27594009	0.070756	0.00558906	0.03984016	0.06170256	0.017424	0.34503876	0.12201049	0.28430224	0.15649936	0.04210704	0.04892944	0.33200644	0.35856144	0.35390601
Rikenella microfusus	0.15264649	0.18258529	0.13601344	0.26790976	0.01132096	0.02140369	0.12666481	0.10725625	0.02050624	0.349281	0.06848689	0.19633761	0.147456	0.12489156	0.01375929	0.20097289	0.28643904	0.19598329
Bacteroides uniformis	0.10969344	0.17438976	0.09247681	0.20187049	0.15241216	0.02414916	0.01814409	0.01912689	0.07091569	0.09504889	0.12327121	0.01763584	0.020164	0.00418868	0.06702921	0.12166144	0.21818241	0.04447881
Desulfonauticus autotrophicus	0.20286016	0.173056	0.37356544	0.35319249	0.01454436	0.03709476	0.05631129	0.04661281	0.02105401	0.52027369	0.13147876	0.43230625	0.28890625	0.13601344	0.07485696	0.50794129	0.44796249	0.33246756
Parabacteroides merdae	0.11458225	0.16621929	0.05349969	0.06295081	0.00151399	0.00625997	0.02152089	0.00419515	0.05442889	0.11323225	0.042436	0.03740356	0.03904576	0.04418404	0.02979076	0.10804369	0.11526025	0.11142244
Dysgonomonas wimpennyi	0.13749264	0.15499969	0.16638241	0.09265936	0.068644	0.0007958	0.01338649	0.09102289	0.09036036	0.217156	0.17682025	0.11242609	0.25060036	0.19412836	0.07112889	0.25260676	0.13920361	0.19061956
Parabacteroides goldsteinii	0.15912121	0.15452761	0.06036849	0.06692569	0.07918596	0.00393756	0.062001	0.01863225	0.11042329	0.121104	0.038809	0.07317025	0.06666724	0.15077689	0.03218436	0.17673616	0.19079424	0.12895281
Faecalibacterium prausnitzii	0.38763076	0.15171025	0.226576	0.21893041	0.16281225	0.02802276	0.03779136	0.04490161	0.022601	0.21631801	0.29246464	0.11276164	0.16032016	0.08105409	0.21224449	0.23794884	0.190969	0.21086464
Bacteroides dorei	0.09891025	0.14417209	0.09803161	0.104976	0.04255969	0.01140624	0.03200521	0.04044121	0.06780816	0.14085009	0.10278436	0.05817744	0.01317904	0.07311616	0.12595401	0.22316176	0.18207289	0.173889
Ruminococcus albus	0.13417569	0.14280841	0.22024249	0.18241441	0.04549689	0.00171644	0.03286969	0.076729	0.089401	0.25280784	0.09728161	0.24117921	0.14243076	0.15872256	0.04888521	0.25623844	0.17901361	0.11607649
Bacteroides rodentium	0.11128896	0.13942756	0.05841889	0.13593969	0.141376	0.02387025	0.00676671	0.01630729	0.05745609	0.07177041	0.08202496	0.00631071	0.01423249	0.00646416	0.04198401	0.07317025	0.15800625	0.02226064
Turicibacter sanguinis	0.10903204	0.13830961	0.12362256	0.06528025	0.01974025	0.00912407	0.011664	0.01625625	0.03374569	0.07447441	0.08479744	0.04372281	0.06817321	0.0019027	0.14025025	0.15202201	0.09865881	0.05678689
Lachnospira pectinoschiza	0.137641	0.13801225	0.126736	0.22771984	0.02418025	0.01968409	0.04372281	0.00047786	0.00811441	0.12802084	0.10169721	0.15069924	0.10131489	0.08386816	0.12257001	0.133225	0.09778129	0.12215025
Anaerobranca zavarzinii	0.18550249	0.11377129	0.23980609	0.15046641	0.02117025	0.00594749	0.068121	0.01530169	0.00934509	0.39803481	0.15178816	0.29724304	0.16418704	0.15824484	0.06906384	0.30338064	0.29669809	0.29084449
Bacteroides cellulosilyticus	0.17572864	0.109561	0.083521	0.18826921	0.02585664	0.00053315	0.05745609	0.04064256	0.0041435	0.06728836	0.079524	0.089401	0.01279161	0.02630884	0.06677056	0.08473921	0.11029041	0.10208025
Parabacteroides johnsonii	0.26173456	0.09891025	0.05171076	0.104329	0.02862864	1.1016E-05	0.04165681	0.02169729	0.03225616	0.15031129	0.02879809	0.05368489	0.0361	0.08202496	0.01420864	0.13380964	0.163216	0.11587216
Parabacteroides distasonis	0.12061729	0.08579041	0.06041764	0.08916196	0.17606416	0.01871424	0.06115729	0.12559936	0.01168561	0.11269449	0.22714756	0.05900041	0.07160976	0.02111209	0.01256641	0.11723776	0.09259849	0.05161984
Sphingobacterium bambusae	0.11128896	0.07529536	0.03450721	0.10074276	0.00361441	0.00071022	0.00039402	0.00096803	0.13950225	0.02140369	0.13741849	0.03179089	0.04507129	0.02262016	0.13242321	0.10705984	0.189225
Sphingobacterium shayense	0.06937956	0.06315169	0.028561	0.04910656	0.14791716	0.01860496	0.04695889	0.09418761	0.02079364	0.05489649	0.14861025	0.02732409	0.03682561	0.01113025	0.00880219	0.06843456	0.04831204	0.02563201
Limnobacter litoralis	0.01517824	0.04566769	0.02298256	0.06007401	0.00260712	0.00760384	0.04515625	0.07969329	0.04137156	0.01147041	0.06661561	0.05139289	0.03179089	0.00363488	0.05885476	0.07739524	0.09381969	0.06017209
Alkaliphilus crotonatoxidans	0.07431076	0.042025	0.17850625	0.142129	0.00707113	0.00147994	0.01677025	0.05044516	0.027889	0.28026436	0.08398404	0.23609881	0.09966649	0.15093225	0.08720209	0.27269284	0.252004	0.14311089
Bifidobacterium longum	0.09641025	0.04133089	0.09721924	0.034969	0.04605316	1.8284E-05	0.00318547	0.02019241	0.00816493	0.09443329	0.07322436	0.038809	0.07263025	0.04881129	0.02951524	0.09418761	0.142884	0.10778089
Prevotella copri	0.10725625	0.03944196	0.11042329	0.05929225	0.09156676	0.06806881	0.0324	0.06360484	0.08213956	0.10182481	0.133956	0.05692996	0.09308601	0.10530025	0.10575504	0.17698849	0.041616	0.038025
Bacteroides graminisolvens	0.05631129	0.03857296	0.00149305	0.03721041	0.18619225	0.10478169	0.0012752	0.02576025	0.03052009	0.01750329	0.06677056	0.00140625	0.00037791	0.01054729	0.02663424	0.02576025	0.02030625	0.04003609
Bacteroides caccae	0.11999296	0.03613801	0.045796	0.10699441	0.02208196	0.00916423	0.02217121	0.02832489	0.00094004	0.09703225	0.09828225	0.04264225	0.07879249	0.049729	0.01500625	0.08334769	0.09941409	0.08254129
Bifidobacterium adolescentis	0.15327225	0.03337929	0.10719076	0.10478169	0.08386816	0.00572229	0.00074161	0.07112889	0.02064969	0.06195121	0.25310961	0.15163236	0.17147881	0.066049	0.06661561	0.10036224	0.09449476	0.13786369
Bacteroides stercorisoris	0.07171684	0.02515396	0.03873024	0.19855936	0.01034289	0.00017876	0.00855995	0.00663573	0.01890625	0.061009	0.123904	0.03115525	0.03988009	0.05134756	0.07198489	0.08732025	0.07862416	0.11269449
Collinsella aerofaciens	0.20115225	0.015625	0.12559936	0.04906225	0.02070721	3.5035E-05	0.02735716	0.02676496	0.00191144	0.09272025	0.03352561	0.024	0.04301476	0.01030225	0.05035536	0.11573604	0.10770089	0.044521
Bacteroides ovatus	0.0004431	0.0042654	0.00540519	0.09591409	0.00704592	0.0060016	0.01573929	0.02569609	0.04347225	0.01121481	0.15264649	0.01503076	0.00012928	0.01435204	0.12837889	0.09114361	0.13808656	0.00753945
Bifidobacterium catenulatum	0.0044716	0.00119439	0.00233676	0.00102913	0.00710818	0.00831379	6.6032E-05	0.00526205	0.00167117	0.00236877	0.00049818	0.00086495	0.01411344	0.007744	0.02093809	0.00914892	0.00742872	0.00519264
Acidaminococcus fermentans	0.00117786	0.0002387	0.00386014	0.02989441	0.00426017	0.01577456	0.01940449	0.04782969	0.03504384	0.002261	0.04541161	0.02265025	0.01075369	0.01787569	0.01216609	0.02185529	0.0374423
Fusobacterium naviforme	0.01026169	0.00530712	0.05447556	0.09030025	0.0024453	0.01836025	8.8757E-05	0.00272693	0.04074632	0.03587236	0.02861056	0.02442969	0.03598609	0.01317904	3.976E-06	0.03214849	0.02380849	0.00637762
Negativicoccus succinicivorans	0.00336052	0.01937664	0.0014402	0.06180196	0.00426017	0.01106704	0.01577536	0.03849444	0.04946176	0.0028569	0.00982874	0.00694389	0.00474308	0.00020164	0.00011946	0.00828775	4.3507E-05	0.00188879
Fusobacterium gonidiaformans	0.11587216	0.02637376	0.04524129	0.09418761	0.03697929	0.00459413	0.00017609	0.00039482	0.03308761	0.10588516	0.05257849	0.04468996	0.01817104	0.12369289	0.01582564	0.06071296	0.06739216	0.055696
Pyramidobacter piscolens	0.119025	0.04477456	0.09647236	0.21631801	0.10778089	0.09229444	0.0021441	0.126736	0.10445824	0.16605625	0.10227204	0.04748041	0.00520096	0.15618304	0.15657849	0.09696996	0.02122849
Acidaminococcus intestini	0.00016641	0.05803281	0.00192019	0.03337929	0.00334778	0.00251201	0.00434545	0.0026605	0.05929225	0.00217902	0.02196324	0.00768252	0.0025808	0.00919681	0.00288154	0.01190281	0.00025408	0.02849344
Fusobacterium nucleatum	0.158404	0.065536	0.02313441	0.0961	0.09647236	0.15731569	0.01386409	0.00780749	0.03996001	0.035856	0.13227769	0.04068289	0.02393209	0.05559649	0.07862416	0.07739524	0.05080516	0.06135529
Escherichia albertii	0.127449	0.08196769	0.04056196	0.25452025	0.073984	0.00106211	0.0007177	0.00848609	0.05271616	0.09960336	0.264196	0.07756225	0.16711744	0.047961	0.15155449	0.25938649	0.14227984	0.16842816
Escherichia coli	0.09778129	0.08381025	0.02563201	0.25371369	0.03052009	0.00089102	0.00031969	0.01096209	0.05202961	0.04879681	0.16654561	0.11703241	0.11744329	0.01652025	0.100489	0.154449	0.12895281	0.03069456
Megasphaera hominis	0.06625476	0.1024	0.050176	0.13046544	0.064516	0.04	0.024649	0.08357881	0.02200947	0.01108809	0.04048144	0.00637283	7.161E-06	0.0067322	5.2349E-06	0.01147041	0.04661281	0.06646084
Veillonella denticariosi	0.04477456	0.110224	0.02377764	0.12931216	0.13571856	0.01734436	0.04020025	0.02157961	0.02162941	0.002961	0.16984	0.17969121	0.11235904	0.131769	0.01315616	0.09253764	0.14784025	0.05790564
Megasphaera micronuciformis	0.15211669056	0.10647169	0.14523721	0.14205361	0.03323329	1.5054E-05	0.03519376	0.05919489	0.09205156	0.11682724	0.09024016	0.00161443	0.00236196	0.064516	0.14861025	0.14356521	0.06832996
Serratia entomophila	0.16679056	0.12866569	0.05588496	0.29746116	0.083521	0.00825736	0.00061603	0.01879	0.07038409	0.12845056	0.30338064	0.13454224	0.19571776	0.09437184	0.01900384	0.18473841	0.20738916	0.259081
Candidatus Endobugula sertula	0.21613201	0.13601344	0.04915089	0.20511841	0.13147876	0.00452391	0.01063458	0.00754987	0.04305625	0.09498724	0.12902464	0.06754801	0.13927824	0.075076	0.07535025	0.20967241	0.11478544	0.15350724
Veillonella montpellierensis	0.06370576	0.15880225	0.08684809	0.28249225	0.07661824	0.00143187	0.03916441	0.09333025	0.05489649	0.08462281	0.18054001	0.12559936	0.08602489	0.01106704	0.08242641	0.18731584	0.10381284	0.09647236

Spearman (r²)	L-Glycine	Beta-Alanine	5-Aminovale	4-Hydroxyph	Cadaverine	D-Glucose	OTMA	Tyramine	Phenylalanin	3-Hydroxybut	Nicotinic Aci	Hydrocinnam	Pyroglutamic	Methyladipic	Tricarballylic	Pantothenic	Linoleic Acid	Sebacic Acid	5β-Coprostan	2-hydroxy-3-	Glutamate	Citrate	Methylamine
Bacteroides caccae	0.00011046	0.12552849	0.14538969	0.00842357	0.12425625	0.02235025	0.12411529	0.02930944	0.14107536	0.04601025	0.14600041	0.06426225	0.05308416	0.20439441	0.08462281	0.02319529	0.00195895	0.00120201	0.18326961	0.1369	0.18558864	0.19289664	0.19989841
Pedobacter kwangyangensis	0.01056784	0.10523536	0.16887449	0.915129	0.15272464	0.015876	0.27217089	0.13905441	0.15912121	0.05112121	0.15233409	0.10666756	0.11812969	0.30680521	0.18224361	0.072361	0.0433889	0.046656	0.31102929	0.25140196	0.198025	0.29214025	0.290521
Bacteroides uniformis	0.03108169	0.06180196	0.18224361	0.0083448	0.117649	0.01551361	0.0625001	0.1089	0.15124321	0.01399489	0.12411529	0.0010608	0.00801025	0.10074276	0.06431296	0.08421604	0.090015	0.01975029	0.08151025	0.09184784	0.07425625	0.14737921	0.23951236
Parabacteroides distasonis	0.00716224	0.05822569	0.06901129	6.1921E-07	0.03876961	0.02322576	0.08334769	0.03150625	0.15397776	0.04199524	0.17380561	0.06922161	0.03810304	0.14002564	0.10621081	0.025281	0.05602689	0.01297321	0.02531281	0.09554281	0.113569	0.10797796	0.06046681
Sphingobacterium shayense	0.00974761	0.054756	0.06927424	9.4809E-05	0.03179089	0.01631861	0.07851204	0.03690241	0.17690436	0.05276209	0.13890529	0.0006225	0.03006756	0.12362256	0.12475024	0.02449225	0.060516	0.01968221	0.06280225	0.08254129	0.11621841	0.07592161	0.07524049
Ruminococcus bromii	0.03869089	0.03916441	0.06365529	0.02502724	0.11269449	0.04528384	0.12299049	0.03363556	0.099856	0.029929	0.02208196	0.09138529	0.02070721	0.12496225	0.07306209	0.04682896	0.05189284	0.05433561	0.24186724	0.100489	0.06859161	0.155236	0.14017536
Parabacteroides merdae	0.00124256	0.03407716	0.022725	0.02091841	0.01923321	0.00594749	0.068121	0.01530169	0.01384641	0.01993744	0.010404	0.01153129	0.10850436	0.08375236	0.01267876	0.00679032	7.6895E-06	0.02675025	0.118336	0.04052169	0.087025	0.14868736
Prevotella copri	0.02930944	0.03404025	0.03129361	0.00309136	0.02452356	0.00150079	0.1024641	0.03990001	0.04674244	0.01602756	0.07403841	0.06646084	0.0008773	0.0533148	0.0004145	0.0575864	0.01762636	0.0902329	0.04709	0.04652649	0.0863721	0.02630884
Dysgonomonas wimpennyi	0.03337929	0.02934369	0.14010049	0.02267082	0.05331481	0.01445296	0.27510025	0.10843849	0.12013156	0.07767369	0.19829209	0.11262736	0.03667225	0.29322225	0.17539344	0.0929034	0.047089	0.04464769	0.265225	0.32216976	0.15896169	0.30404196	0.24423364
Sutterella wadsworthensis	0.00585531	0.02528529	0.03900625	0.00954334	0.02069009	0.00104394	0.01254456	0.04969576	0.02134521	0.01364224	0.01366561	0.019321	0.02449225	0.0383024	9.3335E-05	0.007804	0.00404009	0.00173722	0.02259009	0.014049	0.0401	0.04114123
Prevotella stercorea	0.06528025	0.02556801	0.00264196	0.02184484	0.011025	0.0012034	0.01456849	0.03389281	0.0961	0.06791236	0.03139984	0.00088209	0.01236544	0.04210704	0.01408969	0.05466244	0.00161845	0.01046529	0.03992004	0.0058645	0.036481	0.05008644	0.03655744
Akkermansia muciniphila	0.00093482	0.02524921	0.09957825	0.03207681	0.04473259	0.00143699	0.17156164	0.14167696	0.02234996	0.08886361	0.061009	0.09042049	0.29224836	0.07360369	0.02951524	0.04886449	0.03102929	0.25140196	0.04394	0.23316689	0.13235044	0.15736441	0.13402921
Phascolarctobacterium faecium	0.02483776	0.02214144	0.05803281	0.00471058	0.01590121	0.056696	0.074529	0.01555009	0.03319684	0.03441409	0.02229049	0.05424241	0.05280804	0.1298169	0.0841	0.00224775	5.2969E-05	0.01125721	0.05189284	0.09090225	0.02521744	0.10595025	0.08180196
Bacteroides acidifaciens	0.01108809	0.01827904	0.0125124	0.007921	0.04468996	3.287E-06	0.04367316	0.01067009	0.01602756	0.00933929	0.12278016	0.04089484	0.00675848	0.1527684	0.15227604	0.00361201	0.00157688	8.145E-05	0.00023654	0.01646989	0.06024004	0.02090916	0.06017144
Bilophila wadsworthia	0.01205648	0.01779556	0.08259876	0.008732	0.05326864	0.04739329	0.11063289	0.02907025	0.117649	0.03606201	0.07392961	0.04473224	0.10290169	0.08674009	0.09313704	0.02927521	0.00126736	0.00884761	0.06780816	0.14379264	0.04481689	0.1184041	0.18071001
Bacteroides denticanum	0.02862864	0.01498176	0.04713241	0.01113839	0.02256004	0.025281	0.08720209	0.02996361	0.03560769	0.01205604	0.08105409	0.0534072	0.000841	0.05934096	0.04	0.041616	0.052441	0.08892324	0.09759376	0.077841	0.00681615	0.06651241	0.08168164
Bacteroides thetaiotaomicron	0.04056196	0.01420864	0.03254416	0.00153429	0.0398696	5.0131E-06	0.05387041	0.07096896	0.0574164	0.0011594	0.10771524	0.00790321	0.00818301	0.02208196	0.03946896	0.06974881	0.01276663	0.01149	0.04293184	0.07086244	0.01962801	0.10543009	0.07441984
Alkaliphilus crotonatoxidans	0.03136441	0.00633457	0.04048144	0.00921984	0.05851561	0.04959529	0.29008996	0.09186961	0.06325225	0.15468489	0.07102225	0.104329	0.04405801	0.18550249	0.05049009	0.05230369	0.08520561	0.07230721	0.21827584	0.19351201	0.17969121	0.17081689	0.14853316
Bacteroides dorei	0.03865156	0.0041 6154	0.0048958	0.00010858	0.02772225	0.00062925	0.11502169	0.06340324	0.05040025	0.02770323	0.00070703	0.01999025	0.02343961	0.00535964	0.01127889	0.004754	0.05230369	0.00666481	0.01180264	0.00667489	0.02509033	0.00667817	0.05107076
Bacteroides xylanisolvens	0.02944656	2.4394E-05	0.01350244	0.00080372	0.02295225	0.00485809	3.4798E-05	0.005909	0.01510441	0.00869049	0.01954756	0.00448096	0.0007778	0.018225	0.00916196	0.01545049	0.02908729	6.4561E-05	0.00153476	0.00328651	0.0375929	0.01375929	0.01934881
Collinsella intestinalis	0.03683396	0.00032725	0.00554727	0.00516817	0.00702412	0.01315609	0.03916441	0.02061563	0.00813424	0.00028023	9.1911E-05	0.01934881	3.2262E-05	0.03775249	0.01814409	0.0001974	0.04862025	0.06687396	0.05387041	0.01734489	0.00433227	0.00974809	0.03001489
Fusobacterium nucleatum	0.0340716	0.00060368	0.00085439	0.0059441	0.00690924	0.01085764	4.0272E-05	0.01576384	0.00428788	0.08059921	0.00224771	0.000649	2.1521E-06	0.06766325	0.06677056	0.01774224	0.02692881	0.00044732	0.02032608	0.00593516	0.02196301	0.11792	0.00695056
Caloramator mitchellensis	0.00321149	0.00411907	0.01752976	0.00599231	0.00405514	0.03179089	0.10387729	0.03013696	0.04986289	0.154449	0.03530641	0.11276164	0.01129969	0.21706281	0.08910225	0.00116827	0.013924	0.01782225	0.14638276	0.10719076	0.06220036	0.13734436	0.09369721
Escherichia albertii	0.01164241	0.00646738	0.00457044	2.493E-05	0.02986041	0.01529321	0.09084196	0.01040404	0.00692224	0.01459296	0.08946081	0.02876416	0.05583769	0.06713281	0.07284601	0.05489649	0.00942064	0.01752996	0.12588304	0.090601	0.12533489	0.01369321	0.23953009
Veillonella dispar	0.02490084	0.00840522	0.01572516	2.9117E-05	0.00797092	0.04443664	0.02070316	0.00711644	0.00035081	0.02143296	0.01567504	0.0625	0.04272489	0.10310521	0.21874329	0.02521862	0.01017536	0.00470789	0.00444089	0.4441	0.09853321	0.03229209	0.13995981
Serratia entomophila	0.01625625	0.01062961	0.04635409	5.9737E-05	0.04477456	0.00618268	0.14676769	0.02307361	0.03952144	0.10516996	0.05190025	0.09765625	0.07721841	0.11498801	0.05557929	0.01507904	0.04695204	0.07577424	0.13862649	0.11950849	0.15896169	0.17690436	0.05171076
Veillonella denticariosi	0.00669779	0.01129969	0.03331481	0.00300852	0.00781986	0.06802744	0.04198401	0.01819801	0.06467844	0.01988272	0.02211169	0.1054369	0.116964	3.2689E-06	0.00684094	0.00263169	0.0625	0.09078169	0.08178641	0.15438	0.03944025
Veillonella atypica	0.00495475	0.012321	0.04173649	0.00016282	0.01752976	0.04687225	0.03024121	0.00606374	0.00068173	0.02483776	0.042849	0.06385729	0.06553136	0.14258176	0.19971961	0.00208849	0.00919216	0.01256641	0.051076	0.09078169	0.05593225	0.15960025	0.06275025
Candidatus Endobugula sertula	0.03553225	0.016384	0.01580581	0.00016028	0.03158649	0.01461681	0.06431296	0.036481	0.05069296	0.02322576	0.105625	0.02980364	4.4859E-06	0.03059001	0.04405801	0.023104	0.06220036	0.04884196	0.06466849	0.03944196	0.06471936	0.01517824
Streptococcus vestibularis	0.03135609	0.02205225	0.0093993	0.00270504	0.00362404	0.02096704	0.00758118	0.05574321	0.03426201	0.01739761	0.03125824	0.0090326	0.00567762	0.0071547	0.07001316	0.00299209	0.05171076	0.04791721	0.04749997	0.00493896	0.017161	0.04393216	0.01449
Veillonella montpellierensis	0.00934316	0.04338889	0.02964011	0.02656016	0.33367225	0.01431484	0.11336721	0.01036324	0.04481316	0.061009	0.16691	0.03601744	0.05369601	0.1168964	0.11437924	0.0020694	0.02143296	0.01936881	0.06890625	0.09169324	0.09684049	0.16744464	0.03253264
Bifidobacterium breve	0.054756	0.04394709	0.04173649	0.00153351	0.04751601	0.0073077	0.08282884	0.01350161	0.139876	0.010484	0.05837641	0.027225	0.05393764	0.15838576	0.10236361	0.01775959	0.01376461	0.01779159	0.05813904	0.05361509	0.06360484
Prevotella shahii	0.01324801	0.04418404	0.00128666	0.00021874	0.04799272	0.027225	0.01466521	0.01100401	0.001089	0.01715136	0.01281424	0.00460329	0.01791	0.03316969	0.02244004	0.00972985	0.02702736	0.00776866	0.0121	0.00061108	0.00895484	0.01243225	0.00104071
Acidaminococcus intestini	0.01871424	0.05470921	0.00476790	0.00839056	0.031329	0.00758118	2.232E-06	0.06466849	0.03779136	0.04600091	0.01279161	0.00583696	0.04044769	0.0001110	0.00949455	0.00278467	0.01522756	0.01006009	0.00199809	4.8469E-07	0.02059225	0.00447427	0.01207801
Prosthecobacter fluviatilis	0.017956	0.09193024	0.05276209	0.0060078	0.03200521	0.01560001	0.06416089	0.22155849	0.08105409	0.05466244	0.02442969	0.060516	0.04112784	0.02637376	0.0225	0.01026169	0.05076009	0.04769856	0.00071449	0.05861241	0.12236004	0.10214416	0.04100625

Table. 3: *Microbiome-Metabolome correlation of Obesity*

Spearman (r^2)	Butyrate	Arabinose	Galactose	Trimethylam
Blautia	0	0	0.180625	0
Butyricicoccus	0	0	0.106276	0
Butyricimonas	0	0.119716	0	0
Catenibacterium	0	0	0	0.132496
Coprococcus 1	0.231361	0	0	0
Coprococcus 3	0	0	0	0.30362
Desulfovibrio	0.41362	0	0	0.183184
Eggerthella	0.0841	0	0	0
Erysipelotrichaceae UCG-003	0	0.208849	0.2025	0
Fusinibacter	0	0	0.167281	0
Haemophilus	0.1764	0	0	0
Paraprevotella	0.09	0	0	0.096721
Parasutterella	0	0	0	0.090601
Romboutsia	0	0	0.114921	0
Roseburia	0.092416	0	0	0
Ruminoclostridium 5	0.227529	0	0	0.158404
Ruminoclostridium 6	0.100489	0	0.106929	0
Ruminoclostridium 9	0	0	0.1849	0.142129
Ruminococcaceae NK4A214	0	0	0.222784	0.1296
Ruminococcaceae UCG-002	0	0	0.133956	0
Ruminococcaceae UCG-003	0	0	0.155236	0
Ruminococcaceae UCG-010	0	0	0.126025	0.125316
Slackia	0.121801	0	0	0

Table. 4: *Microbiome-Metabolome correlation of T2D*

Spearman (r²)	Acetate	Propionate	Butyrate	Linolenic acid	Palmitoylcarnitine	LPC (18:2)	PC (16:0/17:0)	DG (15:0/18:3)	DG (15:0/20:3)	Glycoursodeoxycholic acid	Chenodeoxyglycocholate	Glycocholic acid	Cholic acid
Akkermansia	0.0001	0.0001	0.0001	0.0144	0.0049	0.0064	0.0036	0.01	0.0009	0.0009	0.0064	0.0025	0.0004
Prevotella	0.0025	0.0009	0.0049	0.0001	0.1681	0.1936	0.2809	0.0016	0.0049	0.0009	0.0025	0.0081	0.0121
Shuttleworthia	0.0004	0.0001	0	0.0064	0.0961	0	0.0016	0.0961	0.0529	0.0036	0.0009	0.0081	0.0121
Peptoniphilus	0.0004	0.0001	0	0.0064	0.0961	0	0.0016	0.0961	0.0529	0.0036	0.0009	0.0081	0.0121
Atopobium	0.0004	0.0001	0	0.0064	0.0961	0	0.0016	0.0961	0.0529	0.0036	0.0009	0.0081	0.0121
Neisseria	0.0001	0.0225	0.0289	0.0049	0.0025	0.0025	0.0004	0.0009	0	0.0025	0.0009	0.0016	0.0484
Veillonella	0.01	0.0169	0.09	0.1764	0.01	0.1225	0.0196	0.0025	0.0001	0.0025	0.0036	0.0036	0.0081
Weissella	0.01	0.0169	0.09	0.1764	0.01	0.1225	0.0196	0.0025	0.0001	0.0025	0.0036	0.0036	0.0081
Pseudobutyrivibrio	0.01	0.0169	0.09	0.1764	0.01	0.1225	0.0196	0.0025	0.0001	0.0025	0.0036	0.0036	0.0081
Streptococcus	0.01	0.0169	0.09	0.1764	0.01	0.1225	0.0196	0.0025	0.0001	0.0025	0.0036	0.0036	0.0081
Providencia	0	0.0016	0.0025	0.0064	0.0025	0.0016	0.0009	0.0064	0.0009	0.0009	0.0016	0.0016	0.0004
Aeromonas	0	0.0016	0.0025	0.0064	0.0025	0.0016	0.0009	0.0064	0.0009	0.0009	0.0016	0.0016	0.0004
Pseudomonas	0	0.0016	0.0025	0.0064	0.0025	0.0016	0.0009	0.0064	0.0009	0.0009	0.0016	0.0016	0.0004
Acinetobacter	0	0.0016	0.0025	0.0064	0.0025	0.0016	0.0009	0.0064	0.0009	0.0009	0.0016	0.0016	0.0004
Enhydrobacter	0	0.0016	0.0025	0.0064	0.0025	0.0016	0.0009	0.0064	0.0009	0.0009	0.0016	0.0016	0.0004
Allisonella	0.0025	0.0001	0.01	0.0004	0.0025	0.2025	0.49	0.0144	0.0036	0.0016	0.0001	0.0009	0.0004
Ochrobactrum	0.0025	0.0001	0.01	0.0004	0.0025	0.2025	0.49	0.0144	0.0036	0.0016	0.0001	0.0009	0.0004
Butyricicoccus	0.0025	0.0001	0.01	0.0004	0.0025	0.2025	0.49	0.0144	0.0036	0.0016	0.0001	0.0009	0.0004
Ruminococcus (torques group)	0.0025	0.0001	0.01	0.0004	0.0025	0.2025	0.49	0.0144	0.0036	0.0016	0.0001	0.0009	0.0004
Anaerostipes	0.0025	0.0001	0.01	0.0004	0.0025	0.2025	0.49	0.0144	0.0036	0.0016	0.0001	0.0009	0.0004
Blautia	0.0001	0.0036	0.0001	0.0256	0.0121	0.0001	0.0001	0.0081	0.0016	0.0004	0.0016	0.0121	0.0025
Lachnospiraceae NK4A136 group	0.0001	0.0036	0.01	0.0256	0.0121	0.0001	0.0001	0.0081	0.0016	0.0004	0.0016	0.0121	0.0025
Marvinbryantia	0.0001	0.0036	0.01	0.0256	0.0121	0.0001	0.0001	0.0081	0.0016	0.0004	0.0016	0.0121	0.0025
Morganella	0.0784	0.0169	0.09	0.0036	0.0025	0.0016	0.0009	0.0036	0.0025	0.0016	0.0036	0.3249	0.0676
Campylobacter	0.0784	0.0169	0.09	0.0036	0.0025	0.0016	0.0009	0.0036	0.0025	0.0016	0.0036	0.3249	0.0676
Solibacillus	0.0576	0.0001	0.0004	0.0036	0.0036	0.0016	0.0016	0.0064	0.0004	0.1089	0.0484	0.0009	0.0289
Oligella	0.0576	0.0001	0.0004	0.0036	0.0036	0.0016	0.0016	0.0064	0.0004	0.1089	0.0484	0.0009	0.0289
Epulopiscium	0.0576	0.0001	0.0004	0.0036	0.0036	0.0016	0.0016	0.0064	0.0004	0.1089	0.0484	0.0009	0.0289
Parapusillimonas	0.0576	0.0001	0.0004	0.0036	0.0036	0.0016	0.0016	0.0064	0.0004	0.1089	0.0484	0.0009	0.0289
Psychrobacter	0.0576	0.0001	0.0004	0.0036	0.0036	0.0016	0.0016	0.0064	0.0004	0.1089	0.0484	0.0009	0.0289
Flavobacterium	0.0576	0.0001	0.0004	0.0036	0.0036	0.0016	0.0016	0.0064	0.0004	0.1089	0.0484	0.0009	0.0289
Eubacterium (oxidoreducens group)	0.0049	0.0025	0.0025	0.0081	0.0036	0.0049	0.0016	0.0049	0.0049	0.36	0.0841	0.04	0.0064
Prevotellaceae NK3B31 group	0.0049	0.0025	0.0025	0.0081	0.0036	0.0049	0.0016	0.0049	0.0049	0.36	0.0841	0.04	0.0064
Sarcina	0	0.0081	0	0.0169	0.0036	0.0025	0.0009	0.0081	0.0036	0.0036	0.0009	0	0.0484

Table. 5: *Microbiome-Metabolome correlation of Autism*

Spearman (r²)	Fumarate	Uridine	Alanine	Propionate	Acetate	Ethanol	Isoleucine	Leucine	Methionine	Orotate	Phenylalanine	Tyrosine	Aspertate	N-methylhyd	1,3,-dihydrox	Fucose
Lactobacilli	0.1024	0	0.0729	0	0.0529	0.0529	0.1369	0.1681	0	0	0.1024	0	0	0	0	0
Akkermansia	0	0	0.2025	0	0	0.0784	0	0.0729	0.0529	0	0	0	0	0	0	0
Bifidobacteria	0	0.0676	0.1089	0	0.1156	0	0.2601	0.2916	0.1089	0.09	0.2116	0.0961	0	0	0.0529	0
Bacteroides	0	0.09	0.2116	0	0	0	0.0676	0.1024	0	0	0	0	0	0	0	0.0676
Prevotella	0.28	0	0	0.1225	0	0	0	0	0	0	0	0	0	0.0676	0	0
Sutterella	0	0	0.0784	0	0.0484	0.0784	0.1444	0.1681	0	0	0.1156	0.1024	0.1936	0	0	0.0961

Table. 6: *Microbiome-Metabolome correlation of Lupus*

Spearman (r²)	13-HODE	17beta-Nitro-5a	2-hydroxyhexae	2-Methylglutari	3-hydroxy-hexa	9-HETE	Adrenic Acid	Androsterone s	Arachidonic acid	Cholic acid	Dehydroepiand	Dihomo-gamma	Dihydroxyvitrate	Dodecanamide	Dodecanoic aci	Glycocholic acid	LysoPA(16:0/0:	LysoPC(17:0/0:	Oleamide	Oleoyl Ethyl Am	Palmitic amide	PC(O:0/14:0)	PC(18:2(9Z,12Z	PC(P-19:1(11Z)	Pentanoic acid	Phosphatidylch	Stearamide	Undecanoic acid
Acidaminococcus	0.21204616	0	0	0	0.22415538	0	0	0	0	0	0	0	0	0	0	0	0	0	0	0	0	0	0	0	0	0	0	0
Acinetobacter	0	0.17085897	0	0	0	0	0	0	0	0	0	0	0	0	0	0	0	0	0	0	0	0	0	0	0	0	0	0
Actinomyces	0	0	0	0	0	0	0	0	0	0	0.1745083	0	0.15235173	0	0	0.1652029	0	0.17215811	0	0	0.18199857	0	0	0	0.14123053	0	0	0
Adlercreutzia	0	0	0	0	0	0	0	0.14323333	0	0	0	0	0	0	0	0	0	0	0	0	0	0	0	0	0	0	0	0
Agathobacter	0	0.1325782	0	0	0	0	0	0	0	0	0.16515245	0	0	0	0	0	0	0	0	0	0.13493772	0	0	0	0	0	0	0
Alistipes	0	0	0	0	0.13582792	0	0	0	0	0	0	0	0	0	0	0.13305635	0.13050987	0	0.1399672	0	0.15800983	0	0	0	0	0	0	0
Allisonella	0	0.22586416	0	0	0	0	0	0	0	0	0.19789535	0	0	0	0	0	0	0	0	0	0	0	0	0	0	0	0	0
Alloprevotella	0.24881431	0.3977314	0	0.13109324	0.30097578	0.24274344	0	0	0.16198951	0.1516456	0	0.14287455	0	0.32100508	0	0.33597708	0.28856568	0.19005336	0.25826866	0.20603574	0.23833914	0.32471603	0.41123055	0.28289272	0	0.25619835	0.40601186	0
Atopobium	0	0	0	0	0	0	0	0	0	0	0	0	0	0	0.15011456	0	0.23486507	0.25434088	0.26392961	0	0.15211162	0.14945183	0	0.22950165	0	0	0	0
Bacteroides	0	0	0	0.16291637	0	0	0	0	0	0	0	0	0	0	0	0	0	0	0	0	0	0	0	0	0	0	0	0
Bilophila	0	0.19058167	0	0	0.34440468	0	0.23977191	0.16086717	0	0.18225992	0	0.15467742	0.2081564	0.13729226	0.20350501	0.29016828	0.19058167	0	0	0	0.26111139	0	0.2310175	0	0.17790917	0	0	0
Butyricimonas	0	0	0	0	0	0	0	0	0	0.20170815	0	0	0	0	0	0.13565041	0	0.13378889	0	0	0	0	0	0.26753536	0	0	0	0
CAG-56	0	0.13854393	0	0.14893888	0.16132545	0.22052773	0	0.17052349	0	0.29946352	0	0.18653623	0.18117596	0	0	0	0	0	0	0	0	0.21958184	0.22433153	0.16853102	0	0	0	0
Catenibacterium	0.20188658	0.36215602	0.12938236	0.18933342	0.22781424	0	0.37247817	0	0.20115835	0	0	0	0.20812912	0.256128	0.21746214	0.27365746	0.17209928	0	0.30416251	0.3860711	0.21672628	0.35729155	0.24037007	0	0.15664893	0.26398612	0	0
Christensenellaceae_R-7_group	0	0	0.15345537	0	0.14903962	0	0	0	0	0.17243597	0	0.2073898	0	0.14314993	0	0	0	0	0	0	0	0.15697008	0.22089953	0	0	0	0	0
Clostridium_innocuum_group	0	0	0	0	0	0	0	0.13941793	0	0.20908497	0	0	0	0	0	0	0	0	0.13849525	0	0	0	0.16098922	0	0	0.16998771	0	0
Clostridium_sensu_stricto_1	0	0	0	0	0	0.13292959	0	0	0	0	0	0.17796071	0	0	0	0	0	0	0	0	0	0	0	0	0	0	0	0
Coprococcus_1	0	0	0	0	0	0	0	0	0	0	0	0	0	0	0	0	0	0	0	0	0	0	0	0	0	0	0	0
Coprococcus_2	0.24295169	0.26091194	0.19686303	0	0.27758083	0.15005296	0.28080408	0.22524563	0.21081551	0	0.33702867	0.36058326	0.17854419	0.26676078	0	0.15465626	0	0	0.22044612	0.17768602	0.17089501	0.15738708	0.35569582	0.34534275	0.2026795	0	0.2737374	0.23876035
Coprococcus_3	0	0.13306802	0.18121598	0	0	0	0	0	0	0	0	0	0	0.1334608	0	0	0	0	0	0	0	0	0	0	0	0	0	0
Dorea	0	0	0	0	0	0	0	0	0	0	0	0	0	0	0	0.13459316	0	0.15130235	0.25507702	0.17691016	0	0	0	0	0	0	0	0
Eggerthella	0	0.15547635	0	0	0	0	0	0	0	0	0	0.16519738	0.13584252	0	0.25065102	0	0.35674877	0.25750449	0.38453331	0	0.20263367	0	0	0	0.15806715	0.21087255
Enorma	0	0	0	0	0	0	0	0	0	0	0	0	0	0	0	0	0	0	0	0	0	0	0	0	0	0.2984019	0
Enterococcus	0.32233087	0.31369028	0.24518471	0	0.37911826	0.22371377	0.18624404	0.30850507	0.21353345	0	0.3390245	0.27987517	0.13761703	0.18199857	0.20088957	0.23024518	0	0.13316817	0	0.21915993	0.29977105	0.27604852	0.14704748	0.12994864	0	0.23569462
Erysipelatoclostridium	0	0.38834122	0.1857254	0	0.28856332	0.14576589	0.20193385	0.18104668	0	0.26996171	0.24033604	0.20485382	0.27101395	0.15012386	0.36622238	0	0.16032593	0.21919916	0.16440219	0.30800924	0.30375895	0.38682976	0	0.25564926	0.20779466
Escherichia-Shigella	0.2195376	0.23765625	0.14183728	0	0.18754486	0.13612528	0.14612126	0	0.24478558	0	0.15046889	0	0.1302395	0	0.32784854	0	0	0	0.26972941	0.20141273	0	0.15235173	0	0.15268865	0.17823376
Eubacterium	0	0	0	0	0	0	0	0	0	0	0.16149966	0	0	0	0	0	0	0	0	0	0	0	0	0	0	0
Eubacterium_coprostanoligenes_group	0	0.1931744	0	0	0.19282014	0	0	0.14642987	0	0	0	0.19673518	0	0.19673518	0	0	0	0.15286665	0	0.19960719	0	0	0	0	0
Eubacterium_eligens_group	0	0.20628956	0	0	0	0	0	0	0	0	0	0.12715365	0	0	0	0	0	0	0	0	0	0	0	0	0
Eubacterium_oxidoreducens_group	0	0.22785539	0	0	0.17602715	0	0	0	0	0.20482549	0	0.18095078	0.36257306	0	0.23345238	0	0.18177799	0.16956804	0.15932934	0.22924629	0.1821923	0.33504625	0	0.23345238
Eubacterium_ruminantium_group	0	0.40311655	0.23187499	0	0.21828061	0.14749955	0	0.18687534	0	0.15646787	0	0.18095078	0	0.2681802	0	0.3995863	0	0.27174525	0.30244478	0.32390031	0	0.18253863	0.31522992	0	0.39749822	0.15250181
Eubacterium_xylanophilum_group	0	0	0	0	0	0	0	0	0	0	0	0	0	0	0	0	0	0	0	0	0	0	0.16070165	0	0
Faecalibacterium	0.30695179	0	0.19352908	0	0.26805668	0.18894444	0	0.12878839	0	0.13169873	0.12878839	0.17653552	0.33341316	0	0.23765625	0	0.14092756	0.19105361	0.241604	0.22485948	0.26141777	0.32600411	0.27817122	0	0.26763933	0.27224832
Faecalibila	0	0.16273374	0	0	0	0	0	0.13235401	0	0	0	0	0	0	0	0	0	0.17081871	0.20362665	0.25364791	0	0	0	0.53251738
Family_XIII_AD3011_group	0	0	0	0	0	0	0	0	0	0	0	0	0	0.14598497	0	0.13877316	0	0	0	0	0	0	0	0
Fusicatenibacter	0.14427744	0	0	0	0	0	0	0	0	0	0	0	0	0	0	0	0	0	0	0	0	0.14550532	0.28072905
Fusobacterium	0	0.16555272	0	0	0.16654202	0.13649404	0	0.18817489	0	0	0	0	0	0.23618813	0	0	0	0	0	0.15903243	0.18935761	0.2481861	0	0
GCA-900066755	0	0.20186492	0	0	0.22692323	0	0	0	0	0	0.19969244	0	0	0	0	0	0	0	0	0	0	0.19939364	0
Gemella	0	0	0	0	0	0	0	0	0	0	0	0	0	0	0	0	0	0.13113864	0	0	0	0	0.16182711
Haemophilus	0	0	0	0	0	0	0	0	0	0	0	0	0	0	0	0	0	0.1493409	0	0	0	0	0
Holdemanella	0	0	0	0	0	0	0.1471897	0	0	0	0	0	0	0	0	0	0	0	0	0	0	0	0
Holdemania	0	0	0	0	0.18482906	0	0	0	0	0	0.14366847	0	0	0	0	0	0	0	0	0	0	0	0
Hungatella	0	0	0	0	0	0	0	0	0	0	0.14716691	0	0.12677011	0	0	0	0	0	0	0	0	0	0
Klebsiella	0	0	0	0	0	0	0	0	0	0	0	0	0.15329754	0	0	0	0	0	0	0	0	0	0
Lachnoclostridium	0.12849909	0	0	0	0.1768745	0.19459479	0	0.1924662	0.23804953	0	0.16750537	0	0	0.2229515	0	0	0	0	0	0	0	0.1718236	0.23335131
Lachnospira	0	0.18712312	0.13774848	0	0	0	0	0	0	0	0	0	0	0	0	0	0	0	0	0	0	0.33695599
Lachnospiraceae_FCS020_group	0	0.1418888	0	0	0	0	0	0	0	0.17361097	0	0.12979959	0	0	0	0	0	0	0	0.14039544	0	0.1970813	0.12715365
Lachnospiraceae_NC2004_group	0	0	0	0	0	0	0	0	0	0	0	0.19842374	0	0	0	0	0	0	0	0.14039544	0	0.17167608
Lachnospiraceae_ND3007_group	0	0.1830344	0	0	0.15092417	0	0.1830344	0	0	0.26901027	0	0.19110205	0.15472886	0	0.13438933	0	0	0	0.16117519	0
Lachnospiraceae_NK4A136_group	0	0.1876962	0	0	0.25751839	0	0	0.15090358	0	0	0	0	0	0.26680421	0	0.20448348	0	0.208148	0	0.20266347	0	0.31168739
Lachnospiraceae_UCG-008	0.20395421	0	0.14032276	0	0.27817122	0.27987517	0	0.15761703	0.25040336	0	0	0	0.15761703	0	0	0	0	0	0	0	0.21690052
Lactobacillus	0.13555821	0	0	0.13114053	0.29880184	0	0.13055698	0.2561366	0	0	0.16059768	0	0	0.15826266	0	0	0	0.16869659	0	0.1379442	0	0.14522715
Megasphaera	0	0	0	0.17364247	0	0	0	0	0.16059768	0	0	0	0	0	0	0	0.12755112	0.13836704	0
Negativibacillus	0	0.13981283	0	0	0	0	0	0	0	0	0	0	0.12642377	0	0	0	0.11493729	0.18881258	0.17232088	0.12958027	0.21332999	0	0.17897638
Nicoliana_otophora	0	0.13980286	0	0.33954477	0	0.29710316	0	0.20650544	0.155981	0	0.25137067	0	0	0.44259114	0.17540935	0.21317853	0.16753435	0.22052726	0.34096105	0.24874019	0.36916694	0.18329196	0.19312202	0.28014801
Parabacteroides	0	0	0	0	0	0	0	0	0	0	0	0	0	0	0	0	0	0	0	0	0.14984393
Paraprevotella	0	0	0	0	0	0	0	0	0	0	0	0	0	0.15484335	0	0	0	0	0	0	0
Parasutterella	0	0	0.21057939	0	0	0	0	0	0.16100525	0	0	0	0	0	0	0	0	0	0	0	0
Prevotella	0.20949606	0.33394622	0	0.18083288	0.23947693	0.17210396	0	0.13989814	0	0.1544848	0	0	0.28057203	0.39120809	0.31330193	0.24603356	0.23947693	0.26915583	0.28121321	0.23868824	0.27483429	0.31860124	0.30902792	0.23320361	0	0.25227355
Romboutsia	0	0.2516155	0	0	0.24718537	0	0	0.13316617	0	0	0	0.1334608	0.18894444	0.12994864	0	0	0	0.15871228	0	0.13169873
Roseburia	0	0.16585916	0	0.14642987	0	0	0.12878839	0	0.17015625	0	0.21852512	0.34848077	0	0.18510809	0	0.26059381	0.25040336	0.13672105	0.12677046	0.21465291	0	0.20395421	0.22754436
Ruminiclostridium_5	0	0	0	0.21019263	0	0	0	0	0	0	0	0	0	0	0	0	0	0.12705774
Ruminiclostridium_9	0	0.13858406	0.20998326	0	0	0	0.24758078	0	0.20298125	0	0.23917871	0	0.14810175	0	0.22242693	0	0	0.14872669	0	0.18199498	0	0.1337953
Ruminococcaceae_NK4A214_group	0	0.15400142	0	0	0	0	0	0	0	0.15441002	0	0.12879959	0.23287438	0	0.13767974	0	0	0.258128	0.15664893	0	0.22242693
Ruminococcaceae_UCG-002	0.16032272	0.25567707	0.26680562	0	0.18789425	0.12994864	0	0.23024518	0	0.16618774	0	0.21093279	0.15015625	0.33714885	0	0	0.23218405	0	0.23413114	0	0.18337734	0.14890885
Ruminococcaceae_UCG-003	0	0.27680731	0.19493037	0	0.23692478	0	0	0	0	0	0.27329234	0	0.23448441	0.14212923	0	0.17652258	0.21977438	0.19456965	0.19161561	0.21502724	0.16373919	0	0.2401983
Ruminococcaceae_UCG-004	0	0.15400142	0	0	0	0	0	0	0	0	0	0.13429909	0	0.17316426	0	0.13180058
Ruminococcaceae_UCG-005	0	0.1958829	0	0	0.20218332	0	0	0	0	0.19496472	0	0.28935373	0	0.20915311	0.18877869	0.20725775	0.25744035	0.21392919	0.32644562	0	0.27132181
Ruminococcaceae_UCG-014	0.20193771	0.27120608	0	0.20331983	0.22423663	0	0.15328478	0	0.19496891	0	0.2600407	0.2433884	0	0.32903807	0.1578725	0	0.21333295	0.1380277	0.2716264	0.26452537	0.28827246	0	0.28952814
Ruminococcus_1	0	0.20331983	0.22423663	0	0.18421728	0.39397277	0	0.18839593	0.19653617	0	0.2600407	0	0.1382161	0.19211259	0	0	0.21353345	0.16194137
Ruminococcus_2	0	0	0	0	0.14386548	0	0	0.14519788	0	0.1382160	0.19211259	0	0	0	0	0.21127388	0.30790802	0.1526974
Ruminococcus_gauvreauii_group	0	0	0	0.1787809	0.34050329	0	0.26498774	0	0.16229876	0	0.22185532	0	0	0.14766668	0.16194137	0	0.29500671
Ruminococcus_gnavus_group	0	0	0	0	0	0	0	0	0	0	0	0.14766668	0	0.17857436
Ruminococcus_torques_group	0	0	0.15187201	0	0	0	0	0	0	0	0	0
Selimonas	0	0	0	0	0	0	0	0	0	0.13469487	0	0	0.15753755	0.12875488	0.1398256
Senegalimassilia	0	0	0	0	0	0	0	0.14530757	0	0	0	0.16467258	0.16869092	0.18542497
Slackia	0	0	0	0	0	0	0	0	0	0.14092756	0	0.15228156	0.14799486	0.1552931
Solobacterium	0	0	0	0	0	0	0	0	0	0	0.20761255	0.14704748	0	0.16433992
Staphylococcus	0	0	0	0	0	0	0	0	0	0	0	0	0
Subdoligranulum	0	0	0	0	0	0	0	0	0	0	0	0	0
Sutterella	0.25702548	0.33640046	0.14305476	0.17132033	0.24354857	0	0.18757015	0	0.18370105	0	0.21232577	0.35685587	0.21275996	0.13198144	0.221125	0.21540403	0.22343442	0.32239423	0.2920846	0.24435503	0	0.15981893
Tyzzerella_1	0	0	0	0	0.17214342	0	0	0	0	0	0	0	0	0	0
uncultured_bacterium_f_Muribaculaceae	0	0	0	0.30261573	0	0.33339617	0	0.20845884	0	0.13368489	0	0.28257432	0.26096108	0	0.28276696	0	0.17934988	0.18575807	0.16831565	0.24498768	0.30358723	0.23676068	0	0.19421799
uncultured_bacterium_f_Prevotellaceae	0	0	0	0	0	0	0	0	0	0	0	0.13904203	0	0	0.13420939	0.12873945	0.13494735
uncultured_bacterium_f_Saccharimonadaceae	0	0	0	0	0	0	0	0	0	0	0	0.14468834	0.16742107	0	0.16975216
uncultured_bacterium_o_Mollicutes_RF39	0	0	0	0.13273482	0	0.15378594	0	0	0	0	0	0
Weissella	0	0	0	0.19278194	0	0	0	0	0	0.15126919	0	0.18993367	0.13121615	0	0.20714359

Table. 7: *Multi - correlation analysis of physiological & histopathological changes and transcriptomics data.*

Parameters	C57BL/6			BALB/c		
	Day 0 (r)	Day 7 (r)	Day 15 (r)	Day 0 (r)	Day 7 (r)	Day 15 (r)
	Histopathological Score II					
Pathophysiological Score	0.95	0.73	0.99	0.79	0.24	0.18
	Fold Changes of Pro-Inflammatory Genes					
Histopathological Score I	-0.86	0.65	0.99	-0.86	0.32	-0.86
	Fold Changes of Anti-Inflammatory Genes					
Histopathological Score I	0.66	-0.73	-0.92	0.86	-0.99	0.86
	Fold Changes of Gut-Barrier function related Genes					
Histopathological Score II	-0.65	0.87	0.98	-0.46	0.52	-0.46

■ (green) Positive Correlation

■ (red) Negative Correlation

r Correlation Coefficient